

THE GALACTIC O-STAR SPECTROSCOPIC SURVEY (GOSSS). II. BRIGHT SOUTHERN STARS*

A. SOTA^{1,6,7,8}, J. MAÍZ APELLÁNIZ^{1,6,7,8}, N. I. MORRELL², R. H. BARBÁ^{3,6},
 N. R. WALBORN⁴, R. C. GAMEN⁵, J. I. ARIAS³, AND E. J. ALFARO¹

¹ Instituto de Astrofísica de Andalucía-CSIC, Glorieta de la Astronomía s/n, E-18008 Granada, Spain; jmaiz@iaa.es

² Las Campanas Observatory, Observatories of the Carnegie Institution of Washington, La Serena, Chile

³ Departamento de Física, Universidad de La Serena, Av. Cisternas 1200 Norte, La Serena, Chile

⁴ Space Telescope Science Institute, 3700 San Martin Drive, Baltimore, MD 21218, USA

⁵ Instituto de Astrofísica de La Plata (CCT La Plata-CONICET, Universidad Nacional de La Plata), Paseo del Bosque s/n, 1900 La Plata, Argentina

Received 2013 October 30; accepted 2013 December 19; published 2014 February 25

ABSTRACT

We present the second installment of GOSSS, a massive spectroscopic survey of Galactic O stars, based on new homogeneous, high signal-to-noise ratio, $R \sim 2500$ digital observations from both hemispheres selected from the Galactic O-Star Catalog (GOSC). In this paper we include bright stars and other objects drawn mostly from the first version of GOSC, all of them south of $\delta = -20^\circ$, for a total number of 258 O stars. We also revise the northern sample of Paper I to provide the full list of spectroscopically classified Galactic O stars complete to $B = 8$, bringing the total number of published GOSSS stars to 448. Extensive sequences of exceptional objects are given, including the early Of/WN, O Iafpe, Ofc, ON/OC, Onfp, Of?p, and Oe types, as well as double/triple-lined spectroscopic binaries. The new spectral subtype O9.2 is also discussed. The magnitude and spatial distributions of the observed sample are analyzed. We also present new results from OWN, a multi-epoch high-resolution spectroscopic survey coordinated with GOSSS that is assembling the largest sample of Galactic spectroscopic massive binaries ever attained. The OWN data combined with additional information on spectroscopic and visual binaries from the literature indicate that only a very small fraction (if any) of the stars with masses above $15\text{--}20 M_\odot$ are born as single systems. In the future we will publish the rest of the GOSSS survey, which is expected to include over 1000 Galactic O stars.

Key words: binaries: general – binaries: spectroscopic – stars: early-type – stars: emission-line, Be – surveys

Online-only material: color figures, machine-readable tables

1. INTRODUCTION

The Galactic O-Star Spectroscopic Survey (GOSSS) is a long-term project whose main goals are to obtain homogeneous, high SNR, $R \sim 2500$, blue-violet spectra of a large number (1000+) of O stars in the Milky Way and to derive accurate and self-consistent spectral types for all of them (Maíz Apellániz et al. 2011). In Sota et al. (2011), hereafter Paper I, we presented the first installment of the survey, which was composed of the results for 178 northern ($\delta > -20^\circ$) O stars and also included an initial grid of spectral classification standards from both hemispheres. The GOSSS collaboration has also produced two letters: one on the classification of Of stars with C III emission lines (Walborn et al. 2010b) and another one on rapidly rotating nitrogen-enriched O stars (Walborn et al. 2011). GOSSS data have also been used for the discovery of the O star with the strongest magnetic field measured to date (NGC 1624-2; Wade

et al. 2012) and for the study of a shell-like event in the Oe star HD 120 678 (Gamen et al. 2012).

In parallel to GOSSS, four other surveys (OWN, IACOB, NoMaDS, and CAFÉ-BEANS) are obtaining high-resolution optical spectroscopy of a subsample of Galactic O stars. OWN, a high-resolution spectroscopic monitoring survey of southern Galactic O- and WN-type stars, is obtaining multiple-epoch spectroscopy with the aims of detecting binaries, determining their orbits, and deriving their physical parameters (Barbá et al. 2010). The detection of spectroscopic binaries (SBs) plays an important role in this paper and is described in the next section. IACOB is obtaining spectroscopy of bright northern OB stars (minimum of three epochs) with the goal of deriving their physical parameters (Simón-Díaz et al. 2011b, 2011c). NoMaDS is an extension of IACOB to fainter stars in the northern hemisphere (Maíz Apellániz et al. 2012; Pellerin et al. 2012). CAFÉ-BEANS (Calar Alto Fiber-fed Échelle Binary Evolution Andalusian Northern Survey), the latest addition to the group, is the northern counterpart to the study of southern SB2 by OWN using the CAFÉ spectrograph at the 2.2 m Calar Alto telescope. Taken together, the five surveys aim to provide the most complete view to date of Galactic O stars with optical spectroscopy, studying their membership, spectroscopic binarity, intervening interstellar medium, spatial distribution, and initial mass function within a few kpc of the Sun. Another complementary survey is obtaining high spatial resolution images of massive stars to study their visual binarity (Maíz Apellániz 2010). The survey initially used only the AstraLux Norte Lucky Imaging instrument at the 2.2 m Calar Alto telescope but has been recently extended to the southern

* The GOSSS spectroscopic data in this article were gathered with one primary facility, the 2.5 m du Pont Telescope at Las Campanas Observatory (LCO), and three auxiliary ones, the 1.5 m Telescope at the Observatorio de Sierra Nevada (OSN), the 3.5 m Telescope at Calar Alto Observatory (CAHA), and the 4.2 m William Herschel Telescope at Observatorio del Roque de los Muchachos (ORM). The OWN spectroscopic data were gathered at LCO, La Silla Observatory, and CASLEO. Some of the supporting imaging data were obtained by the 2MASS survey and the NASA/ESA *Hubble Space Telescope* (HST). The HST data were obtained at the Space Telescope Science Institute, which is operated by the Association of Universities for Research in Astronomy, Inc., under NASA contract NAS 5-26555.

⁶ Visiting Astronomer, LCO, Chile.

⁷ Visiting Astronomer, CAHA, Spain.

⁸ Visiting Astronomer, WHT, Spain.

Table 1
Telescopes, Instruments, and Settings Used

Telescope	Spectrograph	Grating (l mm ⁻¹)	Spectral Scale (Å px ⁻¹)	Spatial Scale ('' px ⁻¹)	Wav. Range (Å)
LCO 2.5 m (du Pont)	Boller & Chivens	1200	0.80	0.71	3900–5500
OSN 1.5 m	Albireo	1800	0.62	0.83	3750–5070
CAHA 3.5 m	TWIN (blue arm)	1200	0.55	0.58	3930–5020
ORM 4.2 m (WHT)	ISIS (blue arm)	600	0.44	0.20	3900–5600

hemisphere using its counterpart AstraLux Sur at the 3.5 m New Technology Telescope (NTT) at La Silla.

This paper is the second installment of the survey and its main goal is to provide a southern ($\delta < -20^\circ$) counterpart for [Paper I](#). The basis of the southern star sample is version 1 of the Galactic O-Star Catalog (GOSC, Maíz Apellániz et al. 2004). To that we added new stars with $B < 8$, some stars located within a few arcminutes of other O stars, and objects in the Carina region from version 2 of GOSC (Sota et al. 2008). We also eliminated from the sample the O stars in NGC 3603 due to crowding and faintness, leaving a total of 258 southern stars, whose spectral types and other information are listed in Table 7. In addition, we also revised the northern sample to (1) include new results from the literature, (2) re-observe SB2 stars near quadrature or visual binaries (VBs) with close companions, (3) add new stars with $B < 8$, and (4) uniformize the use of the f and z suffixes. The results for the northern sample are presented in Table 6. Those changes bring the total (northern+southern) current GOSSS sample to 448 Galactic O stars.

We will continue GOSSS until we have obtained spectra for more than 1000 O Galactic stars. Of course, that implies observing many stars that turn out to be of a different spectral type (Maíz Apellániz et al. 2013). Over the upcoming years we plan to publish the spectra not only for the remaining O stars but also for the other early-type stars we are observing (mostly B stars but also a few Wolf–Rayets or WRs, subdwarfs or sds, planetary nebula nuclei or PNNs, luminous blue variables or LBVs, and A stars). We will also list the late-type stars that have erroneous classifications in the literature as being of O or early-B type, obtain a revised grid of classification standards that will extend from O2 to A0, and produce a Magellanic Cloud extension with some significant O stars there.

2. DATA AND METHODS

2.1. Blue-violet Spectroscopy with $R \sim 2500$

The GOSSS data were described in [Paper I](#) and the reader is referred there for further information. Here we detail the differences with respect to that previous work.

Most of the spectra presented in [Paper I](#) were obtained with the Observatorio de Sierra Nevada (OSN) 1.5 m and Calar Alto (CAHA) 3.5 m telescopes. This paper concentrates on southern stars, so most of the spectra here were obtained with the 2.5 m du Pont telescope at Las Campanas (LCO).

A change in the telescopes used by GOSSS for northern dim stars took place after [Paper I](#). We are now using the ISIS spectrograph at the 4.2 m William Herschel Telescope (WHT) at the Observatorio del Roque de los Muchachos (ORM) in La Palma, Spain instead of the 3.5 m CAHA telescope. Some of the spectra in this paper were obtained with the WHT or with the OSN and CAHA telescopes.

The information for the four settings is shown in Table 1. Besides the addition of the WHT information, the values have been slightly revised from [Paper I](#). The data from each

observatory cover slightly different wavelength ranges but the spectrograms shown in this paper have been cut to show the same spectral range.

The GOSSS data in this paper were obtained between 2007 and 2013. In some cases, observations were repeated due to focus and other instrument issues detected after the fact. For SB2 and SB3 spectroscopic binaries, multiple epochs were obtained to observe the different orbit phases (see below for OWN data). In cases with known orbits, observations near quadrature were attended.

The spectral classifications which are the main content of this paper are presented in Tables 6 and 7. As we did in [Paper I](#), we give the GOSSS spectral type for all of the targets and in those cases where an alternative spectral type has been obtained using better spectral or spatial resolution than GOSSS we list it in the next column. The classification methodology is presented in Section 2.5, individual stars are discussed in Section 3, and statistics on the spectral types from Papers I and II in Section 4.3.

2.2. Spectroscopic Binarity

GOSSS is limited in its detection capabilities for spectroscopic binaries by its relatively low spectral resolution and the small number of epochs (one to two in most cases) used. For those reasons, OWN data (Barbá et al. 2010) is more appropriate to detect and study spectroscopic binaries. OWN is using high-resolution spectrographs at Las Campanas, La Silla, and CASLEO to monitor (as of 2013) 284 O and WN stars visible from those observatories. Of those, 168 (1) are classified as O stars in GOSSS data, (2) are included in the targets of this paper, (3) have $\delta < -20^\circ$, and (4) have at least five OWN epochs analyzed. This constitutes the largest uniform, high-quality sample of Galactic O-type spectroscopic binaries ever studied.⁹ In many cases, OWN have discovered new spectroscopic binaries which are presented as such for the first time in Section 3 of this paper. Here we identify the new binaries and use the information to discuss the multiplicity of O stars. A forthcoming paper (R. H. Barbá et al., in preparation) will present the orbits.

The spectroscopic binarity information is summarized in column SB of Tables 6 and 7. We have omitted the O (Orbit) qualifier for simplicity and because our main interest in this paper is multiplicity statistics, not orbits. The main source used for column SB is OWN, followed by the references listed at the bottom of the two tables. Most of those references are used for only one or two stars, with the exception of Sana et al. (2008, 2011a). When the 26 O stars with $\delta < -20^\circ$ studied by such multi-epoch high-resolution are added to the OWN sample, we obtain a sample of 194 stars for which binarity has been studied in detail.

We have also used the series of papers by Otero et al. (Otero 2003, 2006, 2007; Otero & Claus 2004; Otero & Wils 2005) to include information on eclipsing binaries. Finally,

⁹ Note that most of the archival FEROS data included in Chini et al. (2012) were obtained within OWN for the purpose of studying spectroscopic binarity.

when no alternative source was available, we resorted to the older compilations of Mason et al. (1998) and Pourbaix et al. (2004) to include additional information. Information about individual stars is presented in Section 3 and O-star multiplicity is discussed in Section 4.4.

2.3. Visual Binarity

In Paper I we included some of the AstraLux Norte images of Maíz Apellániz (2010). As previously mentioned, we have extended the Lucky Imaging survey to the south with AstraLux Sur but the data have not been fully reduced yet, so we cannot use them here. Nevertheless, for 12 complex fields we present Two Micron All Sky Survey (2MASS) images with identifications (Figure 12), as we already did in Paper I, in order to reduce the possible confusion when comparing different works. Those fields include six multiple systems and their surroundings (HD 93 146, HD 93 632, HD 92 206, HD 124 314, HD 150 136, and HDE 319 703), four classical stellar clusters (Trumpler 14, NGC 6231, Havlen–Moffat 1, and Pismis 24), one OB association (IC 2944), and an intermediate cluster/association object (Trumpler 16).

We give in column VB of Tables 6 and 7 the number of visual companions detected within 5'' and 10'' of the target separated by a hyphen. When all of the companions are within 5'', a single number is given. Given the absence of a published large-scale Lucky Imaging or Adaptive Optics survey, the information on visual multiplicity is collected in the first place by combining the information from the Washington Double Star Catalog (WDS; Mason et al. 2001, more complete for companions within 5'') and the 2MASS Point Source Catalog (Skrutskie et al. 2006, more complete in some cases for companions farther away than 5''). We have also searched the literature (e.g., Nelan et al. 2004; Mason et al. 2009; E. J. Aldoretta et al., in preparation) for additional data. For a few selected fields with unsaturated ACS/HRC and WFPC2 exposures from HST GO programs 10 205 (P.I.: N.R.W.), 10 602, 10 898, and 11 981 (P.I.: J.M.A.) we also use those images to supplement the information on multiple visual systems. Information on some individual targets is provided in Section 3. The quality of the input data and the bound character of the visual companions (as opposed to being foreground objects or cluster/association members) is discussed in Section 4.4.

2.4. Distances and Cataloguing

With respect to distances, we follow the policy of Paper I of presenting the revised *Hipparcos* distances of Maíz Apellániz et al. (2008a) whenever they are significant.

The spectral types are available through the latest version (currently v3.1) of GOSC.¹⁰ Starting in version 3, the GOSSS spectral types are the default ones and the basis for the catalog selection, though older classifications and those obtained with high-resolution spectra are also kept as possible additional columns. *B*- and *J*-band photometry are also provided in GOSC for all stars (see Maíz Apellániz et al. 2013 for details, we use B_{ap} and J_{ap} , respectively, to refer to the photometry in GOSC, where “ap” refers to approximate and is intended to be significant only to one tenth of a magnitude). The rectified GOSSS spectra can also be obtained from GOSC as FITS tables.

The GOSSS spectral types were first made available at GOSC in 2013 June as part of the GOSSS Data Release 1.0 (GOSSS-DR1.0, Sota et al. 2013), just in time for the *Massive Stars*:

Table 2

Luminosity Classes for the f Phenomenon as a Function of Spectral Type

Sp. Type	((f))	(f)	f
O2-O5.5	V	III	I
O6-O6.5	V-IV	III-Ib	Iab-Ia
O7-O7.5	V-III	II-Ib	Iab-Ia
O8	V-II	Ib	Iab-Ia
O8.5	V-II	Ib-Iab	Ia

From α to Ω meeting that took place in Rhodes, Greece at that time. The spectral types in this paper are in some cases slight revisions (mostly suffixes that were omitted or added in error) to those in GOSSS-DR1.0 and constitute GOSSS-DR1.1.

2.5. Spectral Classification Methodology

The spectral classification methodology was laid out in Paper I. We emphasize that spectral classification is an “art” that depends on the effects of spectral, spatial, and temporal resolution as well as signal-to-noise ratio (S/N). Hence, targets need to be revisited when better data become available in a process that may seem never ending but which actually converges rapidly in most cases. Since Paper I was published, we have filled some of the gaps in the standard grid presented there but some still remain. In a future paper of the series we will present an updated grid, possibly filling some of the gaps with LMC stars. An important update not related to GOSSS is the building of a standard grid for Galactic O stars at $R \sim 4000$ (H. Sana et al., in preparation) which has been used by N. R. Walborn et al. (in preparation) to classify the large sample of O stars in 30 Doradus observed by the VFTS project (Evans et al. 2011). We are collaborating with those projects to keep the standard grids at both resolutions consistent.

Besides the changes introduced by new, better data, three developments have yielded changes in the Paper I results. First, we have reviewed the suffixes related to the f phenomenon (N III $\lambda\lambda 4634$ –40–42 emission and He II $\lambda 4686$ absorption/emission) according to Table 2, after having found some minor discrepancies in Paper I. The reader is referred to Table 3 in Paper I for the meaning of the suffix. Second, we have recalibrated the z phenomenon,¹¹ defined as having a z ratio:

$$z = \frac{\text{EW}(\text{He II } \lambda 4686)}{\text{Max}[\text{EW}(\text{He I } \lambda 4471), \text{EW}(\text{He II } \lambda 4542)]} \quad (1)$$

greater than ~ 1 by measuring the equivalent widths of He I $\lambda 4471$, He II $\lambda 4542$, and He II $\lambda 4686$ in our main-sequence standard stars. This recalibration will be explained in detail by J. I. Arias et al. (in preparation) and has been applied to the results in this paper. Third, a new spectral subtype, O9.2, has been introduced as a result of the $R \sim 4000$ work mentioned above, as described in the next section.

The spectral classification has been carried out primarily by one of us (J.M.A.) using Marxist Ghost Buster (MGB; Maíz Apellániz et al. 2012) and later reviewed by another author (N.R.W.).

3. RESULTS

This section constitutes the main body of the paper and is divided in three parts. First, we present a new spectral subtype,

¹⁰ Accessible at <http://gosc.iaa.es>.

¹¹ See Walborn (2009b) and Sabín-Sanjulián et al. (2014) for details and a recent analysis.

Table 3
Spectral-type Criteria at Types O8–B0 (Comparisons between
Absorption-line Pairs Based on Peak Intensities)

Spectral Type	He II $\lambda 4542$ He I $\lambda 4388$ and He II $\lambda 4200$ He I $\lambda 4144$	Si III $\lambda 4552$ He II $\lambda 4542$
O8	>1	N/A
O8.5	≥ 1	N/A
O9	$= 1$	$\lll 1$
O9.2	≤ 1	$\ll 1$
O9.5	< 1	< 1
O9.7	$\ll 1$	≤ 1 to ≥ 1
B0	$\lll 1$	> 1

O9.2, introduced since [Paper I](#). Second, we revise some of the results on the northern sample of [Paper I](#). Third, we present the main block of results for this paper, the new southern sample. The information is given later in Tables 6 and 7, with details about each star (sorted by Right Ascension within each subsection) provided in the text.

3.1. The O9.2 Spectral Subtype

A recent development subsequent to [Paper I](#) is the definition of subtype O9.2 by H. Sana et al. (in preparation) and N. R. Walborn et al. (in preparation) based on Galactic and 30 Doradus data, respectively, of higher spectral resolution than GOSSS with criteria easily used at $R \sim 2500$. An O9.2 star has He II $\lambda 4542$ /He I $\lambda 4388$ and He II $\lambda 4200$ /He I $\lambda 4144$ ratios just slightly less than unity; thus, this subtype is symmetrical with respect to O8.5 on the opposite side of O9. See Table 3 for the updated criteria for the O8.5–B0 spectral subtype range. In this paper we present 23 Galactic O9.2 stars (see Figure 1). All but five of them were not classified as such in GOSSS-DR1.0. Ten of them have $\delta > -20^\circ$ and appear in Table 6. The other thirteen have $\delta < -20^\circ$ and appear in Table 7.

HD 5005 D. This star was classified as O9.5 V in [Paper I](#) and is now an O9.2 V.

HD 12 323. This star was classified as ON9.5 V in [Paper I](#) and is now an ON9.2 V.

HD 16 832. In [Paper I](#) this star was classified as O9.5 II–III and is now an O9.2 III.

ζ Ori AaAb = Alnitak AaAb = HD 37 742 AB. As in [Paper I](#), we were able to extract the individual spectra of A and B (= HD 37 743), separated by $2''.424$ and with a Δm of 2.424 mag in the z band. The spectral type has changed from O9.5 Ib var Nwk to O9.2 Ib var Nwk.

HD 46 202. This star was classified as O9.5 V in [Paper I](#) and is now an O9.2 V. E. J. Aldoretta et al. (in preparation) have recently discovered a companion with a separation of 86.7 mas and a Δm of 2.166 mag.

HD 57 682. Grunhut et al. (2012) have recently measured the period, longitudinal magnetic field, and magnetic obliquity of this star. The spectral type has changed from O9.5 IV in [Paper I](#) to O9.2 IV here.

CPD –35 2105 AB = CD–35 4384 AB. This is one of the five O9.2 stars classified as such in GOSSS-DR1.0. This star was not included in Maíz Apellániz et al. (2004) but was classified as O9.5 IV by Garrison et al. (1977). The WDS gives a companion with a separation of $1''.1$ and a Δm of 0.4 mag, which we were unable to spatially resolve in our long-slit spectra. Also, recently E. J. Aldoretta et al. (in preparation) have discovered that the A

component is split into Aa and Ab with a separation of 43 mas and a Δm of 1.5 mag. Therefore, the GOSSS spectral type is likely to be a composite.

HD 76 341. This star was classified as O9.5 IV in GOSSS-DR1.0 and is now an O9.2 IV. E. J. Aldoretta et al. (in preparation) have recently found a faint companion with a separation around $0''.16$. In OWN data the spectra are variable.

HD 76 968. This star was classified as O9.7 Ib by Walborn (1973b) and here we change the spectral subtype to O9.2 (in [Paper I](#) it was O9.5). OWN data indicate that this object is an SB1.

HD 90 087. The spectral subtype was changed from O9.7 to O9.2 in GOSSS-DR1.1.

ALS 15 206 = CPD –58 2625. This star was not included in Maíz Apellániz et al. (2004) but was classified as O9 V by Massey & Johnson (1993). The O9 V classification was kept in GOSSS-DR1.0 but has been changed to O9.2 V here. See Figure 12 for a chart (Trumpler 14 field).

HD 96 622. This star was classified as O9.5 IV in GOSSS-DR1.0 and is now an O9.2 IV. From a preliminary OWN analysis, it is an SB1 with a 98 day period.

HD 101 545 A. This system has a B component $2''.575$ away with a Δm of 0.6 mag. We were able to spatially resolve the two stars and determine that the companion is an early-B star. For the A component the spectral type changed from O9.5 II in GOSSS-DR1.0 to O9.2 II here.

HD 123 008. This is one of the five O9.2 stars classified as such in GOSSS-DR1.0. In [Paper I](#) it appeared as an ON9.5 Iab standard; now it is an ON9.2 Iab. OWN data shows it to be variable in He II $\lambda 4686$ and H α .

HD 124 314 BaBb. This is one of the five O9.2 stars classified as such in GOSSS-DR1.0. HD 124 314 A and BaBb are separated by $2''.5$ and both have O spectral types. Ba and Bb cannot be spatially resolved in our data as they are only $0''.21$ apart. This star was not included in Maíz Apellániz et al. (2004). See Figure 12 for a chart (HD 124 314 field).

CPD –59 5634. This star was classified as O9.7 Ib in GOSSS-DR1.0 and is now an O9.2 Ib.

HD 152 247. This system was found by Sana et al. (2008) to be an SB2 with spectral types of O9 III and O9.7: V. We do not see double lines in the GOSSS data but our combined spectral type of O9.2 III (in GOSSS-DR1.0 it was O9.5 III) is in agreement with that result. See Figure 12 for a chart (NGC 6231 field).

HD 152 424. This is one of the five O9.2 stars classified as such in GOSSS-DR1.0. In [Paper I](#) it appeared as an OC9.7 Ia standard, now it is an OC9.2 Ia. From a preliminary OWN analysis, it is an SB1 with a 133 day period.

HD 154 368 = V1074 Sco. This is one of the five O9.2 stars classified as such in GOSSS-DR1.0. In [Paper I](#) it appeared as an O9.5 Iab standard, now it is an O9.2 Iab. Mason et al. (1998) indicate that it is an eclipsing binary.

ζ Oph = HD 149 757. This is a very fast rotator, a runaway, and the closest O star. In [Paper I](#) its classification was O9.5 IVnn; it is now O9.2 IVnn.

HD 164 438. This object was classified as O9 III in [Paper I](#) and is now an O9.2 IV. It is an SB1 system according to OWN data.

HD 201 345. This used to be the prototype late-ON dwarf until its luminosity class was changed to IV in [Paper I](#). Now its spectral subtype has also changed from ON9.5 to ON9.2.

HD 218 915. This star was classified as O9.5 Iab in [Paper I](#) and is now an O9.2 Iab.

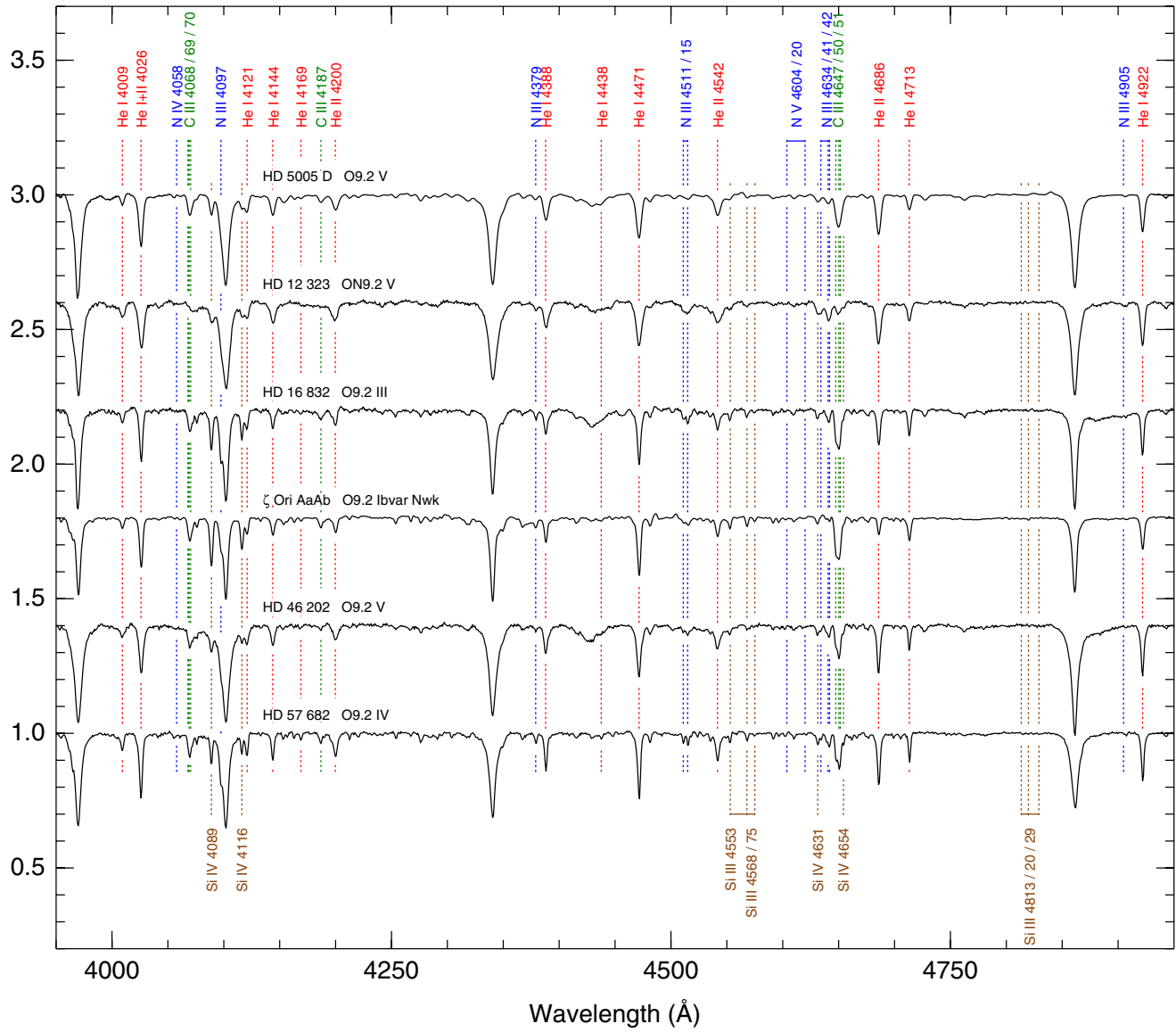


Figure 1. Spectrograms for O9.2 stars. The targets are sorted by Right Ascension.
(A color version of this figure is available in the online journal.)

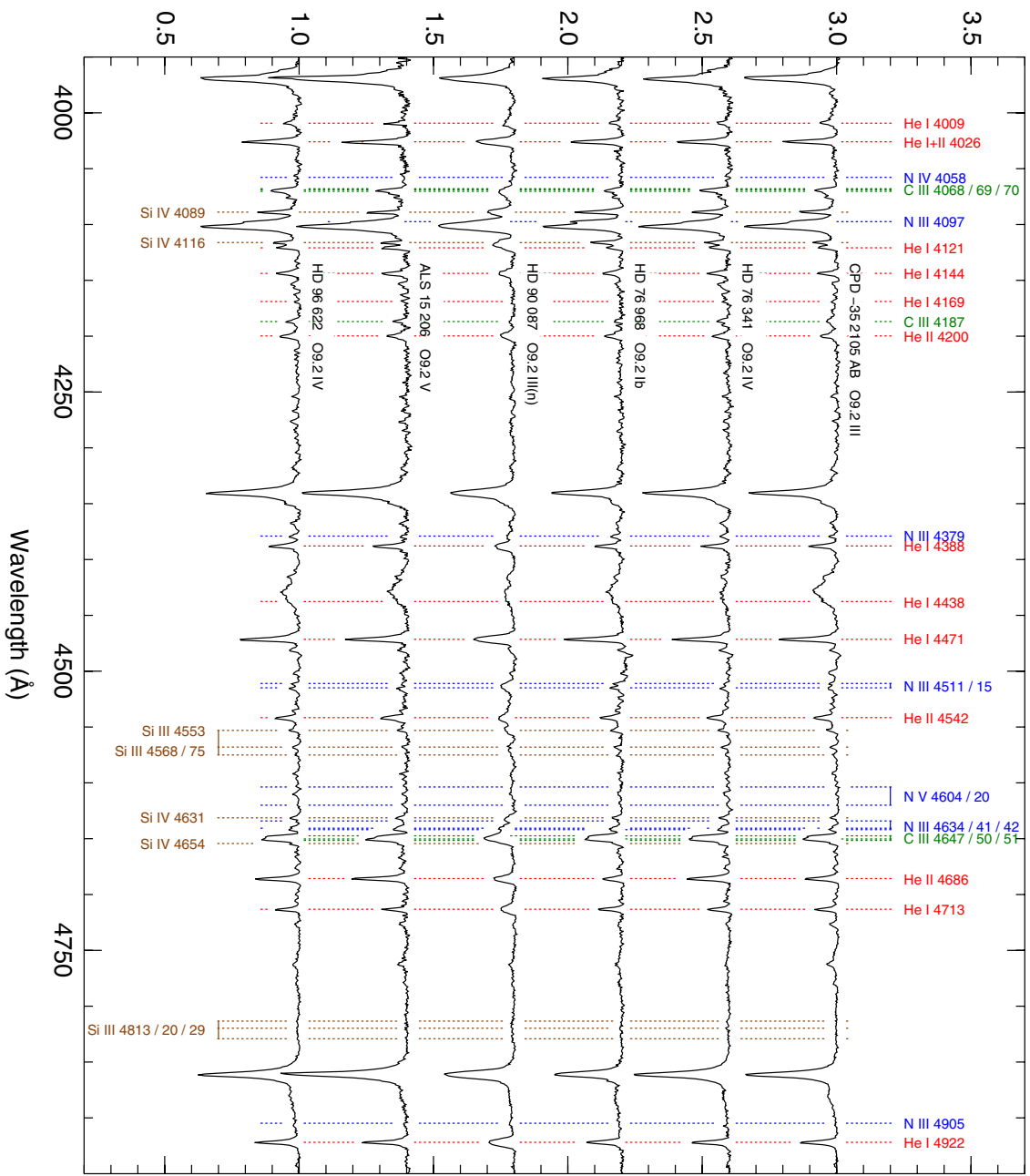


Figure 1. (Continued)

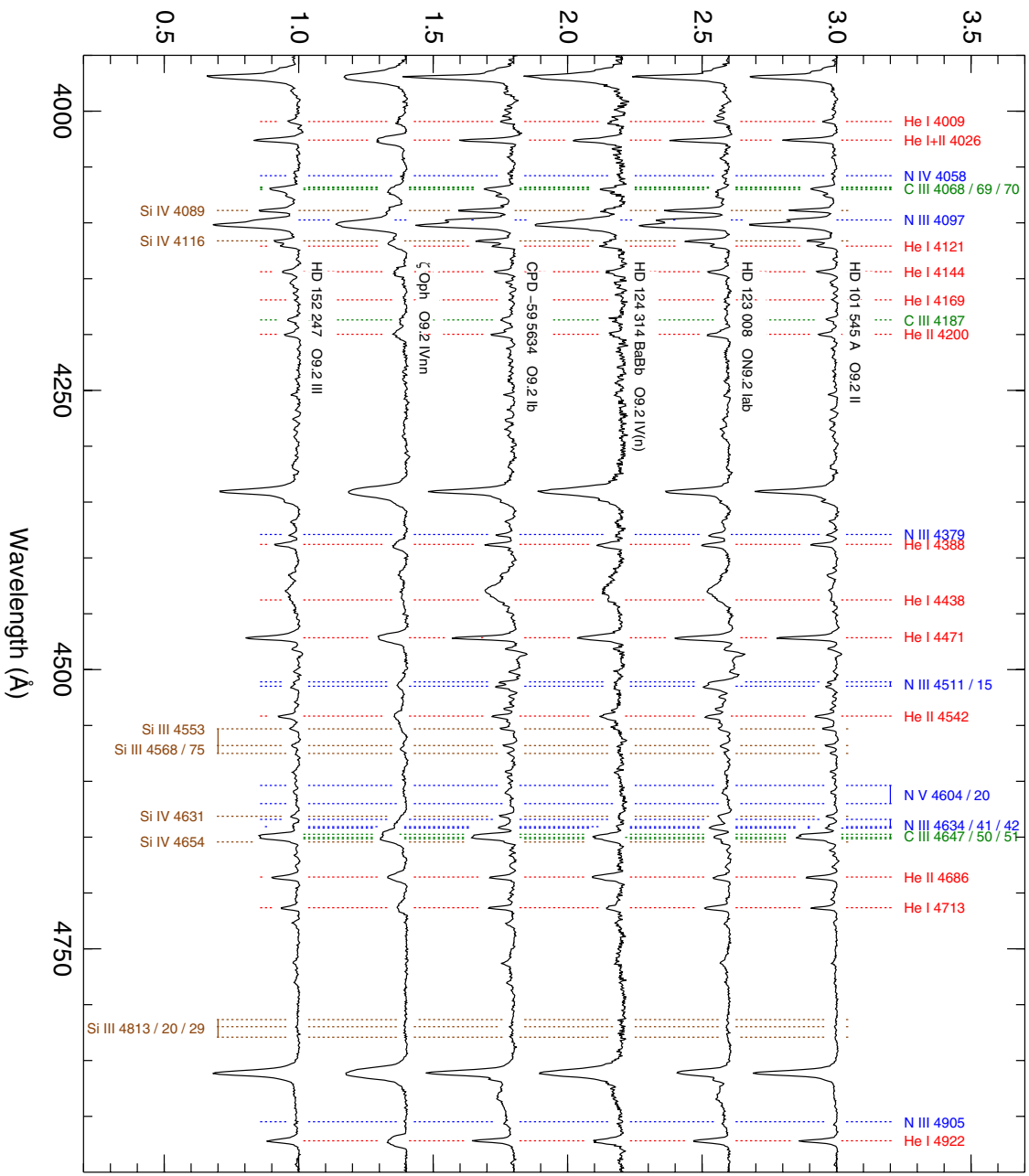


Figure 1. (Continued)

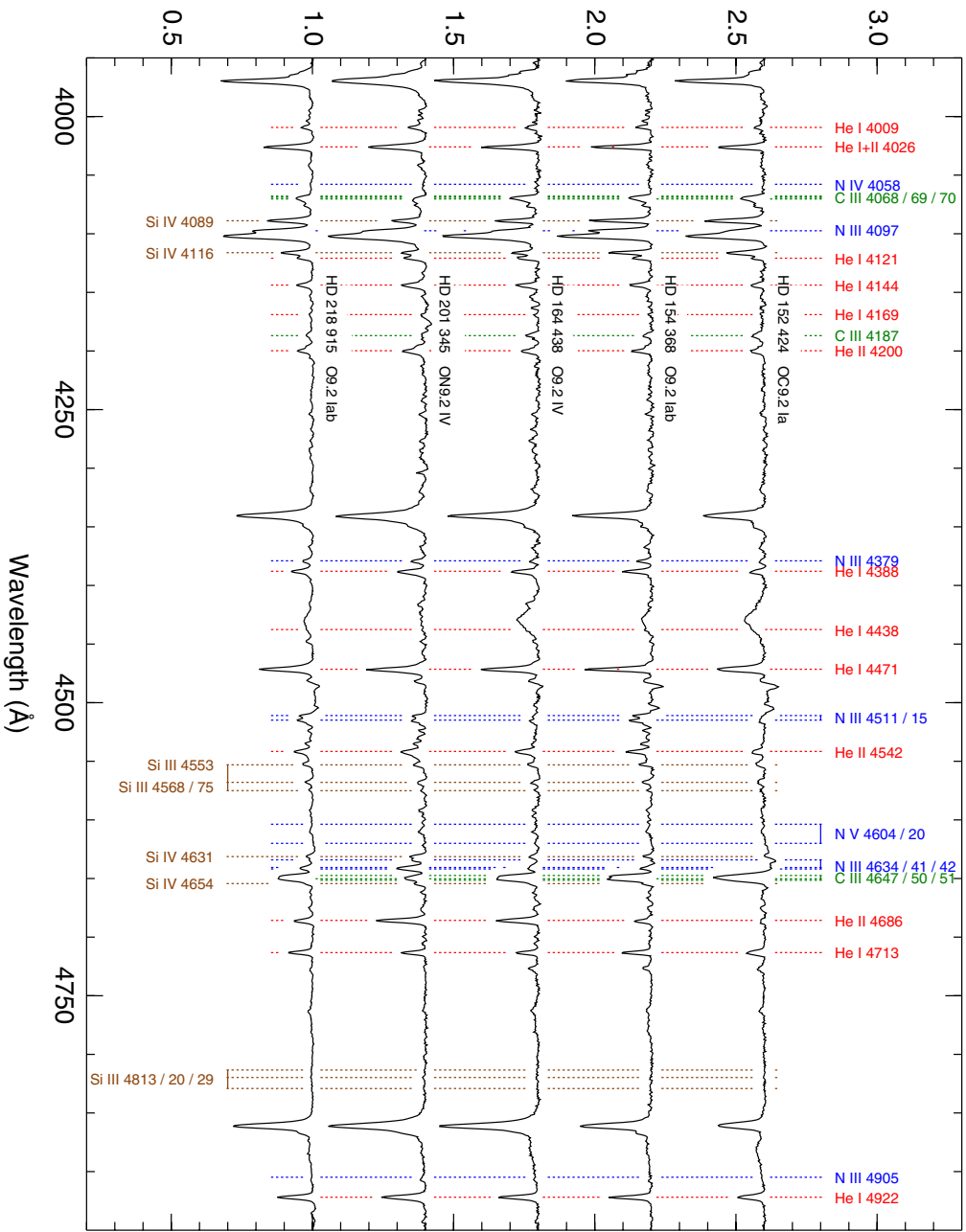


Figure 1. (Continued)

3.2. Revisiting the Northern Sample from *Paper I*

In this subsection we revise the results of *Paper I* due to four reasons:

1. Either we have reobserved an SB2 system with GOSSS or other authors have used high-resolution spectroscopy to obtain resolved (in velocity) spectral types for one of such systems. In the second case we simply recall those new results, since a new GOSSS spectral type was not obtained.
2. We have reobserved some of the stars with close companions under better seeing conditions than those in *Paper I*, leading us to improved (spatially) resolved spectral types.
3. As a result of the redefinition of spectral subtype O9.7, we are observing all stars with previous spectral classifications of B0. In some cases we have found new cases of bright ($B < 8$) O9.7 stars that are presented in order to achieve completeness for that magnitude limit.
4. We have introduced uniform criteria for the definition of the f and z phenomena (see previous section).

Spectrograms are shown in Figure 2. See also Section 3.1 for additional northern stars.

AO Cas = HD 1337. We reobserved this SB2 system and obtained a better velocity resolution for its components. The luminosity class for the secondary has changed from GOSSS-DR1.0. Our spectral type for the secondary is the same as that of Bagnuolo & Gies (1991) but the one for the primary is slightly different. For both components small changes were introduced in GOSSS-DR1.1.

HD 12 993. The Nstr suffix was missing in *Paper I* (see Table 3 in *Paper I* for its definition). Also, its He II $\lambda 4686$ is comparable to He II $\lambda 4542$, making the star only a marginal z. Both of those changes took place after GOSSS-DR1.0 appeared.

HD 15 558 A. The target has C III $\lambda 4650$ in emission but is not strong enough to warrant a c suffix.

BD +60 513. The z suffix was added in GOSSS-DR1.1.

HD 16 429 A. The Nwk suffix was added in GOSSS-DR1.1. This complex SB3 system (see *Paper I*) remains unresolved in velocity in GOSSS but see McSwain (2003) for a high-resolution study that resolves it.

HD 17 505 A. The ((f)) suffix was changed to (f) in GOSSS-DR1.1, according to the rules in Table 2. The spectrum of A is spatially resolved from that of B but no double lines are detected in our spectra (see *Paper I* and Hillwig et al. 2006).

HD 17 520 A. The z suffix was added in GOSSS-DR1.1. Note that A and B are spatially separated in GOSSS data (see *Paper I*).

HD 18 326. The z suffix was added and the (n) suffix dropped in GOSSS-DR1.1 for the primary of this SB2 system.

1 Cam A = HD 28 446 A. 1 Cam A was classified as B0 V by Morgan et al. (1955) and was not included in Maíz Apellániz et al. (2004). With the new definition of O9.7, we obtain a spectral type of O9.7 IIn. According to the WDS, 1 Cam B is located at a distance of $10''.3$ with a Δm of 1.0 mag as of 2009. We placed the slit along the AB line to obtain a spectrum of B and derive a spectral type¹² of B0 V.

NGC 1624-2 = 2MASS J04403728+5027410 = MFJ Sh 2-212 2 = ALS 18 660. The Of?p nature of this object was discovered by Walborn et al. (2010b). Wade et al. (2012) added the c suffix to this star, the O-type with the strongest magnetic field measured to date. The change was incorporated in GOSSS-DR1.1. Figure 2 shows the spectrum of this object in two

epochs that correspond to the “high” and “low” states (note that there is a very slight resolution difference between the two spectra).

HDE 242 908. Penny (1996) flagged this star as a possible SB2. The z suffix was added in GOSSS-DR1.1.

BD +33 1025 A. We observed this star again and obtained a new spectrum with better S/N that made us change its spectral type from O7 to O7.5. We aligned the slit to also measure the B component of the system, located $13''.8$ away, and found it to be an early B star.

HD 35 619. The z suffix was added in GOSSS-DR1.1.

HD 36 879. This star shows peculiar, variable UV Si IV emission lines (Walborn & Panek 1984). The z suffix was added in GOSSS-DR1.1.

σ Ori AB = *HD 37 468 AB.* As described in *Paper I*, σ Ori AB is a visual binary with a well known orbit and a current separation of $0''.26$ and a Δm of 1.6 mag (Turner et al. 2008; Maíz Apellániz 2010). Simón-Díaz et al. (2011a) used multiple-epoch high-resolution spectroscopy to discover that A is a spectroscopic binary and, therefore, that the system is an SB3. They derive spectral types of O9.5 V and B0.5 V for the two components of A and a more uncertain of B0/1 V for B. σ Ori AB remains unresolved in velocity in GOSSS data. The composite spectrum is O9.7 III with the luminosity class estimated from the He lines. However, the Si IV lines are weak, a sign that the real luminosity class of the components of this system is V.

HD 46 106. The luminosity class changed from II-III to III and an (n) suffix was added in GOSSS-DR1.1. The Si IV lines are weak and correspond to a luminosity class of V.

HD 46 485. A weak N III $\lambda\lambda 4634-40-42$ emission is detected. Hence, we introduce an ((f)) suffix. Also, z has been measured to be large enough to warrant the addition of a z suffix.

15 Mon AaAb = HD 47 839 AaAb = S Mon AaAb. The z suffix was added in GOSSS-DR1.1. See also 15 Mon B. Note that the orbital period of Ab with respect to Aa is of the order of a century (Cvetković et al. 2010; Maíz Apellániz 2010) so we cannot see double lines in our spectra. Indeed, the secondary was resolved in velocity from the primary by Gies et al. (1993) using high-resolution spectroscopy thanks to their different rotation speeds. This star was an MK primary standard in the past but GOSSS and other authors have shown it in an O7.5 state on occasion, hence the var suffix.

15 Mon B = HD 47 839 B = S Mon B. In *Paper I* we were able to obtain spatially resolved spectra for 15 Mon AaAb and B (separation of $2''.976$ and Δm of 3.2 mag, Maíz Apellániz 2010) that yielded an early-B type for the B component. A re-analysis of the data and a new long-slit spectrum obtained under better seeing conditions show that B has a clear He II $\lambda 4542$ absorption line. We estimate a spectral type of O9.5. We are unable to estimate a luminosity class due to the uncertainty in the separation of two nearby spectra with such a large Δm .

HD 48 099. We obtained a new GOSSS observation and we were able to resolve in velocity the two SB2 components of this system with a 3.078098 day period (Stickland 1996). Our spectral types are reasonably similar to those obtained by Mahy et al. (2010) with high-resolution spectroscopy.

HD 48 279 A. The z suffix was added in GOSSS-DR1.1.

HD 54 662. As noted in *Paper I*, Boyajian et al. (2007) attempted a tomographic reconstruction of the spectra of this system and could only determine it to within O6.5 V + O7-9.5 V. The OWN analysis indicates a different period for this SB2 (2119 ± 5 days instead of 557.8 days; R. C. Gamen et al.,

¹² Note that in this paper we only list O spectral types in the tables.

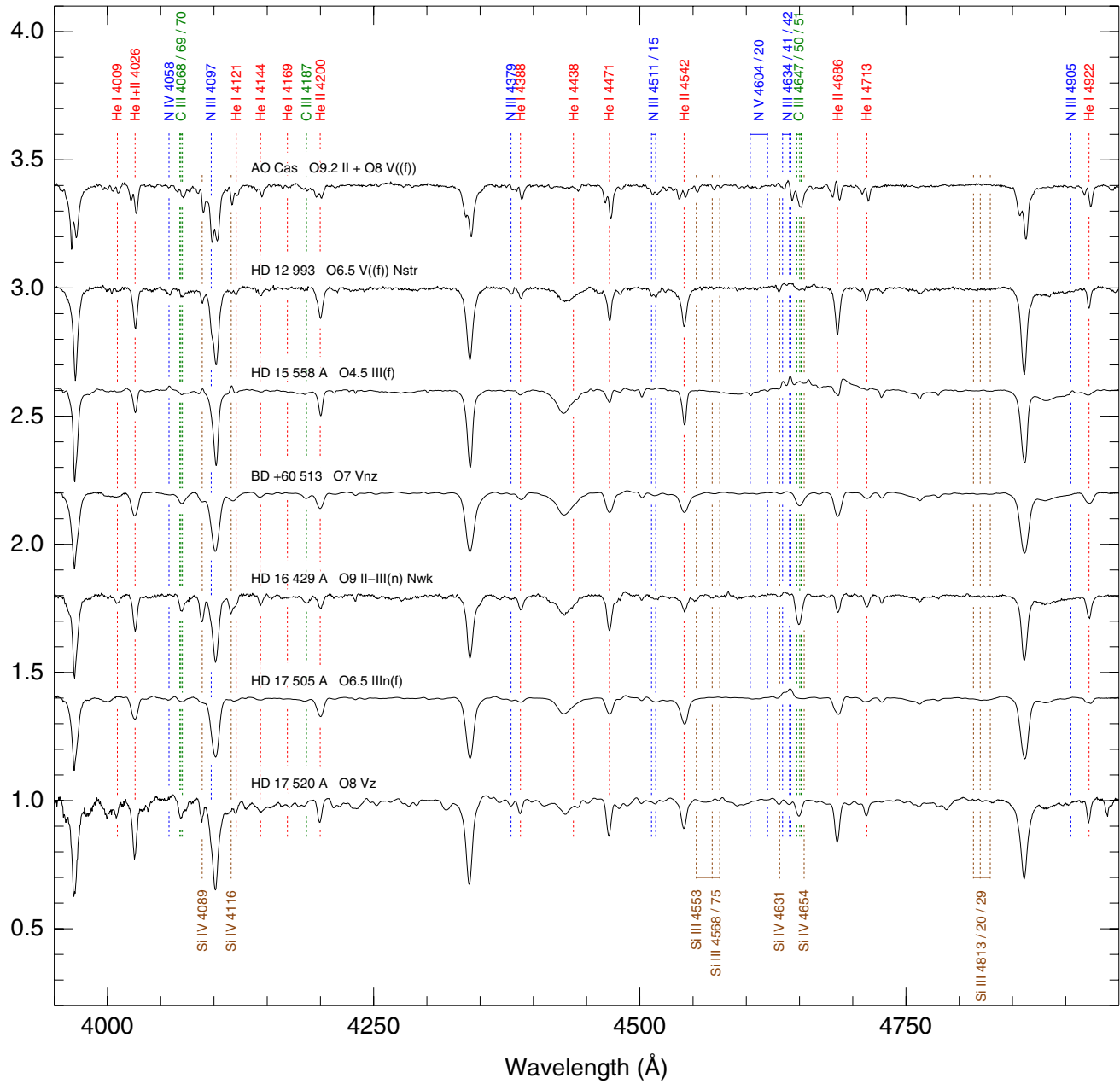


Figure 2. Spectrograms for the northern sample (O9.2 stars not included). The targets are sorted by Right Ascension with the exception of NGC 1624-2, whose two spectrograms (for different epochs with dates in YYMMDD) are shown last.

(A color version of this figure is available in the online journal.)

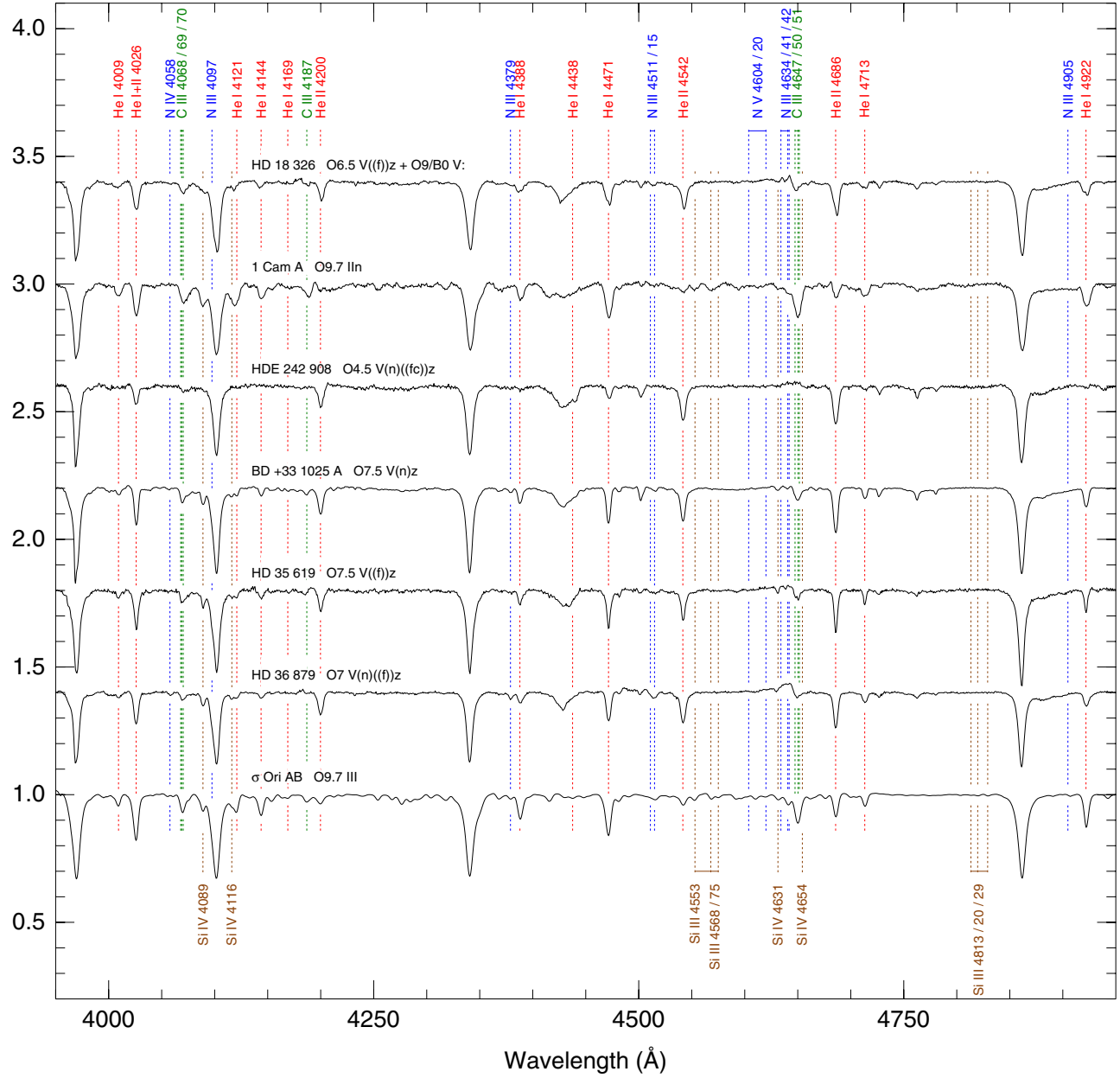


Figure 2. (Continued)

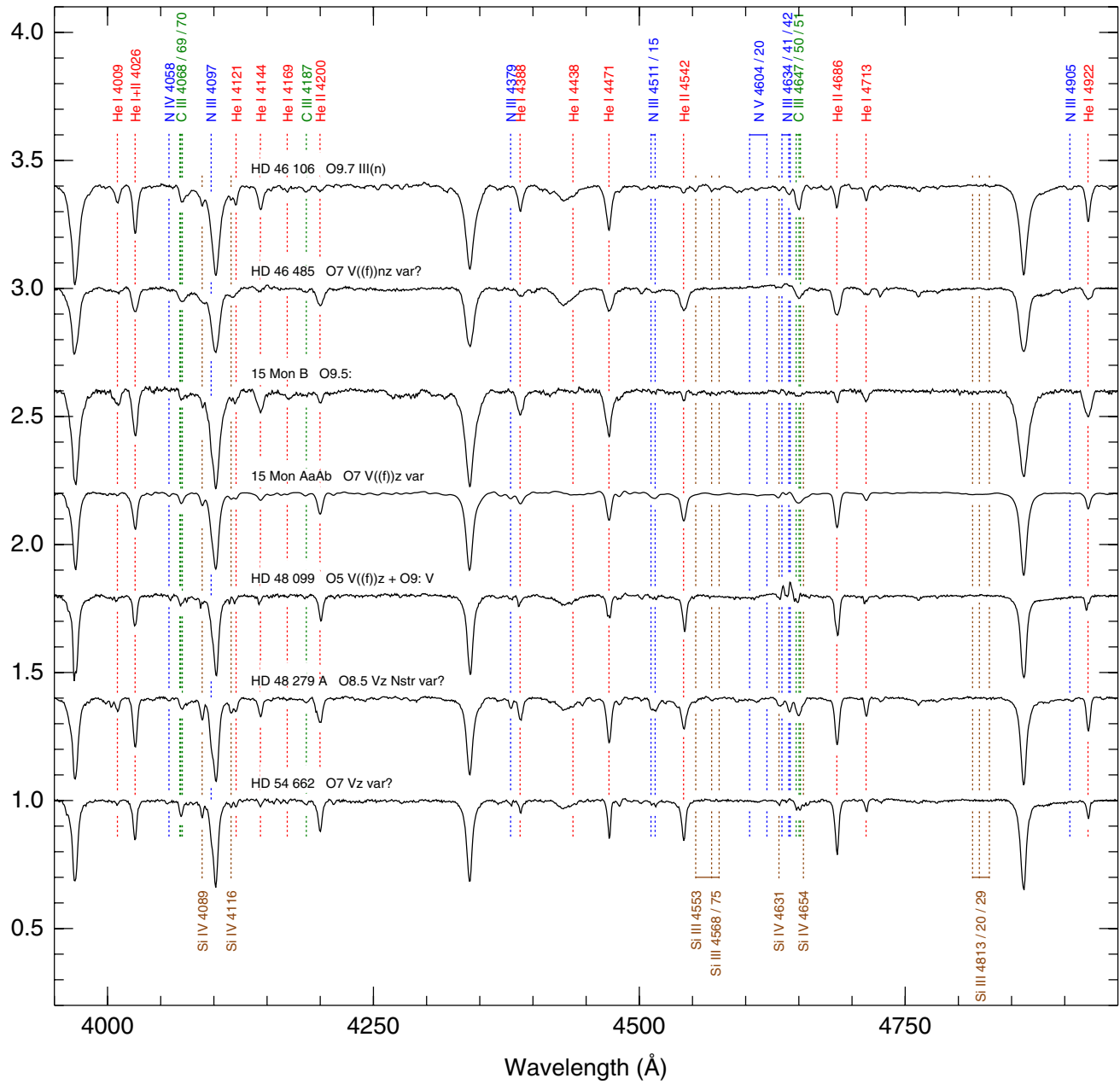


Figure 2. (Continued)

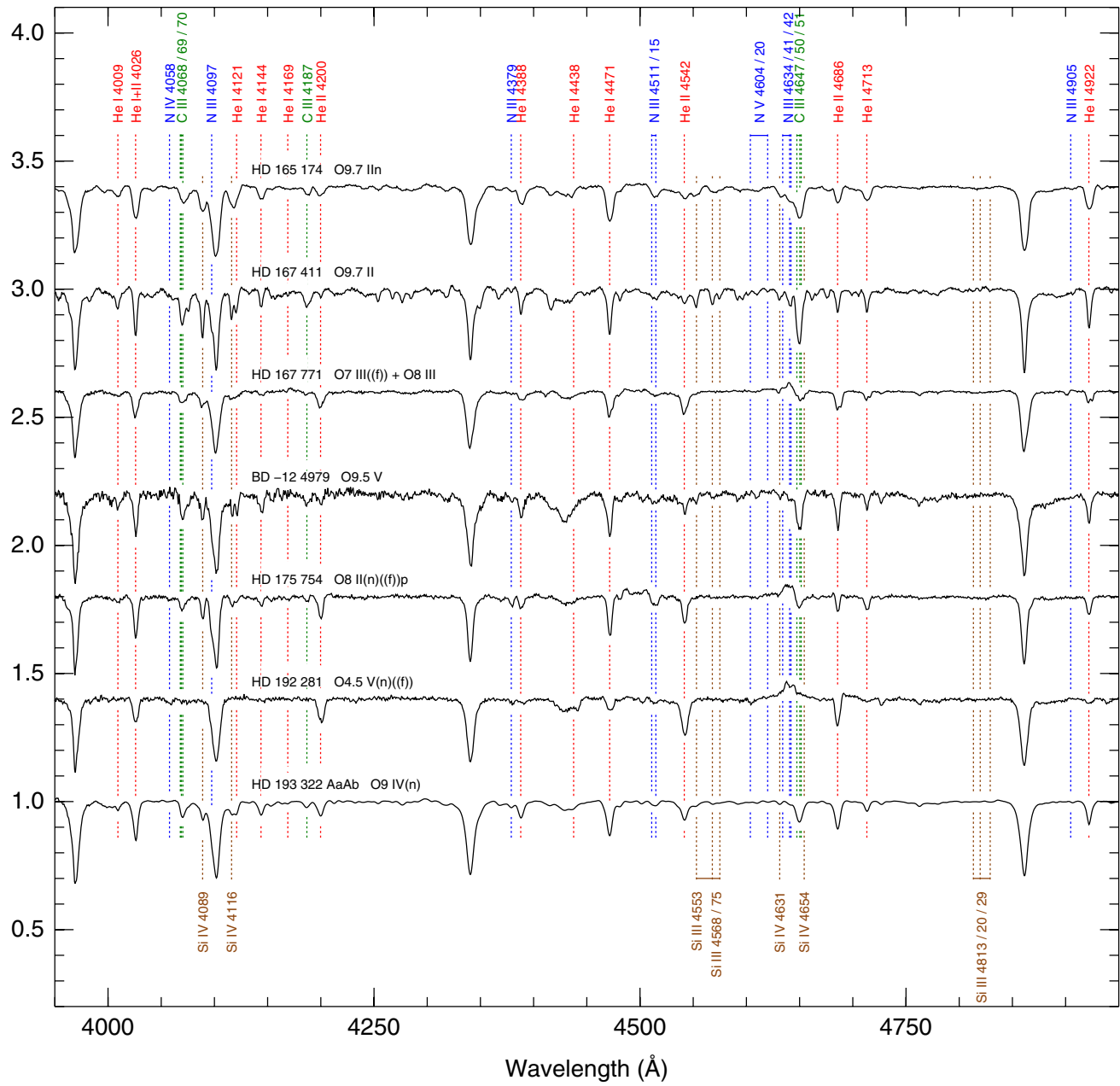


Figure 2. (Continued)

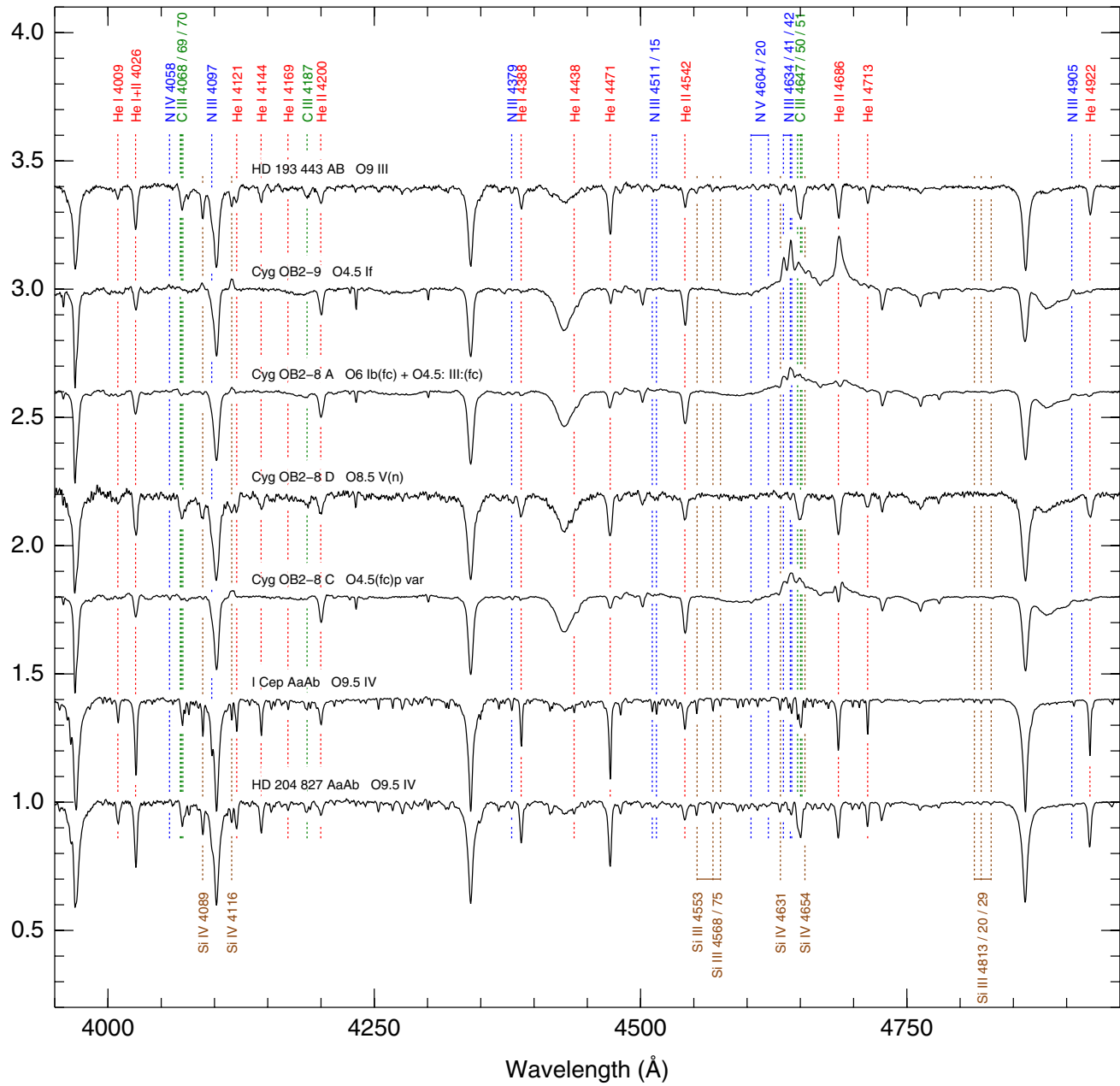


Figure 2. (Continued)

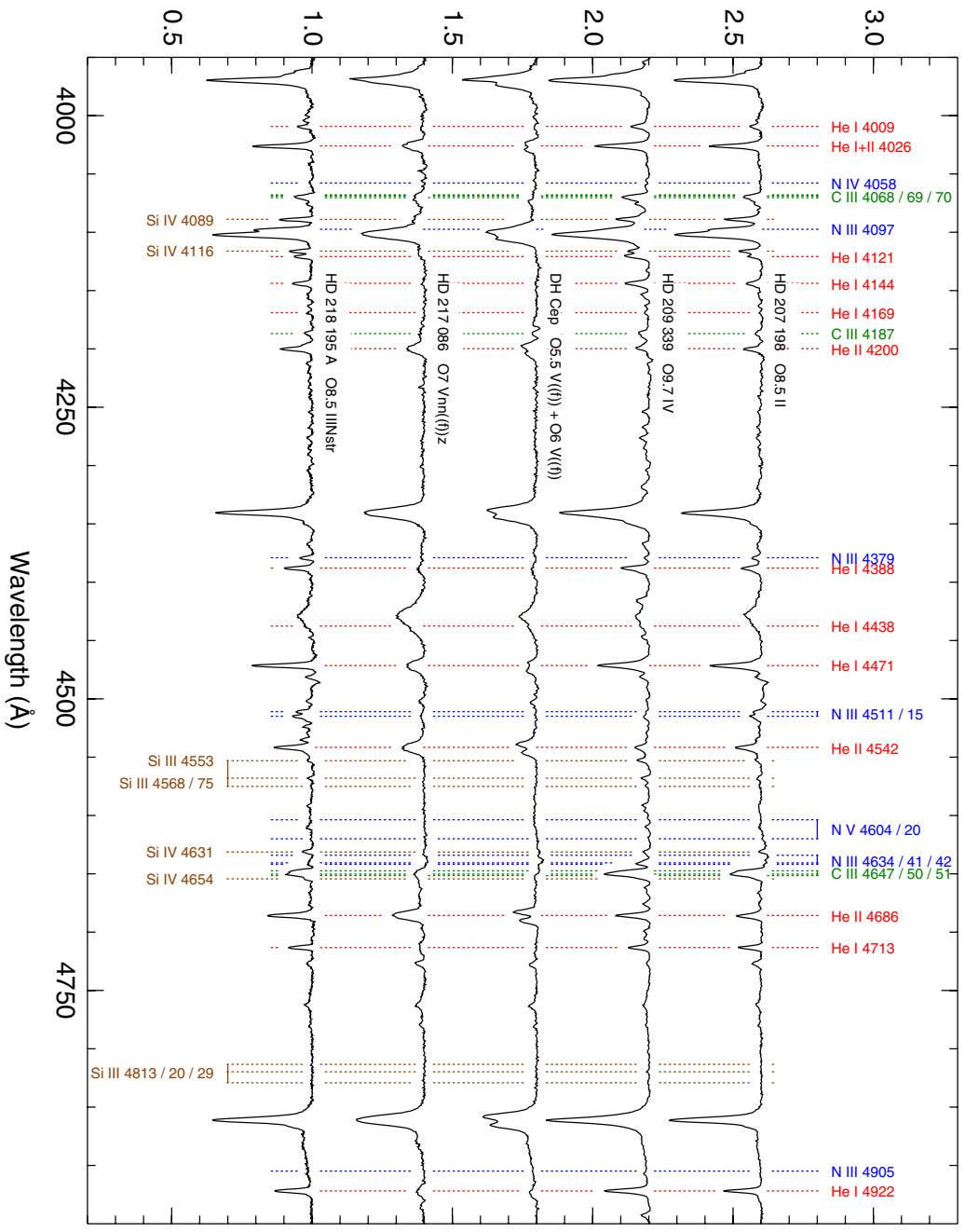


Figure 2. (Continued)

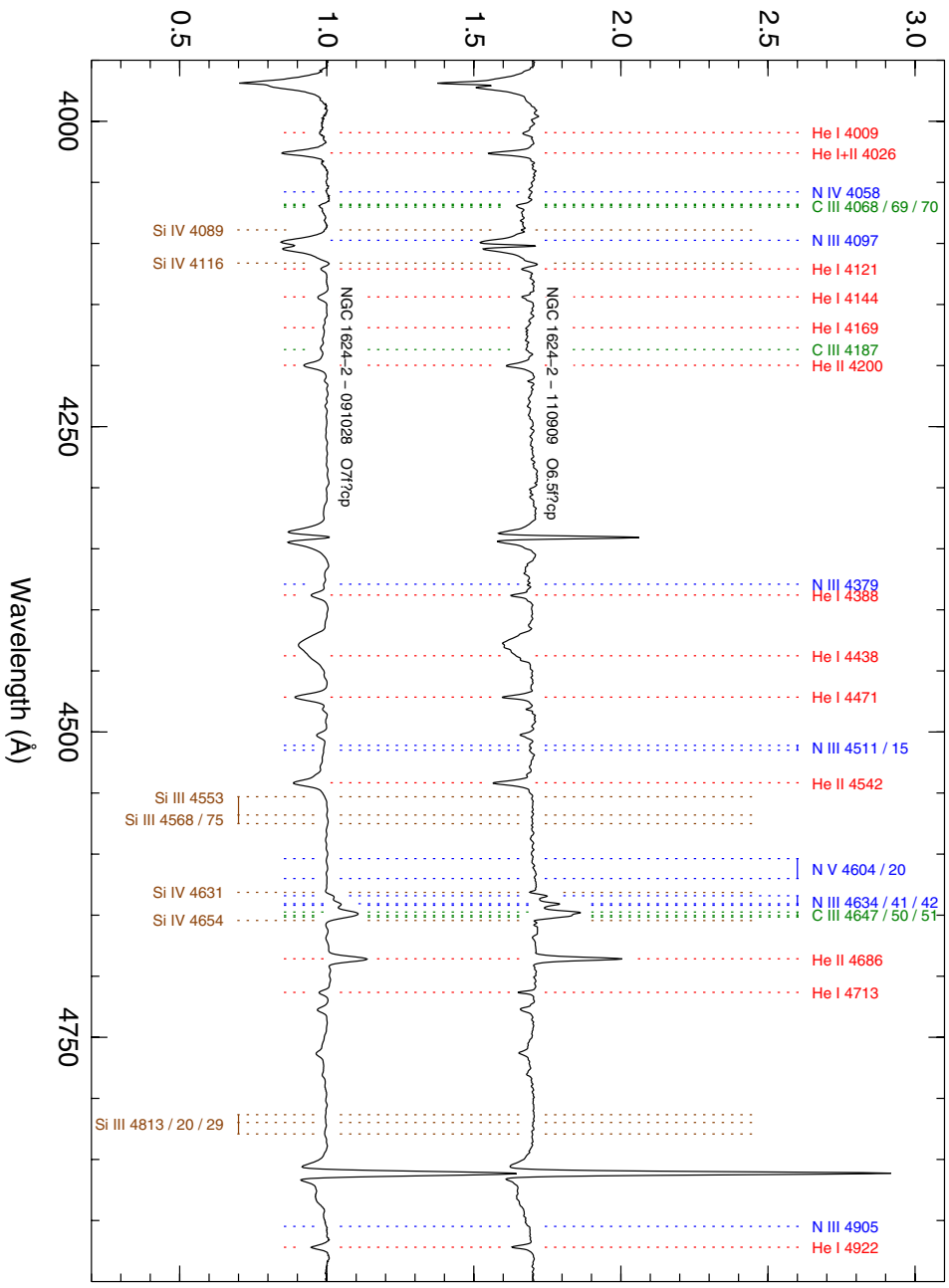


Figure 2. (Continued)

in preparation). We were unable to detect double lines in our spectra so the spectral classification of O7 Vz var? refers to the combined spectrum. In [Paper I](#) an ((f)) suffix was added but we have now determined the N III $\lambda\lambda 4634$ -40-42 emission is not detected in our spectra.

HD 165 174 = V986 Oph. Morgan et al. (1955) classified this star as B0.5 III var and Lesh (1968) as B0 III_n; we are unaware of any classifications as an O star. Therefore, it was not included in Maíz Apellániz et al. (2004) but we observed it in GOSSS as we are doing with all bright stars classified as B0 to check whether they are of late-O type or not. This is one case where we indeed obtain a classification of O9.7 II_n with the definition of O9.7 of Table 3.

HD 167 411. Morris (1961) classified this star as B0 II_k and we are unaware of any classifications as an O star. Under the same circumstances as for HD 165 174, we observed it and obtained a classification of O9.7 II.

HD 167 771. The (f) suffix of the primary component of this SB2 system with a period of 3.97333 days (Pourbaix et al. 2004) was changed to ((f)) in GOSSS-DR1.1, according to the rules in Table 2.

HD 175 754. The (f) suffix was changed to ((f)) in GOSSS-DR1.1 to follow the criteria in Table 2. It has very weak but definite He II $\lambda 4686$ emission wings, making it an Onfp star.

BD -12 4979. This star was classified as O9.5 III-IV in [Paper I](#) and is now an O9.5 V.

HD 192 281. The suffix was changed to (n)((f)) in GOSSS-DR1.1. We suspect that the broadening is not caused by rotation but instead by binarity, as the position of the N III $\lambda\lambda 4634$ -40-42 emission lines appears shifted.

HD 193 322 AaAb. HD 193 322 is a highly complex system that includes at least six stars of spectral types O and B. Aa and Ab are separated by 0'05-0'07 and follow a 35 a orbit (ten Brummelaar et al. 2011; Maíz Apellániz 2010). ten Brummelaar et al. (2011) have used multiple-epoch high-resolution spectroscopy to analyze the AaAb system, determining a spectral type of O9 V_{nn} for Aa and that Ab is an SB2 system with spectral types of O8.5 III and B2.5: V. HD 193 322 AaAb remains unresolved in velocity in GOSSS data.

HD 193 443 AB. Mahy et al. (2013) studied this SB2 system with high-resolution spectroscopy and determined a period of 7.467 days, with spectral types of O9 III/I and O9.5 V/III, respectively. Note, however that the WDS indicates that this system is a visual binary with a separation of 0'1-0'2 and a Δm of 0.3, i.e., there has to be at least a third star in the Mahy et al. (2013) aperture with a much longer period (hence, the designation AB). We have unpublished Lucky Imaging data of HD 193 443 that confirm the approximate separation and Δm in the WDS. HD 193 443 AB remains unresolved in velocity in GOSSS data.

Cyg OB2-9 = LS III +41 36 = Schulte 9 = [MT91] 431. Nazé et al. (2012b) studied this SB2 system with high-resolution spectroscopy and obtained a period of 2.35 a and spectral types of O5-5.5 I for the primary and O3-4 III for the secondary. Cyg OB2-9 remains unresolved in velocity in GOSSS data, which is unsurprising given the short amount of time during the long orbit where velocity differences are large. The target has C III $\lambda 4650$ in emission but is not strong enough to warrant a c suffix.

Cyg OB2-8 A = BD +40 4227 = Schulte 8 A = [MT91] 465. We have obtained several more spectra of this target and we have been able to separate the two components of this SB2

(see De Becker et al. 2004). The spectral type for the primary agrees with the previous result but our result for the secondary is somewhat earlier.

Cyg OB2-8 D = Schulte 8 D = [MT91] 473. A new observation with better S/N has led us to revise the spectral type of this system from O9 to O8.5.

Cyg OB2-8 C = LS III +41 38 = Schulte 8 C = [MT91] 483. Using several more spectra, the He II $\lambda 4686$ profile has been found to be variable and to display the characteristic profile of an Onfp object on occasion. By analogy with similar systems, it is possible that there is a companion in this system.

I Cep AaAb = HD 202 214 AaAb. This system was classified as B0 V by Morgan et al. (1953b) and by several more authors¹³; hence, it was not included in Maíz Apellániz et al. (2004). Nevertheless, Mannino & Humblet (1955) dissented and indicated that it was an O9. The WDS gives three components (Aa, Ab, and B) within 1" and with small values of Δm . We initially observed this system and attempted to spatially resolve AaAb from B (separation of 1'0, and Δm of 0.68 with respect to the combined AaAb system, values confirmed from unpublished Lucky Imaging data) but we were unsuccessful since the observing conditions were not optimal. Hence, the spectral type in GOSSS-DR1.0 (Sota et al. 2013), O9.5 IV, corresponds to the integrated spectrum from Aa+Ab+B. In a later observation with better seeing we were able to spatially resolve AaAb from B (but not Aa from Ab, since they are less than 0'1 apart). AaAb is indeed an O9.5 IV while B is an early-B star.

HD 204 827 AaAb. This system was classified as O9.7 III in [Paper I](#) but the S/N was relatively low compared to the GOSSS typical values. We re-observed the star and obtained a revised spectral type of O9.5 IV. This change took place after GOSSS-DR1.0. The WDS gives a separation of 0'1 and a $\Delta m = 1.2$ for the Aa + Ab system, so the spectral type is likely a composite.

HD 207 198. The spectral type changed from O9 II to O8.5 II in GOSSS-DR1.1 as a consequence of the redefinition of the O9-O9.5 spectral subtypes associated with the introduction of the O9.2 subtype.

HD 209 339. This star was classified as O9 IV by Morgan et al. (1953b) but was accidentally skipped by Maíz Apellániz et al. (2004) even though it is brighter than $B = 8$. According to the WDS, it has a nearby companion with a separation of 0'8 and a Δm of 3.3 (unpublished Lucky Imaging data suggest that the companion may have moved slightly farther away since the last observation recorded in the WDS), so the companion should not influence the combined spectral type. We obtain O9.7 IV with the new definition of the O9.7 subtype.

HD Cep = HD 215 835. We obtained a new GOSSS epoch for this SB2 system with a 2.1109 day period (Pourbaix et al. 2004) that allowed for a better separation in velocity of the two components. Our spectral types agree with those of Burkholder et al. (1997) but our luminosity classes are V instead of III.

HD 217 086. The z suffix was added in GOSSS-DR1.1.

HD 218 195 A. An Nstr suffix was added in GOSSS-DR1.1. Note that the B component is spatially resolved in GOSSS as an early-B star (see [Paper I](#)).

3.3. The New Southern Sample

In presenting the new southern sample, we follow the same strategy of [Paper I](#) of introducing first the members of the

¹³ Note that HD 202 124 is also a late O star (see [Paper I](#)), so it would not be unthinkable that some confusion has existed between the two.

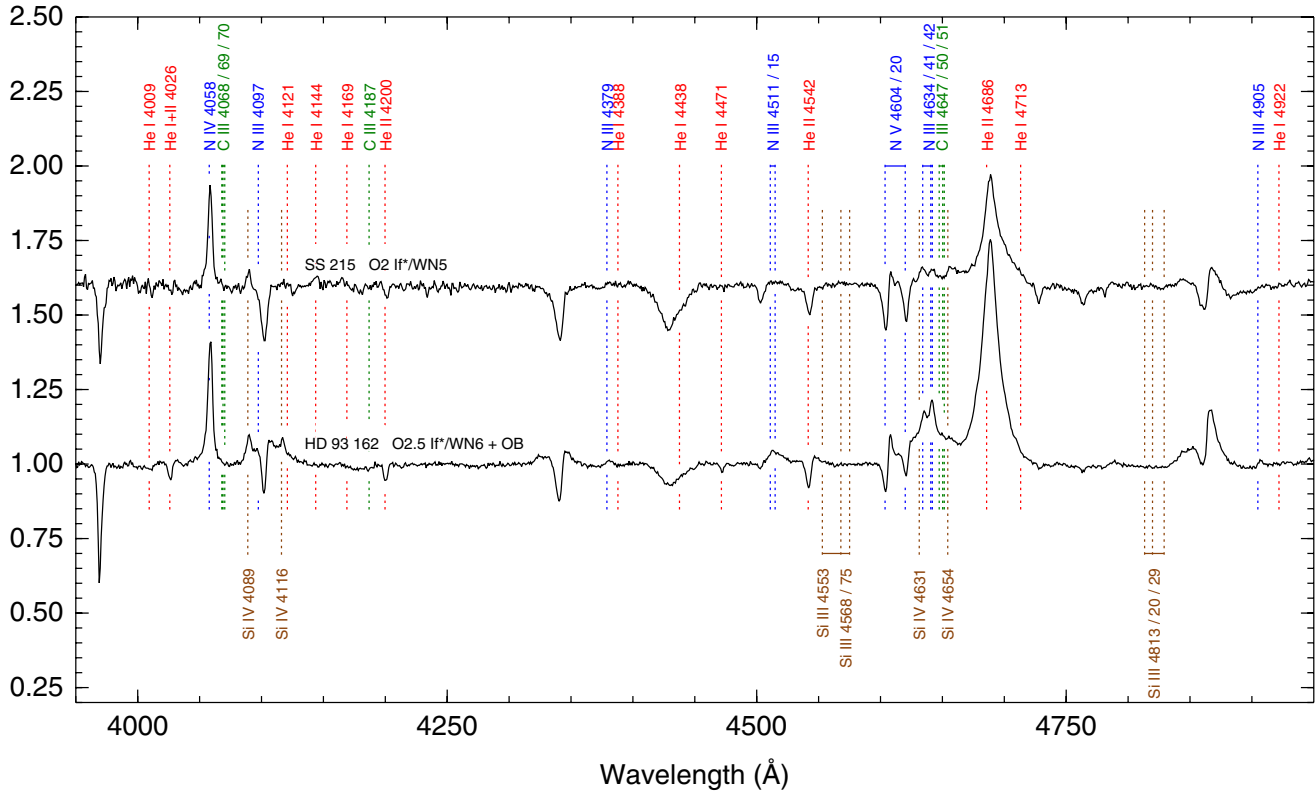


Figure 3. Spectrograms for the early Of/WN stars. The targets are sorted by Right Ascension.
(A color version of this figure is available in the online journal.)

peculiar categories and then those of the normal sample. The reader is referred to [Paper I](#) for the definitions of most of the peculiar categories. There are two new categories in this paper with respect to Sota et al. (2011), the early Of/WN stars and the O Iafpe stars (which are usually grouped together under the name of “slash” stars), since none of them were present in the sample of [Paper I](#). Note that SB2 stars that belong to another peculiar category are listed in the corresponding non-SB2 subsection and that O9.2 stars have already been discussed.

3.3.1. Early Of/WN stars

Walborn (1971) was the first to notice a smooth morphological transition between the earliest O supergiants and the H-rich, high-luminosity, narrow-lined WN sequence. Walborn (1982a) introduced the hybrid O3 If*/WN6 classification for Sk −67 22, the first well defined transition object. Such objects are currently called early Of/WN stars or “hot slash” stars (see below for the “cool slash” category) and are thought to be very massive, core hydrogen-burning stars in an intermediate evolutionary, or at least wind-development, phase. Crowther & Walborn (2011) established the H β profile as the morphological criterion to distinguish among the three related categories: it is in absorption in O2-3.5 If* stars, it has a P-Cygni profile in O2-3.5 If*/WN5-7 stars (“hot slash” stars), and it is in emission in WN5-7 objects. Note that some early “slash” stars have WR numbers for historical reasons though they are no longer considered proper WR stars from the morphological viewpoint. Spectrograms are shown in Figure 3.

SS 215 = WR 20aa. This O2 If*/WN5 was discovered by Roman-Lopes et al. (2011) and could have been ejected from

the massive young Galactic cluster Westerlund 2. This star was not included in Maíz Apellániz et al. (2004) due to its dimness.

HD 93 162 = WR 25. This system was included in the “hot slash” category by Crowther & Walborn (2011) on the basis of its P-Cygni H β profile. Gamen et al. (2006) presented the first SB1 orbit and indicated that some of the absorption lines varied in anti-phase, hence indicating they originated in the secondary. The secondary was clearly detected by Gamen et al. (2008). This object was not included in Maíz Apellániz et al. (2004) since at that time it was thought to be a WR star instead of an early Of/WN. See Figure 12 for a chart (Trumpler 16 field) and Figure 16 for an ACS/HRC image. In the existing ACS/HRC images we detected a previously unpublished¹⁴ visual companion. It has a separation of 790 mas, a position angle of 353°, and a ΔV of 5.8 mag. The magnitude and colors are consistent with an $\sim 8 M_{\odot}$ star.

3.3.2. O Iafpe Stars

A second, cooler flavor of “slash” stars was introduced by Walborn (1982b) and Bohannan & Walborn (1989), the members of which will be referred to here as *either* O Iafpe or WNVL (for Very Late) stars, depending upon whether or not distinct absorption lines are present in their spectra, respectively (see also Walborn & Fitzpatrick 2000). These spectra can be distinguished from their hotter counterparts by the absence of the N IV $\lambda 4058$ emission line used to classify the hot spectra, while in contrast the cool spectra may contain N II $\lambda 3995$

¹⁴ It was presented in JD 13 of the IAU General Assembly in 2009 but did not appear in any proceedings.

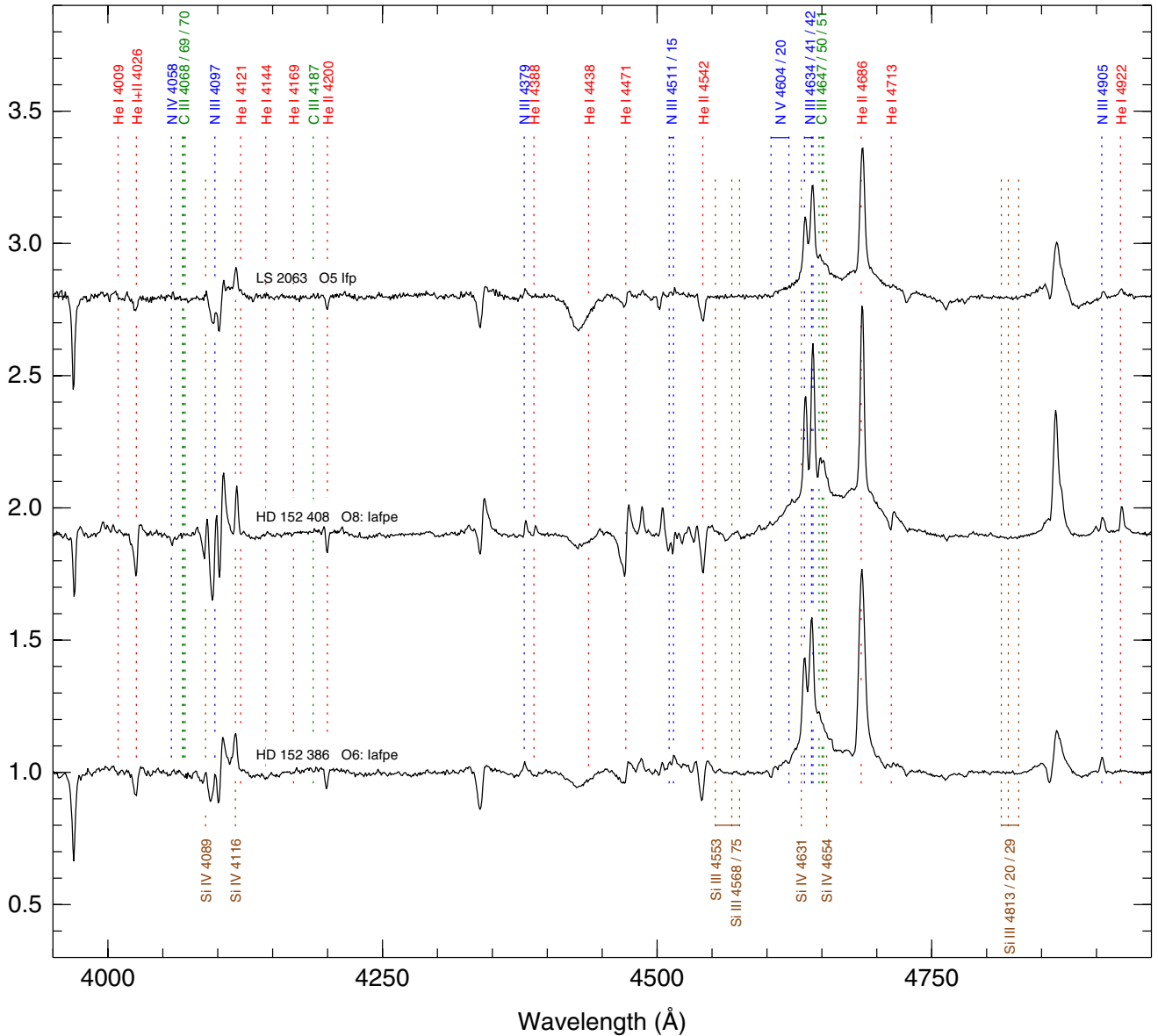


Figure 4. Spectrograms for the O Iafpe stars. The targets are sorted by Right Ascension.
(A color version of this figure is available in the online journal.)

emission instead. The composite late Of/WN or “cool slash” nomenclature will no longer be used in detailed classifications for two important reasons¹⁵: (1) we include two relatively early-type stars in the O Iafpe category here; and (2) a significant difference from the early Of/WN category is that the cooler objects are *not* an intermediate category between Of and WN stars, but rather stars that can be described alternatively as one or the other. Indeed, this sometimes implicit distinction between the two “slash” categories has caused some confusion in the literature. Here we shall follow the criterion of classifying a star as O Iafpe when He I $\lambda 4471$ has a P Cygni profile (which usually introduces some uncertainty in the spectral subclass, as

indicated by “:”); if that line is in pure absorption, the spectrum is a normal Of type. The blended composite morphology of the H δ region and generally stronger emission lines also distinguish the O Iafpe spectra from normal Of. Spectrograms are shown in Figure 4. There are no WNVL stars in the present sample according to our criteria; however, note that Crowther (2007) includes some of our O Iafpe objects in his WN9-10 classes (see also Walborn 2009a).

LS 2063. This object was described by Walborn & Fitzpatrick (2000) and is an extreme supergiant, with strong He II $\lambda 4686$ and N III $\lambda\lambda 4634-40-42$ emission, as well as H β showing a P-Cygni profile. The OWN spectra indicate variability. The suffix was changed in GOSSS-DR1.1.

HD 152 408 = WR 79a. Walborn (1972) classified this object as O8 Iafpe.

HD 152 386 = WR 79b. Walborn (1973b) classified this object as O6: Iafpe. The WDS gives a companion with a separation of 0.6 but without a value for Δm .

¹⁵ Nevertheless, the name “Ofpe/WN9” will continue to be useful to refer to that category as originally discovered in the Large Magellanic Cloud, although it does not represent a detailed classification of individual spectra. One member of that category, Radcliffe 127, has subsequently undergone a classical LBV outburst (Walborn et al. 2008 and references therein).

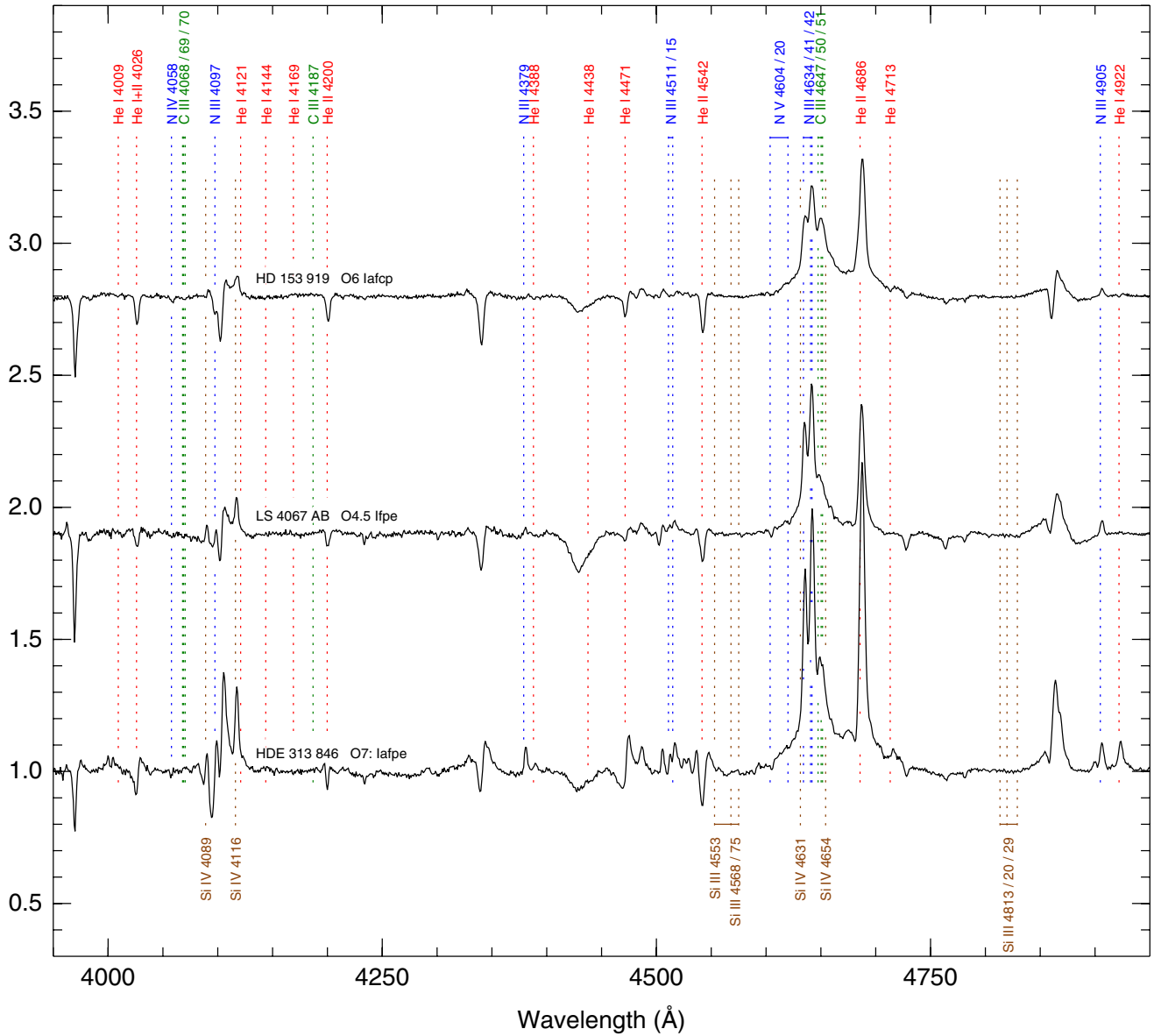


Figure 4. (Continued)

HD 153 919 = V884 Sco. This system is an SB1 with a period of 3.41 days and is the optical counterpart of the X-ray binary 4U 1700–37 (Hutchings et al. 1973; Anay et al. 2001; Clark et al. 2002; Hammerschlag-Hensberge et al. 2003).

LS 4067 AB = HM 1–2 AB = C1715–387–2 AB. This object is the earliest member of the OIafpe category. Its spectral type was changed from O4 to O4.5 in GOSSS-DR1.1. Mason et al. (2009) finds a companion with separation of $1''.3$ and a Δm of 1.2 mag that we were unable to spatially resolve. See Figure 12 for a chart (Havlen–Moffat 1 field).

HDE 313 846 = WR 108. Walborn (1982c) classified this object as O7: Iafpe.

3.3.3. Ofc Stars

The Ofc category was introduced by Walborn et al. (2010b) and amplified by Sota et al. (2011) in qualitative terms, on the basis of the ratio of peak intensities in C III $\lambda 4650$ to N III $\lambda 4634$, albeit without an explicit specification of the boundary between

definite and marginal cases. Also, that definition is complicated by the occurrence of broad emission pedestals underlying the narrow emission lines, especially in the supergiants. To improve this situation, here we have measured the narrow emission-line peaks *relative to the pedestals when they exist* in both Ofc and marginal cases; and a value of the ratio of 1.0 has been adopted as the lower boundary for the Ofc classification. As a result, some prior classifications in terms of this parameter have been revised. In the future, EWs will be preferable to peak intensities to define the phenomenon, to avoid resolution effects (C III $\lambda 4650$ is a blend barely resolved in the GOSSS data), analogously to what has been done for the Vz category here.

Spectrograms are shown in Figure 5. See also Section 3.2.

CPD –47 2963 = ALS 1216 = CD –47 4551. Walborn (1982c) classified this object as O4 III(f) but in GOSSS it is clearly a slightly later supergiant, as already shown in Walborn et al. (2010b). Our classification as O5 Ifc agrees with that of O5 If by Garrison et al. (1977). One of us (N.R.W.) checked

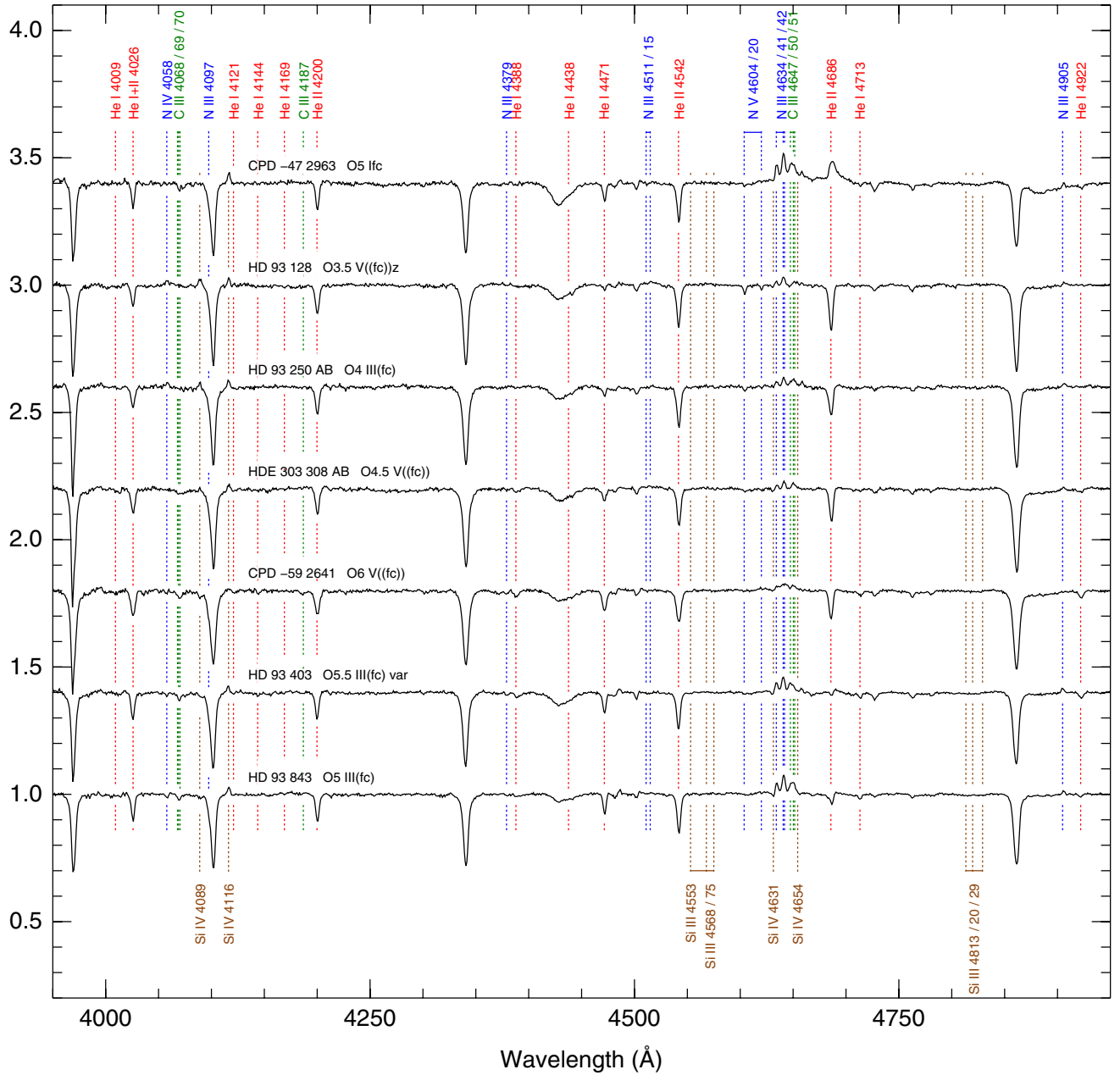


Figure 5. Spectrograms for Ofc stars. The targets are sorted by Right Ascension.
(A color version of this figure is available in the online journal.)

the original plate of the Walborn (1982c) observation, taken on 1974 November 25, and confirmed the presence of weak emission in the 4640–4650 Å region and for He II λ 4686, indicating that the spectrum has not changed in a major way in the last four decades. There are no appreciable differences between the two epochs observed with GOSSS but in OWN data a radial-velocity variation is apparent with a most likely period of 59 days and a low semi-amplitude K of 9.4 km s^{-1} (an alternative classification as an O(n)fcp star is also suggested by the variable profile of He II λ 4686 in the OWN data). The variability could be caused by a binary companion (colliding wind region) or by the existence of a magnetic field (something not entirely surprising for a star with both C III λ 4650 and

He II λ 4686 emission, see Section 3.3.6). The binary hypothesis is supported by the detection of non-thermal radio emission from the system (Benaglia et al. 2001; De Becker & Rauq 2013).

HD 93 250 AB. Rauw et al. (2009) could not find velocity variations in this system but Sana et al. (2011b) used VLTI to spatially resolve it into two stars separated by 1.5 mas with a Δm of 0.2 (such separation is unresolvable by GOSSS by more than two orders of magnitude). The (fc) suffix was missing in the GOSSS-DR1.0 spectral classification of this O4 III system. No companions are seen in the ACS/HRC images. The system is a colliding-wind binary (De Becker & Rauq 2013).

HDE 303 308 AB. Nelan et al. (2004) spatially resolved this system with *HST*/FGS to discover a pair with a separation

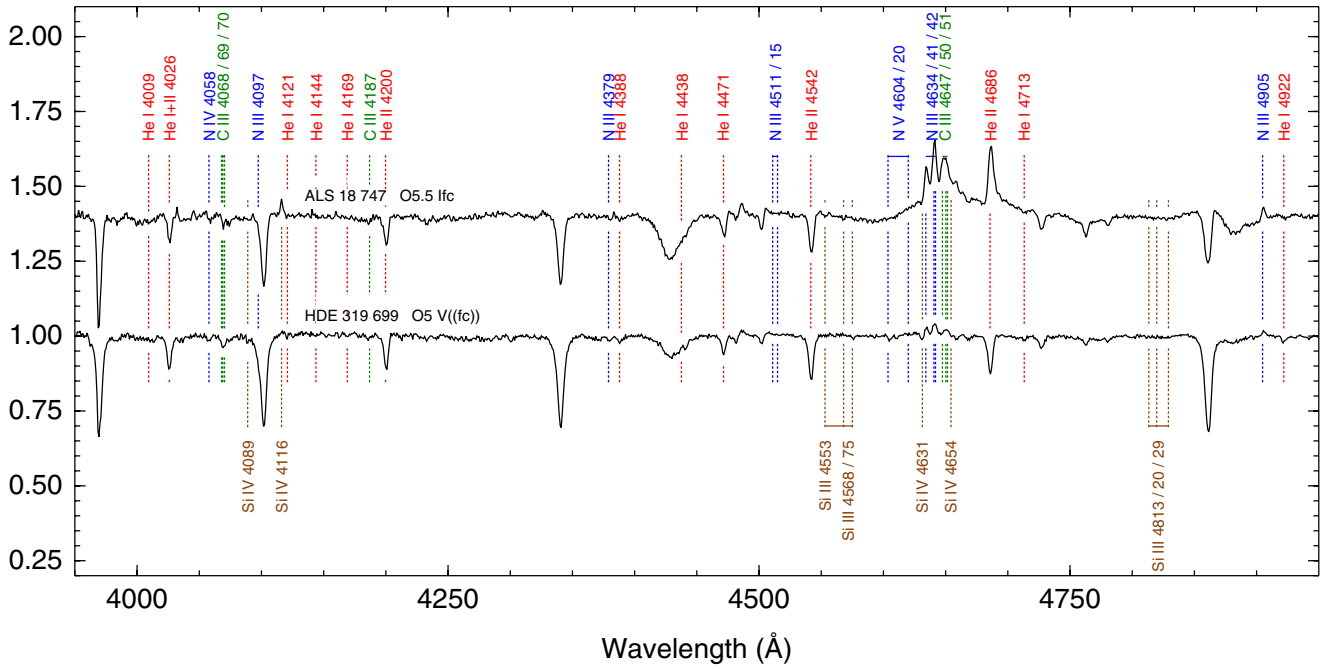


Figure 5. (Continued)

of 15 mas and a Δm of 1.0 mag (obviously unresolved with GOSSS). See Figure 12 for a chart (Trumpler 16 field).

CPD -59 2641 = Trumpler 16-112. This object shows an O6 V((fc)) spectrum in the GOSSS data. Rauw et al. (2009) used high-resolution spectroscopy to derive spectral types for this SB2 system of O5.5-6 V((f+?p)) and B2 V-III. Their spectral types and luminosity classes are compatible with that of our combined spectrum, which does not show double lines. In order to check whether the primary belongs to the Of?p category we obtained spectra in five different epochs between 2008 and 2013 (once a year except for 2009). None of the five spectra show He II $\lambda 4686$ in emission and C III $\lambda 4650$ appears to be constant. Therefore, we conclude that this star is an Ofc star (note that Rauw et al. 2009 appeared before the definition of Ofc in Walborn et al. 2010b) and amend the high-resolution spectral types to O5.5-6 V((fc)) + B2 V-III. See Figure 12 for a chart (Trumpler 16 field).

HD 93 403. Rauw et al. (2000) classified this SB2 system as O5.5 I + O7 V. We observed it three times with GOSSS and we obtained a spectral type of O5.5. We do not see double lines but He II $\lambda 4686$ is variable, going from a P-Cygni profile to a nearly neutral condition, as a result of the SB2 orbit. Therefore, we settled for a III luminosity class, which is consistent with the combination of a dwarf and a supergiant. The spectrum shows C III $\lambda 4650$ greater than N III $\lambda 4634$ in emission; hence, the (fc) suffix. The GOSSS-DR1.1 classification differs from that of GOSSS-DR1.0.

HD 93 843. The (fc) suffix was missing in the GOSSS-DR1.0 spectral classification of this O5 III system. This system appears to be variable in OWN data and was already reported as such by Walborn (1973b); it could be an SB1.

ALS 18 747 = HM 1-6 = C1715-387-6. This star was not included in Maíz Apellániz et al. (2004) due to its dimness (Havlen & Moffat 1977). See Figure 12 for a chart (Havlen-Moffat 1 field).

HDE 319 699. The ((fc)) suffix was missing in the GOSSS-DR1.0 spectral classification of this O5 V system. A preliminary

analysis of the OWN data indicates that this system is an SB1 with a period of 12.62 days.

3.3.4. ON/OC stars

Spectrograms are shown in Figure 6. See Sections 3.1 and 3.2 for additional members of this category.

HD 89 137. This object is a nitrogen-rich rapid rotator (Walborn et al. 2011). According to Levato et al. (1988), it shows velocity variability that could be caused by a companion.

HD 91 651. This system was found to be a likely SB2 by Levato et al. (1988) and is also a nitrogen-rich rapid rotator (Walborn et al. 2011). The OWN data clearly show that is an SB2 and possibly an SB3. We do not see double lines in the GOSSS data. The luminosity class was changed in GOSSS-DR1.1.

HD 102 415. This star is a nitrogen-rich very rapid rotator (Walborn et al. 2011). The OWN data also indicate variability; it could be an SB2. The luminosity class was changed in GOSSS-DR1.1.

HD 104 565. This is a nitrogen-deficient star (Walborn 1976). The luminosity class was changed in GOSSS-DR1.1.

GS Mus = HD 105 056. This nitrogen-rich star is variable (Levato et al. 1988) and could be a low-mass (PAGB?) object (Walborn et al. 2011). The OWN data show variability with a period of 0.71 days that could be due to the system being an SB1, pulsations, or rotating spots.

HD 117 490. This star is a nitrogen-rich very rapid rotator (Walborn et al. 2011). It could be a spectroscopic binary according to OWN data. The n index was changed in GOSSS-DR1.1.

HD 150 574. This system is a nitrogen-rich rapid rotator (Walborn et al. 2011). Levato et al. (1988) suggested that it is an SB2 but that has not been confirmed with OWN data. We do not see double lines in the GOSSS data.

HD 152 003. This is one of the original weakly nitrogen-deficient stars in Walborn (1976). The Nwk suffix was omitted

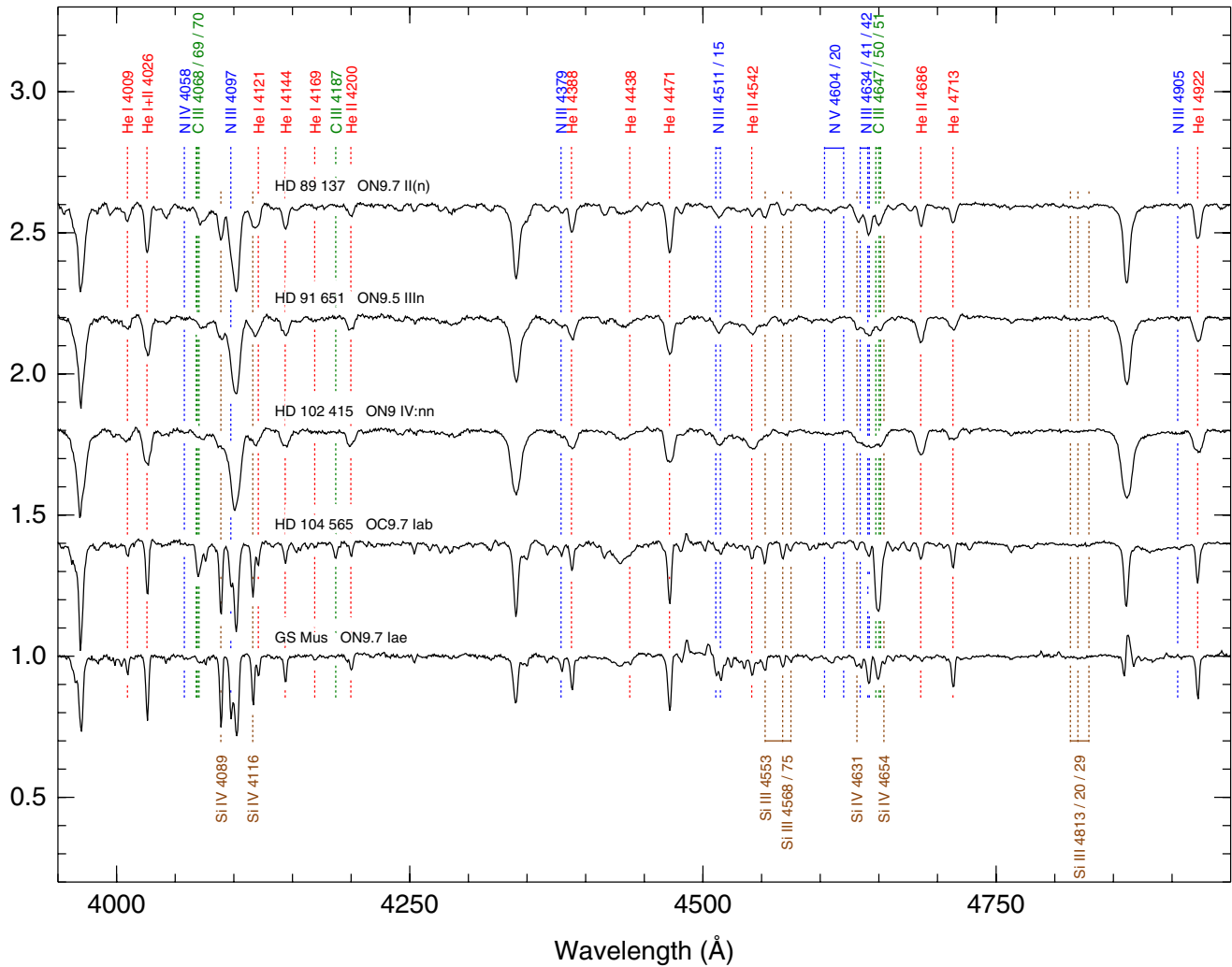


Figure 6. Spectrograms for the ON/OC stars. The targets are sorted by Right Ascension.
(A color version of this figure is available in the online journal.)

by mistake in GOSSS-DR1.0 and the spectral type there was O9.5 instead of O9.7.

HD 152 147. This is one of the original weakly nitrogen-deficient stars in Walborn (1976). The Nwk suffix was omitted by mistake in GOSSS-DR1.0. Williams et al. (2013) indicated that it is an SB1 with a period of 13.8194 days but a preliminary OWN analysis suggests that it is an SB2 with a different orbit.

HD 152 249. This nitrogen-deficient star (Walborn 1976) shows small velocity variations in OWN data. See Figure 12 for a chart (NGC 6231 field).

HD 154 811. Walborn (1973b) classified this star as OC9.7 Ia and here we reclassify it as OC9.7 Ib. The H α line is highly variable in OWN.

3.3.5. Onfp Stars

See Paper I for a description of this class. Spectrograms are shown in Figure 7.

ζ Pup = HD 66 811 = Naos. This is one of the two visually brightest O stars in the sky (the other being ζ Ori Aa), to the point that it presents a challenge to be observed with a 2–4 m telescope at this resolution (the minimum exposure time for our LCO spectra is 1 s) and requires a neutral density filter. The p qualifier was added in GOSSS-DR1.1 (but see Conti & Niemelä

1976 and Walborn et al. 2010a). The new *Hipparcos* calibration gives a revised distance of 335^{+12}_{-11} pc (Maíz Apellániz et al. 2008a).

LM Vel = HD 74 194. Barbá et al. (2006) detected variations in radial velocity and in H α that suggest that this system is an SB1 and the possible optical counterpart of the INTEGRAL hard X-ray source IGR J08408-4503. The (f) suffix was omitted by mistake in GOSSS-DR1.0.

HD 76 556. Walborn (1973b) classified this star as O5.5 Vn(f). Here we make slight adjustments to the spectral subtype, luminosity class, and rotation index and move it to the Onfp category on the basis of the weak He II λ 4686 emission wings revealed by the GOSSS data (some of these changes are also with respect to GOSSS-DR1.0).

HD 94 370 A. This star is a spectroscopic binary with a 2.8 day period according to OWN data. It is possibly an SB2, though the detection of the secondary star is marginal in the available data. It has a companion with a separation of 3".6 and a Δm of 1.8 mag (according to the WDS) which we were able to spatially resolve in our GOSSS spectra: it is an early-B star. The luminosity class was eliminated in GOSSS-DR1.1.

HD 96 670. Walborn (1972) classified this star as O8p. Here we classify it as O8.5(n)fp var, with a variable

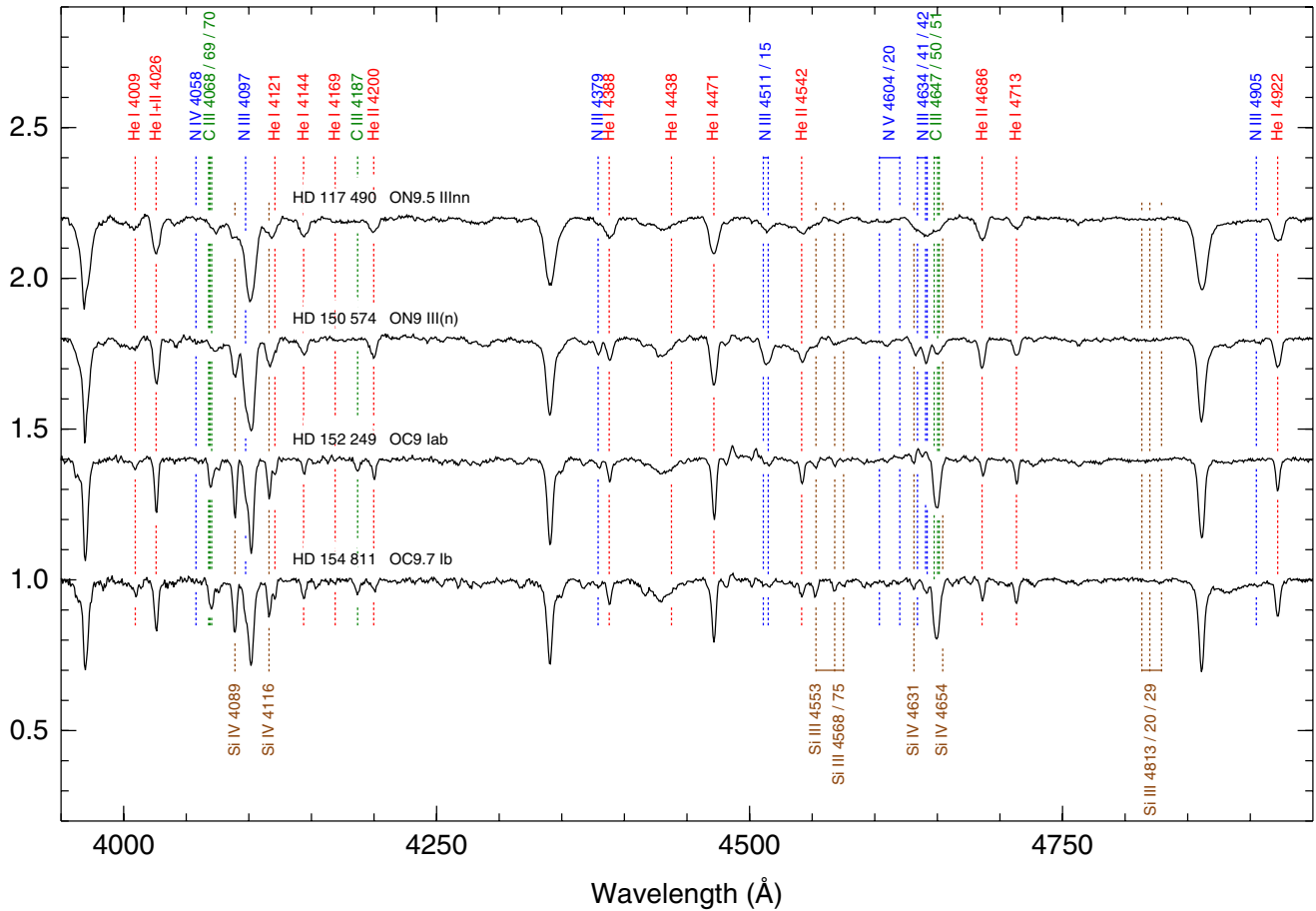


Figure 6. (Continued)

He II λ 4686 profile (this is a change from GOSSS-DR1.0). See Figure 7 for the two GOSSS spectra obtained. According to Stickland & Lloyd (2001) it is an SB1 with a 5.5296 day period.

HD 112 244. According to OWN data, this object is an SB2 with a 7.5 day period. The p suffix was added in GOSSS-DR1.1. We do not see double lines in the GOSSS data.

HD 117 797. This object is a new member of the Onfp category found by GOSSS; it is an SB2 according to OWN data, although we have not seen double lines in the GOSSS data. The classification was modified in GOSSS-DR1.1.

3.3.6. Of?p Stars

See Walborn et al. (2010b) for the characteristics of this class and Section 3.2 for another member of this category. Spectrograms are shown in Figure 8.

CPD -28 2561 = CD -28 5104. Walborn (1973b) and Garrison et al. (1977) reported this star to be a peculiar Of type of an undetermined nature. One of us (R.H.B.) discovered its Of?p nature, as reported in Walborn et al. (2010b). Figure 8 shows two GOSSS spectra taken in 2008 and 2012 that correspond to the “high” and “low” states, respectively (see G. A. Wade et al. (in preparation) for details).

HD 148 937. This star was one of the two original Of?p stars (Walborn 1972). It differs from the rest in its class in that it only shows small photometric changes on seven-day timescales as opposed to larger variations on longer timescales. The period was discovered through the variations in its H β

profile. A possible explanation is that the object is seen pole-on (Nazé et al. 2012c and references therein). It is also the only member of its class to be involved in an ejected, axially symmetric circumstellar nebula (NGC 6164-6165).

3.3.7. Oe Stars

Spectrograms are shown in Figure 9.

HD 93 190. This star in the Carina Nebula was not included in Maíz Apellániz et al. (2004).

HD 120 678. This Oe star experienced a shell-like event in 2008 (Gamen et al. 2012) that was detected with OWN and GOSSS data. Figure 9 shows three GOSSS spectra taken in 2008 May, 2009 July, and 2011 April that correspond to the early shell stage, recovery phase, and normal state, respectively.

HD 155 806 = V1075 Sco. This object has been historically considered an Oe star (see Negueruela et al. 2004 for its H α profile). In our blue-violet spectra, H β is partially filled but not enough to show an emission, hence the (e) suffix. The ((f))z suffix was introduced in GOSSS-DR1.1.

3.3.8. Double- and Triple-lined Spectroscopic Binaries

In this part of this subsection we include the double- (SB2) and triple- (SB3) lined spectroscopic binaries that do not belong to any of the other peculiar categories. More than for any other peculiar categories, membership here is determined by spectral resolution and time coverage, given the large ranges of velocity differences and periods existent among massive spectroscopic

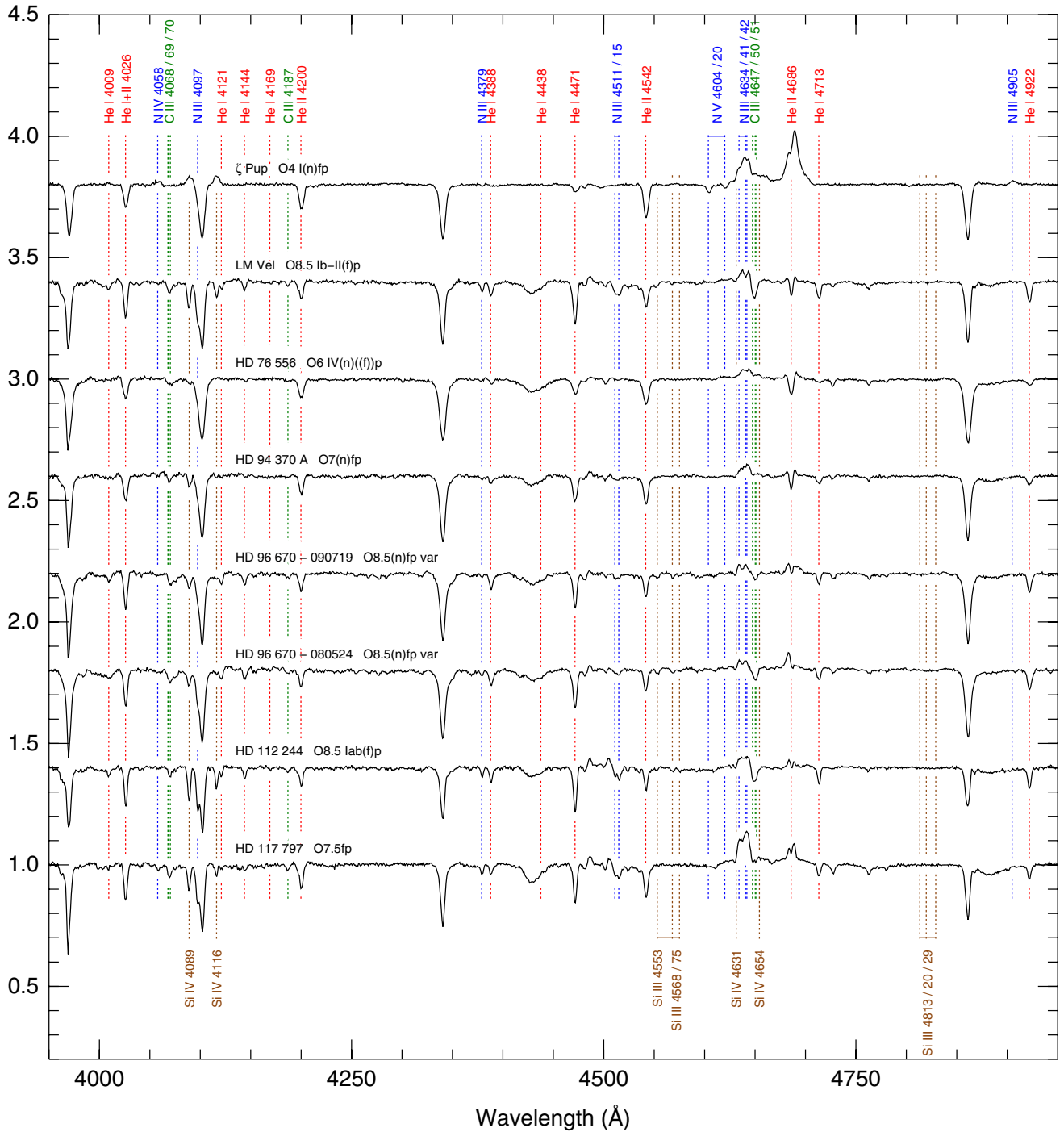


Figure 7. Spectrograms for the Onfp stars. The targets are sorted by Right Ascension. Two HD 96 670 epochs are shown (dates in YYMMDD).
(A color version of this figure is available in the online journal.)

binaries. Therefore, we have included in this category examples that have been identified as SB2s or SB3s by other authors (in most cases using high-resolution spectroscopy) but that are single lined in our spectra. In those cases, we point to the relevant reference. Our classifications were obtained with MGB varying seven input parameters: the spectral types, luminosity classes, and velocities of both the primary and secondary; and the flux fraction of the secondary. Spectrograms are shown in Figure 10.

29 Cma = HD 57 060 = *UW Cma*. We do not see double lines in the GOSSS data of this SB2 system with a 4.39349 day period (Pourbaix et al. 2004), except for He II λ 4686. However, we see clear variability in the emission lines among our four epochs, including for the peculiar H β profile (in absorption but with one or two emission peaks at the line edges). The new *Hipparcos* calibration gives a revised distance of 632^{+137}_{-96} pc (Maíz Apellániz et al. 2008a). The analysis of the light curve

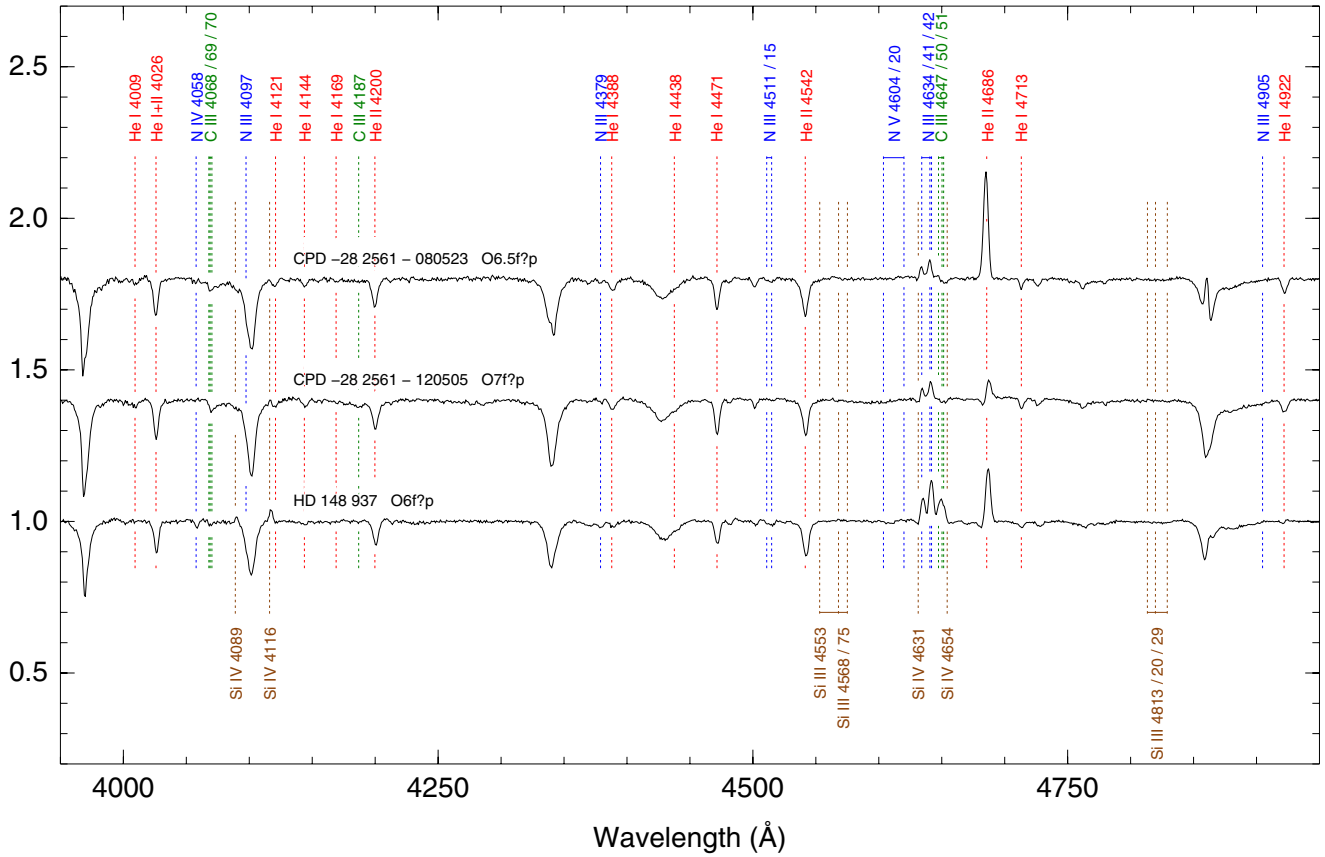


Figure 8. Spectrograms for the Of?p stars. The targets are sorted by Right Ascension. Two CPD–28 2561 epochs are shown (dates in YYMMDD). (A color version of this figure is available in the online journal.)

of this eclipsing binary by Antokhina et al. (2011) suggests a contact configuration.

HD 64 315 AB = V402 Pup AB. Tokovinin et al. (2010) spatially resolved this system into three tight components with speckle interferometry although Mason et al. (2009) and E. J. Aldoretta et al. (in preparation) only see two of them, separated by 63 mas and with a Δm of 0.6 mag. Lorenzo et al. (2010) discovered that HD 64 315 is a double SB2 system composed of four O stars. We observed this system with GOSSS on four different occasions and found the absorption line profiles to be highly varying. For the epoch where there is a better velocity resolution, we see an O5.5 Vz and an O7 V component. The spectral types are consistent with the range of effective temperatures measured by Lorenzo et al. (2010). The z character of the primary component could be caused by its hidden binary nature.

HD 75 759. This system is considered by a number of literature sources to have an early-B spectrum but it is an SB2 (period: 33.311 days, Pourbaix et al. 2004) that contains an O star. The O-type nature was already established by Hiltner et al. (1969) and Walborn (1973b); the latter also commented on the possible existence of a secondary component. With MGB we obtain spectral types of O9 V and B0 V. The new *Hipparcos* calibration gives a revised distance of 947^{+378}_{-203} pc (Maíz Apellániz et al. 2008a).

HD 92 206 C = CPD -57 3580. This object does not appear in the WDS catalog as HD 92 206 C (it is located $34''$ away from the A component), though it is most commonly referred to by that name in the literature. Campillay et al. (2007) discovered its

SB2 nature and assigned it spectral types of O7.5 V and B0 V. We have observed it on three occasions with GOSSS and in two of them it appears clearly as an SB2, with spectral types of O8 Vz and O9.7 V. It is located in NGC 3324 at the NW of the Carina Nebula. See Figure 12 for a chart (HD 92 206 field).

HD 92 206 A. HD 92 206 AB is a closer pair with a separation of $5''.3$ spatially resolved with ease into two O-type systems with GOSSS. OWN data show that it is an SB2. We do not see double lines in the GOSSS data. See Figure 12 for a chart (HD 92 206 field).

HD 93 161 A. HD 93 161 A and B are separated by $2''$ and both are O-type systems, with A itself being an O+O spectroscopic binary (Nazé et al. 2005). When observed within the same aperture, A+B form an SB3 system. We observed A twice and on both occasions we clearly detected it as an SB2. Our best spectral type for the secondary (O9 V) agrees with that of Nazé et al. (2005) but that for the primary (O7.5 V) is half a spectral subtype earlier. See Figure 12 for a chart (Trumpler 14 field).

QZ Car = HD 93 206. This complex SB1+SB1 system was studied by Mayer et al. (2001), who measured the two periods in the system to be 5.991 days (eclipsing) and 20.73596 days (non-eclipsing). See also the previous works by Leung et al. (1979) and Morrison & Conti (1980). The spectral types of Parkin et al. (2011) are consistent with our combined classification (we do not see double lines in the GOSSS data).

HD 93 205 = V560 Car. Conti & Walborn (1976) classified this massive SB2 system in Carina as O3 V + O8 V. We observed it five times with GOSSS and in two of them it is clearly

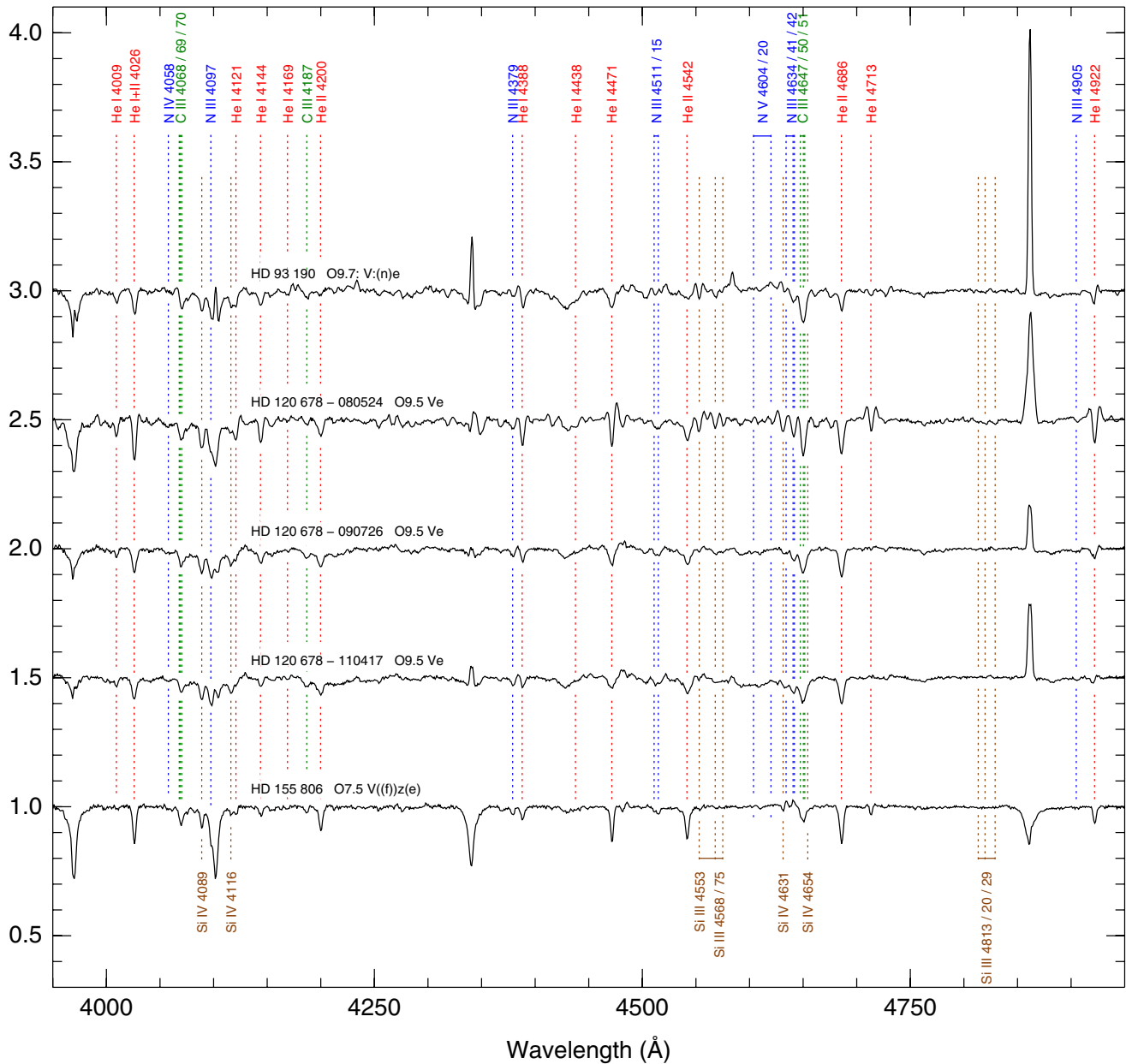


Figure 9. Spectrograms for the Oe stars. The targets are sorted by Right Ascension. Three HD 120 678 epochs are shown (dates in YYMMDD). (A color version of this figure is available in the online journal.)

in a double-lined state. Our best spectral type for the secondary (O8 V) agrees with that of Morrell et al. (2001) but the one for the primary (O3.5 V((f))) is half a spectral subtype later (something that was already modified by Walborn et al. 2002 when the O3.5 subtype was created) and adds the ((f)) suffix. The 4650 Å region is variable between epochs: it is not clear if what we are seeing in some epochs as emission there corresponds to C III λ 4650 from the primary (making it an Ofc) or N III λ 4640-42 from the secondary. See Figure 12 for a chart (Trumpler 16 field). In the existing ACS/HRC images we detect a previously unpublished visual companion. It has a separation of 3".68, a position angle of 272°, and a ΔV of 9.3 mag. Note that both HD 93 205 and HD 93 250 are systems with early-type O stars in them: one should be careful not to confuse them.

CPD −59 2591 = Trumpler 16–21. This star was not included in Maíz Apellániz et al. (2004) but was classified as O8 V by Massey & Johnson (1993). We did not detect that it was an SB2 in GOSSS-DR1.0 but a later analysis prompted by a spectrum obtained for the *Gaia*-ESO Survey (Gilmore et al. 2012) led us to find the weak secondary B spectrum redshifted by ~ 250 km s $^{-1}$ in an existing GOSSS spectrum. See Figure 12 for a chart (Trumpler 16 field).

CPD −59 2600. OWN data show that this system is an SB1 and, possibly, an SB2 with a 626 day period. We do not see double lines in the GOSSS data. See Figure 12 for a chart (Trumpler 16 field).

HD 93 249 A. OWN data show that this system is an SB2 with a 2.9797 day period. We do not see double lines in the GOSSS data. This is the brightest star in Trumpler 15.

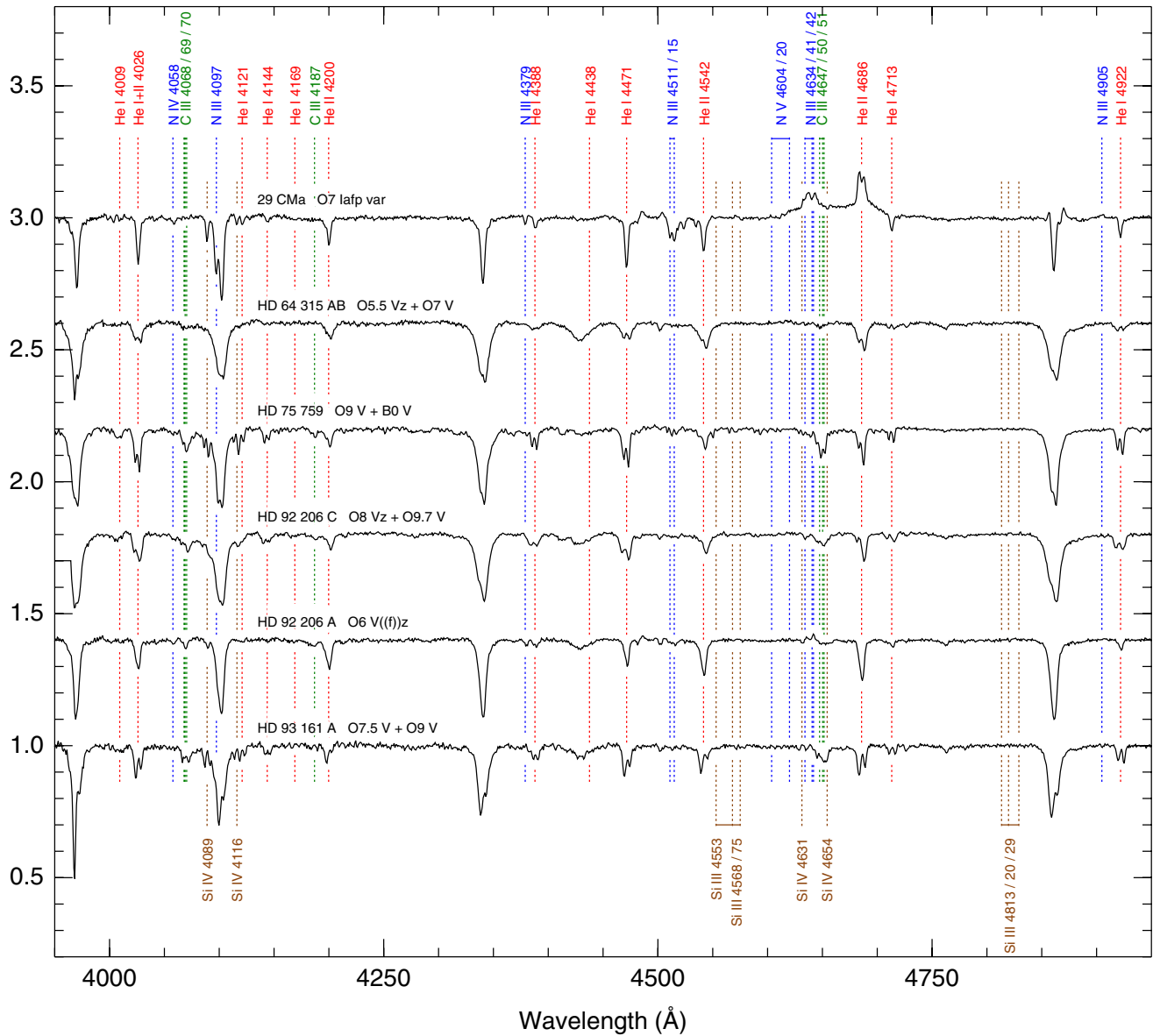


Figure 10. Spectrograms for the SB2 and SB3 stars. The targets are sorted by Right Ascension.
(A color version of this figure is available in the online journal.)

V572 Car = CPD -59 2603 = Trumpler 16-104. Rauw et al. (2001b) classified this system as a hierarchical triple consisting of an inner eclipsing O7 V + O9.5 V binary and an outer B0.2 IV component. In one of our two GOSSS epochs there are two components visible, an O7.5 V(n)z and a B0 Vn, the latter likely being a combination of the two later spectral types detected by Rauw et al. (2001b) in their high-resolution spectra. See Figure 12 for a chart (Trumpler 16 field).

V573 Car = CPD -59 2628. This SB2 system has a period of 1.47 days and was classified by Freyhammer et al. (2001) as O9.5 V + B0.2 V. We observed it twice with GOSSS and in both occasions we clearly detect double lines. Our spectral types (O9.5 V and B0.5 V) are similar to those of Freyhammer et al. (2001) though in both cases qualified with (n) suffixes. This star was not included in Maíz Apellániz et al. (2004). See Figure 12 for a chart (Trumpler 16 field).

HD 93 343. Rauw et al. (2009) classified this SB2 system as O7-8.5 + O8. We do not see double lines in the GOSSS data but our combined spectral type, O8 Vz, is consistent with the Rauw et al. (2009) results. See Figure 12 for a chart (Trumpler 16 field).

CPD -59 2635 = Trumpler 16-34. Albacete Colombo et al. (2001) classified this SB2 system as O8 V + O9.5 V and Otero (2006) discovered its eclipses (period of 2.29995 days). We obtain the same spectral types with GOSSS data with the only difference of an (n) suffix for the primary. See Figure 12 for a chart (Trumpler 16 field).

CPD -59 2636 AB = Trumpler 16-110 AB. This SB3 system was classified as O7 V + O8 V + O9 V by Albacete Colombo et al. (2002). According to the WDS, the B component (called C in Albacete Colombo et al. 2002) is a visual component 0".3 away from the SB2 system and is an SB1 system by itself,

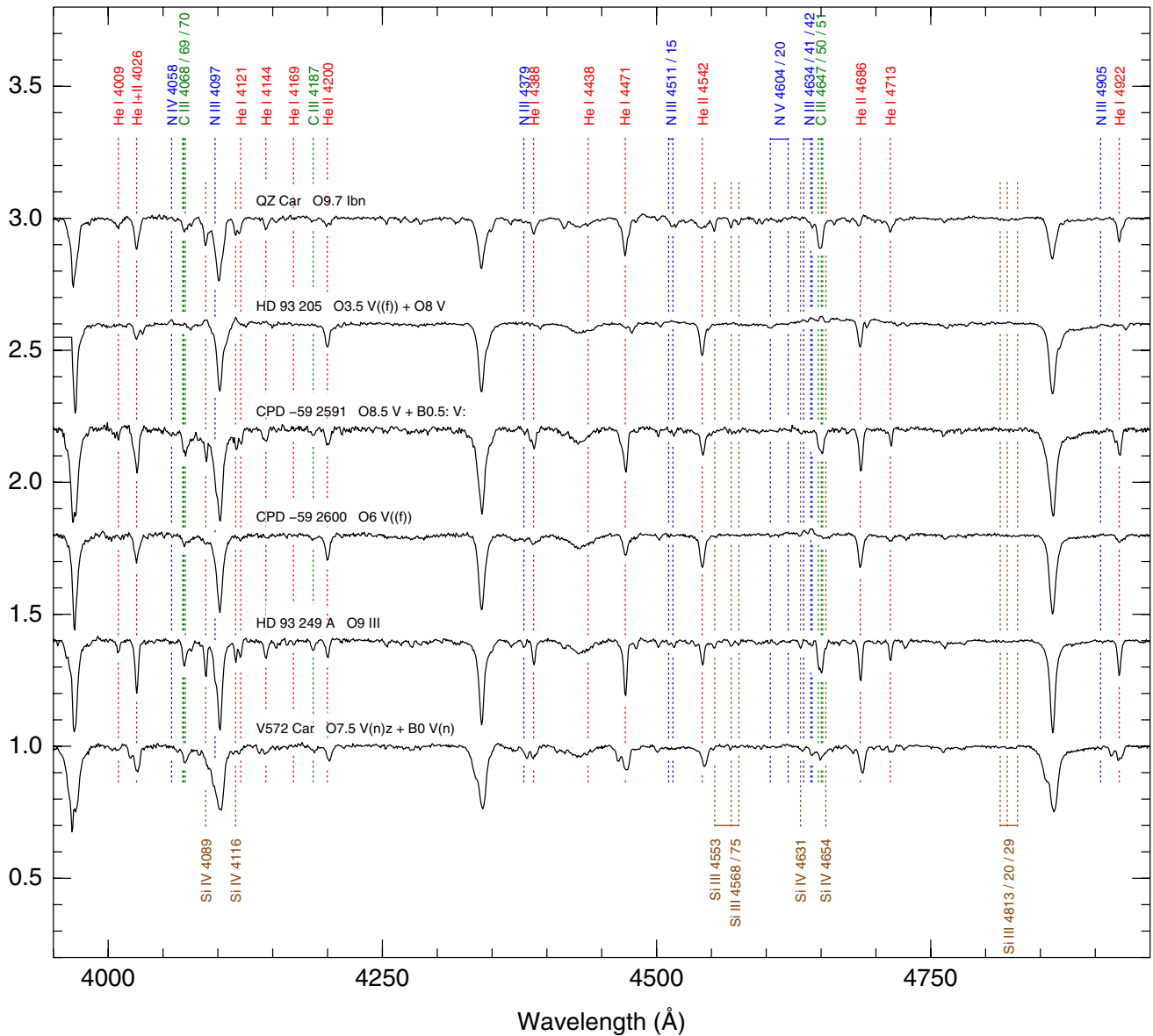


Figure 10. (Continued)

making CPD –59 2636 a quadruple system with one undetected component. We see two of those components in one of the six GOSSS epochs and we obtain spectral types of O8 V + O8 V. One of the set of lines is deeper than the other, likely indicating that is a composite of the O7 V and O9 V components. See Figure 12 for a chart (Trumpler 16 field).

V662 Car = FO 15. Niemelä et al. (2006) classified this SB2 system as O5.5 Vz + O9.5 V. It is an eclipsing binary with a period of 1.41355 days (Otero 2006; Fernández Lajús & Niemelä 2006). We detect double lines in He I λ 4471 for three of the five GOSSS epochs, yielding a classification of O5 Vz + B0: V, which is reasonably consistent with the previous result and confirms the z nature of the primary. This star was not included in Maíz Apellániz et al. (2004).

HD 96 264. This object is an SB2 according to OWN data. Here we do not see double lines and we classify it as O9.5 III.

HD 97 166. According to OWN data, this system is an SB2 and possibly an SB3. We do not see double lines in the GOSSS data. The ((f)) suffix was added in GOSSS-DR1.1.

HD 97 434. According to OWN data, this system is an SB2. We do not see double lines in the GOSSS data.

TU Mus = HD 100 213. Linder et al. (2007) classified this SB2 system as O7.5 V + O9.5 V. We obtained two epochs with GOSSS and double lines were clearly seen in this very fast system (1.3873 days period). Our spectral types are O8 V(n)z + B0 V(n), which are not too different from those in Linder et al. (2007). In particular, an (n) or n index is expected in a contact binary like TU Mus.

HD 101 131 = V1051 Cen. Gies et al. (2002) obtained spectral types of O6.5 V((f)) + O8.5 V. From the GOSSS spectra we derived slightly earlier types of O5.5 V((f)) + O8: V. In GOSSS-DR1.1 we added the missing ((f)) suffix to the primary. See Figure 12 for a chart (IC 2944 field).

HD 101 190. According to Sana et al. (2011a), this system is an SB2 with spectral types O4 V((f)) + O7 V, but they caution that the system could include a third component based on the lack of motion of the N III and N v lines. We do not detect double lines in the GOSSS data and assign this system

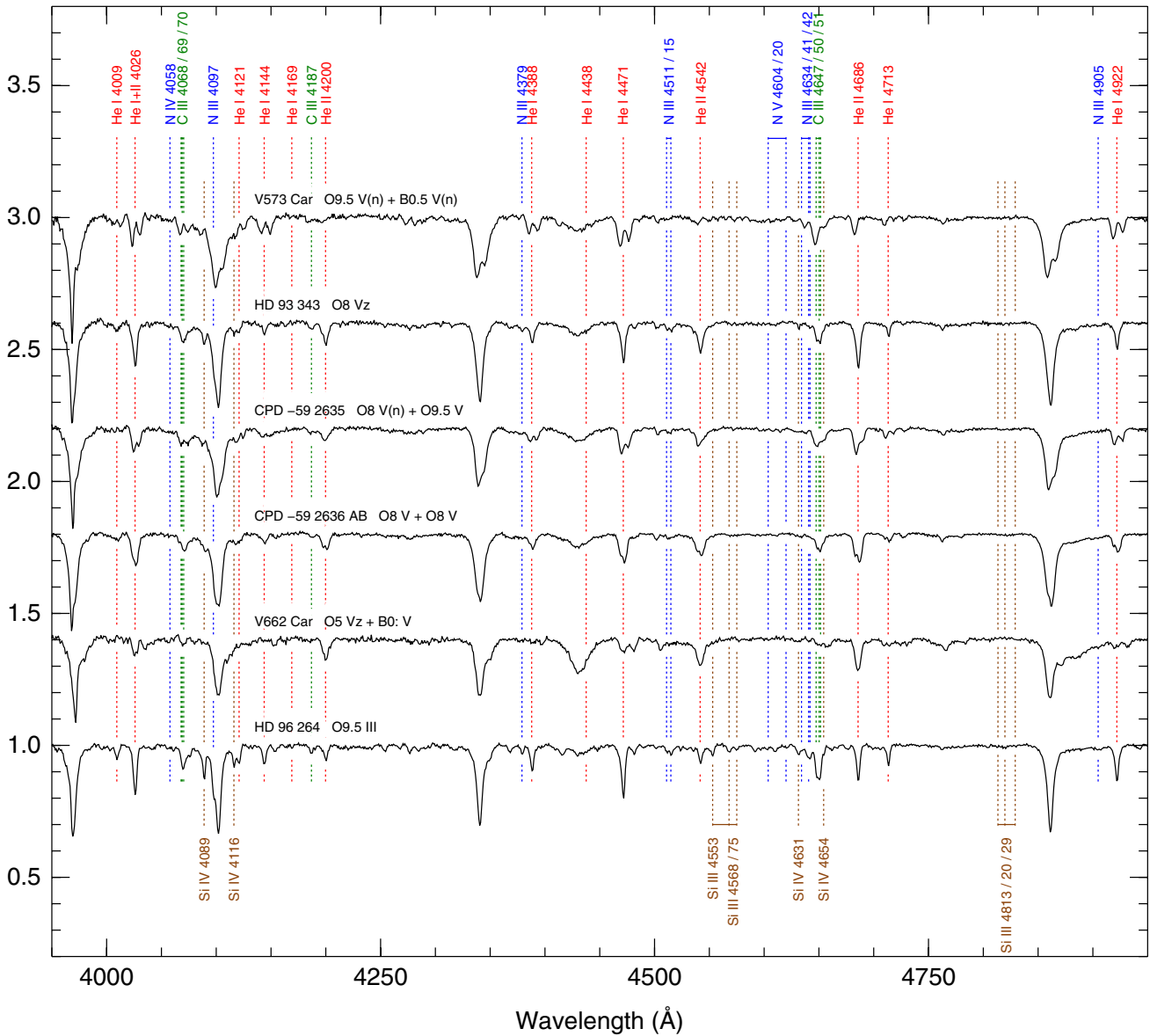


Figure 10. (Continued)

a classification of O6 IV((f)), intermediate between that of the primary and the secondary of Sana et al. (2011a). The WDS lists two dim companions within 15". The ((f)) suffix was added in GOS-DR1.1. See Figure 12 for a chart (IC 2944 field).

HD 101 205 AB = V871 Cen. This system is an SB2 according to OWN data. The WDS lists a B companion with a separation of 0".4 and a Δm of 0.3 mag that we were unable to spatially resolve in the GOSSS data (we do not see double lines, either). Either A or B is an eclipsing binary with a period of 2.090704 days (Otero 2007), which is different from the SB2 period. The luminosity class of II: (changed in GOSSS-DR1.1) is a compromise between the behavior of N III $\lambda\lambda 4634$ -40-42 and of He II $\lambda 4686$, possibly a consequence of the composite nature of the spectrum. See Figure 12 for a chart (IC 2944 field).

HD 101 413. Sana et al. (2011a) obtained spectral types of O8 V + B3: V for this SB2 system. We do not see double lines in the GOSSS data, which is unsurprising given the large

expected Δm (our combined spectral type is the same that Sana et al. (2011a) obtain for the primary). See Figure 12 for a chart (IC 2944 field).

HD 101 436. Sana et al. (2011a) obtained spectral types of O6.5 V + O7 V for this SB2 system. We do not see double lines in the GOSSS data and obtain a combined spectral type of O6.5 V, consistent with the Sana et al. (2011a) result. In GOSSS-DR1.1 we eliminated the z suffix of the primary. See Figure 12 for a chart (IC 2944 field).

HD 114 886 AaAb. According to the WDS (supplemented with additional information), this system is composed of three close components, Aa, Ab, and B with B magnitudes of 7.5, 8.6, and 9.2, respectively. Aa and Ab have a separation of 0".2 and cannot be spatially resolved with GOSSS while B is 1".7 from the other two and is indeed spatially resolved in our spectra. We obtain spectral types of O9 III + O9.5 III for AaAb, consistent with the O9 II-III classification of Walborn (1973b). From OWN data, a period of 13.559 days is derived. The B component is an early B star.

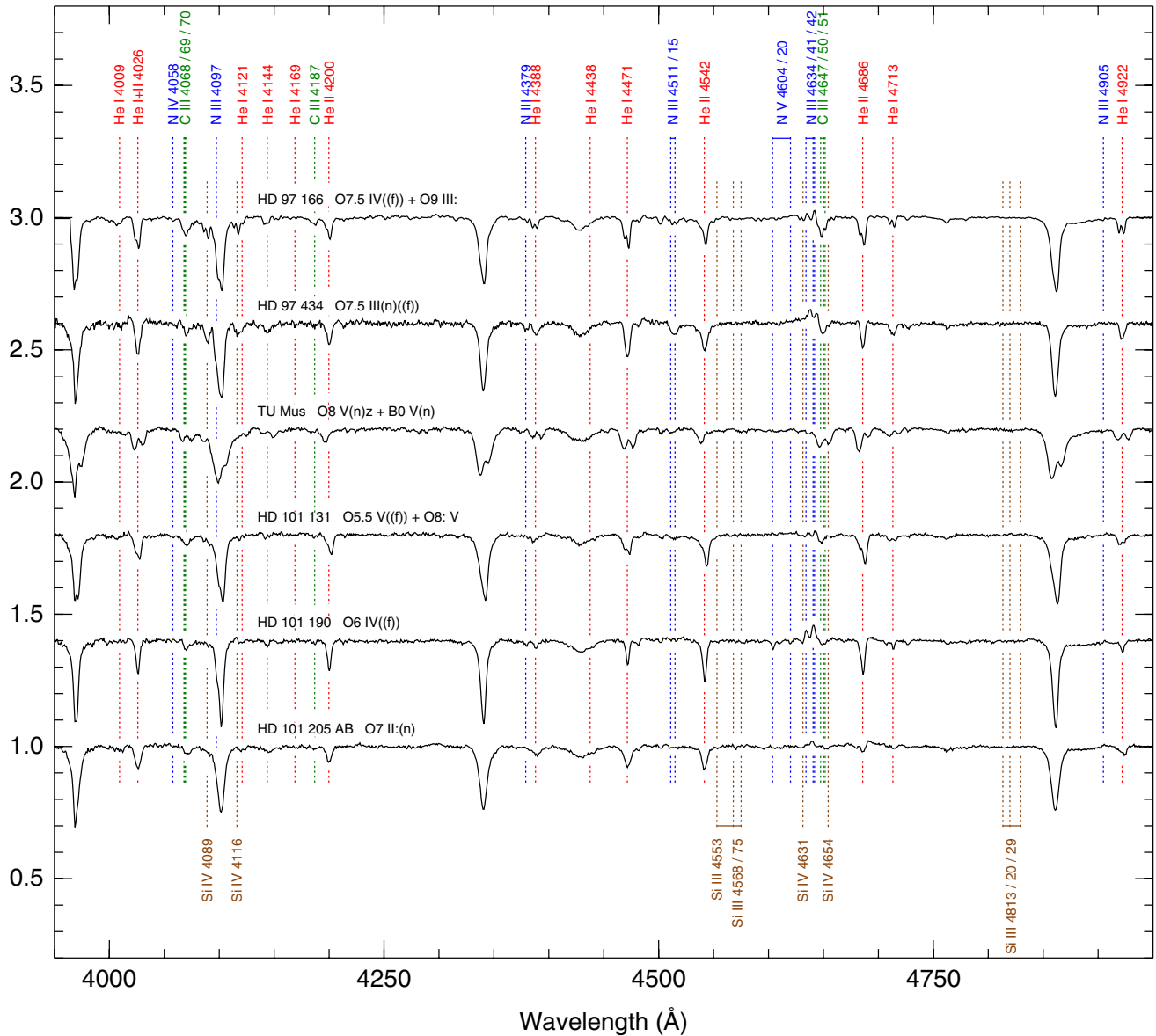


Figure 10. (Continued)

HD 115 071 = V961 Cen. Penny et al. (2002) classified this SB2 system as O9.5 V + B0.2 III. With GOSSS we obtain O9.5 III + B0 Ib, which are similar in spectral subtypes but correspond to higher luminosity classes.

HD 115 455. This SB2 system has a period of 15.08 days according to OWN data. We do not see double lines in the GOSSS data. The ((f)) suffix was missing in GOSSS-DR1.0.

HD 117 856. This SB2 system has a period of 27.6 days according to OWN data. We do not see double lines in the GOSSS data. The classification was changed from O9.7 II to O9.7 II-III in GOSSS-DR1.1.

HD 123 056. This system is at least an SB2 in the OWN data. We do not see double lines in the GOSSS data.

HD 123 590. This SB2 system has a period of 58.9 days according to OWN data. We do not see double lines in the GOSSS data. The z suffix was added in GOSSS-DR1.1.

HD 124 314 A. HD 124 314 A and BaBb are separated by 2''5 and both have O spectral types. A is a likely SB2 system according to preliminary OWN results but is not seen with

double lines in the existing GOSSS spectrum. The luminosity class was changed from III to IV in GOSSS-DR1.1. The system is a colliding-wind binary (De Becker & Rauq 2013). See Figure 12 for a chart (HD 124 314 field).

HD 124 979. This object is an SB2 system according to OWN data. We do not see double lines in the GOSSS data. The (n) suffix was added in GOSSS-DR1.1.

HD 125 206. This object is an SB2 system according to OWN data. We do not see double lines in the GOSSS data.

δ Cir = *HD 135 240.* Penny et al. (2001) classified this SB3 system as O7 III-V + O9.5 V + B0.5 V. We do not see double lines in the GOSSS data and we obtain a combined classification of O8 V (changed from O7.5 V in GOSSS-DR1.1), which is consistent with the Penny et al. (2001) result.

HD 149 404 = V918 Sco. Rauw et al. (2001a) classified this SB2 system¹⁶ as O7.5 I(f) + ON9.7 I (see also Thaller et al. (2001)). We do not see double lines in our three GOSSS epochs,

¹⁶ Note that the (f) suffix cannot be used for an O7.5 supergiant according to Table 2.

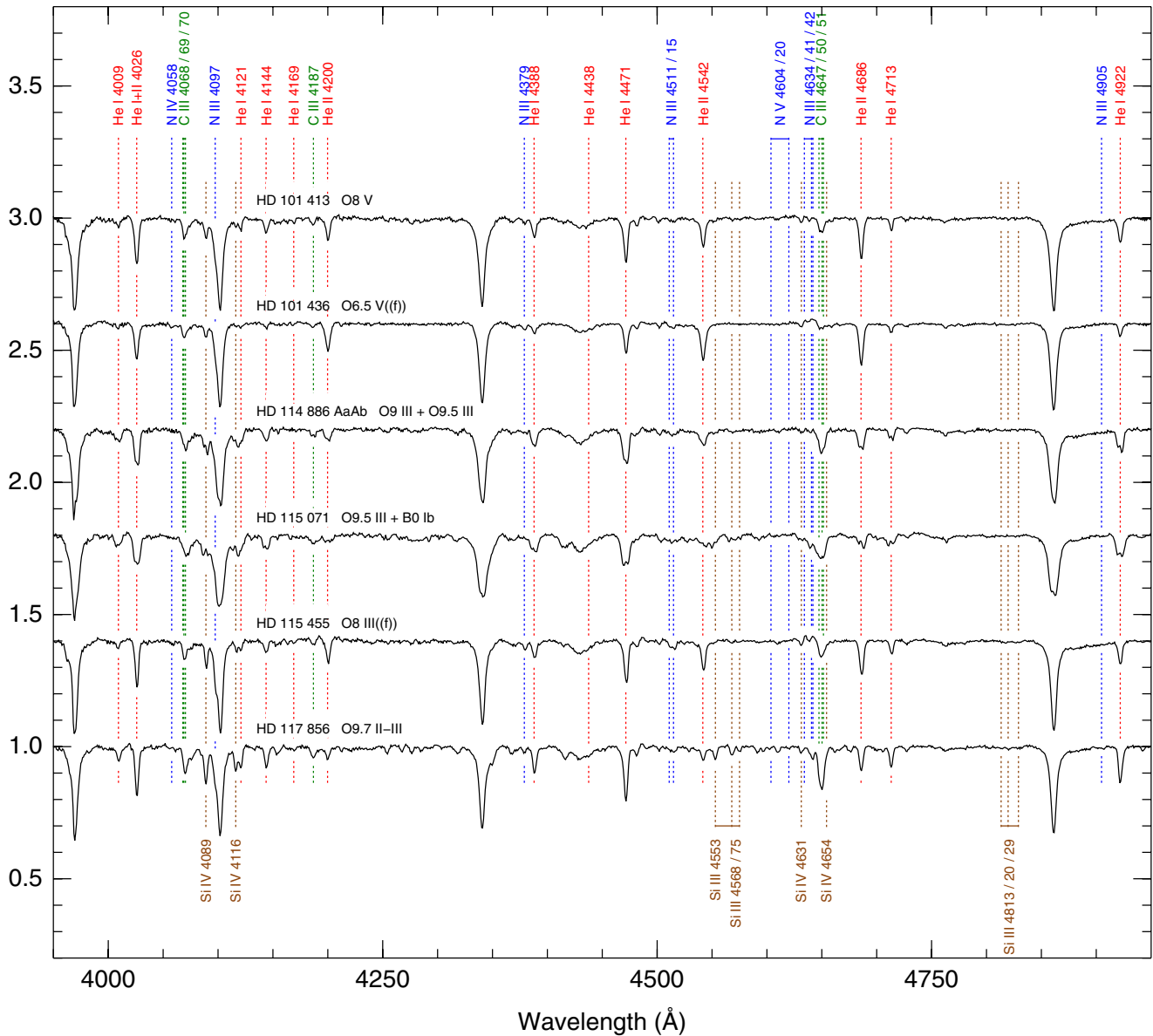


Figure 10. (Continued)

though both He II $\lambda 4686$ and H β have variable and anomalous profiles due to the binarity of the system. The combined spectral type is O8.5 Iab(f), consistent with the Rauw et al. (2001a) classification. Note that the two unidentified emission lines at 4486 Å and 4504 Å discussed by those authors (see also Walborn 2001) were soon afterward discovered to originate in Si IV by Werner & Rauch (2001). The new *Hipparcos* calibration gives a revised distance of 458^{+96}_{-67} pc (Maíz Apellániz et al. 2008a).

HD 150 135. This SB2 system has a period of 181 days according to OWN data. We do not see double lines in the GOSSS data. See Figure 12 for a chart (HD 150 136 field).

HD 150 136. Niemelä & Gamen (2005) classified this object as O3, making it the closest O2/3.5 system, and discovered it was an SB3. Mahy et al. (2012) classified it as O3-3.5 V((f)) + O5.5-6 V((f)) + O6.5-7 V((f)). In the GOSSS data we see it only as SB2, with spectral types of O3.5-4 III(f*) and O6 IV, which is roughly consistent with the three individual spectral types of Mahy et al. (2012) merged into two. Recently, Sana et al.

(2013) and Sánchez-Bermúdez et al. (2013) have independently spatially resolved one of the three components with VLTI with a separation of 7–9 mas and an 8 a orbit around the inner pair of O stars (which are expected to be separated by only ~ 0.1 mas according to the 2.67454 day period of their spectroscopic orbit). Note that in addition to those three stars (all part of the A component), a fainter B component is listed by WDS with a separation of 1''.6. See Figure 12 for a chart (HD 150 136 field). The visual multiplicity for this target was checked in ACS/HRC images (the VLTI-detected companion is obviously not seen there). The system is a colliding-wind binary (De Becker & Raucq 2013).

HD 151 003. This SB2 system has a period of 199 days according to OWN data. We do not see double lines in the GOSSS data. The spectral classification was changed from O9 III to O8.5 III in GOSSS-DR1.1 due to the revision of criteria around spectral type O9.

HD 150 958 AB. This object is an SB2 system according to OWN data. We do not see double lines in the

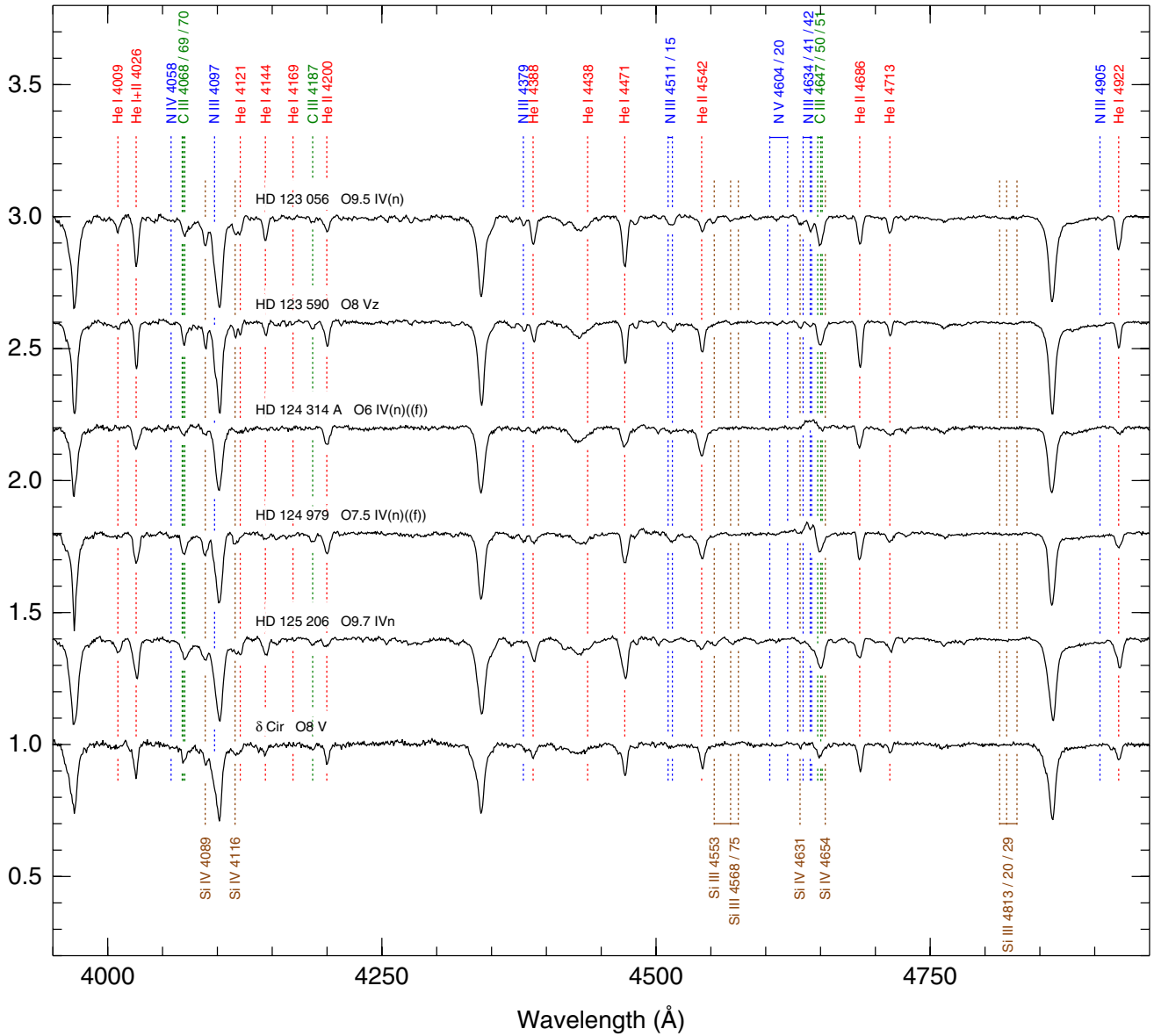


Figure 10. (Continued)

GOSSS data. The WDS lists a B component with a separation of $0''.3$ and a Δm of 1.7 mag that we cannot spatially resolve.

HD 151 804 = V973 Sco. This object is an SB2 system according to OWN data. We do not see double lines in the GOSSS data. The system is a colliding-wind binary (De Becker & Raucq 2013).

HD 152 219 = V1292 Sco. Sana et al. (2008) classified this system as O9 III + B1-2 V/III. We do not see double lines in the GOSSS data and we get a combined spectrum of O9.5 III(n), which is consistent with the previous one. See Figure 12 for a chart (NGC 6231 field).

HD 152 218 = V1294 Sco. Sana et al. (2008) classified this system as O9 IV + O9.7 V. We also resolve in velocity the two components in the GOSSS data and we obtain the very similar classification of O9 IV + B0: V. See Figure 12 for a chart (NGC 6231 field).

HD 152 233. Sana et al. (2008) classified this system as O5.5 + O7.5. We do not see double lines in the GOSSS

data and we get a combined spectrum of O6 II(f), whose spectral subtype is compatible with the previous measurement. The GOSSS luminosity class was adjusted from Ib to II in GOSSS-DR1.1. See Figure 12 for a chart (NGC 6231 field).

HD 152 246. This object is an SB2 system according to OWN data. We do not see double lines in the GOSSS data. The luminosity class was changed from V to IV in GOSSS-DR1.1.

HD 152 248 AaAb = V1007 Sco AaAb. Sana et al. (2008) classified this system as O7 III(f) + O7.5 III(f). We also resolve in velocity the two components in the GOSSS data and we obtain a classification of O7 Iabf + O7 Ib(f), i.e., similar spectral subtypes but somewhat brighter luminosity classes (note that Sana et al. 2008 showed convincingly that both components have He II $\lambda 4686$ in absorption and all the emission in that line arises in the colliding wind region, so their luminosity classes are likely correct). In GOSSS-DR1.0 the luminosity class of the primary was Ib and its suffix (f). According to Mason et al. (2009) there is a visual Ab companion at a distance of $0''.05$ with

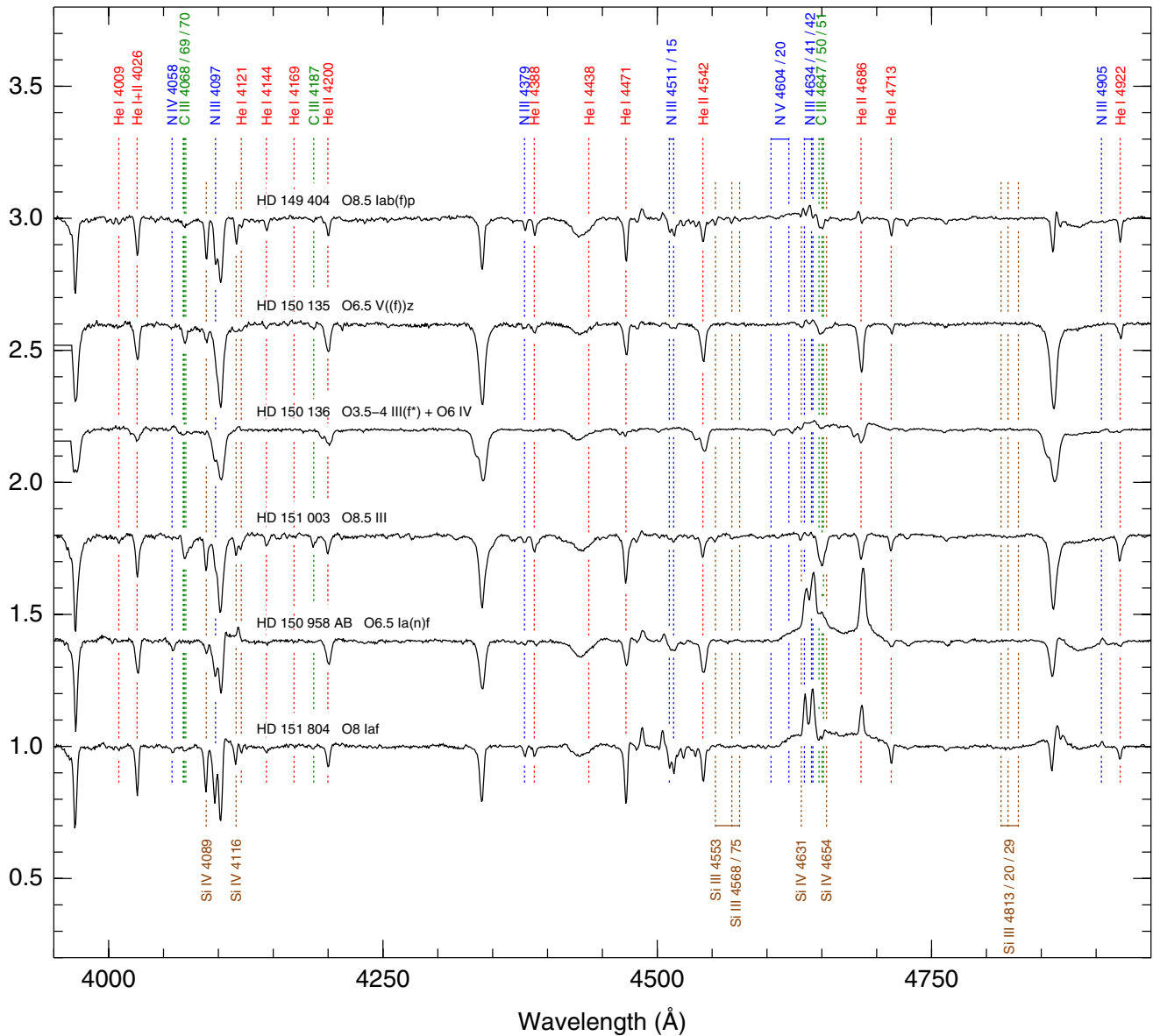


Figure 10. (Continued)

a Δm of 2.0 mag, which we were unable to spatially resolve in our data. See Figure 12 for a chart (NGC 6231 field).

CPD -41 7733. Sana et al. (2008) classified this system as O8.5 V + B3. We do not see double lines in the GOSSS data and we get a combined classification of O9 IV, which is consistent with the previous result. See Figure 12 for a chart (NGC 6231 field).

V1034 Sco = CPD -41 7742. Sana et al. (2008) classified this system as O9.5 V + B1.5 V. We do not see double lines in the GOSSS data and we get a combined classification of O9.5 IV, which is not far from what one would expect from the previous result. In GOSSS-DR1.0 the luminosity class for this system was III. See Figure 12 for a chart (NGC 6231 field).

HDE 326 331. This object is an SB2 system according to OWN data. We do not see double lines in the GOSSS data. The ((f)) suffix was added in GOSSS-DR1.1. See Figure 12 for a chart (NGC 6231 field).

HD 152 314. This system was found by Sana et al. (2008) to be an SB2 with spectral types of O8.5 III and B1-3 V. We

do not see double lines in the GOSSS data but our combined spectral type of O9 IV (in GOSSS-DR1.0 it was O9.5 IV) is in agreement with that result. See Figure 12 for a chart (NGC 6231 field).

HD 152 590 = V1297 Sco. This eclipsing system has a period of 4.487 days (Otero & Claus 2004) and is an SB2 according to OWN data. We do not see double lines in the GOSSS data.

HD 153 426. This object is an SB2 system with a period of 22.4 days according to OWN data. We do not see double lines in the GOSSS data. The classification was changed from O9 II-III to O8.5 III in GOSSS-DR1.1.

HD 155 889 AB. This object is an SB2 system (and possibly an SB3) according to OWN data. We do not see double lines in the GOSSS data. The WDS lists a companion with a separation of 0".2 and a Δm of 0.6 mag than cannot be spatially resolved in our long-slit spectra.

HD 155 913. This object is an SB2 system according to OWN data. We do not see double lines in the GOSSS data. E. J. Aldoretta et al. (in preparation) have

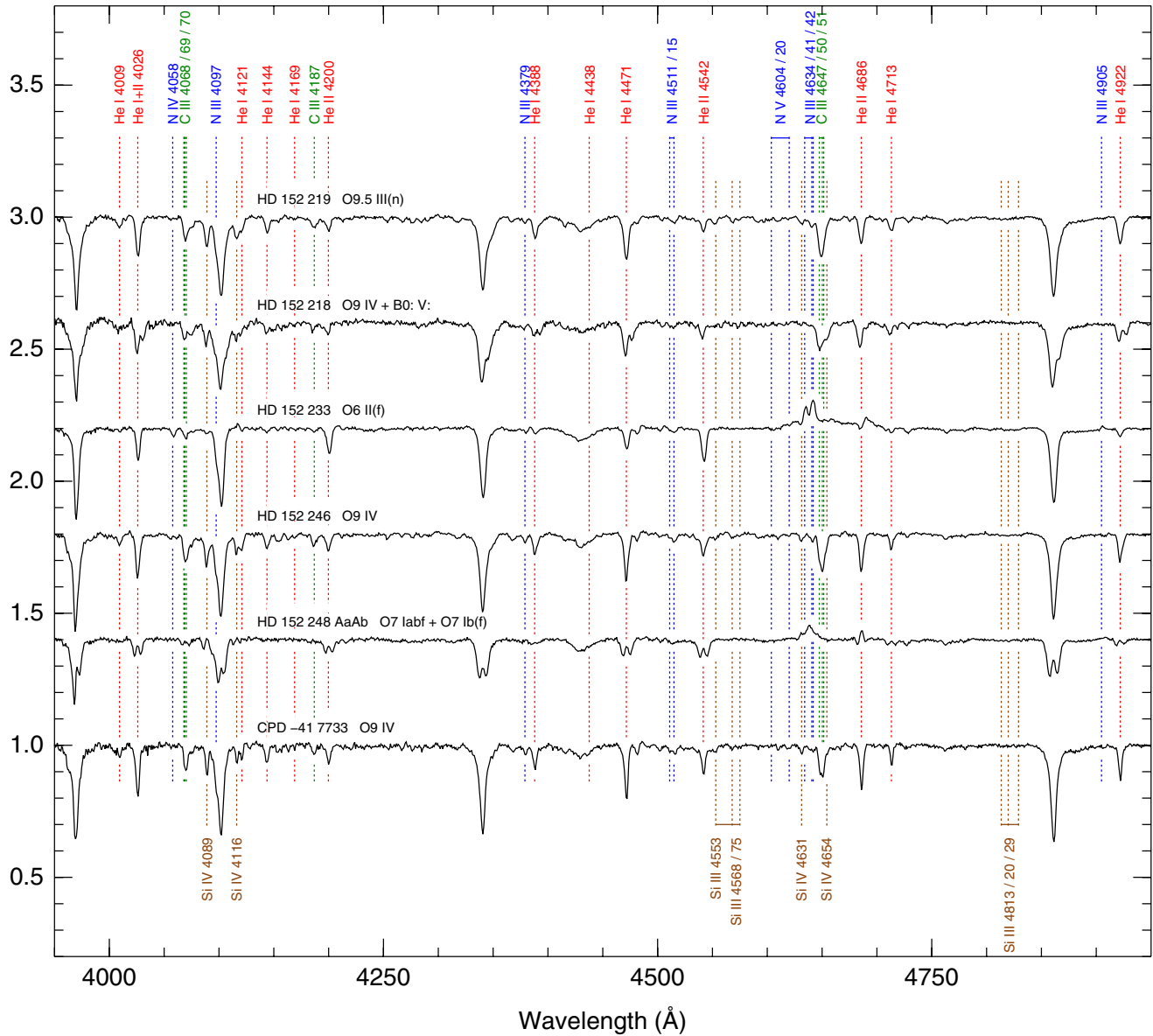


Figure 10. (Continued)

found a new dim companion at a small distance from the primary.

HD 156 292. This object is an SB2 system with a period of 4.94 days according to OWN data. We do not see double lines in the GOSSS data.

ALS 18 748 = HM 1–8 = C1715–387–8. This star was not included in Maíz Apellániz et al. (2004) due to its dimness (Havlen & Moffat 1977). The OWN collaboration has recently discovered that it is an SB2 with a 5.8783 day period. We do not see double lines in our data. The target has C III λ 4650 in emission but the C III λ 4650/N III λ 4634 intensity ratio of 0.9 places this spectrum just below the fc boundary. It is interesting that it is associated with the Ofc star ALS 18 747 in the Havlen–Moffat 1 cluster shown in Figure 12, which may be significant in the context of the Walborn et al. (2010b) finding that this phenomenon occurs in some clusters but not others.

HDE 319 703 A. A chart of the complex HDE 319 703 system in NGC 6334 can be seen in Figure 12 (HDE 319 703 field; see also Figure 1 in Walborn 1982c). The A component is clearly spatially resolved from the others (see Section 3.3.9 for two

additional O stars) and we do not see double lines in its spectrum. This object is an SB2 system with a 16.4 day period according to OWN data. The ((f))z suffix was added in GOSSS-DR1.1, where the star was also moved from O7.5 to O7.

HDE 319 702. This object in NGC 6334 was found to be an eclipsing binary with a period of 2.0 d by Barr Domínguez et al. (2013). OWN data reveal that it is actually an SB3 system. We do not see double lines in the GOSSS data.

Pismis 24-1 AB = HDE 319 718 AaAb. Maíz Apellániz et al. (2007) were able to spatially resolve this close pair (separation of $0''.364$ and Δm of 0.1 mag) with IMACS at the Baade telescope at LCO to obtain spatially resolved spectral types of O3.5 If* and O4 III(f) for A and B, respectively.¹⁷ With the GOSSS data we were unable to spatially resolve the pair, so we can only produce a combined spectral type of O3.5 If*, which is consistent with the expected merged spectrum. Note, however, that the merged spectrum shows a P-Cygni-like profile in He II λ 4686. Maíz Apellániz et al. (2007) also cited a private communication by

¹⁷ Note that the f+ qualifier became obsolete in Paper I.

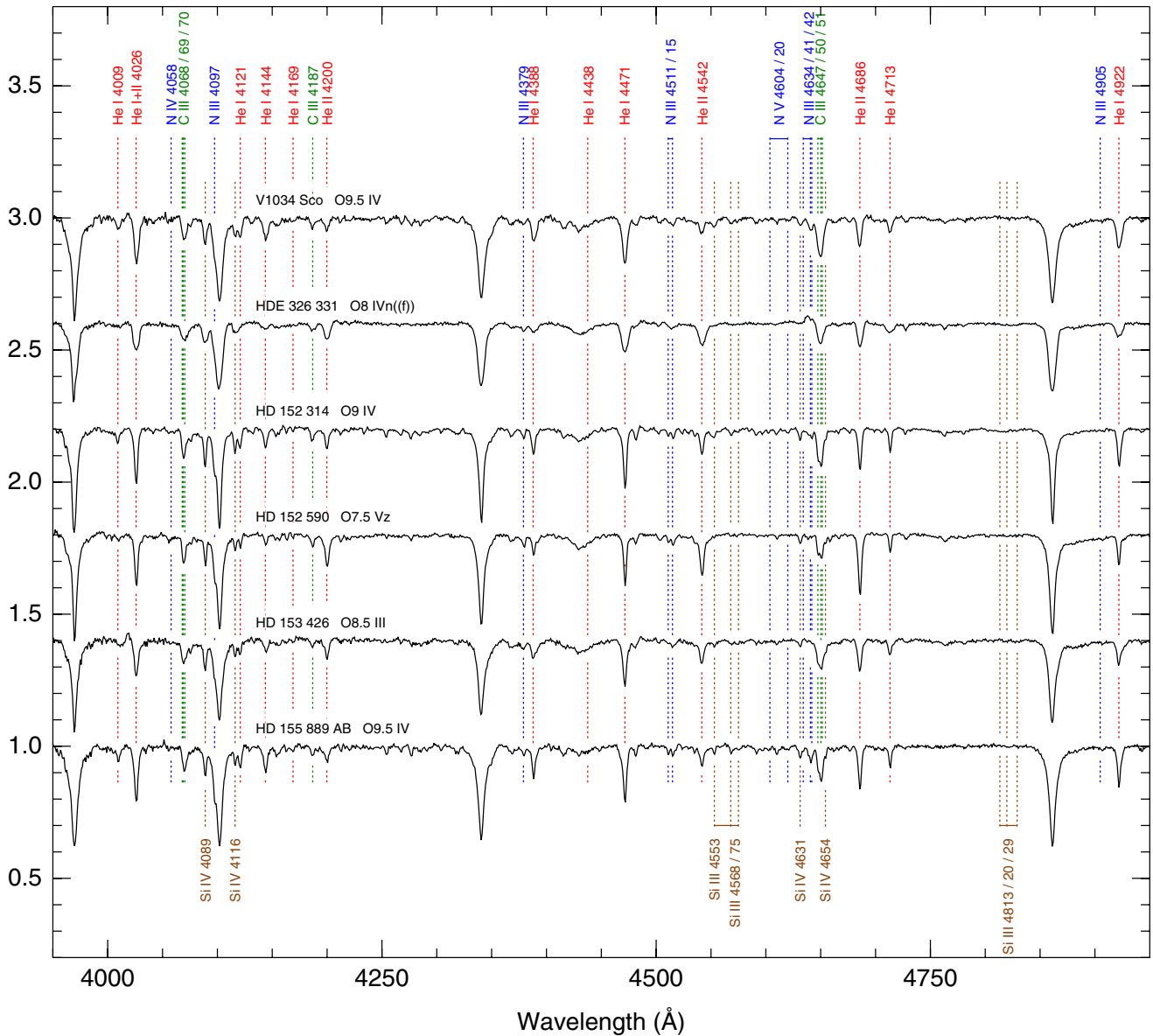


Figure 10. (Continued)

Phil Massey about the photometric variability of the system that indicated the eclipsing binary nature of one of its components, making Pismis 24-1 a system with three very massive O stars.¹⁸ The eclipsing binary nature and the period of 2.36 days has been recently confirmed by Barr Domínguez et al. (2013). OWN data also reveal the period in radial velocity data. See Figure 12 for a chart (Pismis 24 field). The visual multiplicity for this target was measured in ACS/HRC images.

HD 158 186 = V1081 Sco. This object is an SB3 system according to OWN data. We do not see double lines in the GOSSS data. The (n) suffix was added in GOSSS-DR1.1. E. J. Aldoretta et al. (in preparation) and H. Sansa et al. (in preparation) have recently detected a companion with a Δm of 2.1–2.3 mag and a separation in the vicinity of 30 mas (with somewhat discrepant results between the two).

HD 159 176 = V1036 Sco. Linder et al. (2007) classified this system as O7 V((f)) + O7 V((f)), see also Conti et al. (1975). We

obtain exactly the same classification with GOSSS (after adding the ((f)) suffixes missing in GOSSS-DR1.0). According to the WDS, the HD 159 176 system is rather complex. The B and C components are rather faint and well separated from A. A itself is composed of Aa, Ab, and Ac, all less than 1'' from each other and spatially unresolved in the GOSSS data. Ac is considerably fainter than Aa but Ab has no magnitude listed in the WDS. We have unpublished Lucky Imaging obtained with AstraLux Sur at the NTT where Ab does not appear. That indicates that it either does not exist or is too faint. In either case, we do not need to add any component to the star name.

HD 161 853. This object is an SB2 (and possibly an SB3) system according to OWN data. In one of the GOSSS observations we see a weak secondary component in the He I lines that indicate a B-type secondary. This object has a history of confusion with being a post AGB star. However, Szczerba et al. (2007) disqualify it from that category and Urquhart et al. (2009) identify it as the main ionizing source of RCW 134.

HD 163 758. This object is an SB2 system according to OWN data. We do not see double lines in the GOSSS data. We observe

¹⁸ Note that the alternative classification in Table 7 refers to the two visual components, not to a classification based on a velocity resolution of the spectroscopic binary.

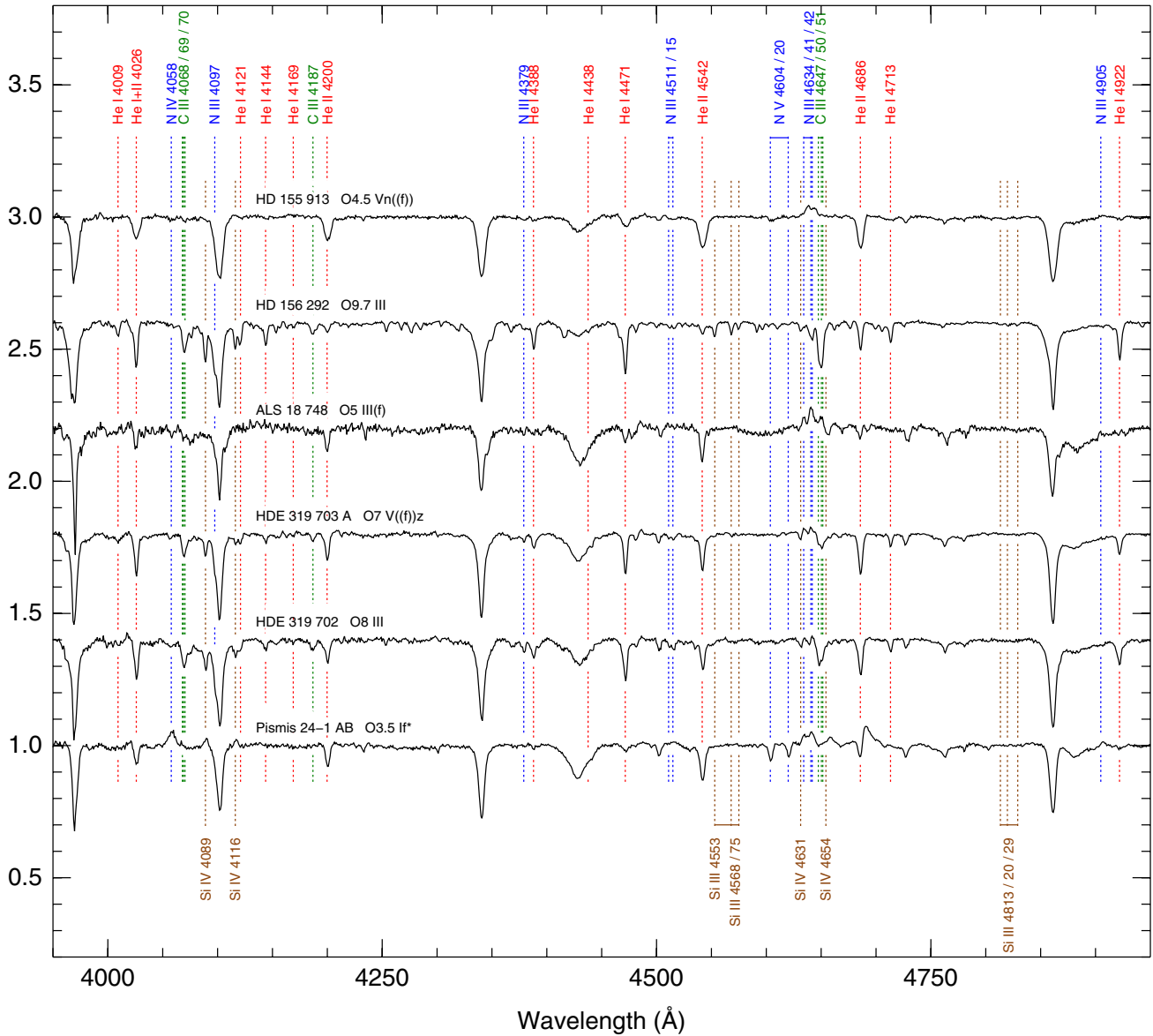


Figure 10. (Continued)

both enhanced C and N absorption lines. That prompted the introduction of the p suffix in GOSSS-DR1.1. Leep (1978) had already suggested that this was a carbon-rich star.

Herschel 36 = HD 164 740. Arias et al. (2010) discovered that *Herschel 36* is an SB3 system with spectral types O7.5 V + O9 V + B0.5 V. We see hints of the secondary in two of the five GOSSS epochs but not full-fledged double lines. The combined spectral type is O7: V + sec. A number of companions can be detected in the IR in this region with heavy and patchy extinction (Arias et al. 2006), including one with a separation of just 0".25 (Goto et al. 2006). The visual multiplicity for this target was measured in WFPC2 images.

9 Sgr = HD 164 794. Rauw et al. (2012) classified this system as O3.5 V((f*)) + O5-5.5 V((f)). We do not see double lines in our spectrum, which is unsurprising given the long period (8.6 a) of the orbit. Our combined spectral subtype (O4) and luminosity class (V) are consistent with those expected from the Rauw et al. (2012) results. The suffixes are different for two reasons: there is no * at O3.5/O4 V and there is a z suffix due to the depth of the He II $\lambda 4686$ absorption with respect to that

of the He II $\lambda 4542$ absorption (this could be a case where the z phenomenon appears due to the existence of a binary). The target has C III $\lambda 4650$ in emission but is not strong enough to warrant a c suffix. The system is a colliding-wind binary (De Becker & Raucq 2013). Note that both 9 Sgr and 9 Sge are O stars: one should be careful not to confuse them.

HD 164 816. This object is an SB2 system according to OWN data. Double lines are clearly seen in two of our five GOSSS epochs. We derive spectral types of O9.5 V + B0 V for the two components.

HD 165 052. Ferrero et al. (2013) used multiple-epoch high-resolution spectroscopy to determine the apsidal motion rate of this SB2 system, calculate the masses of the two components, and assign to them spectral types of O7 Vz and O7.5Vz, respectively (see also the previous work by Arias et al. 2002). We obtained GOSSS spectra at six different epochs and in one of them we barely resolve in velocity the two SB2 components when they had a separation of $\sim 200 \text{ km s}^{-1}$. That is close to our velocity resolution limit, so the GOSSS spectral types are rather uncertain.

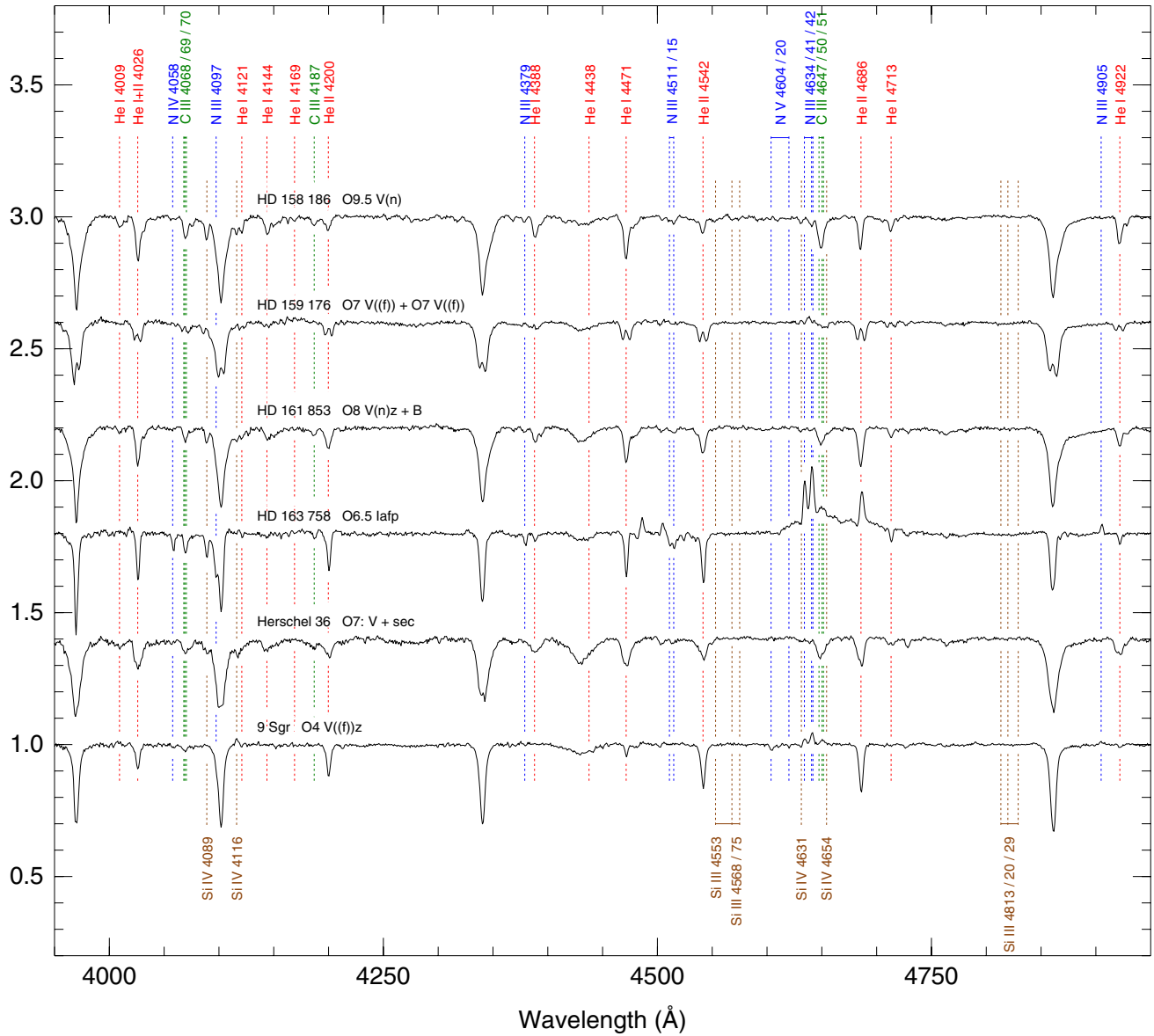


Figure 10. (Continued)

HD 165 246. Otero (2007) discovered that this is an eclipsing binary and Mayer et al. (2013) derived spectral types for this SB2 of O8 V + B7 V. The GOSSS classification is O8 V(n). Other than the difference in the rotation index, the GOSSS spectral type is what one would expect, since detecting a companion with such a large Δm as that between O8 and B7 dwarfs should not be possible with our data.

HD 165 921 = V3903 Sgr. Niemelä & Morrison (1988) obtained spectral types of O7 V + O9 V for this SB2 system. We detect double lines in one of our two GOSSS epochs and derive spectral types of O7 V(n)z + B0: V, which agree (given the uncertainty in the secondary) reasonably well with the previous classification. The z suffix of the primary was added in GOSSS-DR1.1.

3.3.9. Normal Sample

In this subsection we briefly describe the O stars in our sample that do not belong to any of the categories of the previous subsections. Spectrograms are shown in Figure 11.

μ Col = *HD 38 666*. μ Col is a runaway star, likely ejected from the Trapezium 2.5 Ma ago (Hoogerwerf et al. 2001). The new *Hipparcos* calibration gives a revised distance of 412^{+38}_{-32} pc (Maíz Apellániz et al. 2008a).

τ CMa AaAb = *HD 57 061 AaAb*. This is a complex system, with three visual components within 1'' and a number more outside of it (τ CMa is by far the brightest system in the open cluster NGC 2362 and it is unclear where the multiple system ends and the cluster begins). The GOSSS spectrum corresponds to the combined light of Aa+Ab+E. E is too dim to modify the spectral type¹⁹ but the Δm between Aa and Ab is only 0.8 mag and the separation is 0''.122; hence, the O9 II classification is a composite. The system is further complicated by being (1) a single-lined spectroscopic binary with a period of 154.9 days (Stickland et al. 1998) and (2) an eclipsing binary

¹⁹ Hence, it is not included in the GOSSS name. Note that E. J. Aldoretta et al. (in preparation) have recently discovered that the P.A. of E with respect to Aa is 268° , an offset of 180° with respect to the previous value in the WDS, an effect that we have confirmed in unpublished AstraLux data.

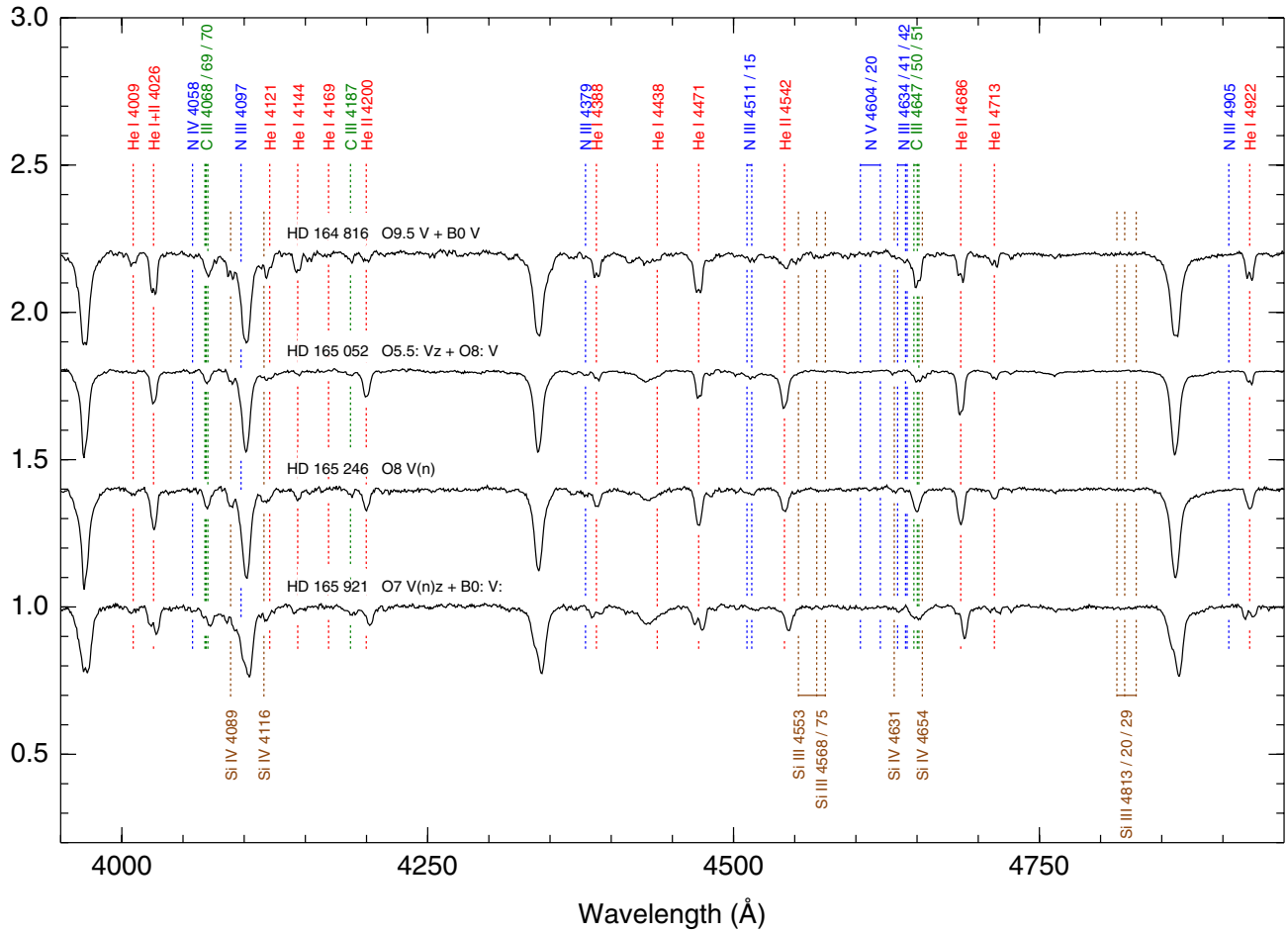


Figure 10. (Continued)

with a 1.282 day period (van Leeuwen & van Genderen 1997). Therefore, the system includes at least five bodies within $1''$.

HD 57 236. This star was classified as O8 V((f)) by Walborn (1982c). Based on the new criteria around spectral subtype O9 we reclassify it as O8.5 V.

CPD -26 2716 = CD -26 5136. He II $\lambda 4686$ is clearly in emission in this star, prompting us to change the luminosity class from Ib (Walborn 1982c) to Iab. This object is variable in OWN spectra on time scales of 1 day.

HD 64 568. This was one of the ten O3 stars in Walborn (1982a). Solivella & Niemelä (1986) indicated that is a possible SB1. The ((f*))z suffix was omitted by mistake in GOSSS-DR1.0. The visual multiplicity for this target was measured in ACS/HRC images.

HD 68 450. The WDS lists two weak companions far away from the primary.

HD 69 106. This bright star was not included in Maíz Apellániz et al. (2004) due to the lack of previous classifications as O type we were aware of. The likely reason for that is the broadening of He II $\lambda 4542$ in this fast O9.7 rotator.

HD 69 464. E. J. Aldoretta et al. (in preparation) have recently discovered a weak secondary $0''.92$ away from the primary. The (f) suffix was omitted by mistake in GOSSS-DR1.0.

HD 71 304. This star was classified as O9.5 Ib by Walborn (1973b) and here we reclassify it as O9 II according to the revised criteria around O9.

NX Vel AB = HD 73 882 AB. We cannot spatially resolve the B component indicated by the WDS with a separation of $0''.7$ and a Δm of 1.3 mag. Otero (2003) discovered that this system is an eclipsing binary with a period of 2.9199 days. OWN data show an SB1 orbit with a preliminary period of 20.6 days, raising the total number of bodies in the system to four.

HD 74 920. This O star was inadvertently excluded from Maíz Apellániz et al. (2004) even though it was classified as O8: by Thackeray & Andrews (1974). The ((f)) suffix was omitted by mistake in GOSSS-DR1.0.

HD 75 211. The ((f)) suffix was omitted by mistake in GOSSS-DR1.0. OWN data indicate that it is an SB1 with a 20.4 day period.

HD 75 222. This star was classified as O9.7 Iab by Walborn (1973b), which is maintained here.

CPD -47 2962 = ALS 1215 = CD -47 4550. This star had no previous classifications as being of O type and was not included in Maíz Apellániz et al. (2004). We placed it on the same slit as CPD -47 2963 and discovered it was an O star.

HDE 298 429. This star was classified as O8 III((f)) by Walborn (1982c) and here we reclassify it as O8.5 V.

HD 91 572. This target is an SB1 according to OWN data. The z suffix was added in GOSSS-DR1.1.

HD 91 824. The ((f))z suffix was added in GOSSS-DR1.1. OWN data indicate that it is an SB1 with a 112 day period.

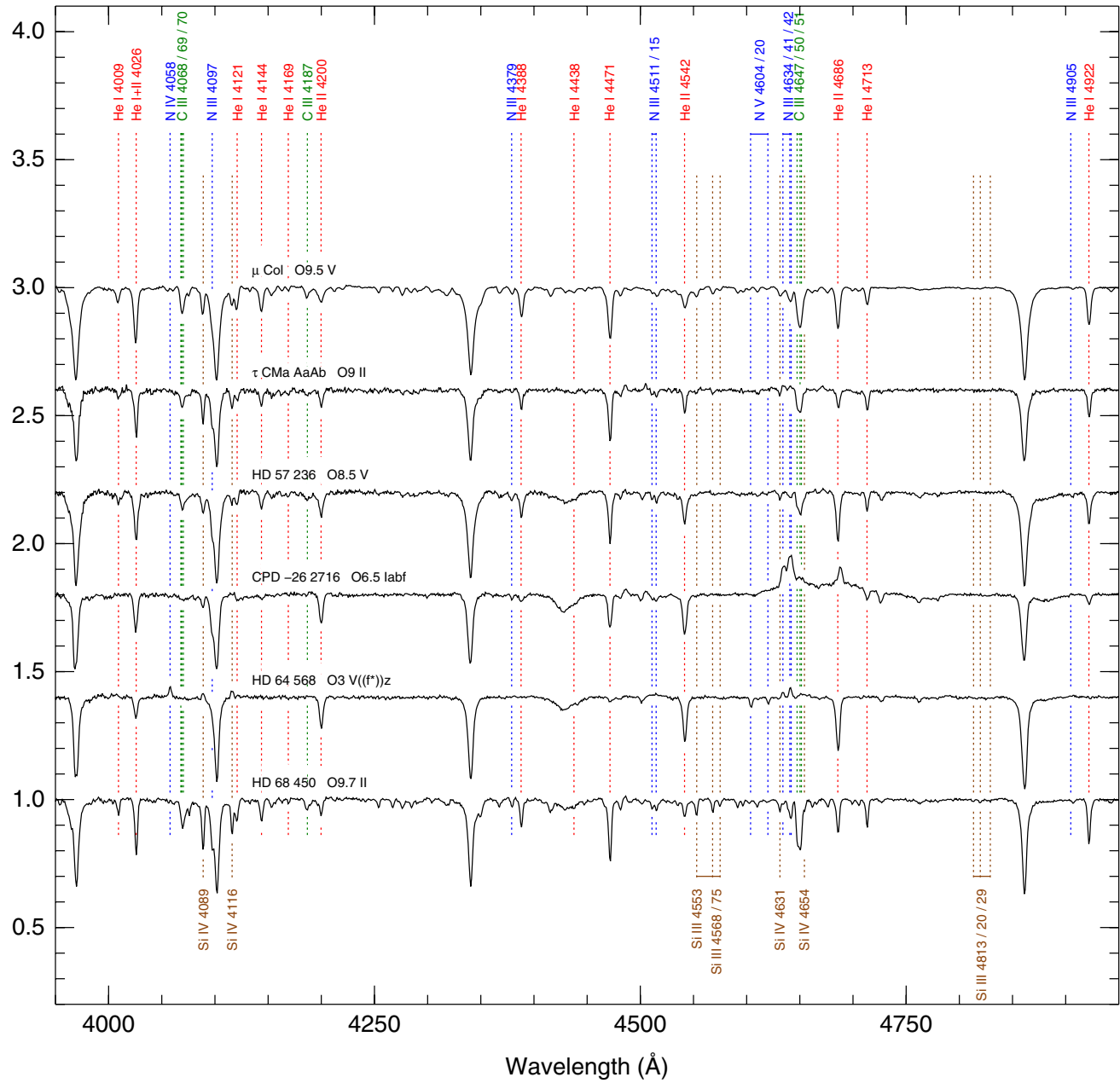


Figure 11. Spectrograms for the stars in the normal sample. The targets are sorted by Right Ascension.
(A color version of this figure is available in the online journal.)

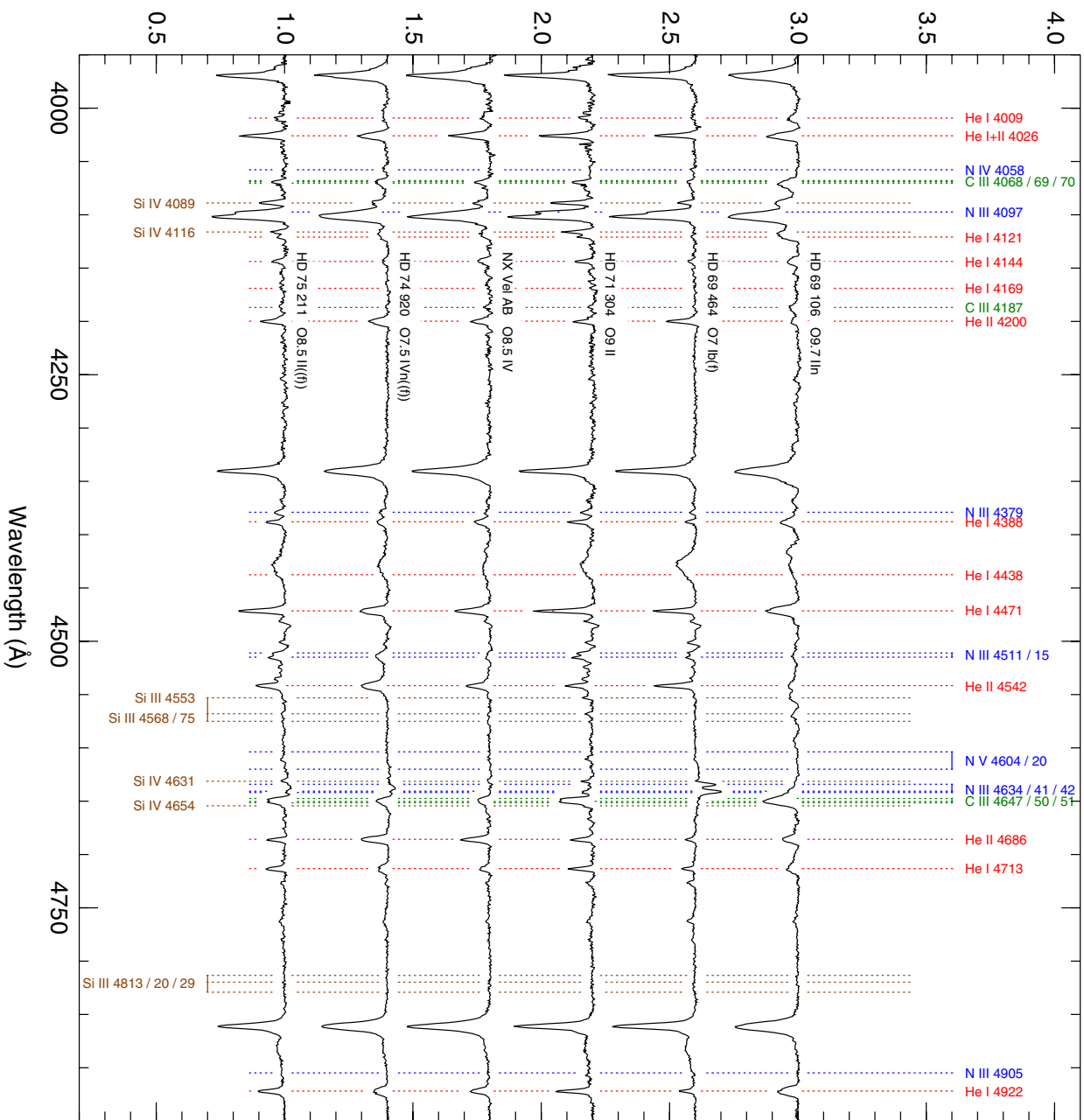


Figure 11. (Continued)

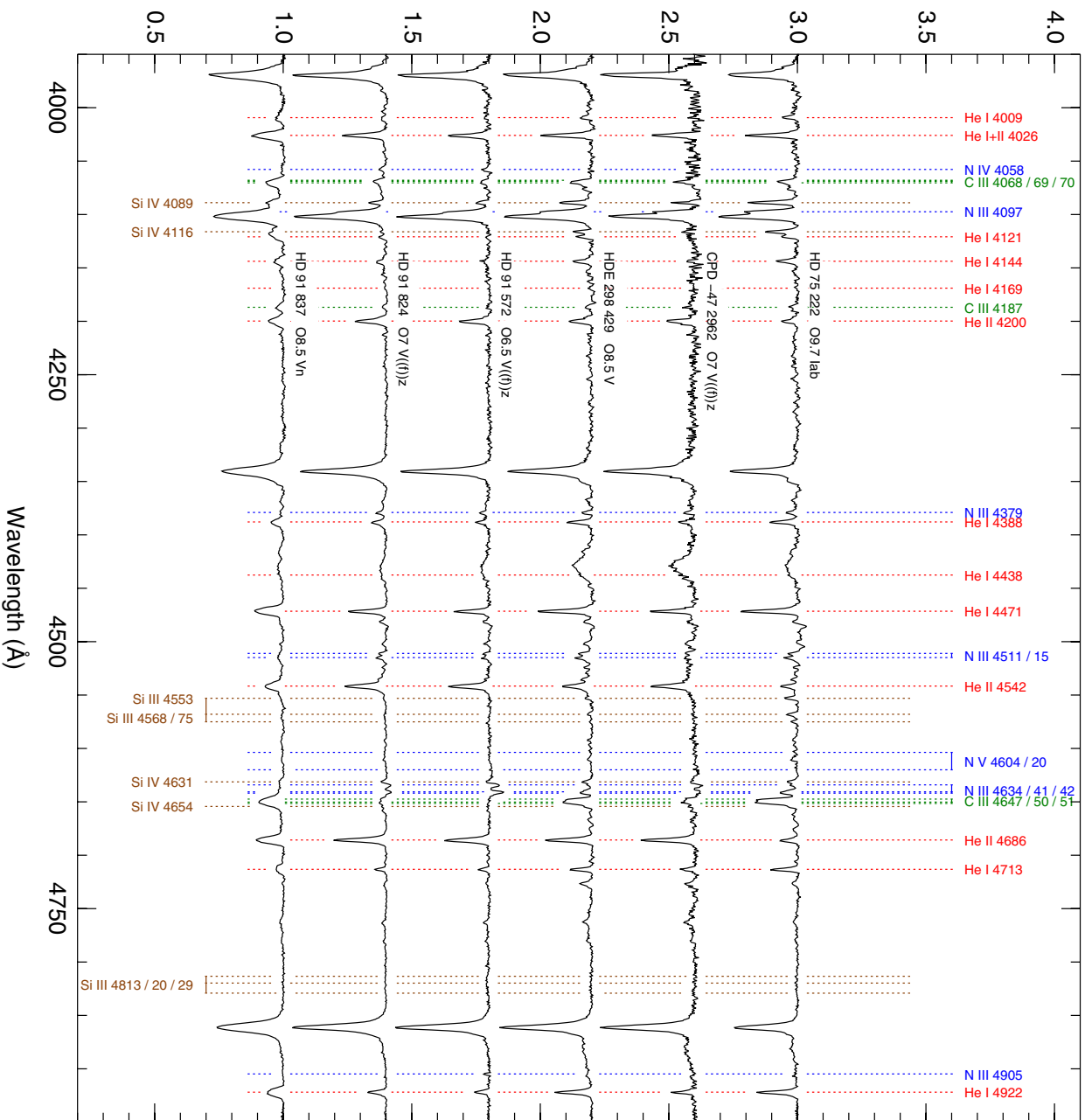


Figure 11. (Continued)

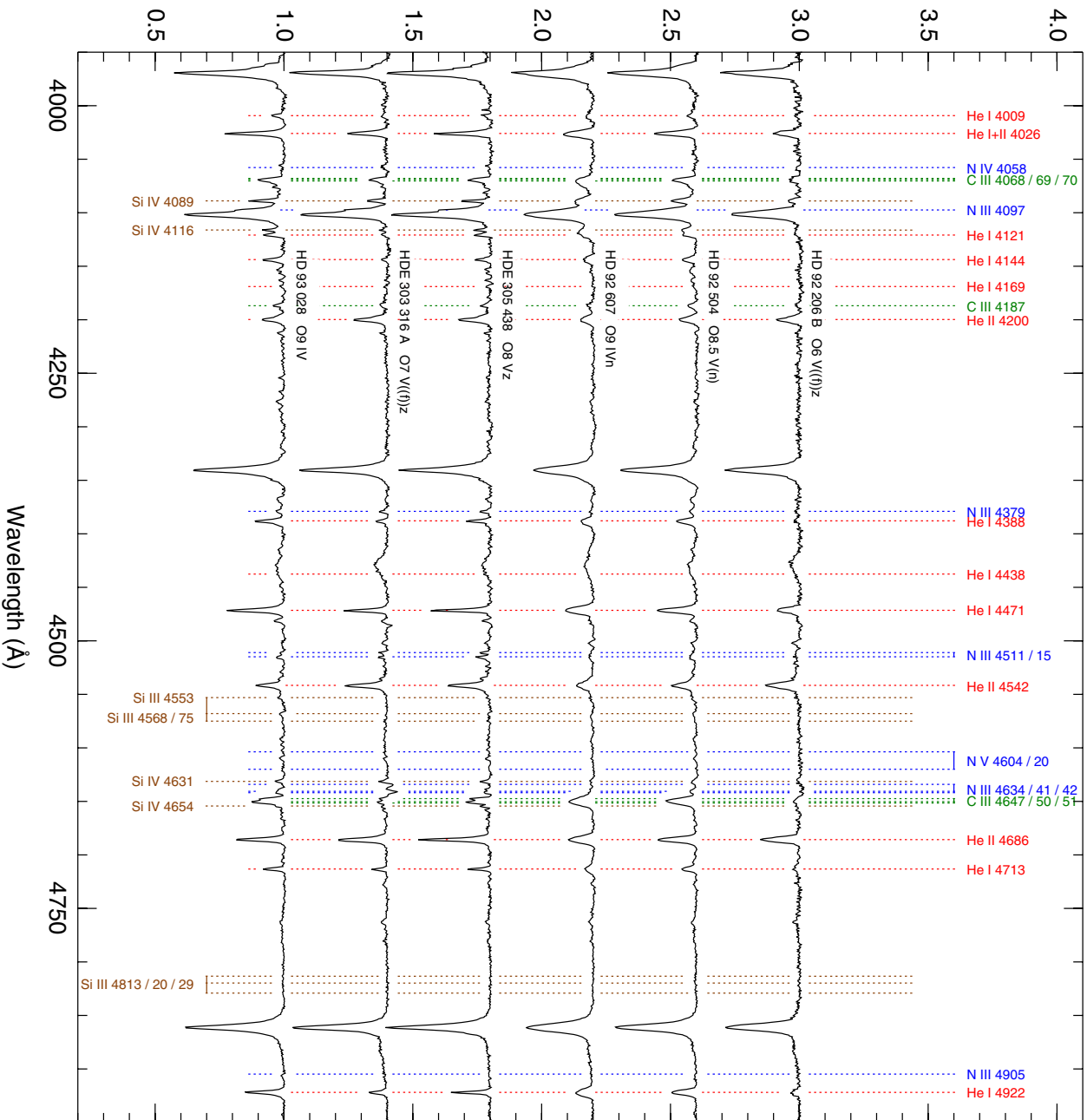


Figure 11. (Continued)

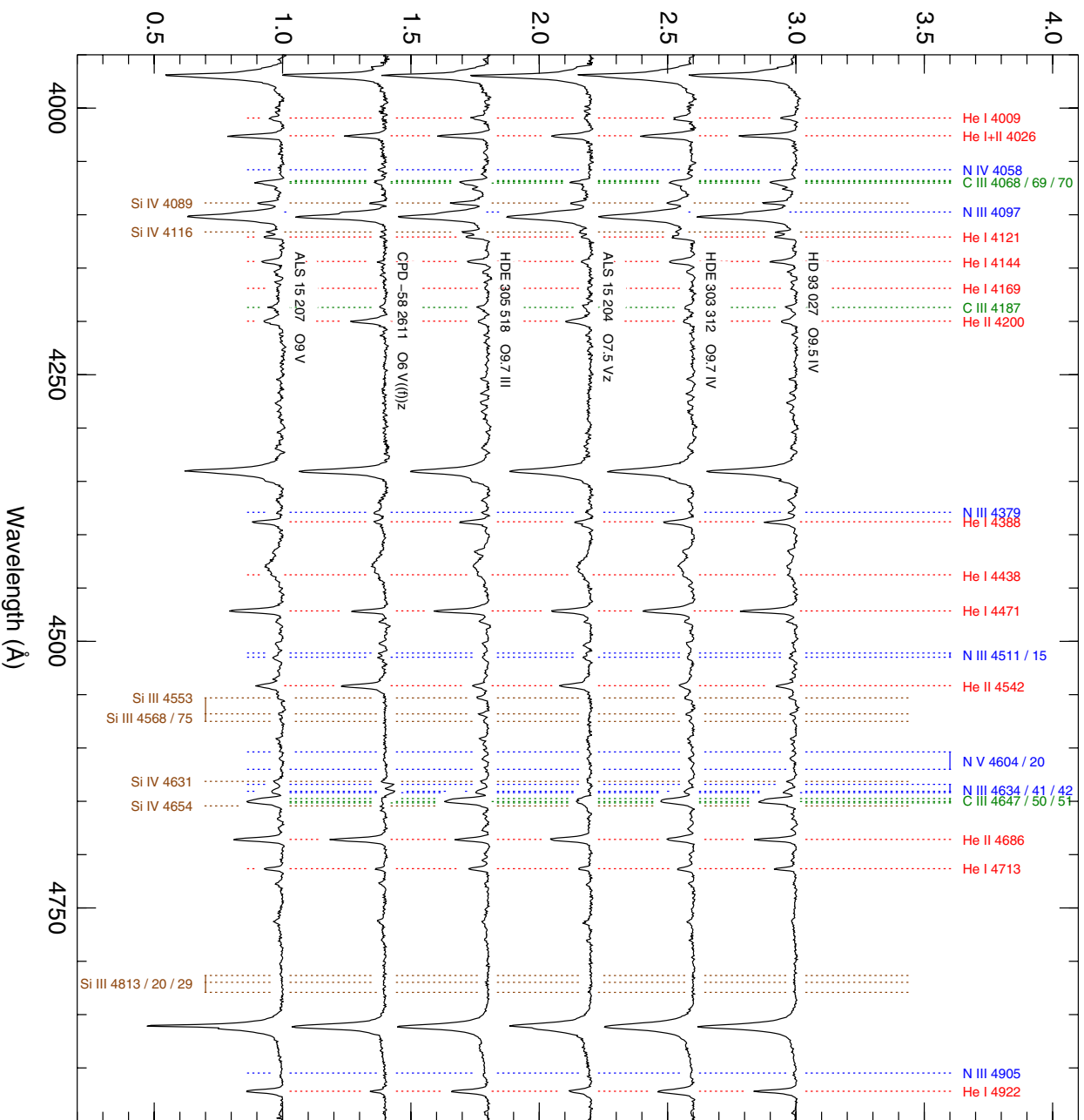


Figure II. (Continued)

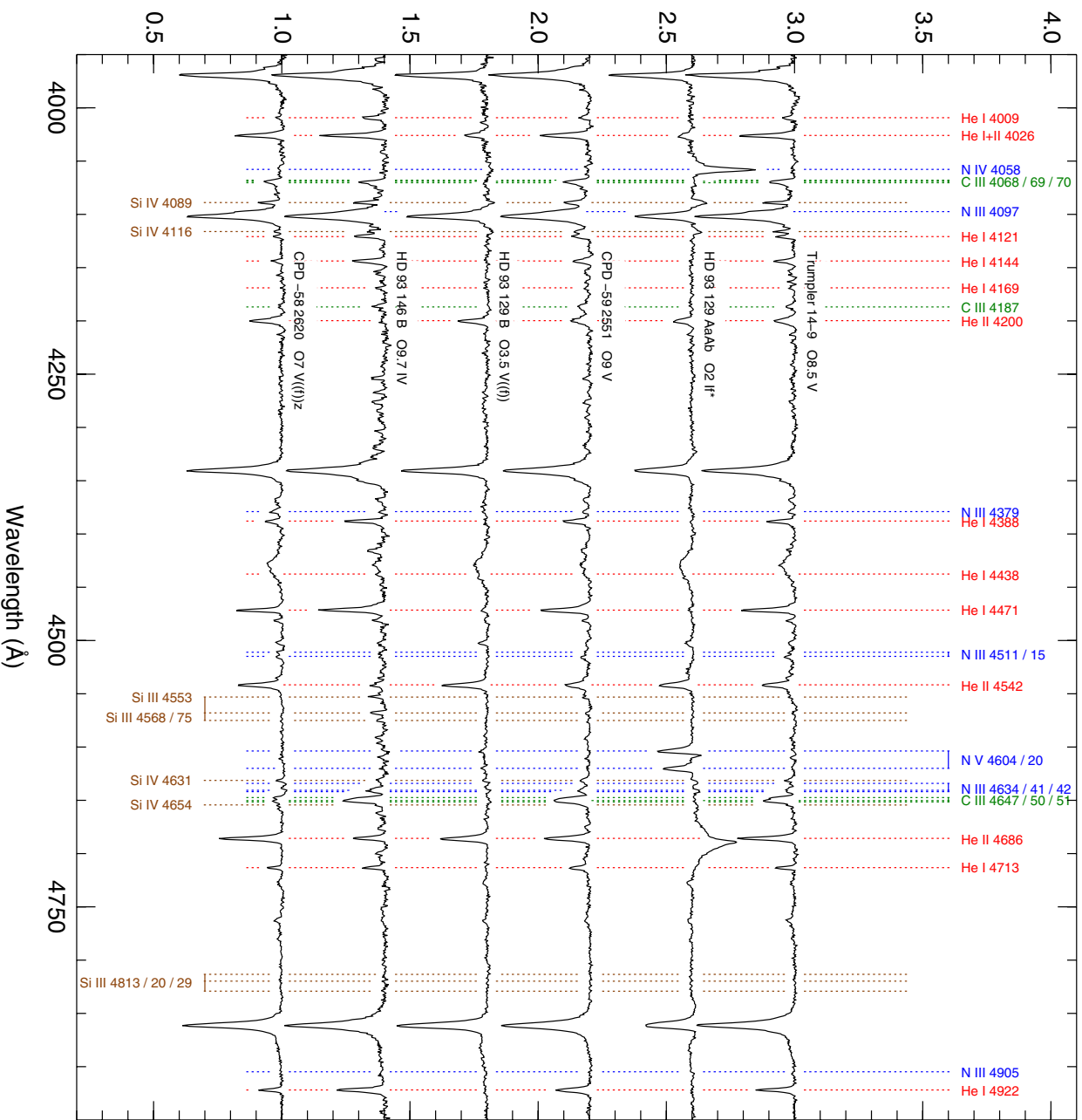


Figure 11. (Continued)

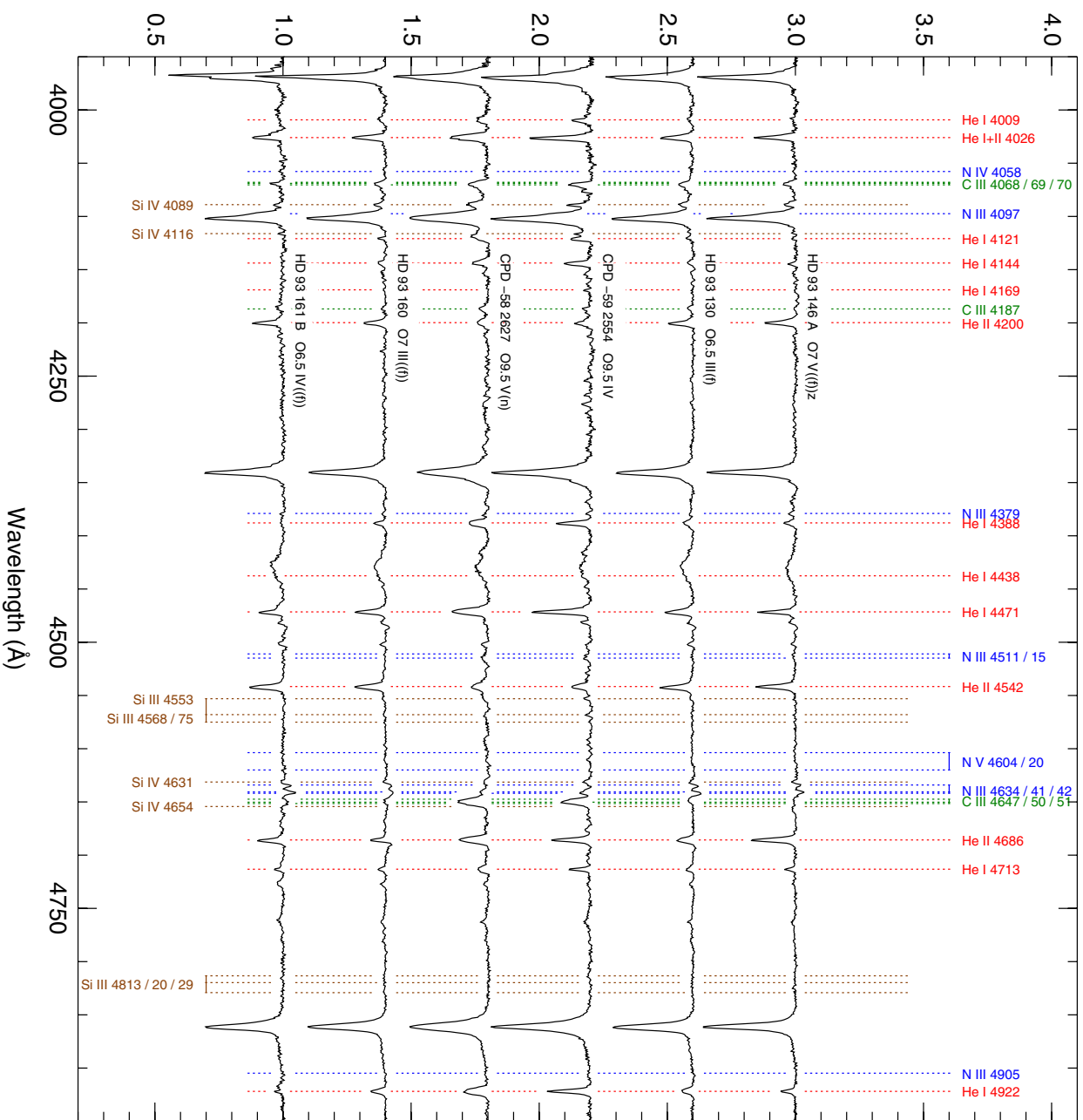
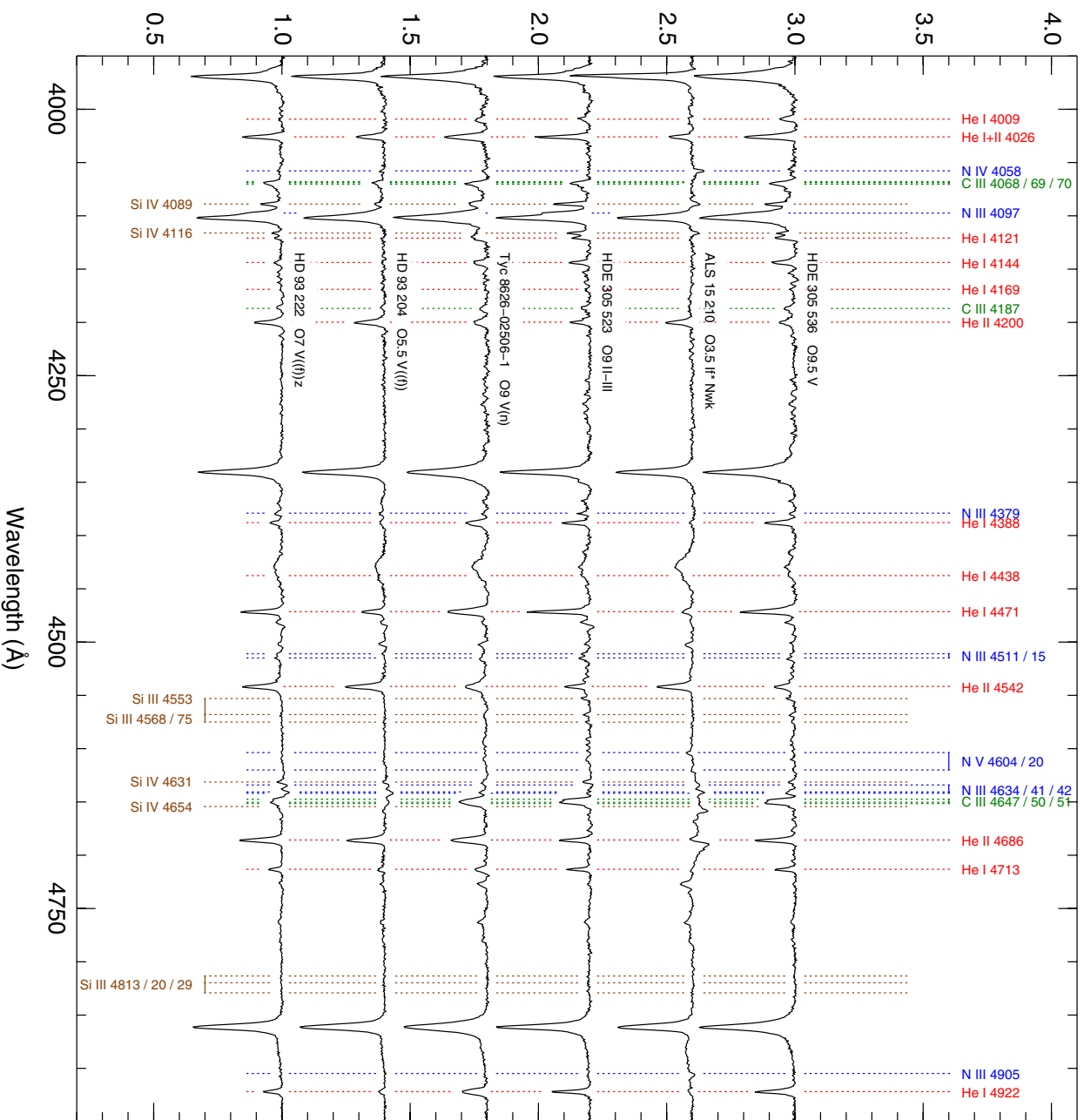


Figure 11. (Continued)



Wavelength (Å)
Figure 11. (Continued)

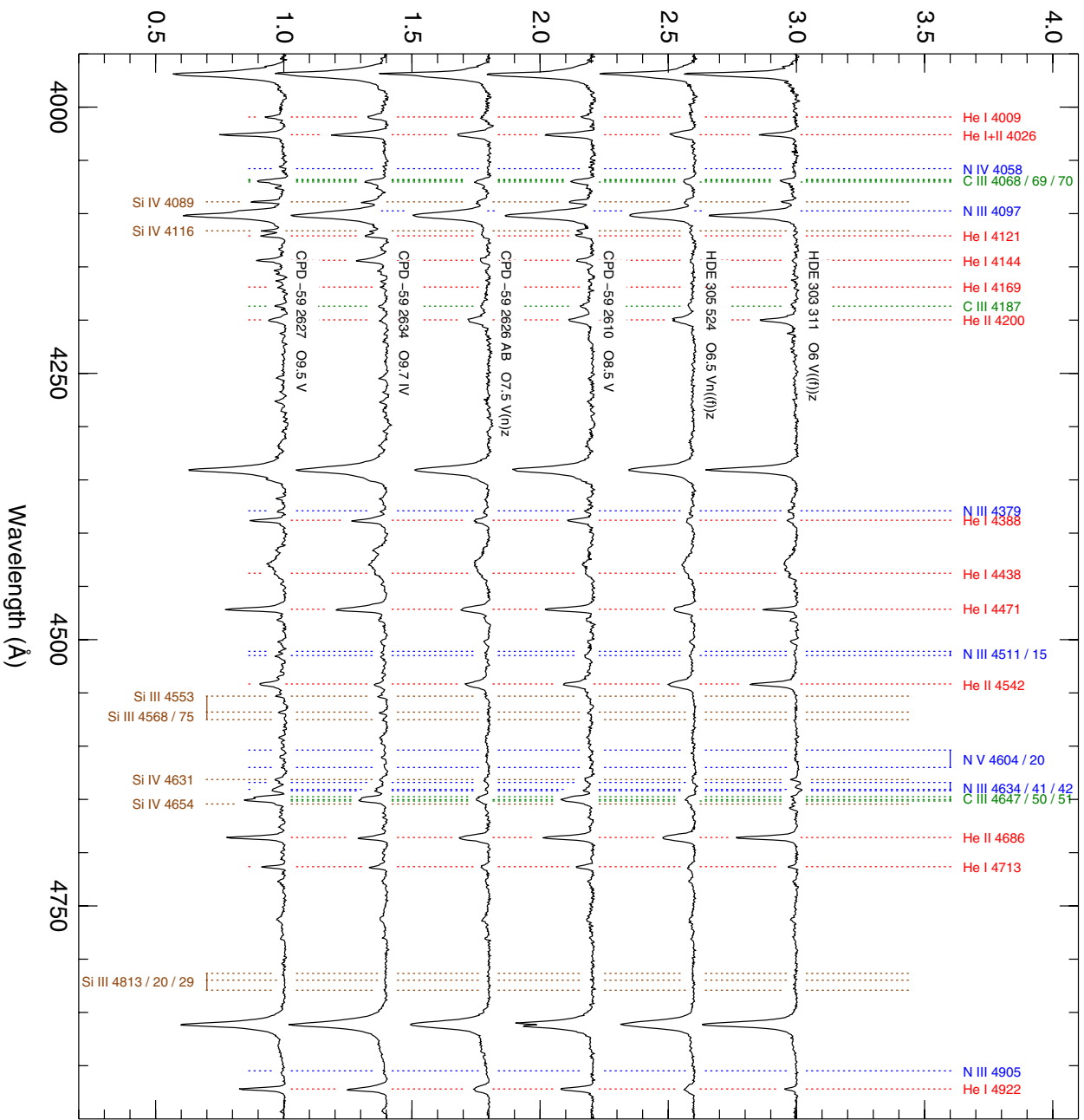


Figure 11. (Continued)

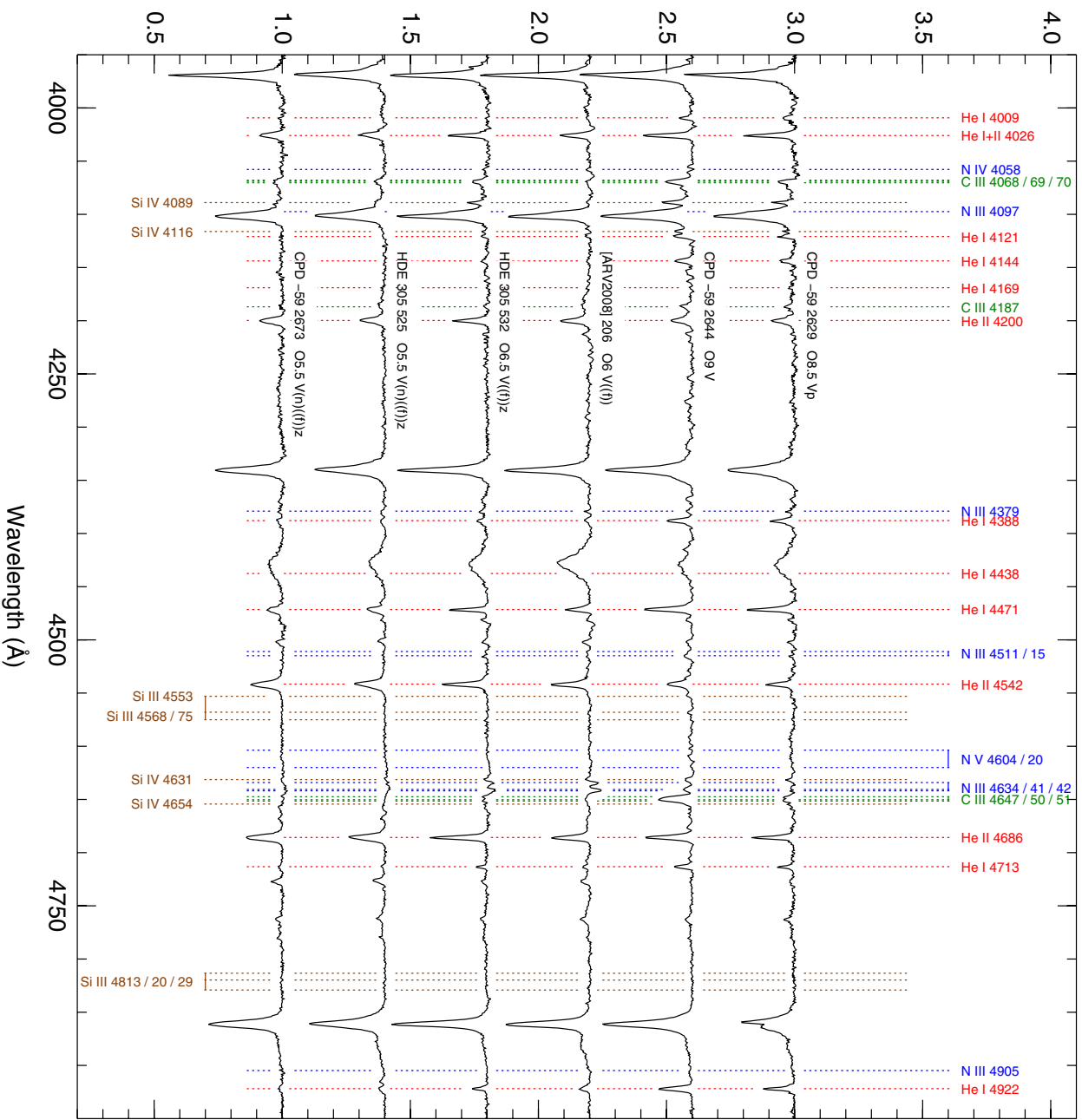


Figure 11. (Continued)

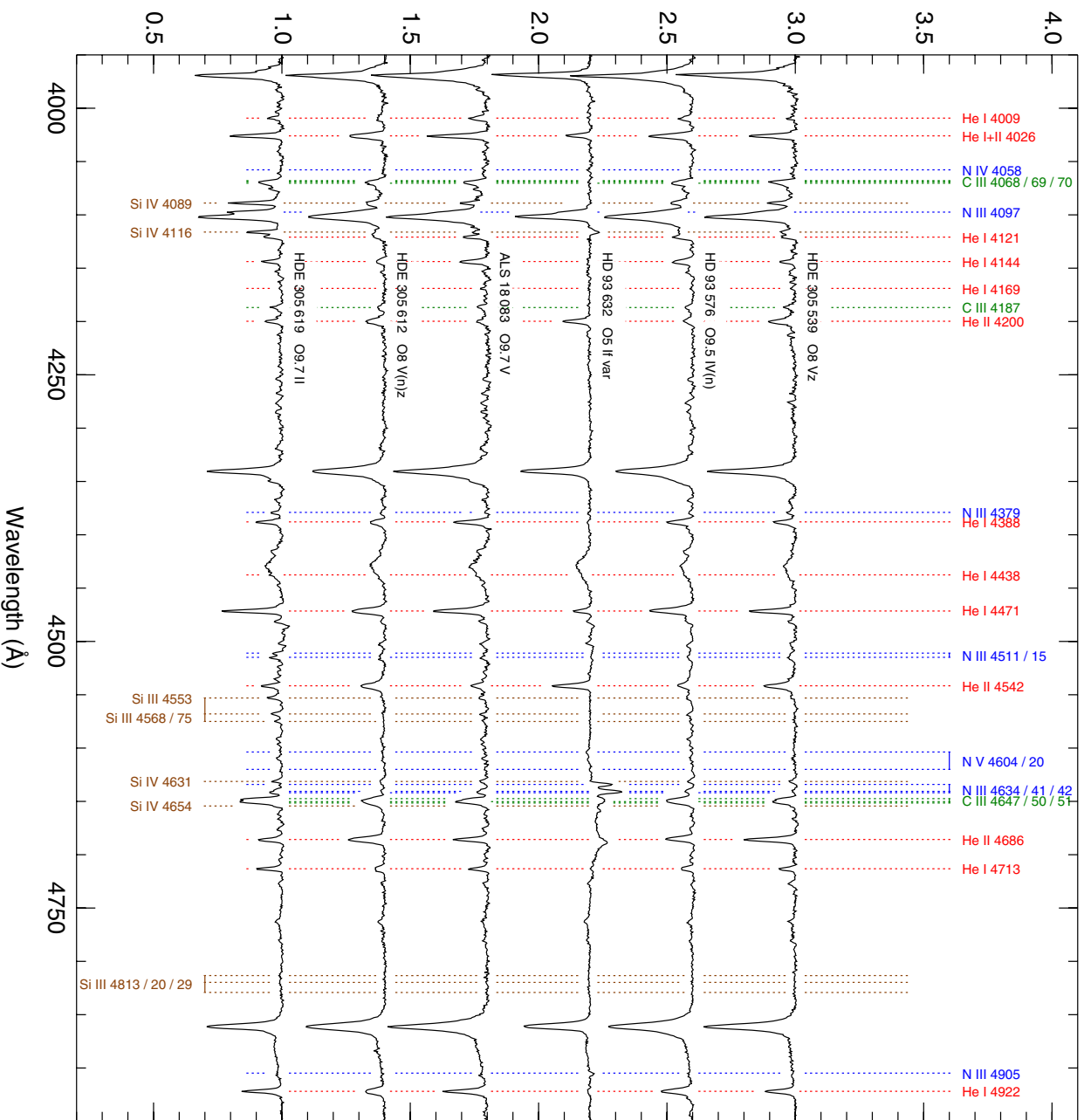


Figure 11. (Continued)

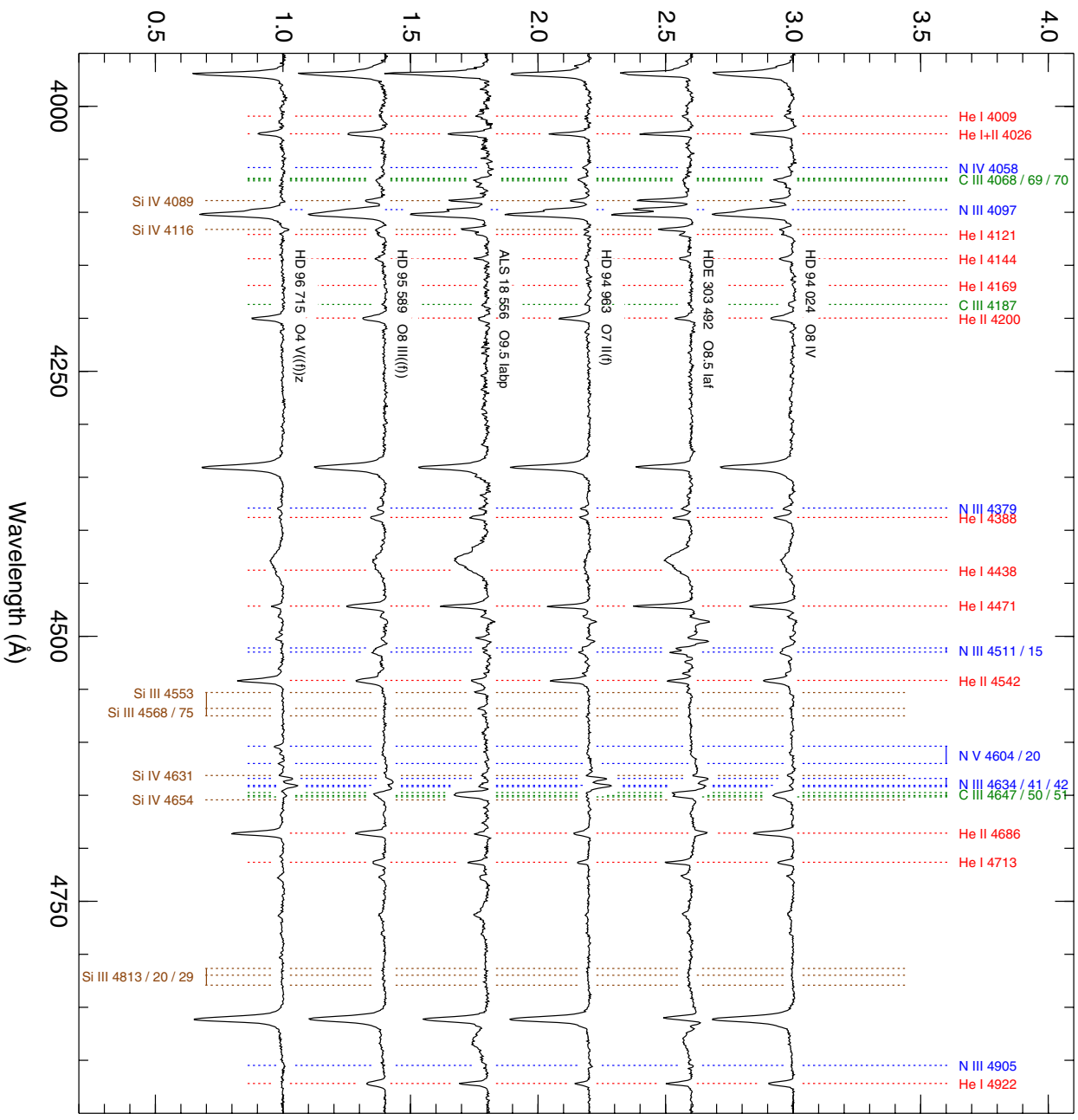


Figure 11. (Continued)

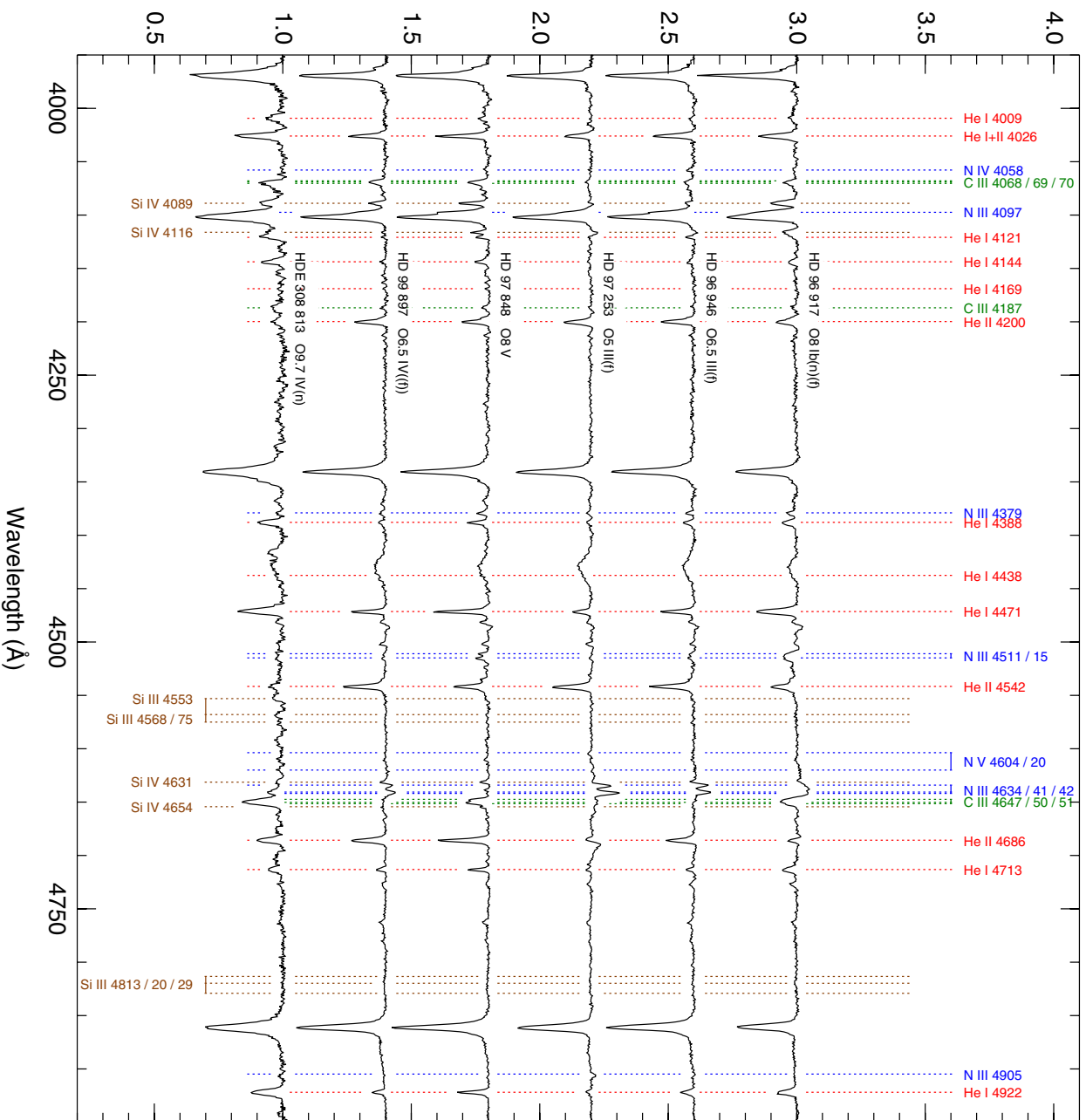
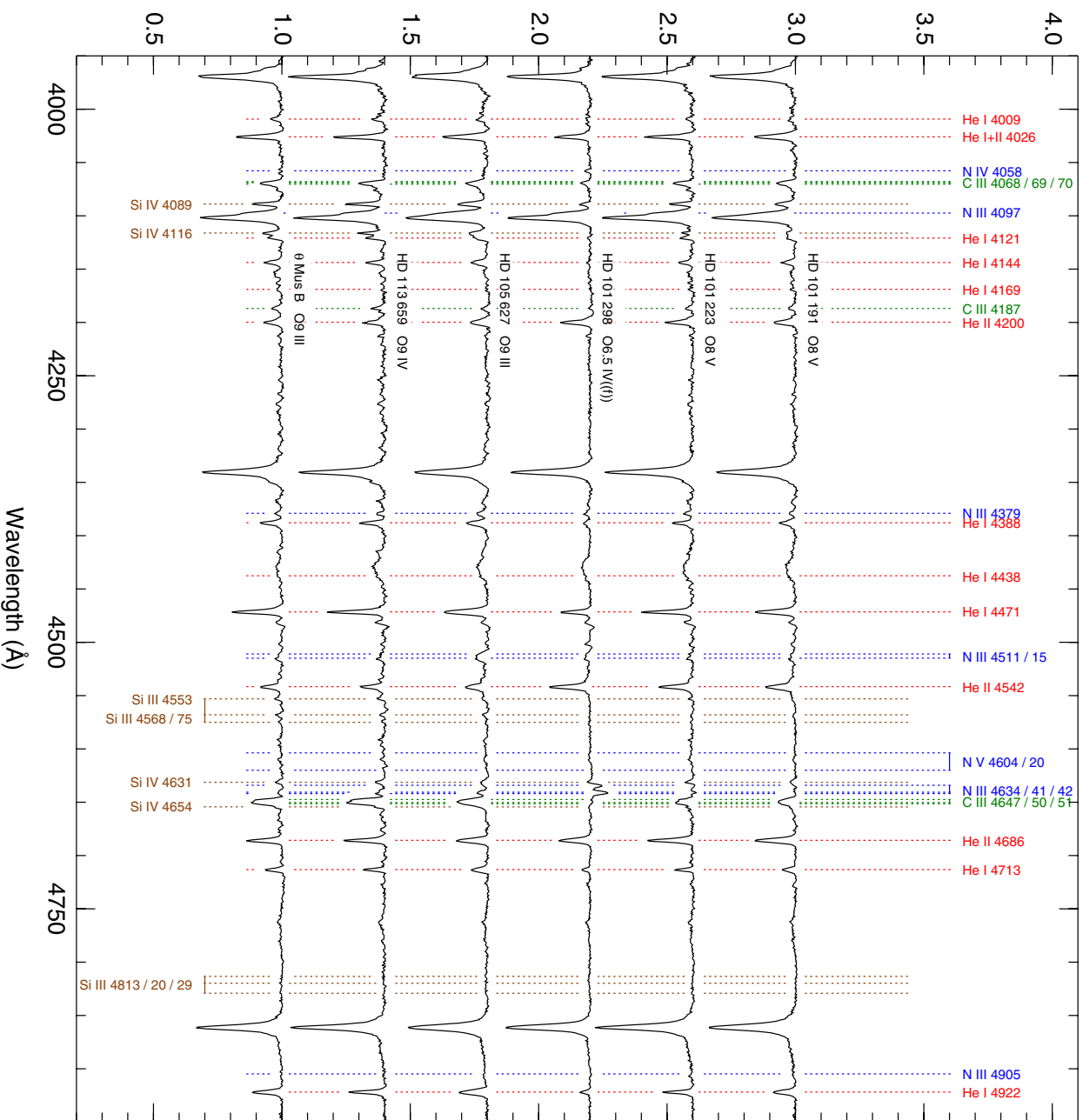


Figure 11. (Continued)



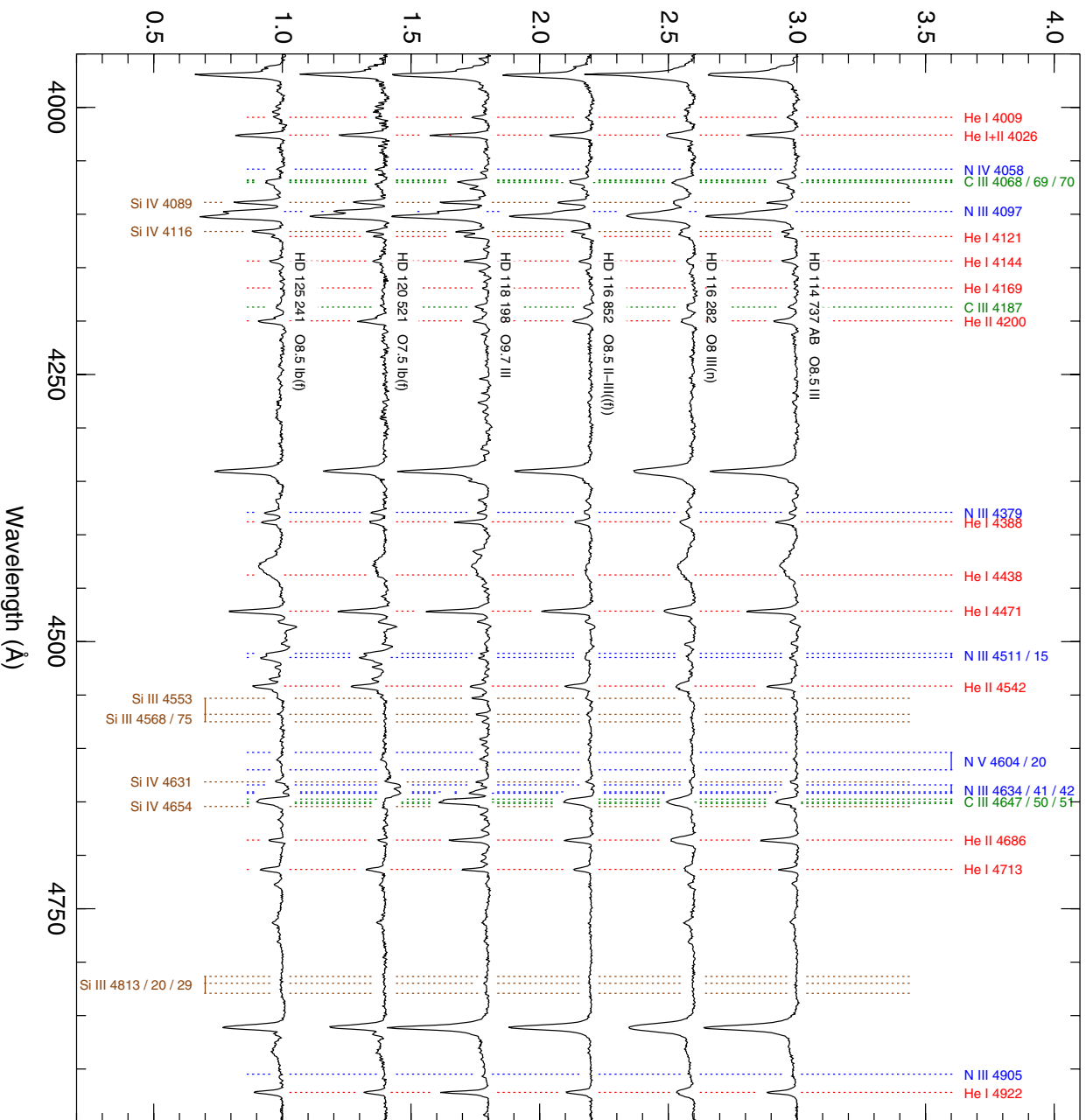
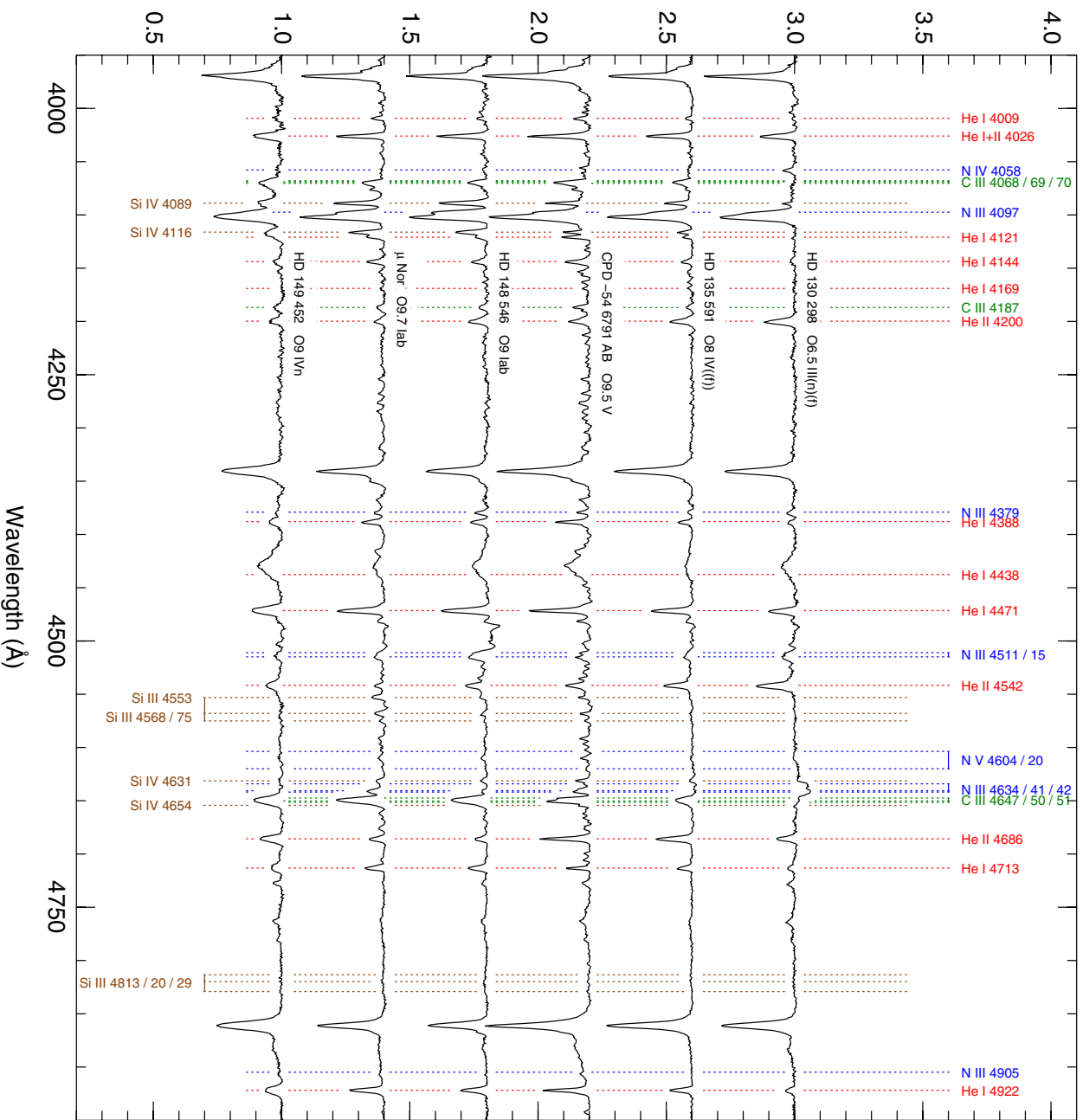


Figure 11. (Continued)



Wavelength (Å)
Figure 11. (Continued)

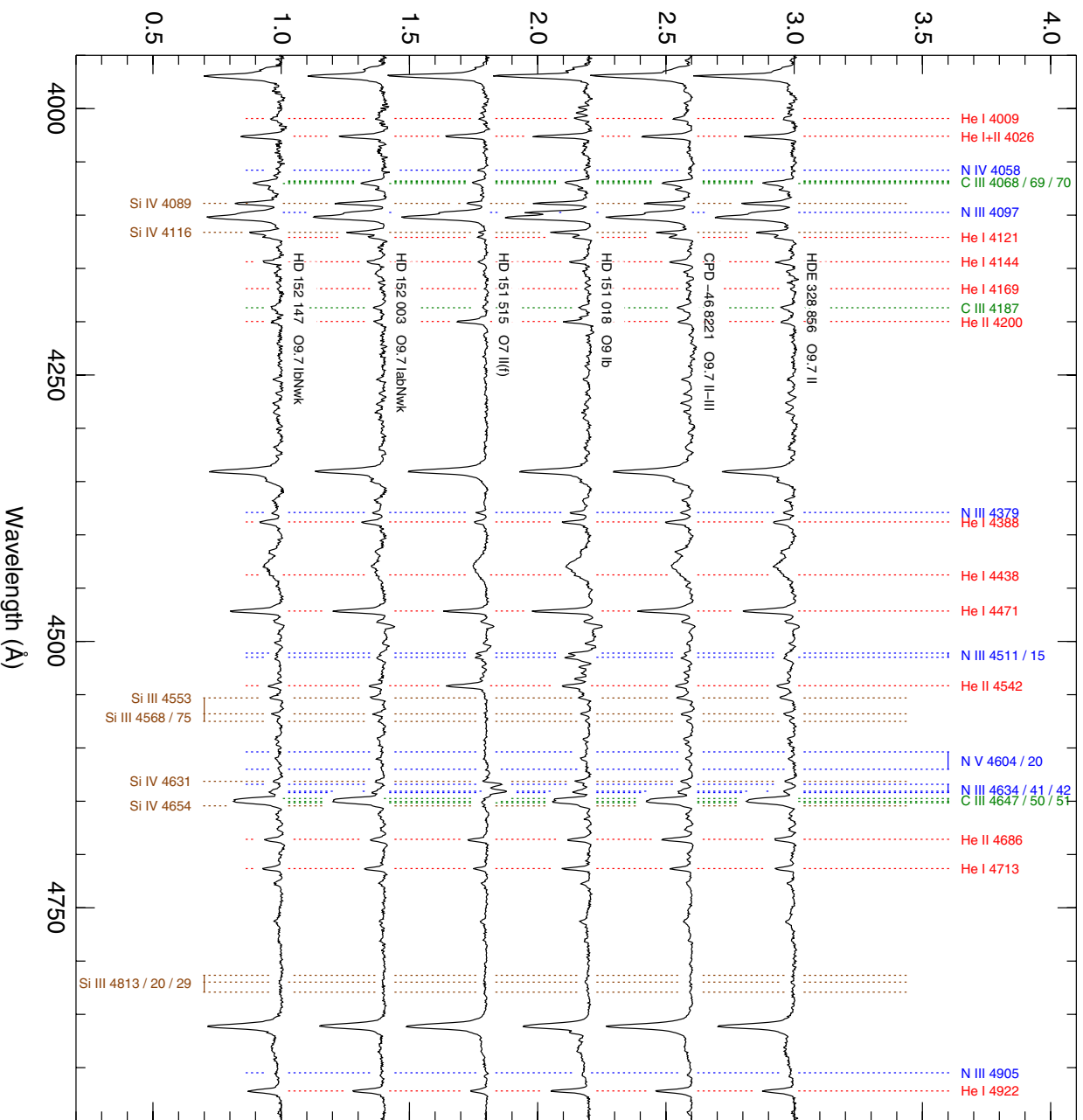
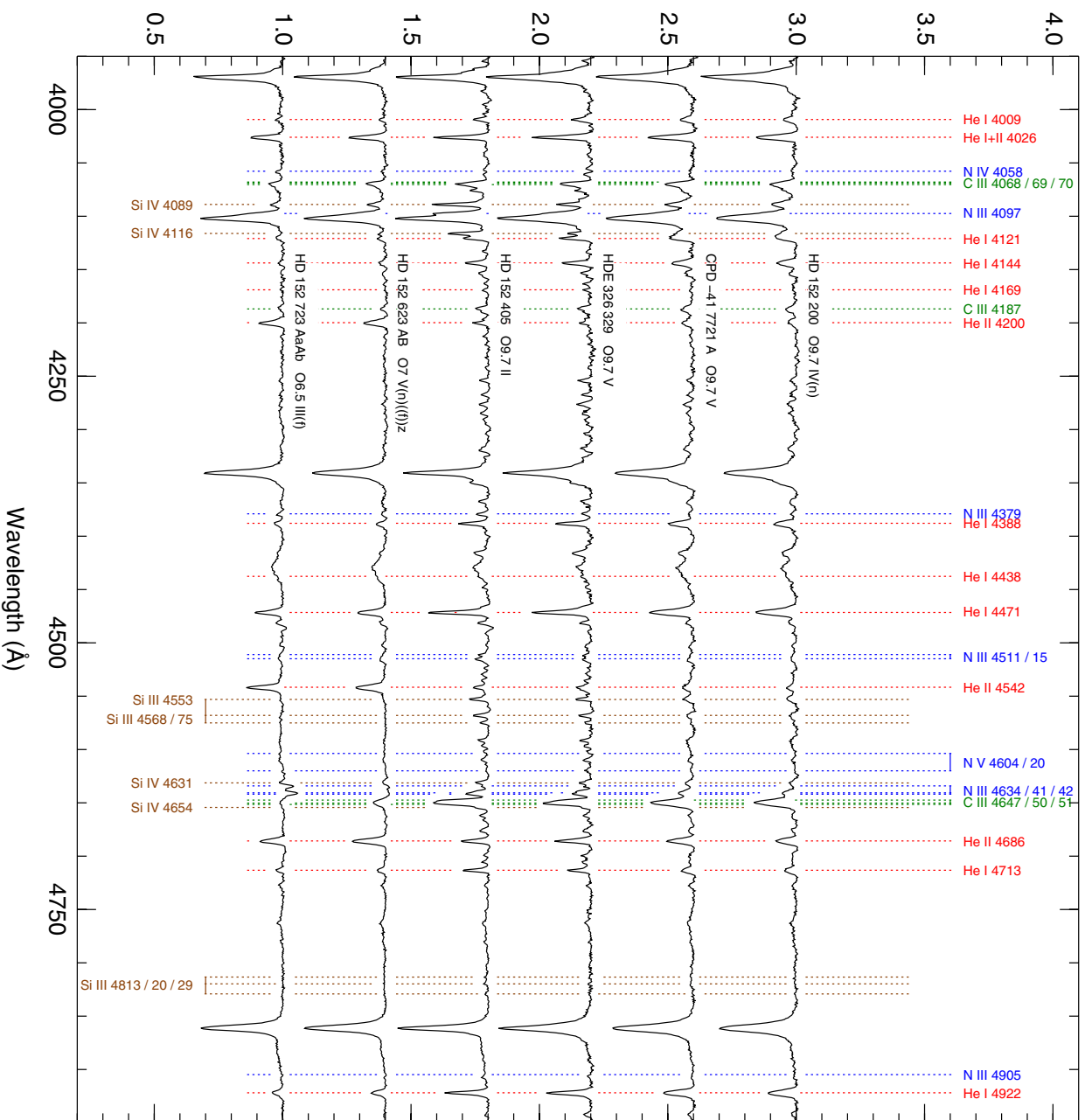
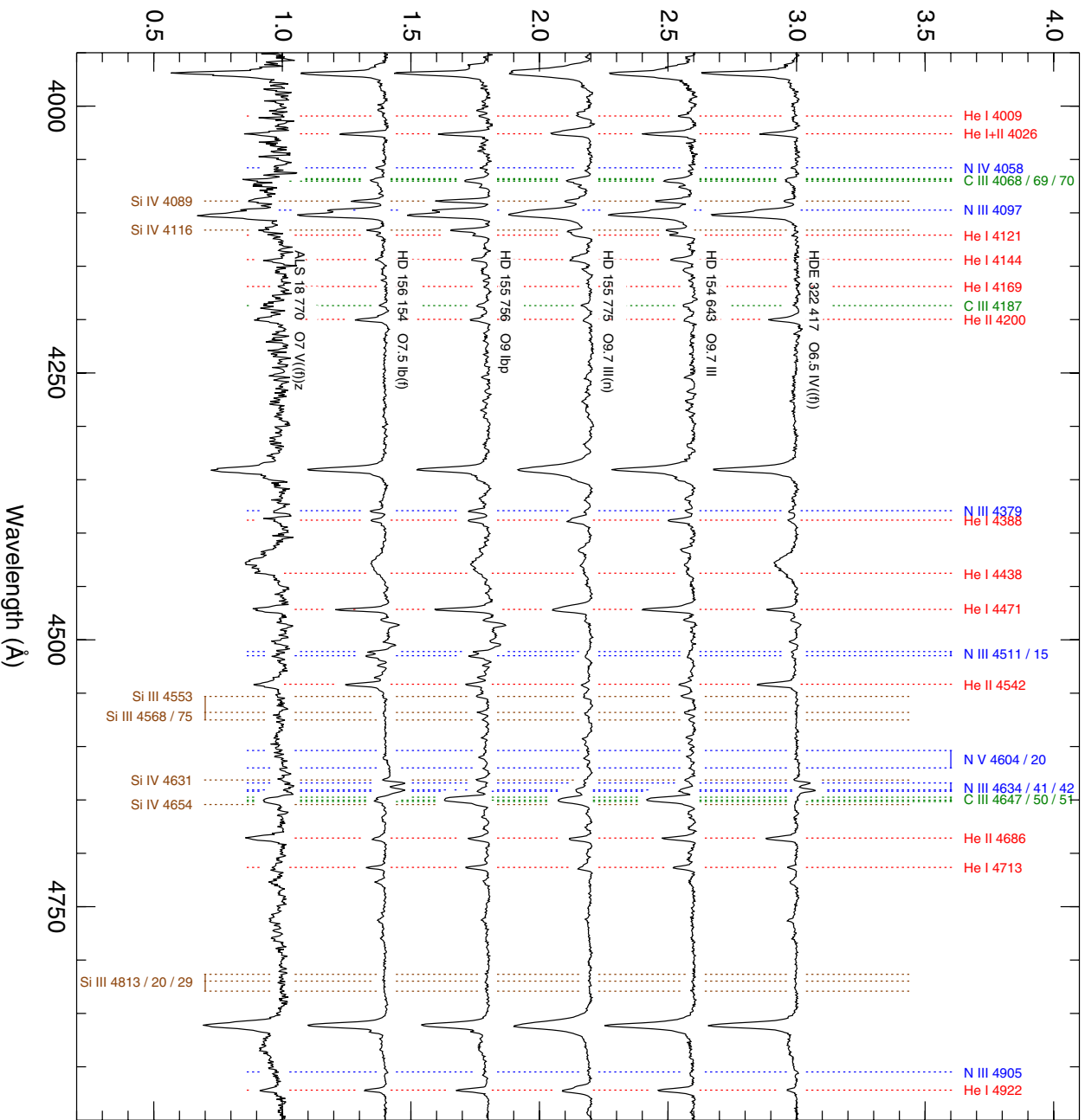


Figure 11. (Continued)





Wavelength (Å)

Figure 11. (Continued)

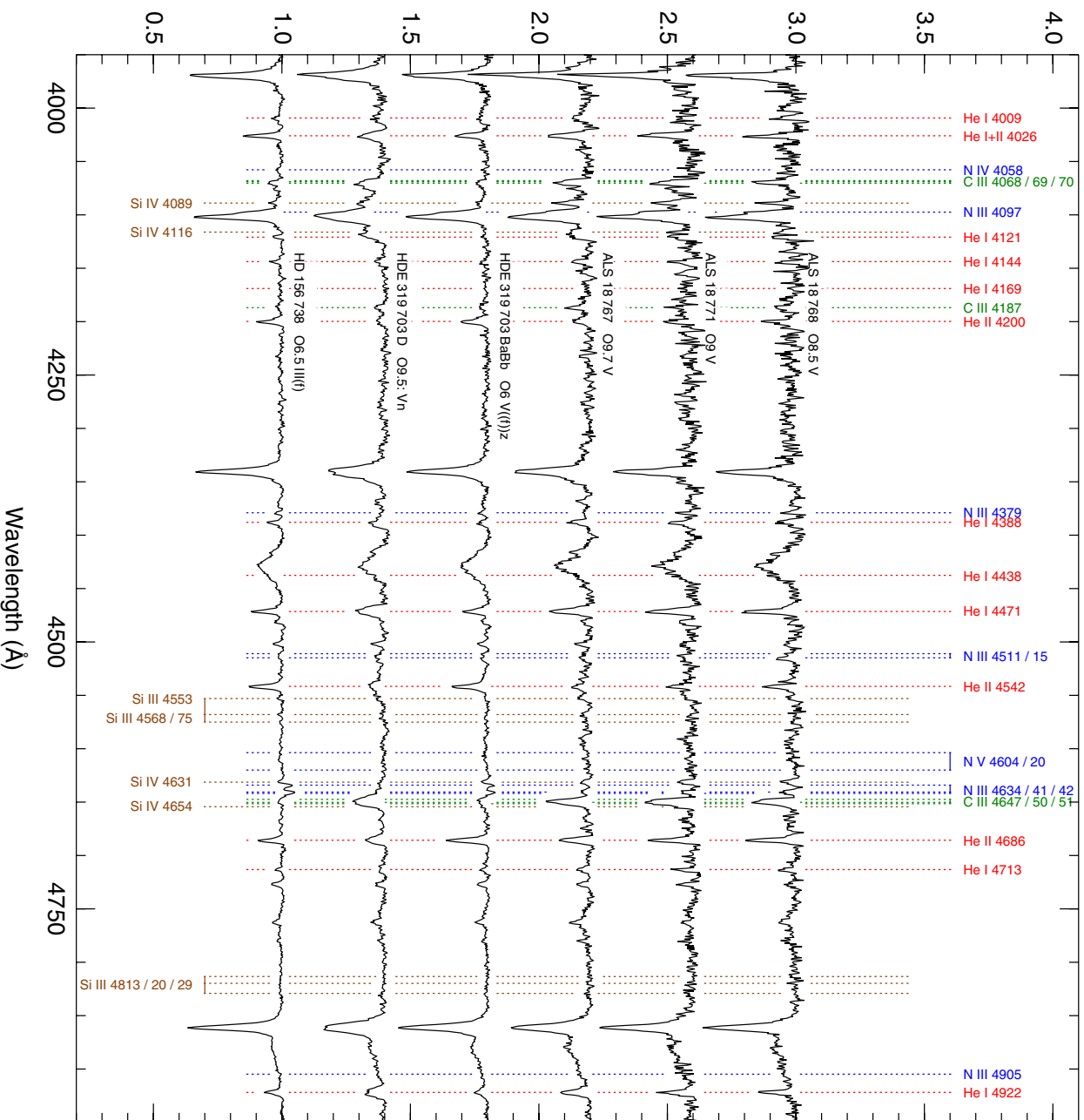


Figure 11. (Continued)

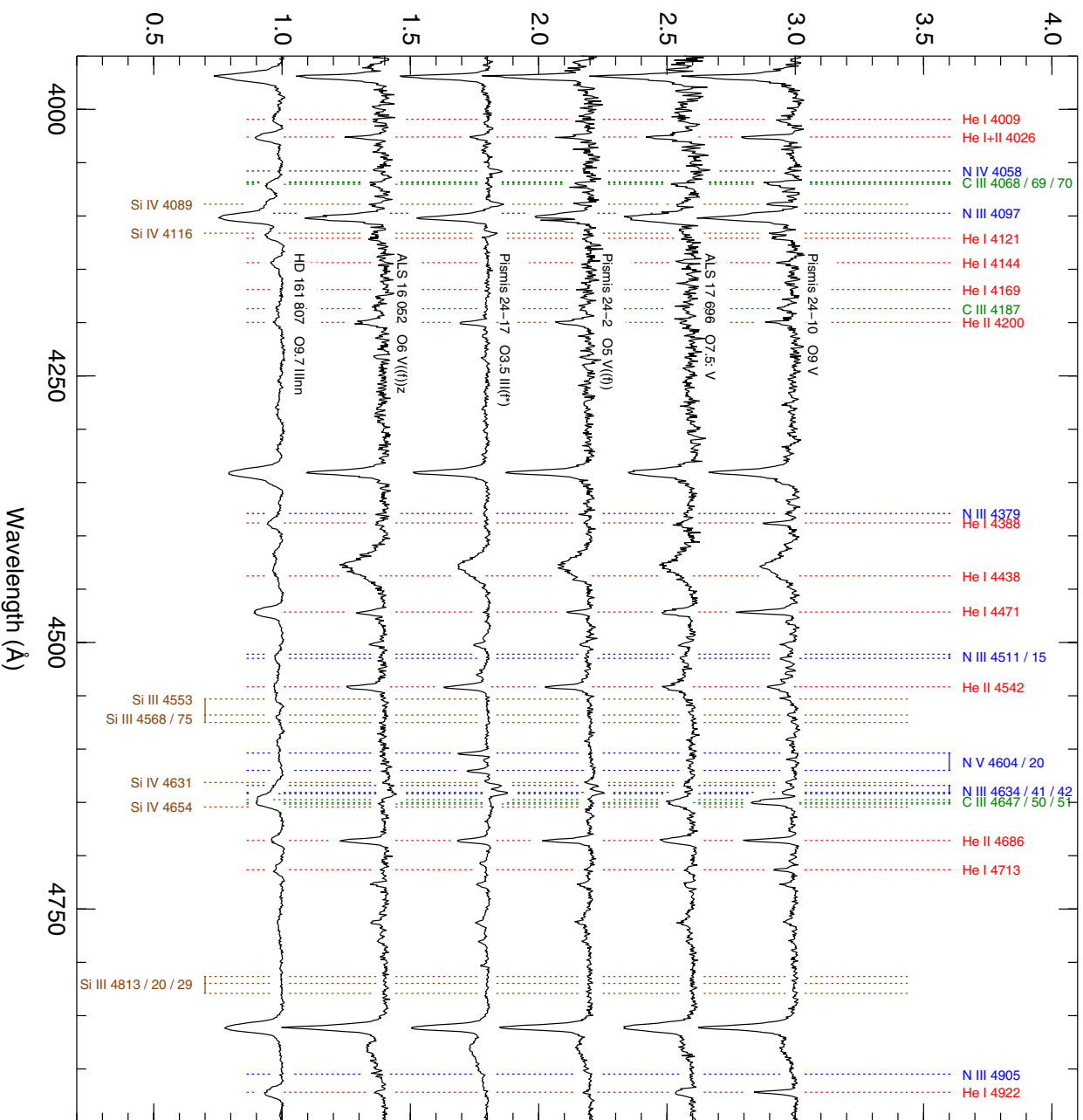


Figure 11. (Continued)

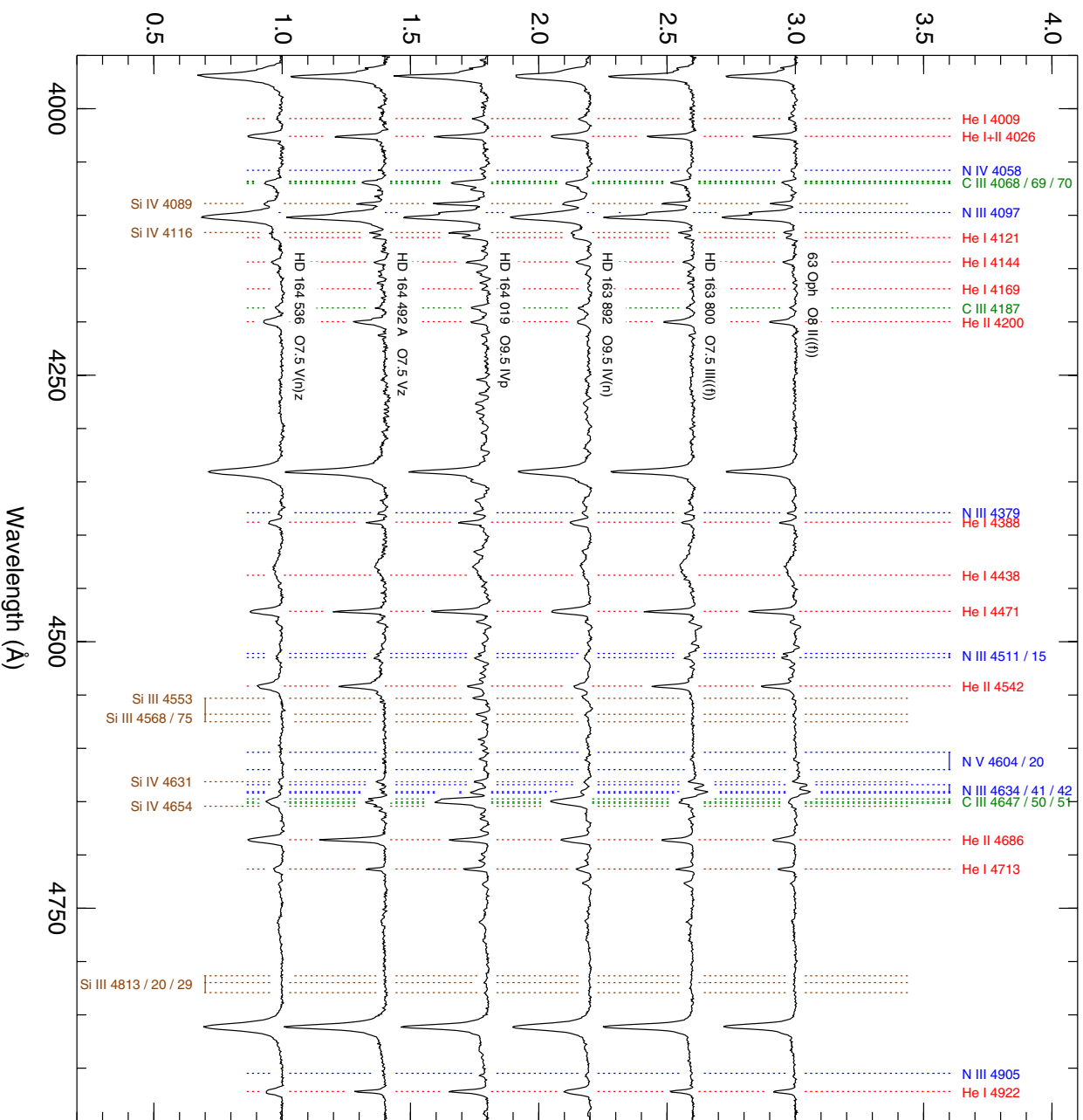


Figure 11. (Continued)

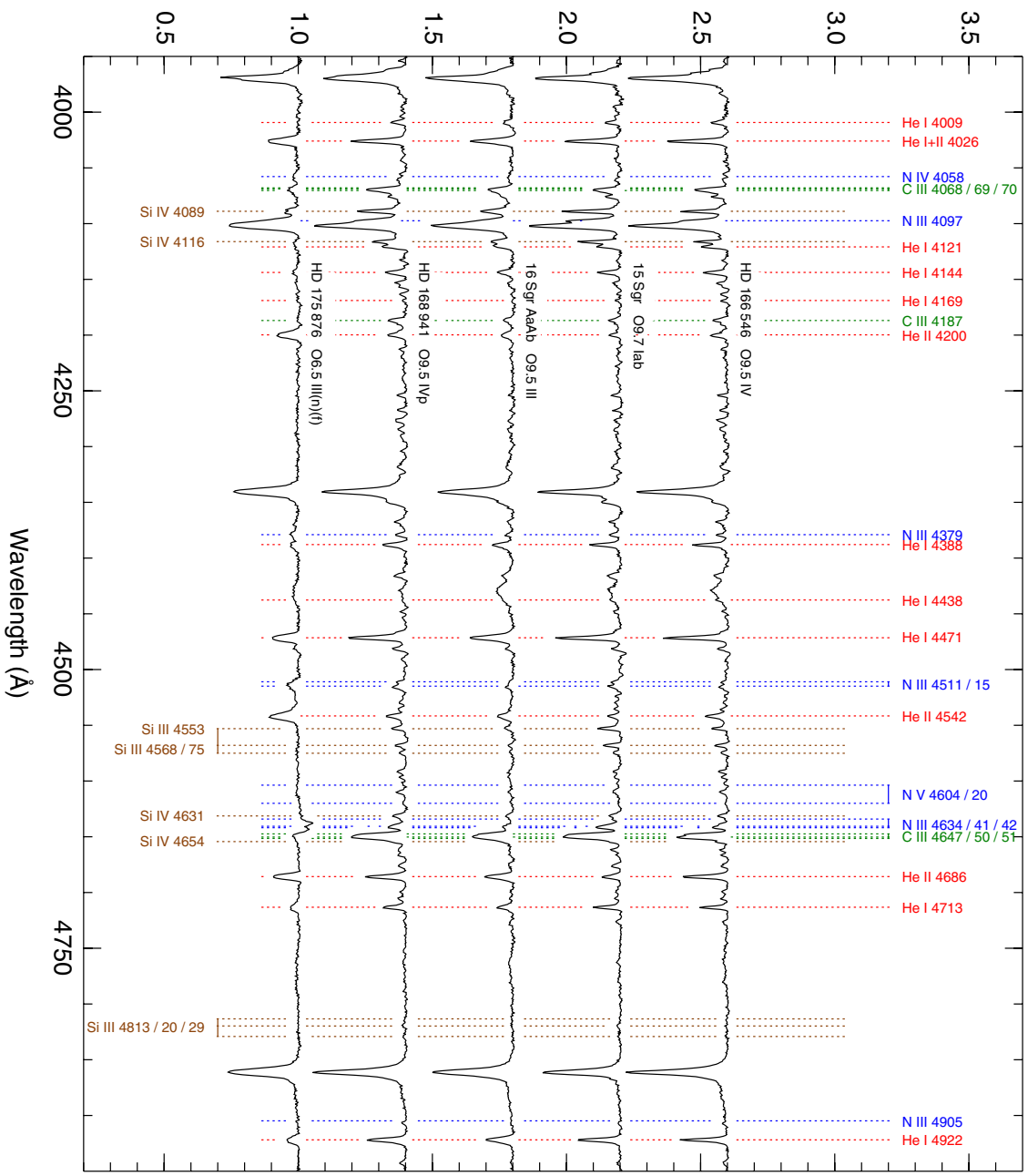


Figure 11. (Continued)

HD 91 837. This star was not included in Maíz Apellániz et al. (2004) and, to our knowledge, had been never classified as an O star.

HD 92 206 B. This star in NGC 3324 was not included in Maíz Apellániz et al. (2004), probably because its spectrum had been previously analyzed only together with that of A (see, e.g., Walborn 1982c). Note that in this system, each of the A, B, and C components contain at least one O star (see previous comments on A and C). See Figure 12 for a chart (HD 92 206 field).

HD 92 504. The WDS lists a companion with a separation of 8".7 and a small Δm . A look at images available in Aladin and the 2MASS Point Source Catalog reveals that the separation is correct but the magnitude difference is significantly larger (over 2 mag).

HD 92 607. This star in the Carina Nebula was not included in Maíz Apellániz et al. (2004) but was previously classified as an O star by Forte & Orsatti (1981).

HDE 305 438. This star in the Carina Nebula was not included in Maíz Apellániz et al. (2004) but was previously classified as an O star by Thackeray & Andrews (1974).

HDE 303 316 A. This star in the Carina Nebula was not included in Maíz Apellániz et al. (2004) but was previously classified as an O star by Forte & Orsatti (1981). A companion with a separation of 10".9 and a Δm of 1.9 mag was spatially resolved with GOSSS; it is an early-B star.

HD 93 028. According to Levato et al. (1990), this object is an SB1 with a 51.554 day period. OWN data indicate that the period is close to four times that value. This star was classified as O9 V by Walborn (1972) and that was revised to O9 IV by Sota et al. (2011).

HD 93 027. This star was classified as O9.5 V by Walborn (1973a) and that was revised to O9.5 IV by Sota et al. (2011).

HDE 303 312 = CPD -58 2604 = V725 Car = CD -58 3523. This star was not included in Maíz Apellániz et al. (2004) but was previously classified as an O star by Forte & Orsatti (1981). Otero (2006) finds it to be an eccentric eclipsing binary with a 9.4109 day period.

ALS 15 204 = Trumpler 14 MJ 92. This object is a serendipitous discovery (hence, it was not included in Maíz Apellániz et al. 2004): it was placed on the slit because another O star was observed nearby. A weak redward component may indicate the presence of a dim spectroscopic B companion. The z suffix was added in GOSSS-DR1.1. See Figure 12 for a chart (Trumpler 14 field).

HDE 305 518. This star was not included in Maíz Apellániz et al. (2004) but was previously classified as an O star by Levato & Malaroda (1982).

CPD -58 2611 = Trumpler 14-20. Walborn (1982c) classified this star as O6 V((f)). We have now added the z suffix but kept the rest unchanged. This star was flagged as a possible SB1 by García et al. (1998). See Figure 12 for a chart (Trumpler 14 field). The visual multiplicity for this target was measured in ACS/WFC images.

ALS 15 207 = Trumpler 14-21. This star was not included in Maíz Apellániz et al. (2004) but was previously classified as an O star by Morrell et al. (1988). See Figure 12 for a chart (Trumpler 14 field).

HD 93 128 = 2MASS J10435441-5932574. This object in the core of Trumpler 14 was one of the O3 stars in Walborn (1982a). Its spectral subtype was revised to O3.5 by Walborn et al. (2002). The ((f))z suffix was inadvertently omitted in GOSSS-DR1.0. Note that there is an error in Table 3 of Paper I:

the range of validity of the ((f*)) suffix is O2-O3, not O2-O3.5 (the latter is applicable only to (f*) and f*). Levato et al. (1991) indicate that it is an SB1 but its radial velocity appears to be constant in OWN data. See Figure 12 for a chart (Trumpler 14 field). The visual multiplicity for this target was measured in ACS/HRC images.

Trumpler 14-9 = Trumpler 14 MJ 165 = 2MASS J10435540-5932493. This star was not included in Maíz Apellániz et al. (2004) but was previously classified as an O star by Morrell et al. (1988). The z suffix was removed in GOSSS-DR1.1. See Figure 12 for a chart (Trumpler 14 field) and Figure 16 for an ACS/HRC image. The visual multiplicity for this target was measured in ACS/HRC images.

HD 93 129 AaAb. This object was considered an O3 star in Walborn (1982a) and later became the prototype O2 If* (Walborn et al. 2002). It is the most massive system at the core of Trumpler 14 in the Carina Nebula. It was split by Nelan et al. (2004) into two components (Aa and Ab) using *HST*/FGS. Later observations with *HST*/HRC and *HST*/FGS by Maíz Apellániz et al. (2005, 2008b) detected a proper motion along the radius vector (i.e., near-constant position angle) between Aa and Ab with an average value (updated with unpublished data) of 2.14 ± 0.21 mas/a and a separation of ≈ 40 mas in early 2009. The Δm of 0.9 indicates that both Aa and Ab must be very early-type O stars. See Figure 12 for a chart (Trumpler 14 field), Figure 16 for an ACS/HRC image, and below for the B component. The visual multiplicity for this target was measured in ACS/HRC images. The system is a colliding-wind binary (Benaglia et al. 2010; De Becker & Rauq 2013).

CPD -59 2551 = Collinder 228-21. This star was not included in Maíz Apellániz et al. (2004) but was previously classified as an O star by Levato & Malaroda (1981). See Figure 12 for a chart (HD 93 146 field).

HD 93 129 B. This object was the third O3 star in Walborn (1982a) (besides HD 93 129 A - now AaAb and an O2 - and HD 93 128) located in the core of Trumpler 14. It is separated by 2".5 from AaAb and has magnitudes similar to its siblings HD 93 129 Ab and HD 93 128. The target has C III $\lambda 4650$ in emission but is not strong enough to warrant a c suffix. See Figure 12 for a chart (Trumpler 14 field) and Figure 16 for an ACS/HRC image. The visual multiplicity for this target was measured in ACS/HRC images.

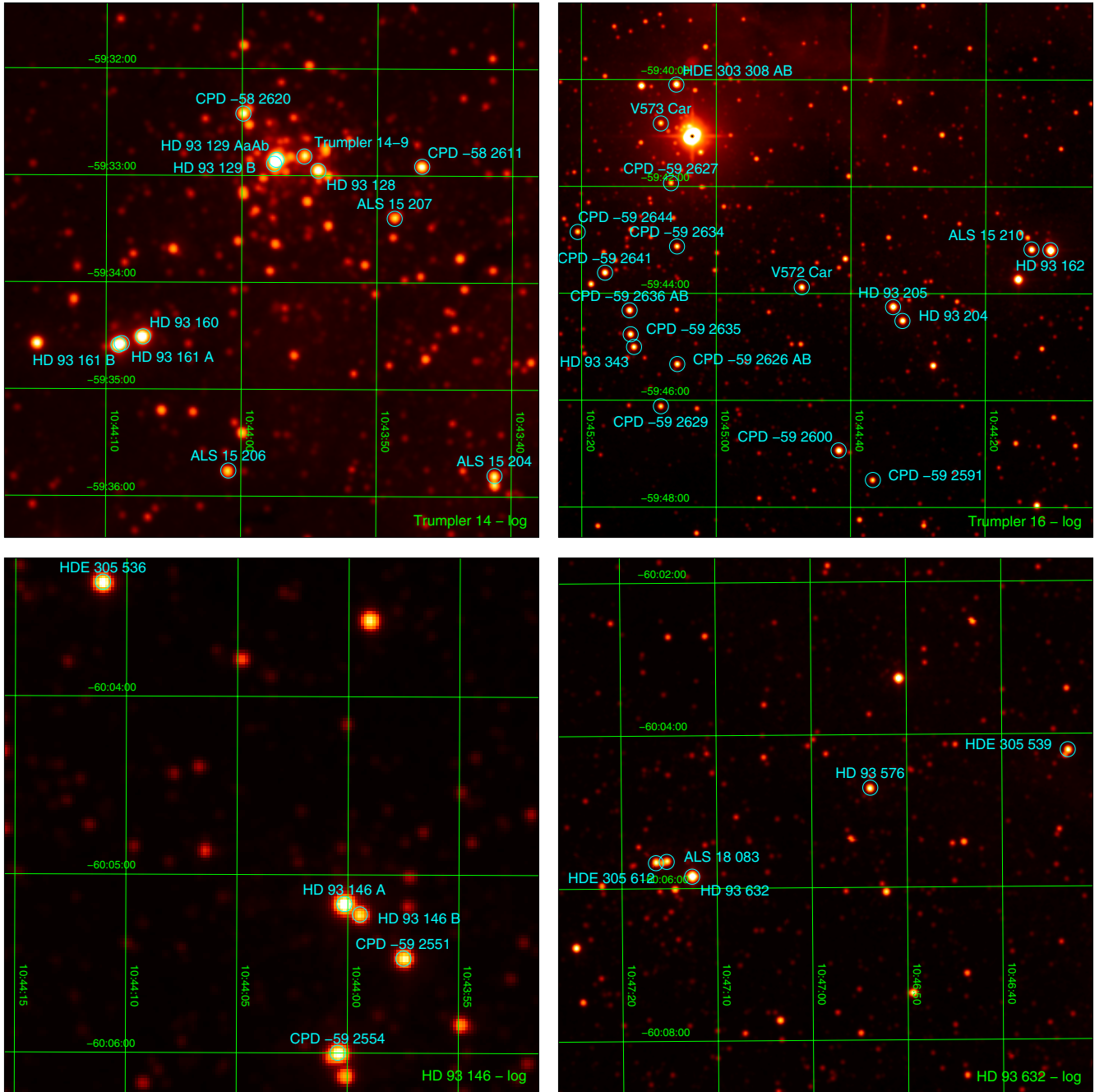
HD 93 146 B. This star was not included in Maíz Apellániz et al. (2004) but was previously classified as an O star by Levato & Malaroda (1981). According to the WDS, the A (see below) and B components of HD 93 146 have a Δm of 1.5 mag and a separation of 6".5. Both are O stars. See Figure 12 for a chart (HD 93 146 field).

CPD -58 2620 = Trumpler 14-8. The ((f)) suffix was omitted by mistake in GOSSS-DR1.0. See Figure 12 for a chart (Trumpler 14 field).

HD 93 146 A. The ((f))z suffix was added in GOSSS-DR1.1. See Figure 12 for a chart (HD 93 146 field) and above for a brief description of HD 93 146 B. OWN data indicate that it is an SB1 with a 1130 day period.

HD 93 130 = V661 Car. This object is an eccentric eclipsing binary with a 23.944 day period (Otero 2006). OWN data also show that it is an SB1.

CPD -59 2554 = Collinder 228-67. This star was not included in Maíz Apellániz et al. (2004) but was classified as an O star by Massey et al. (2001). See Figure 12 for a chart (HD 93 146 field).



(a)

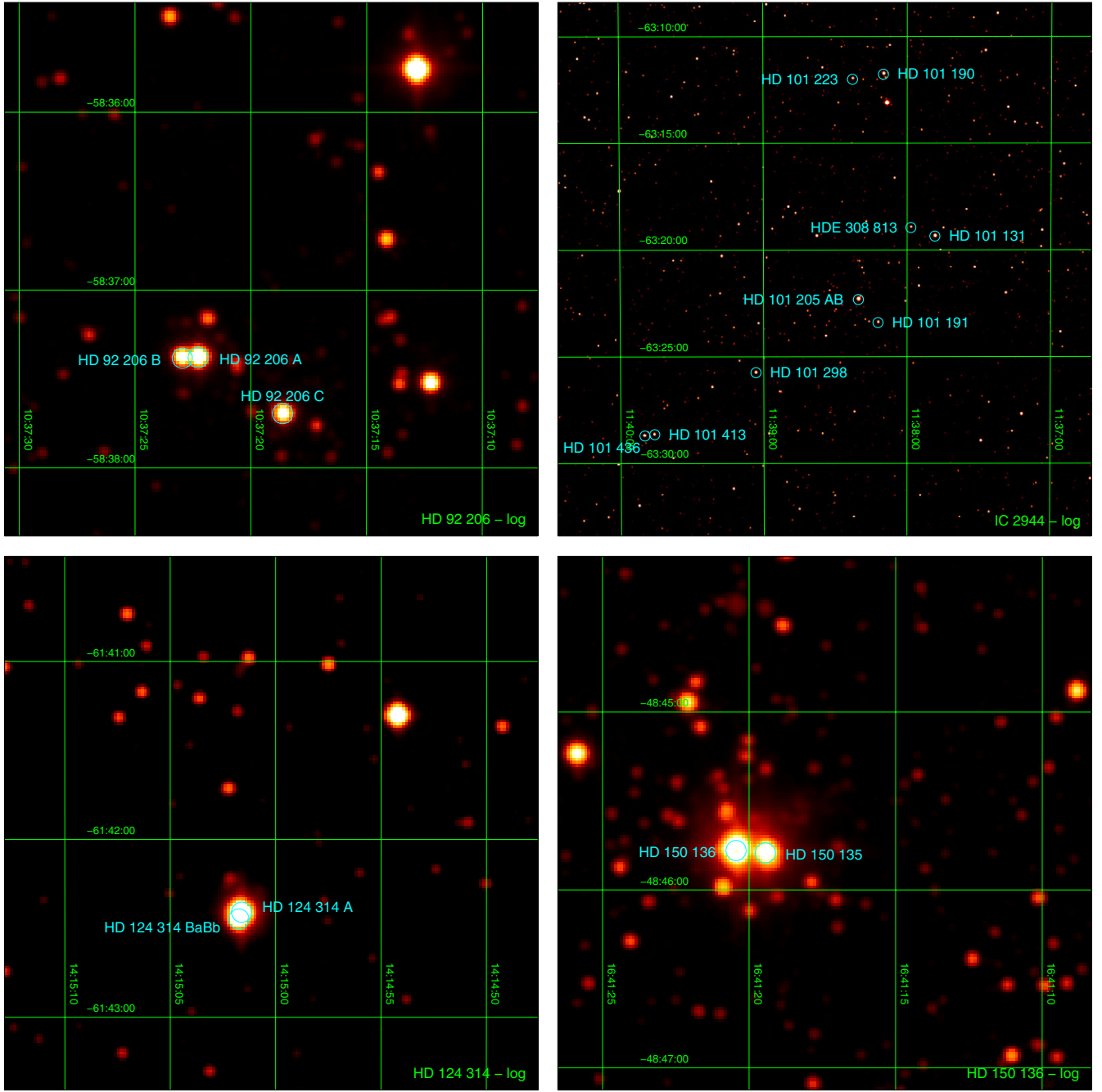
Figure 12. (a) Twelve fields that include O stars for which we have obtained spectral types (marked in cyan or black). The background image is the 2MASS *J* band and is shown with a logarithmic stretch. The four panels displayed here (from left to right and from top to bottom) have linear sizes of 5', 10', 3', and 7', respectively, and correspond to the Trumpler 14, Trumpler 16, HD 93 146, and HD 93 632 fields. (b) The four panels displayed here (from left to right and from top to bottom) have linear sizes of 3', 25', 3', and 3', respectively, and correspond to the HD 92 206, IC 2944, HD 124 314, and HD 150 136 fields. (c) The four panels displayed here (from left to right and from top to bottom) have linear sizes of 15', 5', 3', and 10', respectively, and correspond to the NGC 6231, Havlen–Moffat 1, HDE 319 703, and Pismis 24 fields.

(A color version of this figure is available in the online journal.)

CPD –58 2627. This star was not included in Maíz Apellániz et al. (2004) but was classified as an O star by Forte & Orsatti (1981).

HD 93 160. The (f) suffix was changed to ((f)) in GOSSS-DR1.1 according to the rules in Table 2. HD 93 160 is 12"6 away from HD 93 161 A. See Figure 12 for a chart (Trumpler 14 field).

HD 93 161 B. HD 93 161 A and B are separated by 2" and both are O-type systems. This star was not included in Maíz Apellániz et al. (2004) because Walborn (1972) produced a spectral type for the combined AB system (but see Nazé et al. 2005). The luminosity class was changed from V to IV in GOSSS-DR1.1. The target has C III λ 4650 in emission but is not strong enough to warrant a c suffix. One of us (N.R.W.) disagrees about the



(b)

Figure 12. (Continued)

spectral subtype of this star and thinks that it should be O6 instead of O6.5 based on the ratio of He I λ 4206/He II λ 4200. However, any of the combinations among the strong He lines excluding He I + He II λ 4206 (He II λ 4200, He I λ 4471, He II λ 4542, and He II λ 4686) yields ratios essentially identical to those of the O6.5 IV standard used in Paper I and in this work, hence the O6.5 classification. See Figure 12 for a chart (Trumpler 14 field).

HDE 305 536. This star was not included in Maíz Apellániz et al. (2004) but Levato & Malaroda (1981) classified it as an O type. Levato et al. (1990) discovered that it is an SB1 with a 2.018 day period. See Figure 12 for a chart (HD 93 146 field).

ALS 15 210 = Trumpler 16–244. This star was not included in Maíz Apellániz et al. (2004) but Massey & Johnson (1993) classified it as O3/4 If. We obtain O3.5 If* Nwk, making it the most extincted O2–O3.5 star in the Carina Nebula known to date. He II λ 4686 shows a P-Cygni profile which, by analogy with Pismis 24–1 A, could imply the existence of a companion. The Nwk suffix was added in GOSSS-DR1.1 based on weak N V λ 4604–4620 and strong C IV λ 4658. Smith et al. (2004) considered that this star and/or the adjacent HD 93 162 are the main sources responsible for creating Carina’s defiant finger.²⁰

²⁰ See <http://www.spacetelescope.org/images/heic0822b/>.

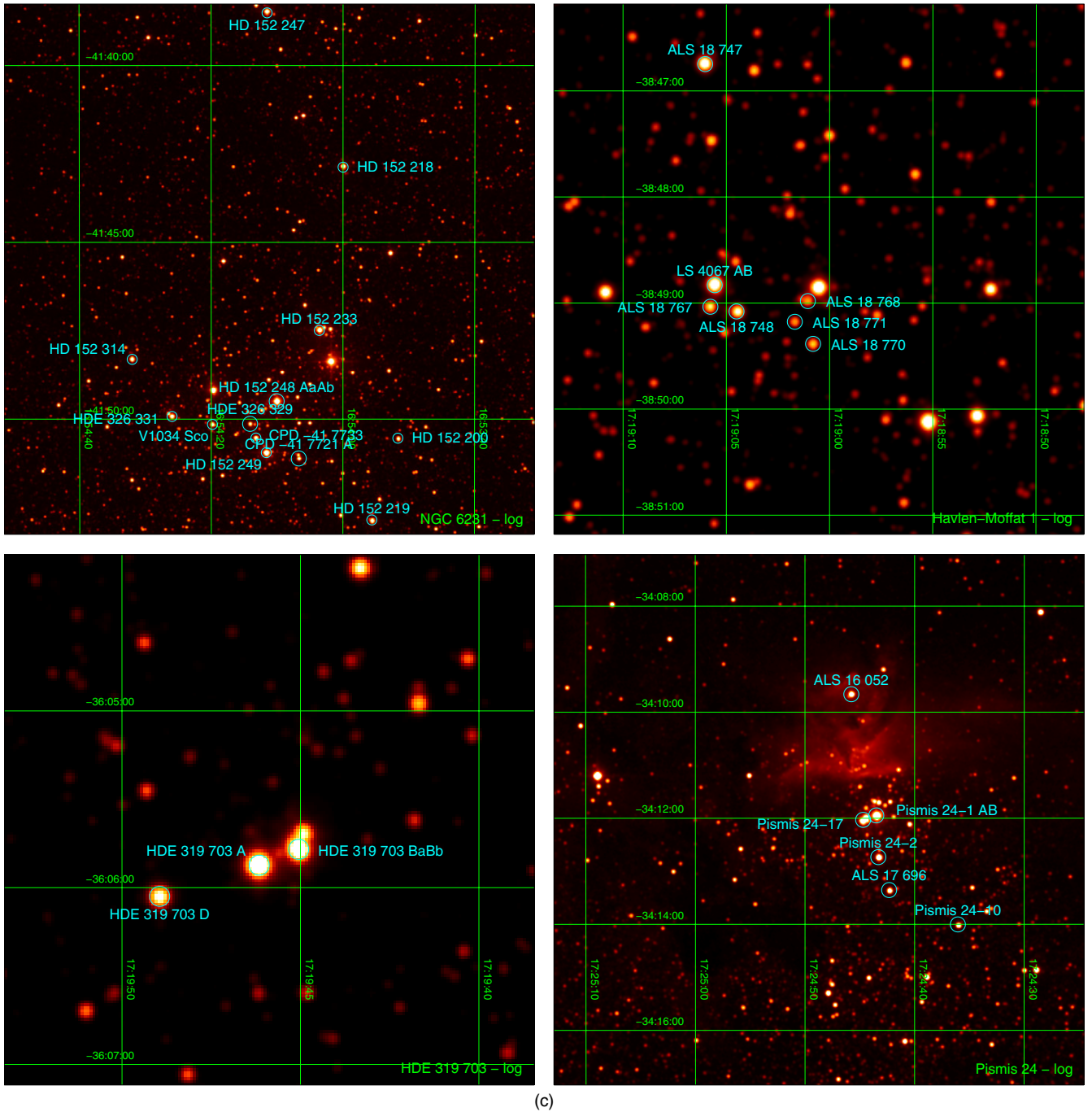


Figure 12. (Continued)

See Figure 12 for a chart (Trumpler 16 field) and Figure 16 for an ACS/HRC image. In the existing ACS/HRC images we detect a previously unpublished²¹ visual companion. It has a separation of $1''.09$, a position angle of 314° , and a ΔV of 8.9 mag. The magnitude and colors are consistent with those of a $\sim 1 M_\odot$ star. An even fainter companion (separation of $1''.49$, position angle of 102° , and ΔV of 10.7 mag) is seen in the saturated ACS/WFC images.

HDE 305 523. Walborn (1973b) classified this star as O9 II. Here we change its luminosity class to II-III.

²¹ It was presented in the JD 13 of the IAU General Assembly in 2009 but did not appear in any proceedings.

Tyc 8626-02506-1. This star was not included in Maíz Apellániz et al. (2004) and, to our knowledge, this is the first time it receives a clear classification as an O type.

HD 93 204. See Figure 12 for a chart (Trumpler 16 field). In the existing ACS/HRC images we detect three previously unpublished visual companions. They have separations of $1''.40$, $1''.67$, and $4''.81$; position angles of 42° , 209° , and 0° ; and ΔV of 6.7, 8.9, and 8.7 mag, respectively. The C III $\lambda 4650$ /N III $\lambda 4634$ intensity ratio (in emission) of 0.9 places this spectrum just below the boundary of the fc category.

HD 93 222. The ((f))z suffix was added in GOSSS-DR1.1.

HDE 303 311. The WDS lists a companion with a separation of $2''.3$ and a Δm of 2.9 mag, i.e., not bright enough to

influence the spectral type. The ((f))z suffix was added in GOSSS-DR1.1.

HDE 305 524. This star was not included in Maíz Apellániz et al. (2004) but was classified as O type by Levato & Malaroda (1981).

CPD -59 2610 = Collinder 228-39. This star was not included in Maíz Apellániz et al. (2004) but was classified as O type by Levato & Malaroda (1981).

CPD -59 2626 AB = Trumpler 16-23 AB. This star was not included in Maíz Apellániz et al. (2004) but was classified as O type by Levato & Malaroda (1982). A spatially unresolved B component has a separation of 16 mas and a Δm of 1.6 mag (Nelan et al. 2004, 2010). The z suffix was added in GOSSS-DR1.1. See Figure 12 for a chart (Trumpler 16 field).

CPD -59 2634 = Trumpler 16-9. This star was not included in Maíz Apellániz et al. (2004) but was classified as O type by Massey & Johnson (1993). A spatially unresolved B component has a separation of 77 mas and a Δm of 2.4 mag (Nelan et al. 2004). The luminosity class was changed to IV in GOSSS-DR1.1. See Figure 12 for a chart (Trumpler 16 field).

CPD -59 2627 = Trumpler 16-3. This star was not included in Maíz Apellániz et al. (2004) but was classified as O type by Massey & Johnson (1993). See Figure 12 for a chart (Trumpler 16 field).

CPD -59 2629 = Trumpler 16-22. This star was not included in Maíz Apellániz et al. (2004) but was classified as O8.5 V by Massey & Johnson (1993). Nazé et al. (2012a) discovered a magnetic field in this star with a strong H α emission. We observe a weak emission in H β in the middle of the stellar absorption, something that is also detected in other magnetic O stars. See Figure 12 for a chart (Trumpler 16 field).

CPD -59 2644. This star was not included in Maíz Apellániz et al. (2004) but was classified as O type by Levato & Malaroda (1982). The spectral subtype was changed to O9 in GOSSS-DR1.1. See Figure 12 for a chart (Trumpler 16 field).

[ARV2008] 206 = *Trumpler 16 MJ 568*. This star was not included in Maíz Apellániz et al. (2004) and, to our knowledge, had never been optically classified as an O star.

HDE 305 532. This star was classified as O6 V((f)) by Walborn (1982c). Here we reclassify it as O6.5 V((f))z. Levato et al. (1990) found variable velocities, possibly indicating a spectroscopic binary.

HDE 305 525. This star was not included in Maíz Apellániz et al. (2004) but was classified as O type by Levato & Malaroda (1981). The WDS lists a companion with a separation of 4".7 and a Δm of 3.7 mag.

CPD -59 2673 = Feinstein 97 = Collinder 228-97. The ((f)) suffix was added in GOSSS-DR1.1.

HDE 305 539. This star was classified as O7p by Walborn (1982c). Here it appears as a relatively normal O8 Vz, with the strength of its metallic lines typical for that spectral type. See Figure 12 for a chart (HD 93 632 field).

HD 93 576. This star was not included in Maíz Apellániz et al. (2004) but was classified as O type by Levato & Malaroda (1981). According to Levato et al. (1990), it is an SB1 with a 2.02 day period. See Figure 12 for a chart (HD 93 632 field).

HD 93 632. Walborn (1973b) classified HD 93 632 as O5 III(f) var but in our GOSSS spectra it clearly has a luminosity class of I, based on He II $\lambda 4686$ strongly in emission. Recent OWN spectra show a weaker He II $\lambda 4686$, indicating unusual variability, possibly related to the presence of a magnetic field.

The target has C III $\lambda 4650$ in emission but is not strong enough to warrant a c suffix. See Figure 12 for a chart (HD 93 632 field).

ALS 18 083 = Bochum 11-5. This star was not included in Maíz Apellániz et al. (2004) but was classified as O type by Fitzgerald & Mehta (1987). See Figure 12 for a chart (HD 93 632 field).

HDE 305 612. This star was not included in Maíz Apellániz et al. (2004) but was classified as O type by Fitzgerald & Mehta (1987). See Figure 12 for a chart (HD 93 632 field).

HDE 305 619. The luminosity class of this star was changed from Ib to II in GOSSS-DR1.1.

HD 94 024. Walborn (1973b) classified this star as O8 V((n)). Here we find it to be O8 IV. OWN data indicate that this system is an SB1.

HDE 303 492. Walborn (1982c) classified this star as O9 Ia. In Paper I it was adopted as the O8.5 Iaf standard in accordance with the revised criteria around O9 discussed there.

HD 94 963. The (f) suffix was added in GOSSS-DR1.1.

ALS 18 556. This star was not included in Maíz Apellániz et al. (2004). Simbad gives a spectral type of O5 but we have been unable to find any reference that has previously obtained an optical spectrum for this target. Apparently, the source of the "spectral type" in Simbad is a purely photometric estimate by Wramdemark (1976) assuming that the star is a main-sequence object. Actually, its spectral type is O9.5 Iabp, with the p arising from discrepant ratios between the He lines used to determine the precise spectral type for late-O stars.

HD 95 589. The ((f)) suffix was added in GOSSS-DR1.1.

HD 96 715. The ((f))z suffix was added in GOSSS-DR1.1.

HD 96 917. Walborn (1973b) classified this star as O8.5 Ib(f) and here we change the classification to O8 Ib(n)(f), which is slightly different from the one in GOSSS-DR1.0. According to OWN data, it is an SB1 with a likely period of 4.03 days.

HD 96 946. According to OWN data, this system is an SB1 with a likely period of 4.34 days. The (f) suffix was added in GOSSS-DR1.1.

HD 97 253. Walborn (1973b) classified this star as O5.5 III(f). We obtain the same luminosity class and suffix but as an O5.

HD 97 848. Walborn (1982c) classified this star as O8 V and that same spectral type is also found here. This star is a marginal z.

HD 99 897. Walborn (1973b) classified this star as O6 V(f). Here we obtain O6.5 IV((f)).

HDE 308 813. This star was not included in Maíz Apellániz et al. (2004) but Schild (1970) classified it as an O star. According to Williams et al. (2013), it is an SB1 with a 6.340 day period. The spectral type was changed from O9.5 to O9.7 in GOSSS-DR1.1. See Figure 12 for a chart (IC 2944 field).

HD 101 191. Walborn (1973b) classified this star as O8 V((n)). We obtain O8 V. Sana et al. (2011a) indicate that it is a long-period SB1 system. OWN data, however, point toward a 25.8 day period. See Figure 12 for a chart (IC 2944 field).

HD 101 223. Walborn (1973b) classified this star as O8 V((f)). We obtain the same spectral type without the suffix. See Figure 12 for a chart (IC 2944 field).

HD 101 298. The classification was changed from O6 V((f)) to O6.5 IV((f)) in GOSSS-DR1.1. See Figure 12 for a chart (IC 2944 field).

HD 105 627. According to OWN data, this system is an SB1 with a likely period of 2.692 days.

HD 113 659. This object was not included in Maíz Apellániz et al. (2004) even though it has $B = 8.0$. The spectral type changed from O9.5 V in GOSSS-DR1.0 to O9 IV here. It is an eclipsing binary with a period of 3.4273 days (Otero 2007).

θ Mus B = *HD 113 904 B*. This O star is located 5".5 to the south of the brighter A component, a WR + O binary (WR 48) which itself has a companion separated by 47 mas (Hartkopf et al. 1999). We easily spatially resolve the spectra of A and B. θ Mus B is an SB1 according to OWN data.

HD 114 737 AB. The WDS lists a B component with a separation of 0".2 and a Δm of 1.5 mag. According to OWN data, this system is an SB1 with a 12.38 day period.

HD 116 282. Walborn (1982c) classified this star as O8 III(n)((f)). We obtain the same classification but only with (n) as suffix.

HD 116 852. The ((f)) suffix was added in GOSSS-DR1.1.

HD 118 198. Walborn (1973b) classified²² this star as O9.5 II-III. Here we obtain O9.7 III (in GOSSS-DR1.0 the luminosity class was IV).

HD 120 521. Walborn (1973b) classified this star as O8 Ib(f). Here we obtain O7.5 Ib(f) (in GOSSS-DR1.0 the luminosity class was Ib-II). OWN data indicate it is variable.

HD 125 241. The (f) suffix was added in GOSSS-DR1.1. OWN data indicate it is variable.

HD 130 298. This object is an SB1 with a 14.63 day period according to OWN data. The (n)((f)) suffix was changed to (n)(f) in GOSSS-DR1.1.

HD 135 591. The ((f)) suffix was added in GOSSS-DR1.1.

CPD -54 6791 AB = Muzzio I-116. The WDS lists a B component with a separation of 1".1 and a Δm of 0.4 mag that we are unable to spatially resolve in the GOSSS data. OWN data indicate that a long-period SB1 may be present in the system but not necessarily involving the brightest component.

HD 148 546. Walborn (1973b) classified this object as O9 Ia and here the luminosity class is changed to Iab. OWN data indicate it is variable.

μ Nor = *HD 149 038.* Walborn (1972) classified this star as O9.7 Iab and that spectral type is also the one derived from GOSSS data.

HD 149 452. Walborn (1972) classified this star as O8 Vn((f)) and with GOSSS data we obtain O9 IVn.

HDE 328 856. This star was not included in Maíz Apellániz et al. (2004) but was classified as O type by Whiteoak (1963). The luminosity class was changed to II in GOSSS-DR1.1.

CPD -46 8221. This star was not included in Maíz Apellániz et al. (2004) but was classified as O type by Vijapurkar & Drilling (1993). The luminosity class was changed to II-III in GOSSS-DR1.1.

HD 151 018. Garrison et al. (1977) classified this star as O9 Ia. We derive the same spectral subtype but a Ib luminosity class.

HD 151 515. The (f) suffix was omitted by mistake in GOSSS-DR1.1.

HD 152 200. This star was not included in Maíz Apellániz et al. (2004) but was classified as O type by Schild et al. (1969). See Figure 12 for a chart (NGC 6231 field).

CPD -41 7721 A = CD -41 11027 p. This star was not included in Maíz Apellániz et al. (2004) but was classified as O type by Sana et al. (2008). The WDS lists a B companion with a separation of 5".7 and a Δm of 1.0 mag that was not included in the GOSSS spectrum. See Figure 12 for a chart (NGC 6231 field).

HDE 326 329 = CPD -41 7735. This star was not included in Maíz Apellániz et al. (2004) but was classified as O type by Morgan et al. (1953a). The WDS lists a dim companion 7".7 away. See Figure 12 for a chart (NGC 6231 field).

HD 152 405. This object is an SB1 system with a period of 25.5 days according to OWN data.

HD 152 623 AB. This object is an SB1 system according to OWN data. The WDS lists a companion with a separation of 0".3 and a Δm of 1.3 mag that we were unable to spatially resolve in the GOSSS data. The system is a colliding-wind binary (De Becker & Raucq 2013).

HD 152 723 AaAb. This object is an SB1 system with a period of 18.9 days according to OWN data. The WDS lists three (B, C, and D) well resolved companions within 15" that are not included in the GOSSS data. Ab, however, has a separation of 0".098 and a Δm of 1.7 mag (Mason et al. 2009), so it likely contributes to the spectral classification.

HDE 322 417 = Trumpler 24-430. This object is an SB1 system with a period of 223 days according to OWN data. The ((f)) suffix was omitted by mistake in GOSSS-DR1.0

HD 154 643. This object is an SB1 system with a period of 28.6 days according to OWN data.

HD 155 775 = V1012 Sco. This star was not included in Maíz Apellániz et al. (2004) but was classified as O type by Goy (1973). It is an eclipsing binary according to Malkov et al. (2006).

HD 155 756. This star was classified as O9.5 Iab in GOSSS-DR1.0 and is now an O9 Ibp. The peculiarity arises from the discrepancies between luminosity criteria and the presence of both strong N and C lines (except for N III $\lambda\lambda 4634-40-42$).

HD 156 154. This object is an SB1 system according to OWN data. The (f) suffix was added in GOSSS-DR1.1.

ALS 18 770 = HM 1-18 = C1715-387-18. This star was not included in Maíz Apellániz et al. (2004) and, to our knowledge, had never been classified as O type before. The z suffix was changed to ((f))z in GOSSS-DR1.1. See Figure 12 for a chart (Havlen-Moffat 1 field).

ALS 18 768 = HM 1-10 = C1715-387-10. This star was not included in Maíz Apellániz et al. (2004) and, to our knowledge, had never been classified as O type before. Our data are noisy but there is a hint of the C and Si absorption lines being stronger than expected while N lines are not weak. That could be a sign of high metallicity. See Figure 12 for a chart (Havlen-Moffat 1 field).

ALS 18 771 = HM 1-19 = C1715-387-19. This star was not included in Maíz Apellániz et al. (2004) and, to our knowledge, had never been classified as O type before. The spectral type was changed from O8.5 to O9 in GOSSS-DR1.1. See Figure 12 for a chart (Havlen-Moffat 1 field).

ALS 18 767 = HM 1-9 = C1715-387-9. This star was not included in Maíz Apellániz et al. (2004) and, to our knowledge, had never been classified as O type before. See Figure 12 for a chart (Havlen-Moffat 1 field).

HDE 319 703 BaBb. The B component in HDE 319 703 is well separated (14") from A but is closer to C (5".4). According to the WDS, B itself comprises Ba and Bb, with a Δm of 1.5 mag and a separation of 0".2. Our spectrum corresponds to the composite BaBb. C is clearly spatially resolved in the GOSSS data: it is an early-B star. See Figure 12 for a chart (HDE 319 703 field), where C is to the north of BaBb.

HDE 319 703 D = 2MASS J17194894-3606029. This star was not included in Maíz Apellániz et al. (2004). Indeed, to our knowledge, no spectra had ever been obtained. We placed

²² Note that a luminosity class of II-III means "intermediate between II and III" while one of III-II means "uncertain between II and III."

it on the slit with HDE 319 703 A because of its proximity and we discovered it was also an O star. See Figure 12 for a chart (HDE 319 703 field).

HD 156 738. The (f) suffix was added in GOSSS-DR1.1. The O6.5 III(f) classification is the same as that of Walborn (1982c).

Pismis 24–10. This star was not included in Maíz Apellániz et al. (2004) but was classified as O type by Massey et al. (2001). The spectral subtype was changed from O9.5 to O9 in GOSSS-DR1.1. See Figure 12 for a chart (Pismis 24 field).

ALS 17 696 = Pismis 24–3. This star was not included in Maíz Apellániz et al. (2004) but was classified as O type by Massey et al. (2001). The luminosity class was changed to V in GOSSS-DR1.1. See Figure 12 for a chart (Pismis 24 field).

Pismis 24–2 = ALS 17 695. This star was not included in Maíz Apellániz et al. (2004) but was classified as O type by Massey et al. (2001). See Figure 12 for a chart (Pismis 24 field).

Pismis 24–17 = HDE 319 718 B = ALS 18 752. Due to an error in GOSSS-DR1.0, the (f*) suffix was omitted there. The spectral type we obtain in GOSSS is the same as that in Maíz Apellániz et al. (2007). See Figure 12 for a chart (Pismis 24 field). The visual multiplicity for this target was measured in ACS/HRC images.

ALS 16 052 = Pismis 24–13. This star was not included in Maíz Apellániz et al. (2004) but was classified as O type by Massey et al. (2001). See Figure 12 for a chart (Pismis 24 field). This is the star that has evacuated the cave-like hole at the bottom of the iconic *HST* image <http://www.spacetelescope.org/images/heic0619a/> and is likely to be one of the youngest stars in our sample (which is consistent with the interpretation of the z suffix indicating a young age). The pillar above it has been likely produced by Pismis 24-1 AB and Pismis 24-17 (the two brightest point sources in the image), since those are the main sources of ionizing photons in the region.

HD 161 807. This star was not included in Maíz Apellániz et al. (2004) and, to our knowledge, it had never been classified as O type. We observed it because it was a bright star classified as B0 (Garrison et al. 1977). Garrison et al. (1983) note that it is an eclipsing binary.

63 Oph = HD 162 978. The spectral subtype was changed from O7.5 to O8 in GOSSS-DR1.1.

HD 163 800. The ((f)) suffix was added in GOSSS-DR1.1.

HD 163 892. This object is an SB1 system with a period of 7.83 days according to OWN data.

HD 164 019. Walborn (1982c) classified this star as O9.5 III and here we revise the luminosity class to IV. The metallic lines are particularly strong, hence the p suffix.

HD 164 492 A. This star is the main ionizing source of the Trifid Nebula and has three companions within 20'' according to the WDS. Of those, the brightest is C, with a separation of 10''.9 and a Δm of 1.1 mag. We placed C on the slit and determined it is an early-B star.

HD 164 536. This star was not included in Maíz Apellániz et al. (2004) but MacConnell & Bidelman (1976) classified it as O type. This system is an SB1 with a 13.4 day period (Williams et al. 2013). The WDS lists a faint companion 1''.7 away. The (n) suffix was changed to (n)z in GOSSS-DR1.1.

HD 166 546. Walborn (1973b) classified this star as O9.5 II-III and here we revise the luminosity class to IV.

15 Sgr = HD 167 264. This system is an SB1 with a 668 day period according to OWN data. The WDS lists a faint companion with a separation of 1''.3.

16 Sgr AaAb = HD 167 263 AaAb. This system is an SB1 with a 14.75825 day period (Stickland & Lloyd 2001). Mason et al. (2009) measure a Δm of 2.0 mag and a separation of 69 mas between Aa and Ab, obviously spatially unresolved in GOSSS. E. J. Aldoretta et al. (in preparation) give a similar separation but with a lower Δm (as well as a position angle that differs by nearly 180°). The luminosity class was changed from II-III to III in GOSSS-DR1.1.

HD 168 941. Walborn (1982c) classified this star as O9.5 II-III and here we revise the luminosity class to IV. The metallic lines are particularly strong, hence the p suffix.

HD 175 876. Walborn (1973b) classified this star as O6.5 III(n)(f) and here we confirm that classification.

4. ANALYSIS

4.1. Sample Selection and Completeness

The definition of an O star is a purely spectroscopic one: it is a star that shows He II $\lambda 4542$ in absorption and, if Si III $\lambda 4552$ in absorption is present (as it happens for late-O stars), it has to be equal to or weaker than He II $\lambda 4542$ (see Table 3). Some low-mass stars can show those characteristics at the end of their lives (as sdO, PAGB, or PNN) but are excluded specifically from our sample since our interest lies in the study of massive stars (see Drilling et al. 2013 for the spectral classification of sdO objects). Objects with masses above $20 M_{\odot}$ spend most of their lives as O stars,²³ so using the O-type selection criterion provides the most straightforward way of choosing a large and uniform sample of massive stars. The main objections that can be made to this strict criterion to study massive stars are that (1) we are excluding the later stages of stellar evolution, (2) the limit between O and non-O stars is not a fixed boundary in T_{eff} , and (3) multiplicity and rotation may complicate the otherwise straightforward definition of what an O star is.

1. The first objection is indeed valid and one should always keep it in mind not to identify massive stars exclusively with O stars. For a complete picture, one should also study the relatively short-lived high-luminosity B stars, supergiants of any type (including LBVs), and WR stars. If we want to extend the lower mass limit to stars that explode as core-collapse supernovae, we should also include the stars that are of spectral types B0-B2.5 during their main sequence lives.
2. The T_{eff} limit between the O and B spectral types depends not only on luminosity class (for the same subtype, a supergiant is cooler than a dwarf) but also on metallicity. The Si III $\lambda 4552$ line becomes weaker when metallicity decreases, so an O9.7 star at low metallicity will have a lower T_{eff} than one at solar metallicity. Therefore, when considering how much of its lifetime does a massive star consume as an O star using evolutionary tracks, those effects have to be considered.
3. Multiplicity is a ubiquitous issue with massive stars, as the results of this paper emphasize. Probably nothing else complicates more the determination of the spectral type of an O star, forcing the use of multiple epoch spectroscopy and high-resolution imaging to establish how many objects one is looking at and whether a straightforward spectral type derived from a single observation can be trusted. Indeed, it is possible that some stars classified as B0 are in reality, e.g.,

²³ With the exception of the most massive ones, that likely show a WR spectrum during most of their existence.

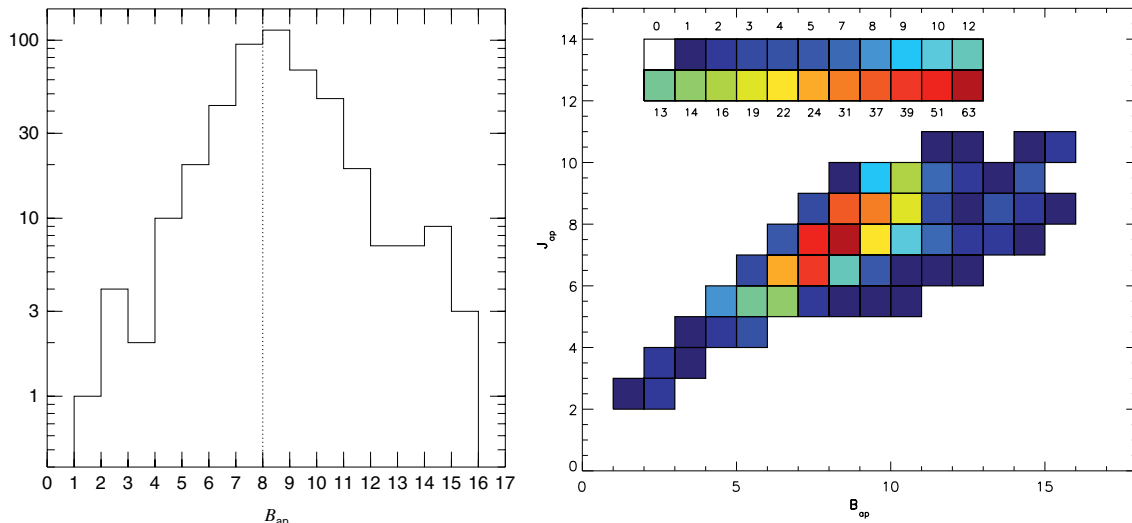


Figure 13. (Left) B_{ap} histogram and (right) $B_{\text{ap}}-J_{\text{ap}}$ density diagram for the stars in GOSSS-DR1.1. The dotted line in the left panel marks the expected completeness limit in GOSSS-DR1.1.

(A color version of this figure is available in the online journal.)

O9.7 + B0.2 binaries yet undiscovered. Fast rotation also complicates the identification of O stars as such, as some of the examples in GOSSS demonstrate (e.g., HD 161 807). This occurs because at the O-B boundary, He II $\lambda 4542$ and Si III $\lambda 4552$ are relatively weak and close together, so in a fast rotator they may merge or become so diluted as to be hard to identify. In this respect, a tool such as MGB becomes quite useful since it artificially broadens the standard spectra for a more adequate comparison. Finally, multiplicity can also lead to interactions, which may alter the observed spectra and even change the fate of the star.

GOSSS aims to build a collection of spectra of optically observable O stars as complete as possible. That implies observing many candidates that turn out to be non-O stars a posteriori as well as a small fraction of massive stars that are known a priori to be non-O but that are needed to establish an adequate knowledge of the rest of the spectra. More specifically, an object is included in the GOSSS sample if it is within the accessible magnitude range and:

1. It has previously received a classification as O type by an author (the primary criterion).
2. It has previously received a classification as B0 by an author (the spectral proximity criterion).
3. It is located within $3'$ of another star in the sample and has a ΔB small enough to allow the two stars to be observed within the slit (the spatial proximity or opportunity criterion).
4. It is a known or suspected early-type star of an interesting small-sized category (the “zoo” criterion).
5. Additional information such as cluster membership, photometry, or X-ray data suggests that it can be an O star (the “other” criterion).
6. It is a known or potential standard for early-type spectral classification (the standard criterion).

The goal is to attain completeness in the first two categories down to a certain B magnitude. Most objects ($\sim 90\%$) observed in the survey so far belong to the first three categories. As previously mentioned, in the first two papers we only present objects that turn out to be O stars.

Given the selection criteria and the ongoing status of the project, the GOSSS-DR1.1 sample is somewhat heterogeneous and covers a wide range in magnitude (Figure 13). Nevertheless, we have concentrated on observing all of the targets with $B_{\text{ap}} < 8$ and 175 (henceforth, the bright sample) out of the total 448 (henceforth, the full sample) are within that range. We believe that the O-star sample in GOSSS-DR1.1 is quite complete up to that magnitude, given that most bright stars have been classified before and that the tendency is to have more non-O stars classified as O than the other way around and that most missed O stars had been previously classified as B0 (Maíz Apellániz et al. 2013), so they are included in the GOSSS sample.²⁴ We will continue evaluating the completeness of the sample by searching for additional sources in the literature and, in the long term, by using photometric methods to select O-star candidates (Maíz Apellániz & Sota 2008; Maíz Apellániz 2013). That solution will become more necessary as we reach into dimmer magnitudes, where most stars have never been classified before. A word of caution: there are 175 systems with $B_{\text{ap}} < 8$ containing an O star but that is not the total number of individual O stars within that magnitude range because some of those contain two or more unresolved O stars. An entry in GOSSS may have two or more individual O stars due to multiplicity.

4.2. Magnitude and Spatial Distributions

The B_{ap} histogram in Figure 13 shows that the number density per unit magnitude as a function of B_{ap} for $B_{\text{ap}} < 8$ grows approximately as $10^{\alpha B_{\text{ap}}}$, with α slightly under 0.4, the value expected for an unextincted uniform spatial disk distribution. Beyond $B_{\text{ap}} = 8$, extinction and the decrease in the spatial density (especially toward the outer Galaxy) are expected to bend the distribution below the extrapolated behavior from bright magnitudes (Maíz Apellániz et al. 2013), but even taking into account that effect it is obvious that the GOSSS-DR1.1 sample is heavily incomplete already in the $B_{\text{ap}} = 9-10$ bin.

²⁴ Note, however, that the GOSSS sample specifically excludes unresolved O+WR systems due to the difficulty of deducing information about the O star from the combined spectrum.

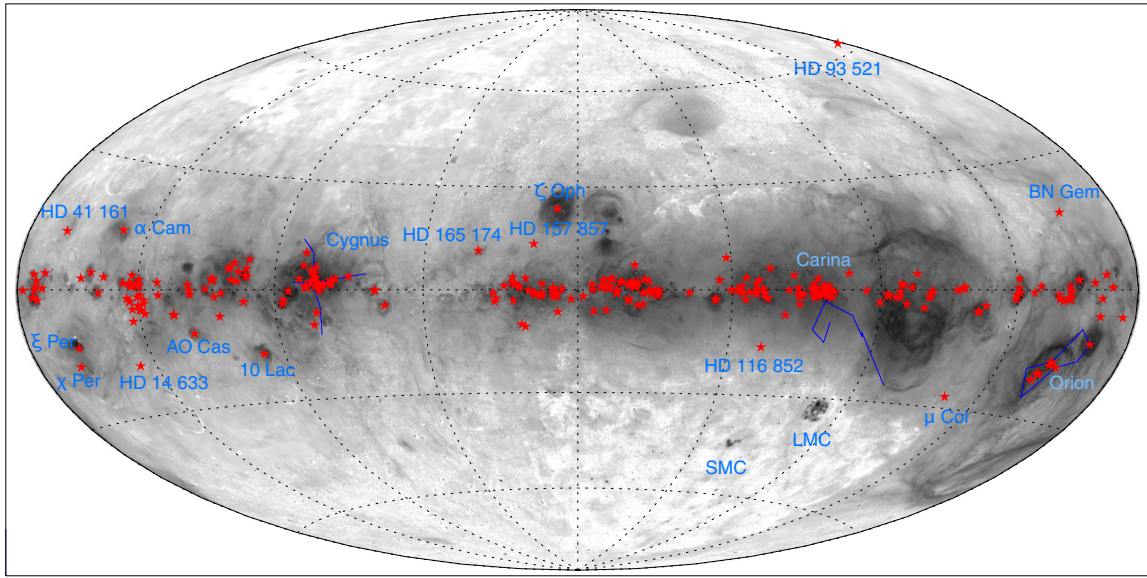


Figure 14. Spatial distribution of the GOSSS-DR1.1 sample in Galactic coordinates. The background image is the $H\alpha$ full-sky map of Finkbeiner (2003). Some regions of the sky and the stars located far from the Galactic Plane are labeled.

(A color version of this figure is available in the online journal.)

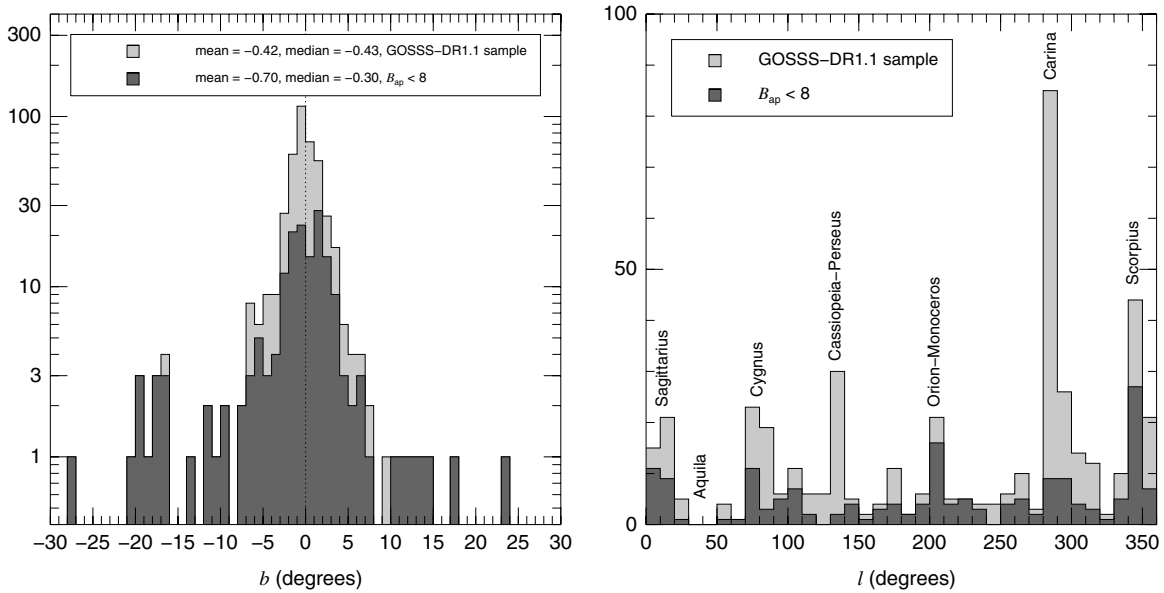


Figure 15. Galactic latitude (left) and longitude (right) histograms for the full and bright samples. HD 93 521 is outside the range in the left panel (see Figure 14). Some regions are labeled in the right panel.

The magnitude density diagram in Figure 13 also reflects the effect of extinction. Nearby stars have $B_{\text{ap}} - J_{\text{ap}}$ values close to the unreddened ones (between -1.0 and -0.7), clustering close to the $B_{\text{ap}} = J_{\text{ap}}$ line. As more distant stars are included, they become dimmer in J_{ap} but even more so in B_{ap} due to reddening. Hence, in the density diagram they concentrate around $J_{\text{ap}} \sim 8$. If dimmer stars were included, we would expect the locus in B_{ap} as a function of J_{ap} to become broader and more distant from the $B_{\text{ap}} = J_{\text{ap}}$ line.

Maíz Apellániz et al. (2013) have evaluated the number of systems with O stars in the GOSSS-DR1.1 sample and included additional systems with $B_{\text{ap}} \geq 8$ already observed by GOSSS, using a simple model to evaluate the number of O-type systems in the Galaxy. They conclude that, at a minimum, 14,000–18,000

such systems exist in the Milky Way. Allowing for effects such as the radial density gradient in the Galaxy, spectroscopic binaries (which are counted just once), WR+O systems, and patchy extinction may raise this number to 30,000–50,000 individual O stars. Those numbers can be compared with the 6500 predicted Galactic WR stars (van der Hucht 2001; Shara et al. 2009) and are roughly consistent in terms of the expected evolutionary paths and relative lifetimes of each phase.

Figure 14 shows the distribution in the sky of the GOSSS-DR1.1 sample and Figure 15 shows the latitude and longitude histograms. The latitude distribution is significantly more irregular for the bright sample than for the full one. This effect is caused by the off-the-plane stars, which are concentrated in the bright sample and the southern hemisphere (hence, the

Table 4

Distribution by Spectral Subtypes and Luminosity Classes in GOSSS-DR1.1

	O2-3.5	O4-5.5	O6-7.5	O8-8.5	O9-9.2	O9.5-9.7	Total
Ia	8	4	2	3	17
I/Iab	7	13	7	4	8	10	49
Ib	7	3	7	7	24
II	9	4	3	14	30
III	1	8	17	11	12	22	71
IV	10	6	17	25	58
V	4	24	65	38	15	21	167
other	0	2	7	6	4	13	32
Total	12	47	130	76	68	115	448

Notes. The other category includes the Of?p class as well as stars without accurate luminosity classifications.

relatively large difference between the mean and median latitudes for the bright sample). In particular, the classical Gould's belt structure is clearly seen in the anticenter direction but not so toward the Galactic Center (where only three O stars, ζ Oph, HD 157 857 and HD 165 174 are clearly above the plane). This is the same asymmetry detected in the cluster population by Elías et al. (2009). Both samples have negative values for their mean and median latitudes, a sign of the location of the Sun above the Galactic Plane, detected for early-type stars with *Hipparcos* measurements (Maíz Apellániz 2001; Maíz Apellániz et al. 2008a).

In the longitude histogram the largest OB associations (or groups of them) are easily identifiable. Also, the Aquila Rift and its surrounding area are notorious in that histogram, as there are no GOSSS-DR1.1 stars between longitudes 30 and 55 degrees. The differences between the two samples are remarkable. Carina represents the largest peak in the full sample but is difficult to identify in the bright sample, as expected for a moderately distant and extincted region. Similar contrasts are seen for Cygnus and Cassiopeia-Perseus. In the other extreme, Orion-Monoceros dominates the two outer Galactic quadrants in the bright sample due to its proximity and low extinction.

4.3. Spectral Classification Statistics

Table 4 shows the distribution by spectral subtypes and luminosity classes in GOSSS-DR1.1. Note that luminosity classes Ia, Iab, Ib, II, and IV are not defined for O2-O5.5. Also, in that range all supergiants are simply called I. The O stars in the sample are heavily concentrated toward luminosity classes III-V even though selection biases favor supergiants. The concentration of O dwarfs toward the middle spectral subtypes is a likely selection effect, as late-type dwarfs are dimmer and tend to be less conspicuous in their spectral characteristics and their ionizing effect (hence, they have been more likely missed by the previous studies that were used to build the sample). The proportion between middle and late subtypes is reversed for brighter luminosity classes, as expected by the elimination of that selection effect and the decrease in initial stellar mass as a function of spectral subtype for constant luminosity class. It will be interesting to compare Table 4 with future GOSSS data releases, where a larger fraction of dimmer stars will be included.

Another interesting statistical issue regarding the GOSSS sample was presented by Maíz Apellániz et al. (2013). The false positive rate in a sample of 1014 stars previously classified as being of O type is 24.9% (i.e., one quarter of those stars

appear as O in the literature but GOSSS reveals them not to be so). That number was calculated using a sample of 1014 objects, larger than that in GOSSS-DR1.1 and shows a clear tendency with magnitude: the quality of the literature spectral classifications decreases as the stars become dimmer. Therefore, we expect that when GOSSS is completed, the false positive rate will be even higher. On the other hand, the false negative rate (stars without previous classifications as O that turned out to be of that type) is 6.4%. Those objects were observed in most cases because they had previous classifications as B0 or because they could be placed within the same slit as an O star that was being observed. This indicates that there are still relatively bright O stars waiting to be discovered. Doing so will likely require large-scale photometric surveys of the Galactic Plane (that do not saturate stars around magnitude 12 and brighter) followed up by spectroscopic surveys with wide-angle multi-fiber spectrographs.

4.4. Multiplicity

4.4.1. The Multiplicity Sample

To study O-star multiplicity, we restrict ourselves to the sample defined in Section 2.2: 194 O stars with $\delta < -20^\circ$ with existing multi-epoch high-resolution studies (mostly OWN). Defining spectroscopic binarity is relatively straightforward though in some cases the current data are inconclusive and the star is labeled as SB1?, SB2? or SB3? in Table 7. For that reason, SB1? and SB2? systems are considered *possible SBs*, while SB3? systems (which are SB2 systems with a possible third component) and the rest of the SB-labeled objects are considered as *certain SBs*. This gives us two estimates (low and high) for spectroscopic binarity according to the current data, depending on whether we include the possible SBs or not²⁵. With respect to the number of components in the system, those labeled as SB1, SB1E, SB2, SB2E, and SBE²⁶ are considered to have two; those labeled as SB3 or SB3E, three; and those labeled as SB1+SBE, SB1E+SB1, SB2+SB1, SB2+SB1E, or SB2+SB2, four. SB1? and SB2? systems have one certain and two possible components while SB3? systems have two certain and three possible components.

Visual binarity is more difficult to ascertain, since in most cases the time baseline is not long enough to establish an orbit with certainty or even that the system is bound and not a chance alignment with a foreground or cluster member (indeed, in many cases only a single epoch is available). Given the need to analyze a large sample, we estimate the probability that a given candidate is a real companion. That is what Maíz Apellániz (2010) did for his Lucky Imaging study of northern massive (mostly O) stars, in which he compared the number of components detected with those expected from the density of 2MASS sources in the surrounding area. That paper found that for separations below 5'' likely all the detected objects are real companions while in the 8''–14'' range $78\% \pm 6\%$ are also so. Note that for a distance of 1 kpc, 10'' corresponds to 10,000 AU. That is a large value but not an unreasonable one: Proxima Centauri is 15,000 AU away from α Cen AB and possibly bound to it (Wertheimer & Laughlin 2006), and is a low-mass, old system.

²⁵ Of course, there should be many systems with periods comparable to those analyzed by OWN that remain undetected because the companion is too dim or the orientation is unfavorable. See Mayer et al. (2013) for the borderline case of HD 165 246. Also note that the companion mass distribution appears to be relatively flat (Maíz Apellániz 2008 and references therein).

²⁶ The E stands for eclipsing.

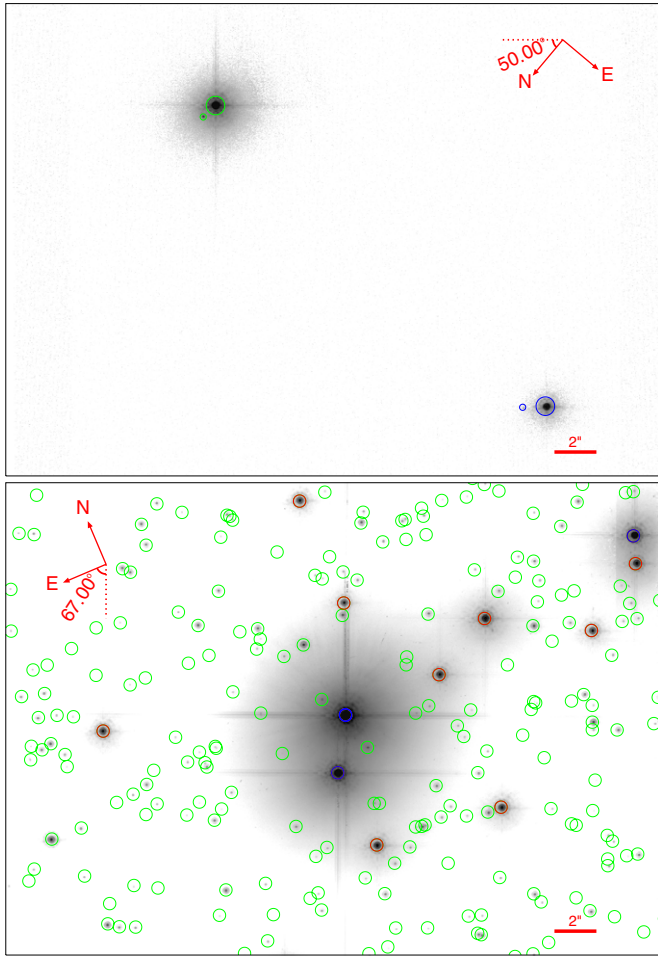


Figure 16. Top: short exposure time (2.4 s) image of a field in the Carina Nebula obtained with ACS/HRC using the F850LP filter. Green circles mark the position of HD 93 162 and its companion while blue circles mark the position of ALS 15210 and its companion. Bottom: combination of short- and long-exposure (total = 256 s) images of the core of Trumpler 14 obtained with ACS/HRC using the F850LP filter. Blue circles mark the position of the three GOSSS systems: HD 93 129 AaAb (center of the field, a double system in the same image when observed at the proper contrast and magnification), HD 93 129 B (SE of AaAb), and Trumpler 14-9 (top right corner). Red circles mark the position of stars with magnitudes similar to or brighter than those of the two companions in the top field. Green circles mark the positions of the stars detected with dimmer magnitudes.

Similar intermediate- and low-mass systems with separations of up to several parsecs are known (Duchêne & Kraus 2013 and references therein). One would expect high-mass, short-lived massive stars to remain bound at large distances in time scales of a few Ma even more easily.²⁷

Our sample differs from that of Maíz Apellániz (2010) in that it consists of southern stars and that the companions were detected in a heterogeneous manner. The distances and spectral types, however, are similar so the southern character should not make a difference. Also, the nearest companions should also be bound in most (if not all, but see below for an exception) cases and most of the objects between 5'' and 10'' are detected by 2MASS, as in Maíz Apellániz (2010). In any case, in analogy with SBs, we produce two estimates of *certain VBs* and *possible*

²⁷ Note, however, that for distances in the range 50,000–100,000 AU, the orbital timescale becomes larger than the life time of an O star and defining such a system as bound becomes meaningless, since it should become unbound by the first supernova explosion before a full orbit takes place.

Table 5
Multiplicity Numbers and Frequencies (Sample Size: 194)

Type	No.	%
Total binaries (low)	126	64.9 ± 3.4
Total binaries (high)	176	90.7 ± 2.1
SBs (low)	97	50.0 ± 3.6
VBs (low)	58	29.9 ± 3.3
SBs (high)	117	60.3 ± 3.5
VBs (high)	148	76.3 ± 3.1
S+VBs (low)	29	14.9 ± 2.6

VBs: the first corresponds to the detections of companions with separations inferior to 5'' and the second to those between 5'' and 10'' (hence we also derive low and high estimates for visual binarity). This is a conservative approach, since we expect most of the *possible VBs* (and even some with larger separations not included here) to be bound objects except when we are observing a star in a dense cluster.

Some of those issues are illustrated by the two ACS/HRC images shown in Figure 16. On the top panel, we see that the two bright stars (both in GOSSS-DR1.1 and outside a well defined cluster) have apparent companions with separations close to 1''. Given the absence of any other sources in the field and the proximity to the two sources, it is quite likely that these are bound systems.²⁸ However, either companion would likely be undetected in a Lucky Imaging survey such as the one by Maíz Apellániz (2010) because they are in an inaccessible part of the Δm -separation plane. Indeed, there is plenty of parameter space to explore for VBs and our current estimates are likely to err on the cautious side. The bottom panel illustrates another issue: what happens when the data are extremely good (in terms of spatial resolution and exposure time) and the star is located at the core of a rich compact cluster such as Trumpler 14. In that case, we start detecting cluster members (even within 5'') that are likely not bound to the star. This contamination may turn out to be a problem for future data if one is trying to measure multiplicity but it should not worry us for this work: Trumpler 14 is the densest cluster in our sample and is also the one with the best quality ACS/HRC data. Therefore, the bottom panel in Figure 16 is an extreme case. Also, note that it is quite possible that HD 93 129 B is bound to Aa+Ab. The total mass of the system is above 100 M_{\odot} and the projected separation is only 6000 AU.

4.4.2. Multiplicity Statistics

Our multiplicity statistics for the studied systems (not for the individual components within a system) are shown in Table 5. The difference between the low and high estimates is smaller for SBs than for VBs. This is expected, given that the properties of spectroscopic binaries are easier to establish (if one has the required data, as it is the case with OWN) than those of visual binaries, given their much shorter orbital periods. The values shown are not corrected for completeness.

We detect certain (spectroscopic or visual) companions in 64.9% of the sample and the value increases to 90.7% when the possible detections are included. To our knowledge, the second value is the highest binary fraction ever measured for a large

²⁸ Furthermore, in each case the mass in the system is of the order of 50 M_{\odot} or higher and the physical separations in the plane of the sky are relatively low, 2000–3000 AU.

Table 6
Spectral Classifications for Stars with $\delta > -20^\circ$

Name	GOSSS ID	R.A. (J2000)	decl. (J2000)	SC	LC	Qual.	Second.	Altern. Classification	Ref.	SB	VB	Sect.	Flag
AO Cas	GOS 117.59–11.09_01	00:17:43.059	+51:25:59.12	O9.2	II	...	O8 V((f))	O9.5 III + O8 V	B91	SB2E	1	3.2	ch
HD 5005 D	GOS 123.12–06.25_01	00:52:48.954	+56:37:30.83	O9.2	V	0–3	3.1	ch
HD 12 323	GOS 132.91–05.87_01	02:02:30.126	+55:37:26.38	ON9.2	V	SB1	0	3.1	ch
HD 12 993	GOS 133.11–03.40_01	02:09:02.473	+57:55:55.93	O6.5	V	((f)) Nstr	1–2	3.2	ch
HD 15 558 A	GOS 134.72+00.92_01	02:32:42.536	+61:27:21.56	O4.5	III	(f)	...	O5.5 III(f) + O7 V	D06	SB2	2–5	3.2	ch
BD +60 513	GOS 134.90+00.92_01	02:34:02.530	+61:23:10.87	O7	V	nz	0	3.2	ch
HD 16 429 A	GOS 135.68+01.15_01	02:40:44.951	+61:16:56.04	O9	II-III	(n) Nwk	...	O9.5II+O8 III-IV + B0 V?	M03	SB3	2–3	3.2	ch
HD 16 832	GOS 138.00–02.88_01	02:44:12.717	+56:39:27.23	O9.2	III	1	3.1	ch
HD 17 505 A	GOS 137.19+00.90_01	02:51:07.971	+60:25:03.88	O6.5	III	n(f)	...	O6.5III((f))+ O7.5 V((f)) + O7.5 V((f))	H06	SB3	2–3	3.2	ch
HD 17 520 A	GOS 137.22+00.88_01	02:51:14.434	+60:23:09.97	O8	V	z	SB1	1–3	3.2	ch
HD 18 326	GOS 138.03+01.50_01	02:59:23.171	+60:33:59.50	O6.5	V	((f))z	O9/B0 V:	SB2	1–4	3.2	ch
1 Cam A	GOS 151.91+03.95_01	04:32:01.845	+53:54:39.03	O9.7	II	n	0	3.2	new
NGC 1624-2	GOS 155.36+02.61_01	04:40:37.266	+50:27:40.96	O7	...	f?cp	0–5	3.2	ch
HDE 242 908	GOS 173.47–01.66_01	05:22:29.302	+33:30:50.43	O4.5	V	(n)((fc))z	SB2?	0	3.2	ch
BD +33 1025 A	GOS 173.56–01.66_01	05:22:44.001	+33:26:26.65	O7.5	V	(n)z	0	3.2	ch
HD 35 619	GOS 173.04–00.09_01	05:27:36.146	+34:45:18.97	O7.5	V	((f))z	1	3.2	ch
HD 36 879	GOS 185.22–05.89_01	05:35:40.527	+21:24:11.72	O7	V	(n)((f))z	0–1	3.2	ch
σ Ori AB	GOS 206.82–17.34_01	05:38:44.765	–02:36:00.25	O9.7	III	O9.5 V + B0.5 V + B0/1 V	S11	SB3	2	3.2	...
ζ Ori AaAb	GOS 206.45–16.59_01	05:40:45.527	–01:56:33.26	O9.2	Ib	var Nwk	2	3.1	ch
HD 46 106	GOS 206.20–02.09_01	06:31:38.395	+05:01:36.38	O9.7	III	(n)	0	3.2	ch
HD 46 202	GOS 206.31–02.00_01	06:32:10.471	+04:57:59.79	O9.2	V	1–2	3.1	ch
HD 46 485	GOS 206.90–01.84_01	06:33:50.957	+04:31:31.61	O7	V	((f))nz var?	0–1	3.2	ch
15 Mon B	GOS 202.94+02.20_02	06:40:58.546	+09:53:42.23	O9.5:	2	3.2	new
15 Mon AaAb	GOS 202.94+02.20_01	06:40:58.656	+09:53:44.71	O7	V	((f))z var	...	O7 V(f) + O9.5: Vn	G93	SB2	2	3.2	ch
HD 48 099	GOS 206.21+00.80_01	06:41:59.231	+06:20:43.54	O5	V	((f))z	O9: V	O5.5 V((f)) + O9 V	M10	SB2	0	3.2	ch
HD 48 279 A	GOS 210.41–01.17_01	06:42:40.548	+01:42:58.23	O8.5	V	z Nstr var?	0–1	3.2	ch
HD 54 662	GOS 224.17–00.78_01	07:09:20.249	–10:20:47.64	O7	V	z var?	...	O6.5 V + O7–9.5 V	B07	SB2	0	3.2	ch
HD 57 682	GOS 224.41+02.63_01	07:22:02.053	–08:58:45.77	O9.2	IV	0	3.1	ch
ζ Oph	GOS 006.28+23.59_01	16:37:09.530	–10:34:01.75	O9.2	IV	nn	0	3.1	ch

Table 6
(Continued)

Name	GOSSS ID	R.A. (J2000)	decl. (J2000)	SC	LC	Qual.	Second.	Altern. Classification	Ref.	SB	VB	Sect.	Flag
HD 164 438	GOS 010.35+01.79_01	18:01:52.279	−19:06:22.07	O9.2	IV	SB1	0	3.1	ch
HD 165 174	GOS 029.27+11.29_01	18:04:37.358	+01:55:08.37	O9.7	II	n	0	3.2	new
HD 167 411	GOS 012.72−00.70_01	18:15:55.747	−18:14:27.06	O9.7	II	0−1	3.2	new
HD 167 771	GOS 012.70−01.13_01	18:17:28.556	−18:27:48.43	O7	III	((f))	O8 III	SB2	0−1	3.2	ch
HD 175 754	GOS 016.39−09.92_01	18:57:35.709	−19:09:11.25	O8	II	(n)((f))p	0−1	3.2	ch
BD −12 4979	GOS 018.25+01.69_01	18:18:03.112	−12:14:34.28	O9.5	V	0−2	3.2	ch
HD 192 281	GOS077.12+03.40_01	20:12:33.121	+40:16:05.45	O4.5	V	(n)((f))	0−1	3.2	ch
HD 193 322 AaAb	GOS 078.10+02.78_01	20:18:06.977	+40:43:55.40	O9	IV	(n)	...	O9 Vnn + O8.5 III + B2.5: V:	T11	SB3	2	3.2	...
HD 193 443 AB	GOS 076.15+01.28_01	20:18:51.707	+38:16:46.50	O9	III	O9 III/I + O9.5 V/III	M13	SB2	1−3	3.2	...
Cyg OB2−9	GOS 080.17+00.76_01	20:33:10.734	+41:15:08.25	O4.5	I	f	...	O5−5.5 I + O3−4 III	N12	SB2	0	3.2	ch
Cyg OB2−8 A	GOS080.22+00.79_01	20:33:15.078	+41:18:50.51	O6	Ib	(fc)	O4.5: III:(fc)	O6 + O5.5	D04	SB2	2−3	3.2	ch
Cyg OB2−8 D	GOS080.23+00.79_01	20:33:16.328	+41:19:02.01	O8.5	V	(n)	0	3.2	ch
Cyg OB2−8 C	GOS080.23+00.78_01	20:33:17.977	+41:18:31.19	O4.5		(fc)p var	SB2?	0	3.2	ch
HD 201 345	GOS 078.44−09.54_01	21:07:55.416	+33:23:49.25	ON9.2	IV	SB2?	0−1	3.1	ch
I Cep AaAb	GOS 098.52+07.99_01	21:11:48.235	+59:59:11.79	O9.5	IV	2	3.2	new
HD 204 827 AaAb	GOS 099.17+05.55_01	21:28:57.763	+58:44:23.20	O9.5	IV	SB1?	2−3	3.2	ch
HD 207 198	GOS 103.14+06.99_01	21:44:53.278	+62:27:38.05	O8.5	II	1	3.2	ch
HD 209 339	GOS 104.58+05.87_01	22:00:39.266	+62:29:16.08	O9.7	IV	1	3.2	new
DH Cep	GOS 107.07−00.90_01	22:46:54.111	+58:05:03.55	O5.5	V	((f))	O6 V((f))	O5.5 III(f) + O6 III(f)	B97	SB2E	0−1	3.2	ch
HD 217 086	GOS 110.22+02.72_01	22:56:47.194	+62:43:37.60	O7	V	nn((f))z	2	3.2	ch
HD 218 195 A	GOS 109.32−01.79_01	23:05:12.928	+58:14:29.34	O8.5	III	Nstr	2	3.2	ch
HD 218 915	GOS 108.06−06.89_01	23:11:06.948	+53:03:29.64	O9.2	Iab	0	3.1	ch

Notes. *GOSSS ID* is the identification for each star with “GOS” standing for “Galactic O Star.” *Ref.* is the reference for the alternative classification. *SB* and *VB* are the spectroscopic and visual binary status, respectively. *Sect.* is the section where the star is discussed. *Flag* can be either “ch” (GOSSS O-type classification changes from Sota et al. 2011), “...” (O-type classification does not change from Sota et al. 2011), “new” (star is not present in Sota et al. 2011).

References. B91: Bagnuolo & Gies (1991), B97: Burkholder et al. (1997), B07: Boyajian et al. (2007), D04: De Becker et al. (2004), D06: De Becker et al. (2006), G93: Gies et al. (1993), H06: Hillwig et al. (2006), M03: McSwain (2003), M10: Mahy et al. (2010), M13: Mahy et al. (2013), N12: Nazé et al. (2012b), S11: Simón-Díaz et al. (2011a), T11: ten Brummelaar et al. (2011).

(This table is also available in a machine-readable form in the online journal.)

Table 7
Spectral Classifications for Stars with $\delta < -20^\circ$

Name	GOSSS ID	R.A. (J2000)	decl. (J2000)	SC	LC	Qual.	Second.	Altern. classification	Ref.	Sam.	SB	VB	Sect.	Flag
μ Col	GOS 237.29–27.10_01	05:45:59.895	–32:18:23.18	O9.5	V	yes	...	0	3.3.9	...
29 CMa	GOS 237.82–05.37_01	07:18:40.378	–24:33:31.32	O7	Ia	fp var	SB2E	0	3.3.8	ch
τ CMa AaAb	GOS 238.18–05.54_01	07:18:42.487	–24:57:15.78	O9	II	yes	SB1+SBE	2–3	3.3.9	...
HD 57 236	GOS 235.64–04.02_01	07:19:30.102	–22:00:17.29	O8.5	V	yes	...	0–1	3.3.9	ch
HD 64 315 AB	GOS 243.16+00.36_01	07:52:20.284	–26:25:46.69	O5.5	V	z	O7 V	yes	SB2+SB2	2	3.3.8	ch
CPD –26 2716	GOS 243.82+00.14_01	07:53:01.007	–27:06:57.75	O6.5	Iab	f	yes	...	0–1	3.3.9	ch
HD 64 568	GOS 243.14+00.71_01	07:53:38.206	–26:14:02.62	O3	V	((f*))z	yes	SB1?	1–3	3.3.9	ch
CPD –28 2561	GOS 245.45–00.10_01	07:55:52.854	–28:37:46.78	O6.5	...	f?p	yes	...	0–2	3.3.6	ch
ζ Pup	GOS 255.98–04.71_01	08:03:35.047	–40:00:11.33	O4	I	(n)fp	yes	...	0	3.3.5	ch
HD 68 450	GOS 254.47–02.02_01	08:11:01.683	–37:17:32.55	O9.7	II	yes	...	0	3.3.9	ch
HD 69 106	GOS 254.52–01.33_01	08:14:03.800	–36:57:07.95	O9.7	II	n	0	3.3.9	new
CPD –35 2105 AB	GOS 253.64–00.45_01	08:15:17.182	–35:44:14.85	O9.2	III	2	3.1	new
HD 69 464	GOS 253.61–00.30_01	08:15:48.565	–35:37:52.88	O7	Ib	(f)	yes	...	1	3.3.9	ch
HD 71 304	GOS 261.76–03.77_01	08:24:55.790	–44:18:03.01	O9	II	yes	...	0–1	3.3.9	ch
NX Vel AB	GOS 260.18+00.64_01	08:39:09.524	–40:25:09.28	O8.5	IV	yes	SB1+SBE	1	3.3.9	ch
LM Vel	GOS 264.04–01.95_01	08:40:47.792	–45:03:30.22	O8.5	Ib-II	(f)p	yes	SB1	0	3.3.5	ch
HD 74 920	GOS 265.29–01.95_01	08:45:10.340	–46:02:19.25	O7.5	IV	n((f))	0	3.3.9	new
HD 75 211	GOS 263.96–00.47_01	08:47:01.592	–44:04:28.85	O8.5	II	((f))	yes	SB1	0	3.3.9	ch
HD 75 222	GOS 258.29+04.18_01	08:47:25.137	–36:45:02.68	O9.7	Iab	yes	...	0	3.3.9	...
HD 75 759	GOS 262.80+01.25_01	08:50:21.017	–42:05:23.27	O9	V	...	B0 V	SB2	0	3.3.8	ch
HD 76 341	GOS 263.53+01.52_01	08:54:00.615	–42:29:08.75	O9.2	IV	yes	...	1	3.1	ch
HD 76 556	GOS 267.58–01.63_01	08:55:07.144	–47:36:27.15	O6	IV	(n)((f))p	yes	SB1?	0	3.3.5	ch
HD 76 968	GOS 270.22–03.37_01	08:57:28.850	–50:44:58.21	O9.2	Ib	yes	SB1	0–1	3.1	ch
CPD –47 2962	GOS 268.00–01.38_01	08:57:51.661	–47:45:43.94	O7	V	((f))z	0	3.3.9	new
CPD –47 2963	GOS 267.98–01.36_01	08:57:54.620	–47:44:15.71	O5	I	fc	yes	SB1?	0	3.3.3	ch
HDE 298 429	GOS 274.47–00.25_01	09:30:37.253	–51:39:34.68	O8.5	V	yes	...	0–1	3.3.9	ch
HD 89 137	GOS 279.69+04.45_01	10:15:40.086	–51:15:24.08	ON9.7	II	(n)	yes	SB1?	0–1	3.3.4	ch
HD 90 087	GOS 285.16–02.13_01	10:22:20.878	–59:45:19.69	O9.2	III	(n)	yes	...	0–2	3.1	ch
SS 215	GOS 284.33–00.58_01	10:23:23.500	–58:00:20.80	O2	I	f*/WN5	0–2	3.3.1	new
HD 91 572	GOS 285.52–00.05_01	10:33:12.266	–58:10:13.64	O6.5	V	((f))z	yes	SB1	0–1	3.3.9	ch
HD 91 651	GOS 286.55–01.72_01	10:33:30.301	–60:07:40.04	ON9.5	III	n	yes	SB3?	0–2	3.3.4	ch
HD 91 824	GOS 285.70+00.07_01	10:34:46.633	–58:09:22.02	O7	V	((f))z	yes	SB1	0–1	3.3.9	ch
HD 91 837	GOS 286.72–01.69_01	10:34:49.506	–60:11:14.06	O8.5	V	n	0–2	3.3.9	new
HD 92 206 C	GOS 286.22–00.18_01	10:37:18.627	–58:37:41.73	O8	V	z	O9.7 V	O7.5 V + B0 V	C07	yes	SB2	0–5	3.3.8	ch
HD 92 206 A	GOS 286.22–00.17_01	10:37:22.276	–58:37:22.81	O6	V	((f))z	yes	...	1–2	3.3.8	ch
HD 92 206 B	GOS 286.22–00.17_02	10:37:22.960	–58:37:23.00	O6	V	((f))z	yes	...	0–1	3.3.9	new
HD 92 504	GOS 285.92+00.99_01	10:39:36.873	–57:27:40.65	O8.5	V	(n)	yes	...	0–1	3.3.9	ch
HD 92 607	GOS 287.11–01.02_01	10:40:12.429	–59:48:10.10	O9	IV	n	0	3.3.9	new
HDE 305 438	GOS 287.44–00.96_01	10:42:43.772	–59:54:16.47	O8	V	z	0–5	3.3.9	new
HDE 303 316 A	GOS 287.41–00.79_01	10:43:11.178	–59:44:21.02	O7	V	((f))z	0–1	3.3.9	new
HD 93 028	GOS 287.64–01.19_01	10:43:15.340	–60:12:04.21	O9	IV	yes	SB1	0	3.3.9	ch
HD 93 027	GOS 287.61–01.13_01	10:43:17.954	–60:08:03.29	O9.5	IV	yes	...	0–1	3.3.9	ch
HDE 303 312	GOS 287.33–00.55_01	10:43:30.842	–59:29:23.80	O9.7	IV	SBE	0–1	3.3.9	new
ALS 15 204	GOS 287.40–00.63_02	10:43:41.237	–59:35:48.18	O7.5	V	z	SB2?	1–3	3.3.9	new
HDE 305 518	GOS 287.51–00.81_01	10:43:44.006	–59:48:17.96	O9.7	III	0	3.3.9	new
CPD –58 2611	GOS 287.39–00.59_01	10:43:46.695	–59:32:54.82	O6	V	((f))z	yes	SB1?	1–2	3.3.9	ch
ALS 15 207	GOS 287.40–00.59_01	10:43:48.707	–59:33:24.10	O9	V	0–1	3.3.9	new
HD 93 128	GOS 287.40–00.58_01	10:43:54.372	–59:32:57.37	O3.5	V	((fc))z	yes	...	3–22	3.3.3	ch

Table 7
(Continued)

Name	GOSSS ID	R.A. (J2000)	decl. (J2000)	SC	LC	Qual.	Second.	Altern. classification	Ref.	Sam.	SB	VB	Sect.	Flag
Trumpler 14–9	GOS 287.41–00.58_01	10:43:55.354	–59:32:48.61	O8.5	V		many	3.3.9	new
HD 93 129 AaAb	GOS 287.41–00.57_01	10:43:57.462	–59:32:51.27	O2	I	f*	yes	...	many	3.3.9	...
CPD –59 2551	GOS 287.67–01.05_02	10:43:57.488	–60:05:28.16	O9	V	0–1	3.3.9	new
HD 93 129 B	GOS 287.41–00.57_02	10:43:57.638	–59:32:53.50	O3.5	V	((f))	yes	...	many	3.3.9	ch
HD 93 146 B	GOS 287.67–01.05_03	10:43:59.454	–60:05:13.33	O9.7	IV	0–1	3.3.9	new
CPD –58 2620	GOS 287.41–00.56_01	10:43:59.917	–59:32:25.36	O7	V	((f))z	yes	...	1–6	3.3.9	ch
HD 93 146 A	GOS 287.67–01.05_01	10:44:00.158	–60:05:09.86	O7	V	((f))z	yes	SB1	0–1	3.3.9	ch
HD 93 130	GOS 287.57–00.86_01	10:44:00.371	–59:52:27.50	O6.5	III	(f)	SB1E	0	3.3.9	ch
CPD –59 2554	GOS 287.67–01.06_01	10:44:00.433	–60:05:59.96	O9.5	IV	1–2	3.3.9	new
ALS 15 206	GOS 287.44–00.61_01	10:44:00.927	–59:35:45.74	O9.2	V	0–2	3.1	new
CPD –58 2627	GOS 287.39–00.52_01	10:44:02.445	–59:29:36.77	O9.5	V	(n)	1–2	3.3.9	new
HD 93 160	GOS 287.44–00.59_01	10:44:07.267	–59:34:30.61	O7	III	((f))	yes	...	1–2	3.3.9	ch
HD 93 161 A	GOS 287.44–00.59_02	10:44:08.840	–59:34:34.49	O7.5	V	...	O9 V	O8 V + O9 V	N05	yes	SB2	1–2	3.3.8	ch
HD 93 161 B	GOS 287.44–00.59_03	10:44:09.080	–59:34:35.30	O6.5	IV	((f))	yes	SB1?	1–3	3.3.9	new
HD 93 162	GOS 287.51–00.71_01	10:44:10.389	–59:43:11.09	O2.5	I	f*/WN6	OB	yes	SB2	1	3.3.1	new
HDE 305 536	GOS 287.67–01.01_01	10:44:11.078	–60:03:21.58	O9.5	V	SB1	0	3.3.9	new
ALS 15 210	GOS 287.52–00.71_01	10:44:13.199	–59:43:10.33	O3.5	I	f* Nwk	2	3.3.9	new
HD 93 190	GOS 287.33–00.32_01	10:44:19.615	–59:16:58.81	O9.7:	V:	(n)e	1	3.3.7	new
QZ Car	GOS 287.67–00.94_01	10:44:22.910	–59:59:35.95	O9.7	Ib	n	...	O9.7 I + O8 III	P11	...	SB1E+SB1	1–3	3.3.8	ch
HDE 305 523	GOS 287.66–00.90_01	10:44:29.479	–59:57:18.11	O9	II-III	yes	...	0–2	3.3.9	ch
Tyc 8626–02506–1	GOS 287.42–00.44_01	10:44:30.218	–59:26:12.97	O9	V	(n)	0–1	3.3.9	new
HD 93 204	GOS 287.57–00.71_01	10:44:32.336	–59:44:31.00	O5.5	V	((f))	yes	...	3	3.3.9	ch
HD 93 205	GOS 287.57–00.71_02	10:44:33.740	–59:44:15.46	O3.5	V	((f))	O8 V	O3 V + O8 V	M01	yes	SB2E	1–2	3.3.8	ch
HD 93 222	GOS 287.74–01.02_01	10:44:36.250	–60:05:28.88	O7	V	((f))z	yes	...	0–1	3.3.9	ch
CPD –59 2591	GOS 287.60–00.75_01	10:44:36.688	–59:47:29.63	O8.5	V	...	B0.5: V:	SB2	0–1	3.3.8	new
HDE 303 311	GOS 287.48–00.54_01	10:44:37.463	–59:32:55.44	O6	V	((f))z	yes	...	1	3.3.9	ch
CPD –59 2600	GOS 287.60–00.74_01	10:44:41.795	–59:46:56.42	O6	V	((f))	yes	SB2?	0–3	3.3.8	...
HD 93 249 A	GOS 287.41–00.36_01	10:44:43.875	–59:21:25.15	O9	III	yes	SB2	0–4	3.3.8	...
HD 93 250 AB	GOS 287.51–00.54_01	10:44:45.027	–59:33:54.67	O4	III	(fc)	yes	...	1–2	3.3.3	ch
HDE 305 524	GOS 287.67–00.85_01	10:44:45.238	–59:54:41.55	O6.5	V	n((f))z	0–1	3.3.9	new
V572 Car	GOS 287.59–00.69_01	10:44:47.307	–59:43:53.23	O7.5	V	(n)z	B0 V(n)	O7 V + O9.5 V + B0.2 IV	R01a	yes	SB3E	0–3	3.3.8	ch
CPD –59 2610	GOS 287.70–00.86_01	10:44:54.714	–59:56:01.91	O8.5	V	0	3.3.9	new
CPD –59 2626 AB	GOS 287.63–00.69_01	10:45:05.794	–59:45:19.60	O7.5	V	(n)z	1–2	3.3.9	new
CPD –59 2634	GOS 287.62–00.66_01	10:45:05.828	–59:43:07.57	O9.7	IV	1	3.3.9	new
HDE 303 308 AB	GOS 287.59–00.61_01	10:45:05.919	–59:40:05.93	O4.5	V	((fc))	yes	SB1?	1	3.3.3	ch
CPD –59 2627	GOS 287.61–00.64_01	10:45:06.721	–59:41:56.58	O9.5	V	0	3.3.9	new
CPD –59 2629	GOS 287.64–00.70_01	10:45:08.225	–59:46:06.96	O8.5	V	p	yes	...	0–2	3.3.9	new
V573 Car	GOS 287.60–00.62_01	10:45:08.226	–59:40:49.48	O9.5	V	(n)	B0.5 V(n)	O9.5 V + B0.2 V	F01	yes	SB2E	0	3.3.8	new
HD 93 343	GOS 287.64–00.68_01	10:45:12.217	–59:45:00.42	O8	V	z	...	O7–8.5 + O8	R09	yes	SB2	0–3	3.3.8	ch
CPD –59 2635	GOS 287.64–00.68_02	10:45:12.715	–59:44:46.18	O8	V	(n)	O9.5 V	O8 V + O9.5 V	A01	yes	SB2E	0–2	3.3.8	ch
CPD –59 2636 AB	GOS 287.64–00.67_01	10:45:12.870	–59:44:19.24	O8	V	...	O8 V	O7 V + O8 V + O9 V	A02	yes	SB3	1–2	3.3.8	ch
CPD –59 2641	GOS 287.64–00.65_01	10:45:16.517	–59:43:36.98	O6	V	((fc))	...	O5.5–6 V((fc)) + B2 V-III	R09	yes	SB2	0–2	3.3.3	ch
CPD –59 2644	GOS 287.64–00.64_01	10:45:20.573	–59:42:51.25	O9	V	0	3.3.9	new
[ARV2008] 206	GOS 287.71–00.75_01	10:45:22.276	–59:50:47.07	O6	V	((f))	0	3.3.9	new
HDE 305 532	GOS 287.78–00.84_01	10:45:34.066	–59:57:26.66	O6.5	V	((f))z	yes	SB1?	1	3.3.9	ch
V662 Car	GOS 287.71–00.71_01	10:45:36.320	–59:48:23.20	O5	V	z	B0: V	O5.5 Vz + O9.5 V	N06	yes	SB2E	0–3	3.3.8	new
HD 93 403	GOS 287.54–00.34_01	10:45:44.122	–59:24:28.15	O5.5	III	(fc) var	...	O5.5 I + O7 V	R00	yes	SB2	0	3.3.3	ch
HDE 305 525	GOS 287.79–00.71_01	10:46:05.704	–59:50:49.45	O5.5	V	(n)((f))z	1–3	3.3.9	new

Table 7
(Continued)

Name	GOSSS ID	R.A. (J2000)	decl. (J2000)	SC	LC	Qual.	Second.	Altern. classification	Ref.	Sam.	SB	VB	Sect.	Flag
CPD −59 2673	GOS 287.84−00.73_01	10:46:22.461	−59:53:20.46	O5.5	V	(n)((f))z	yes	...	0–1	3.3.9	ch
HDE 305 539	GOS 287.94−00.88_01	10:46:33.069	−60:04:12.62	O8	V	z	yes	...	1–3	3.3.9	ch
HD 93 576	GOS 287.98−00.87_01	10:46:53.839	−60:04:41.92	O9.5	IV	(n)	SB1	0–3	3.3.9	new
HD 93 632	GOS 288.03−00.87_01	10:47:12.631	−60:05:50.80	O5	I	f var	yes	...	0–1	3.3.9	ch
ALS 18 083	GOS 288.03−00.87_02	10:47:15.289	−60:05:39.04	O9.7	V	1–3	3.3.9	new
HDE 305 612	GOS 288.03−00.86_01	10:47:16.420	−60:05:39.97	O8	V	(n)z	1–3	3.3.9	new
HDE 305 619	GOS 288.22−00.96_01	10:48:15.523	−60:15:56.76	O9.7	II	yes	...	0	3.3.9	ch
HD 93 843	GOS 288.24−00.90_01	10:48:37.769	−60:13:25.53	O5	III	(fc)	yes	SB1?	0	3.3.3	ch
HD 94 024	GOS 287.34+01.27_01	10:50:01.505	−57:52:26.26	O8	IV	yes	SB1	0–3	3.3.9	ch
HDE 303 492	GOS 288.05+00.40_01	10:51:52.753	−58:58:35.31	O8.5	Ia	f	yes	...	0–2	3.3.9	ch
HD 94 370 A	GOS 288.01+00.63_01	10:52:23.284	−58:44:47.52	O7	...	(n)fp	yes	SB2?	1–3	3.3.5	ch
HD 94 963	GOS 289.76−01.81_01	10:56:35.786	−61:42:32.27	O7	II	(f)	yes	...	0–1	3.3.9	ch
LS 2063	GOS 289.77−01.22_01	10:58:45.475	−61:10:43.01	O5	I	fp	yes	...	0–2	3.3.3	ch
ALS 18 556	GOS 289.80−01.23_01	10:58:56.158	−61:12:09.93	O9.5	Iab	p	0–1	3.3.9	new
HD 95 589	GOS 290.51−02.24_01	11:00:50.448	−62:24:34.25	O8	III	((f))	yes	...	0–2	3.3.9	ch
HD 96 264	GOS 290.40−00.80_01	11:04:55.501	−61:03:05.79	O9.5	III	yes	SB2	0–2	3.3.8	ch
HD 96 622	GOS 290.09+00.57_01	11:06:59.781	−59:40:04.38	O9.2	IV	yes	SB1	0–1	3.1	ch
HD 96 670	GOS 290.20+00.40_01	11:07:13.933	−59:52:23.17	O8.5	...	(n)fp var	SB1	0	3.3.5	ch
HD 96 715	GOS 290.27+00.33_01	11:07:32.817	−59:57:48.68	O4	V	((f))z	yes	...	0	3.3.9	ch
HD 96 917	GOS 289.28+03.06_01	11:08:42.620	−57:03:56.93	O8	Ib	(n)(f)	yes	SB1	0	3.3.9	ch
HD 96 946	GOS 290.73−00.34_01	11:08:51.764	−60:45:33.90	O6.5	III	(f)	yes	SB1	0–2	3.3.9	ch
HD 97 166	GOS 290.67+00.19_01	11:10:05.991	−60:14:56.90	O7.5	IV	((f))	O9 III:	yes	SB3?	0–2	3.3.8	ch
HD 97 253	GOS 290.79+00.09_01	11:10:42.046	−60:23:04.15	O5	III	(f)	yes	SB1?	0	3.3.9	ch
HD 97 434	GOS 291.04−00.15_01	11:11:49.574	−60:41:58.24	O7.5	III	(n)((f))	yes	SB2	1	3.3.8	...
HD 97 848	GOS 290.74+01.53_01	11:14:31.902	−59:01:28.84	O8	V	yes	...	0–1	3.3.9	...
HD 99 897	GOS 293.61−01.28_01	11:28:54.180	−62:39:09.83	O6.5	IV	((f))	yes	...	0	3.3.9	ch
TU Mus	GOS 294.81−04.14_01	11:31:10.927	−65:44:32.10	O8	V	(n)z	B0 V(n)	O7.5 V + O9.5 V	L07	yes	SB2E	0	3.3.8	ch
HD 101 131	GOS 294.78−01.62_01	11:37:48.436	−63:19:23.51	O5.5	V	((f))	O8: V	O6.5 V((f)) + O8.5 V	G02	yes	SB2E	0–1	3.3.8	ch
HDE 308 813	GOS 294.79−01.61_01	11:37:58.453	−63:18:59.46	O9.7	IV	(n)	yes	SB1	0	3.3.9	new
HD 101 190	GOS 294.78−01.49_01	11:38:09.912	−63:11:48.61	O6	IV	((f))	...	O4 V((f)) + O7 V	S11	yes	SB2	0–1	3.3.8	ch
HD 101 191	GOS 294.84−01.68_01	11:38:12.167	−63:23:26.78	O8	V	yes	SB1	0–2	3.3.9	ch
HD 101 205 AB	GOS 294.85−01.65_01	11:38:20.375	−63:22:21.95	O7	II:	(n)	yes	SB2+SB1E	2–3	3.3.8	ch
HD 101 223	GOS 294.81−01.49_01	11:38:22.768	−63:12:02.80	O8	V	yes	...	0–1	3.3.9	ch
HD 101 298	GOS 294.94−01.69_01	11:39:03.277	−63:25:47.07	O6.5	IV	((f))	yes	...	0	3.3.9	ch
HD 101 413	GOS 295.03−01.71_01	11:39:45.836	−63:28:40.14	O8	V	O8 V + B3: V	S11	yes	SB2	0–1	3.3.8	...
HD 101 436	GOS 295.04−01.71_01	11:39:49.961	−63:28:43.56	O6.5	V	((f))	...	O6.5 V + O7 V	S11	yes	SB2	0–2	3.3.8	ch
HD 101 545 A	GOS 294.88−00.81_01	11:40:37.007	−62:34:05.07	O9.2	II	yes	...	1	3.1	ch
HD 102 415	GOS 295.30+00.45_01	11:46:54.404	−61:27:46.99	ON9	IV:	nn	yes	SB2?	0–3	3.3.4	ch
HD 104 565	GOS 296.51+04.02_01	12:02:27.795	−58:14:34.36	OC9.7	Iab	yes	...	0	3.3.4	ch
GS Mus	GOS 298.95−07.06_01	12:05:49.879	−69:34:23.00	ON9.7	Ia	e	yes	SB1?	0	3.3.4	...
HD 105 627	GOS 298.15−00.10_01	12:09:44.579	−62:34:54.61	O9	III	yes	SB1	0	3.3.9	ch
HD 112 244	GOS 303.55+06.03_01	12:55:57.134	−56:50:08.89	O8.5	Iab	(f)fp	yes	SB2	0	3.3.5	ch
HD 113 659	GOS 304.52−02.26_01	13:06:32.350	−65:04:49.53	O9	IV	SBE	0	3.3.9	new
θ Mus B	GOS 304.67−02.49_01	13:08:07.048	−65:18:26.98	O9	III	0–3	3.3.9	ch
HD 114 737 AB	GOS 305.41−00.82_01	13:13:45.528	−63:35:11.75	O8.5	III	yes	SB1	1–3	3.3.9	ch
HD 114 886 AaAb	GOS 305.52−00.83_01	13:14:44.381	−63:34:51.77	O9	III	...	O9.5 III	yes	SB2	2	3.3.8	ch
HD 115 071	GOS 305.76+00.15_01	13:16:04.802	−62:35:01.47	O9.5	III	...	B0 Ib	O9.5 V + B0.2 III	P02	yes	SB2E	0–1	3.3.8	ch

Table 7
(Continued)

Name	GOSSS ID	R.A. (J2000)	decl. (J2000)	SC	LC	Qual.	Second.	Altern. classification	Ref.	Sam.	SB	VB	Sect.	Flag
HD 115 455	GOS 306.06+00.22_01	13:18:35.360	−62:29:28.39	O8	III	((f))	yes	SB2	0−2	3.3.8	ch
HD 116 282	GOS 307.01+02.80_01	13:23:56.255	−59:48:34.80	O8	III	(n)	yes	...	0−2	3.3.9	ch
HD 116 852	GOS 304.88−16.13_01	13:30:23.519	−78:51:20.57	O8.5	II-III	((f))	yes	...	0	3.3.9	ch
HD 117 490	GOS 307.88+01.66_01	13:32:08.600	−60:48:55.47	ON9.5	III	nn	yes	...	0−2	3.3.4	ch
HD 117 797	GOS 307.86+00.04_01	13:34:11.983	−62:25:01.80	O7.5		fp	yes	SB2	0	3.3.5	ch
HD 117 856	GOS 307.77−00.87_01	13:34:43.414	−63:20:07.52	O9.7	II-III	yes	SB2	1	3.3.8	ch
HD 118 198	GOS 307.96−01.22_01	13:36:59.493	−63:38:45.70	O9.7	III	yes	...	1−3	3.3.9	ch
HD 120 521	GOS 310.73+03.42_01	13:51:33.984	−58:32:22.29	O7.5	Ib	(f)	yes	...	0−1	3.3.9	ch
HD 120 678	GOS 309.91−00.69_01	13:52:56.414	−62:43:14.24	O9.5	V	e	yes	...	0−2	3.3.7	ch
HD 123 056	GOS 312.17+01.03_01	14:07:25.640	−60:28:14.11	O9.5	IV	(n)	yes	SB2	0	3.3.8	ch
HD 123 008	GOS 311.02−02.80_01	14:07:30.650	−64:28:08.82	ON9.2	Iab	yes	...	0−1	3.1	ch
HD 123 590	GOS 311.95−01.00_01	14:10:43.969	−62:28:44.42	O8	V	z	yes	SB2	0	3.3.8	ch
HD 124 314 A	GOS 312.67−00.43_01	14:15:01.616	−61:42:24.59	O6	IV	(n)((f))	yes	SB2?	2−3	3.3.8	ch
HD 124 314 BaBb	GOS 312.67−00.43_02	14:15:01.745	−61:42:26.88	O9.2	IV	(n)	2	3.1	new
HD 124 979	GOS 316.40+09.08_01	14:18:11.937	−51:30:13.85	O7.5	IV	(n)((f))	yes	SB2	0−1	3.3.8	ch
HD 125 206	GOS 313.45−00.03_01	14:20:09.041	−61:04:54.61	O9.7	IV	n	yes	SB2	0−1	3.3.8	ch
HD 125 241	GOS 313.54+00.14_01	14:20:22.788	−60:53:22.26	O8.5	Ib	(f)	yes	...	0	3.3.9	...
CPD −59 5634	GOS 315.37−00.08_01	14:34:54.430	−60:25:39.77	O9.2	Ib	0−1	3.1	ch
HD 130 298	GOS 318.77+02.77_01	14:49:33.762	−56:25:38.44	O6.5	III	(n)(f)	yes	SB1	0−2	3.3.9	...
δ Cir	GOS 319.69−02.91_01	15:16:56.894	−60:57:26.12	O8	V	O7 III-V + O9.5 V + B0.5 V	P01	yes	SB3E	0	3.3.8	ch
HD 135 591	GOS 320.13−02.64_01	15:18:49.142	−60:29:46.80	O8	IV	((f))	yes	...	0−1	3.3.9	ch
CPD −54 6791 AB	GOS 327.56−00.83_01	15:55:39.607	−54:38:36.67	O9.5	V	yes	SB1?	2−6	3.3.9	ch
HD 148 546	GOS 343.38+07.15_01	16:30:23.312	−37:58:21.15	O9	Iab	yes	...	0	3.3.9	ch
HD 148 937	GOS 336.37−00.22_01	16:33:52.387	−48:06:40.47	O6	...	f?p	yes	...	1	3.3.6	ch
μ Nor	GOS 339.38+02.51_01	16:34:05.023	−44:02:43.14	O9.7	Iab	yes	...	0−1	3.3.9	...
HD 149 404	GOS 340.54+03.01_01	16:36:22.564	−42:51:31.91	O8.5	Iab	(f)p	...	O7.5 I(f) + ON9.7 I	R01b	yes	SB2	0	3.3.8	ch
HD 149 452	GOS 337.47+00.03_01	16:37:10.514	−47:07:49.85	O9	IV	n	yes	...	0−1	3.3.9	ch
HD 150 135	GOS 336.71−01.57_01	16:41:19.446	−48:45:47.54	O6.5	V	((f))z	yes	SB2	0−2	3.3.8	ch
HD 150 136	GOS 336.71−01.57_02	16:41:20.445	−48:45:46.74	O3.5-4	III	(f*)	O6 IV	O3-3.5 V((f*)) + O5.5-6 V((f)) + O6.5-7 V((f))	M12	yes	SB3	2−3	3.3.8	ch
HD 150 574	GOS 339.00−00.20_01	16:44:07.209	−46:08:29.85	ON9	III	(n)	yes	SB2?	0−2	3.3.4	...
HDE 328 856	GOS 338.56−01.13_01	16:46:33.353	−47:04:50.95	O9.7	II	0	3.3.9	new
HD 151 003	GOS 342.72+02.41_01	16:46:34.194	−41:36:38.52	O8.5	III	yes	SB2	0−1	3.3.8	ch
CPD −46 8221	GOS 338.56−01.14_01	16:46:36.028	−47:05:11.52	O9.7	II-III	0	3.3.9	new
HD 150 958 AB	GOS 338.56−01.15_01	16:46:38.866	−47:05:24.65	O6.5	Ia	(n)f	yes	SB2	1−2	3.3.8	ch
HD 151 018	GOS 339.51−00.41_01	16:46:56.117	−45:53:14.33	O9	Ib	yes	...	0−1	3.3.9	ch
HD 151 515	GOS 342.81+01.70_01	16:49:48.253	−42:00:06.20	O7	II	(f)	yes	...	0−2	3.3.9	...
HD 151 804	GOS 343.62+01.94_01	16:51:33.722	−41:13:49.92	O8	Ia	f	yes	SB2	0	3.3.8	...
HD 152 003	GOS 343.33+01.41_01	16:52:47.373	−41:47:09.00	O9.7	Iab	Nwk	yes	...	0	3.3.9	ch
HD 152 147	GOS 343.15+01.10_01	16:53:28.619	−42:07:17.06	O9.7	Ib	Nwk	yes	SB2	0−2	3.3.9	ch
HD 152 200	GOS 343.41+01.22_01	16:53:51.655	−41:50:32.71	O9.7	IV	(n)	yes	SB1?	0−2	3.3.9	new
HD 152 219	GOS 343.39+01.18_01	16:53:55.606	−41:52:51.47	O9.5	III	(n)	...	O9 III + B1-2 V/III	S08	yes	SB2E	0−1	3.3.8	ch
HD 152 218	GOS 343.53+01.28_01	16:53:59.989	−41:42:52.83	O9	IV	...	B0: V:	O9 IV + O9.7 V	S08	yes	SB2E	0−1	3.3.8	ch
HD 152 233	GOS 343.48+01.22_01	16:54:03.591	−41:47:29.91	O6	II	(f)	...	O5.5 + O7.5	S08	yes	SB2	1−4	3.3.8	ch
HD 152 246	GOS 344.03+01.67_01	16:54:05.300	−41:04:46.11	O9	IV	yes	SB2	0	3.3.8	ch
CPD −41 7721 A	GOS 343.44+01.17_01	16:54:06.709	−41:51:07.17	O9.7	V	yes	...	0−3	3.3.9	new
HD 152 248 AaAb	GOS 343.46+01.18_01	16:54:10.063	−41:49:30.12	O7	Iab	f	O7 Ib(f)	O7 III(f) + O7.5 III(f)	S08	yes	SB2E	1	3.3.8	ch
HD 152 247	GOS 343.61+01.30_01	16:54:11.517	−41:38:30.96	O9.2	III	O9 III + O9.7: V	S08	yes	SB2	0−2	3.1	ch
HD 152 249	GOS 343.45+01.16_01	16:54:11.641	−41:50:57.27	OC9	Iab	yes	SB1?	0	3.3.4	ch

Table 7
(Continued)

Name	GOSSS ID	R.A. (J2000)	decl. (J2000)	SC	LC	Qual.	Second.	Altern. classification	Ref.	Sam.	SB	VB	Sect.	Flag
CPD −41 7733	GOS 343.46+01.17_01	16:54:13.222	−41:50:32.52	O9	IV	O8.5 V + B3	S08	yes	SB2	0−1	3.3.8	ch
HDE 326 329	GOS 343.46+01.17_02	16:54:14.106	−41:50:08.48	O9.7	V	yes	...	0−4	3.3.9	new
V1034 Sco	GOS 343.48+01.15_01	16:54:19.824	−41:50:09.38	O9.5	IV	O9.5 V + B1.5 V	S08	yes	SB2E	1−2	3.3.8	ch
HDE 326 331	GOS 343.49+01.14_01	16:54:25.958	−41:49:55.89	O8	IV	n((f))	yes	SB2	0−2	3.3.8	ch
HD 152 314	GOS 343.52+01.14_01	16:54:32.003	−41:48:18.86	O9	IV	O8.5 III + B1-3 V	S08	yes	SB2	0−1	3.3.8	ch
HD 152 405	GOS 344.56+01.89_01	16:54:55.371	−40:31:29.38	O9.7	II	yes	SB1	0−2	3.3.9	ch
HD 152 408	GOS 344.08+01.49_01	16:54:58.505	−41:09:03.08	O8:	Ia	fpe	yes	...	0−1	3.3.3	...
HD 152 424	GOS 343.36+00.89_01	16:55:03.331	−42:05:27.00	OC9.2	Ia	yes	SB1	0	3.1	ch
HD 152 386	GOS 341.11−00.94_01	16:55:06.451	−44:59:21.37	O6:	Ia	fpe	yes	...	1−2	3.3.3	...
HD 152 590	GOS 344.84+01.83_01	16:56:05.216	−40:20:57.60	O7.5	V	z	yes	SB2E	0−1	3.3.8	ch
HD 152 623 AB	GOS 344.62+01.61_01	16:56:15.026	−40:39:35.76	O7	V	(n)((f))z	SB1	1	3.3.9	ch
HD 152 723 AaAb	GOS 344.81+01.61_01	16:56:54.676	−40:30:44.39	O6.5	III	(f)	yes	SB1	1−4	3.3.9	...
HDE 322 417	GOS 345.26+01.47_01	16:58:55.392	−40:14:33.34	O6.5	IV	((f))	yes	SB1	0−2	3.3.9	ch
HD 153 426	GOS 347.14+02.38_01	17:01:13.007	−38:12:11.88	O8.5	III	yes	SB2	0−1	3.3.8	ch
HD 153 919	GOS 347.75+02.17_01	17:03:56.773	−37:50:38.91	O6	Ia	fcp	SB1E	0	3.3.3	ch
HD 154 368	GOS 349.97+03.22_01	17:06:28.371	−35:27:03.76	O9.2	Iab	yes	SBE	1−2	3.1	ch
HD 154 643	GOS 350.54+03.19_01	17:08:13.983	−35:00:15.68	O9.7	III	yes	SB1	0−2	3.3.9	ch
HD 154 811	GOS 341.06−04.22_01	17:09:53.086	−47:01:53.19	OC9.7	Ib	yes	...	0	3.3.4	ch
HD 155 806	GOS 352.59+02.87_01	17:15:19.247	−33:32:54.30	O7.5	V	((f))z(e)	yes	...	1	3.3.7	ch
HD 155 775	GOS 348.80+00.15_01	17:15:22.325	−38:12:46.70	O9.7	III	(n)	SB1	0−2	3.3.9	new
HD 155 756	GOS 342.57−04.39_01	17:15:50.150	−45:54:38.77	O9	Ib	p	yes	...	0	3.3.9	ch
HD 155 889 AB	GOS 352.50+02.67_01	17:15:50.752	−33:44:13.21	O9.5	IV	yes	SB3?	1−2	3.3.8	ch
HD 155 913	GOS 345.29−02.61_01	17:16:26.336	−42:40:04.13	O4.5	V	n((f))	yes	SB2	1	3.3.8	ch
HD 156 154	GOS 351.22+01.36_01	17:17:27.009	−35:32:12.00	O7.5	Ib	(f)	yes	...	0−2	3.3.9	ch
HD 156 292	GOS 345.35−03.08_01	17:18:45.814	−42:53:29.92	O9.7	III	yes	SB2	0−2	3.3.8	ch
ALS 18 770	GOS 348.71−00.79_01	17:19:00.800	−38:49:23.13	O7	V	((f))z	0−1	3.3.9	new
ALS 18 768	GOS 348.72−00.79_02	17:19:01.052	−38:48:58.94	O8.5	V	1−4	3.3.9	new
ALS 18 771	GOS 348.72−00.79_01	17:19:01.683	−38:49:10.64	O9	V	0−1	3.3.9	new
ALS 18 748	GOS 348.72−00.80_01	17:19:04.508	−38:49:04.81	O5	III	(f)	yes	SB2	1−2	3.3.8	new
LS 4067 AB	GOS 348.73−00.80_01	17:19:05.564	−38:48:49.95	O4.5	I	fpe	yes	...	1−2	3.3.3	ch
ALS 18 767	GOS 348.72−00.80_02	17:19:05.771	−38:49:02.14	O9.7	V	0−2	3.3.9	new
ALS 18 747	GOS 348.76−00.78_01	17:19:06.027	−38:46:44.88	O5.5	I	fc	0−1	3.3.3	new
HDE 319 699	GOS 351.32+00.92_01	17:19:30.417	−35:42:36.14	O5	V	((fc))	yes	SB1	0	3.3.3	ch
HDE 319 703 BaBb	GOS 351.03+00.66_01	17:19:45.050	−36:05:47.00	O6	V	((f))z	yes	...	1−4	3.3.9	ch
HDE 319 703 A	GOS 351.03+00.65_01	17:19:46.156	−36:05:52.37	O7	V	((f))z	yes	SB2	0−1	3.3.8	ch
HDE 319 703 D	GOS 351.03+00.64_01	17:19:48.945	−36:06:02.96	O9.5:	V	n	0−1	3.3.9	new
HDE 319 702	GOS 351.35+00.61_01	17:20:50.609	−35:51:45.97	O8	III	yes	SB3E	0	3.3.8	ch
HD 156 738	GOS 351.18+00.48_01	17:20:52.656	−36:04:20.54	O6.5	III	(f)	yes	...	0−1	3.3.9	...
Pismis 24−10	GOS 353.13+00.90_01	17:24:36.050	−34:14:00.30	O9	V	1	3.3.9	new
ALS 17 696	GOS 353.15+00.88_01	17:24:42.325	−34:13:21.43	O7.5:	V	0−4	3.3.9	new
Pismis 24−2	GOS 353.16+00.89_01	17:24:43.313	−34:12:44.15	O5	V	((f))	0−2	3.3.9	new
Pismis 24−1 AB	GOS 353.17+00.89_01	17:24:43.500	−34:11:56.96	O3.5	I	f*	...	O3.5 If* + O4 III(f)	M07	yes	SB2E	1−2	3.3.8	...
Pismis 24−17	GOS 353.17+00.89_02	17:24:44.700	−34:12:02.00	O3.5	III	(f*)	3−6	3.3.9	...
ALS 16 052	GOS 353.20+00.91_01	17:24:45.777	−34:09:39.86	O6	V	((f))z	0−2	3.3.9	new
HD 158 186	GOS 355.91+01.60_01	17:29:12.925	−31:32:03.44	O9.5	V	(n)	yes	SB2+SB1E	1−2	3.3.8	ch

Table 7
(Continued)

Name	GOSSS ID	R.A. (J2000)	decl. (J2000)	SC	LC	Qual.	Second.	Altern. classification	Ref.	Sam.	SB	VB	Sect.	Flag
HD 159 176	GOS 355.67+00.05_01	17:34:42.491	−32:34:53.97	O7	V	((f))	O7 V((f))	O7 V((f)) + O7 V((f))	L07	yes	SB2E	2–4	3.3.8	ch
HD 161 853	GOS 358.42−01.88_01	17:49:16.559	−31:15:18.07	O8	V	(n)z	B	yes	SB3?	0–1	3.3.8	ch
HD 161 807	GOS 351.78−05.85_01	17:49:24.753	−38:59:01.63	O9.7	III	nn	SBE	0–1	3.3.9	new
63 Oph	GOS 004.54+00.30_01	17:54:54.042	−24:53:13.55	O8	II	((f))	yes	...	0	3.3.9	ch
HD 163 800	GOS 007.05+00.69_01	17:58:57.259	−22:31:03.17	O7.5	III	((f))	yes	...	0	3.3.9	ch
HD 163 892	GOS 007.15+00.62_01	17:59:26.312	−22:28:00.87	O9.5	IV	(n)	yes	SB1	0–2	3.3.9	ch
HD 163 758	GOS 355.36−06.10_01	17:59:28.367	−36:01:15.58	O6.5	Ia	fp	yes	SB2	1–2	3.3.8	ch
HD 164 019	GOS 001.91−02.62_01	18:00:19.956	−28:37:14.66	O9.5	IV	p	yes	...	0–1	3.3.9	ch
HD 164 492 A	GOS 007.00−00.25_01	18:02:23.553	−23:01:51.06	O7.5	V	z	yes	SB1?	1–5	3.3.9	ch
HD 164 536	GOS 005.96−00.91_01	18:02:38.619	−24:15:19.38	O7.5	V	(n)z	1–4	3.3.9	new
Herschel 36	GOS 005.97−01.17_01	18:03:40.333	−24:22:42.74	O7:	V	...	sec	O7.5 V + O9 V + B0.5 V	A10	yes	SB2+SB1	9–19	3.3.8	ch
9 Sgr	GOS 006.01−01.20_01	18:03:52.446	−24:21:38.64	O4	V	((f))z	...	O3.5 V((f*)) + O5-5.5 V((f))	R12	yes	SB2	0	3.3.8	ch
HD 164 816	GOS 006.06−01.20_01	18:03:56.843	−24:18:45.11	O9.5	V	...	B0 V	SB2	0	3.3.8	ch
HD 165 052	GOS 006.12−01.48_01	18:05:10.551	−24:23:54.85	O5.5:	V	z	O8: V	O7 Vz + O7.5 Vz	F13	yes	SB2	0–2	3.3.8	ch
HDE 313 846	GOS 007.36−00.85_01	18:05:25.737	−23:00:20.35	O7:	Ia	fpe	yes	...	0–2	3.3.3	...
HD 165 246	GOS 006.40−01.56_01	18:06:04.679	−24:11:43.88	O8	V	(n)	...	O8 V + B7 V	M13	yes	SB2E	1–3	3.3.8	...
HD 165 921	GOS 006.94−02.10_01	18:09:17.700	−23:59:18.25	O7	V	(n)z	B0: V:	O7 V + O9 V	N88	yes	SB2E	0	3.3.8	ch
HD 166 546	GOS 010.36−00.92_01	18:11:57.099	−20:25:24.16	O9.5	IV	yes	...	0–2	3.3.9	ch
15 Sgr	GOS 010.46−01.74_01	18:15:12.905	−20:43:41.76	O9.7	Iab	yes	...	1	3.3.9	...
16 Sgr AaAb	GOS 010.76−01.58_01	18:15:12.970	−20:23:16.69	O9.5	III	yes	SB1	1–2	3.3.9	ch
HD 168 941	GOS 005.82−06.31_01	18:23:25.562	−26:57:10.83	O9.5	IV	p	yes	...	0–2	3.3.9	ch
HD 175 876	GOS 015.28−10.58_01	18:58:10.765	−20:25:25.53	O6.5	III	(n)(f)	yes	...	0	3.3.9	...

Notes. *GOSSS ID* is the identification for each star with “GOS” standing for “Galactic O Star.” *Ref.* is the reference for the alternative classification. *Sam.* marks the stars belonging to the binarity sample (see Section 2.2). *SB* and *VB* are the spectroscopic and visual binary status, respectively. *Sect.* is the section where the star is discussed. *Flag* can be either “ch” (O-type classification changes from Maíz Apellániz et al. 2004), “...” (O-type classification does not change from Maíz Apellániz et al. 2004), “new” (star is not present or is not O type in Maíz Apellániz et al. 2004).

References. A01: Albacete Colombo et al. (2001), A02: Albacete Colombo et al. (2002), A10: Arias et al. (2010), C07: Campillay et al. (2007), F01: Freyhammer et al. (2001), F13: Ferrero et al. (2013), G02: Gies et al. (2002), L07: Linder et al. (2007), M01: Morrell et al. (2001), M07: Maíz Apellániz et al. (2007), M12: Mahy et al. (2012), M13: Mayer et al. (2013), N88: Niemelä & Morrison (1988), N05: Nazé et al. (2005), N06: Niemelä et al. (2006), P01: Penny et al. (2001), P02: Penny et al. (2002), P11: Parkin et al. (2011), R00: Rauw et al. (2000), R01a: Rauw et al. (2001b), R01b: Rauw et al. (2001a), R09: Rauw et al. (2009) amended in text, R12: Rauw et al. (2012), S08: Sana et al. (2008), S11: Sana et al. (2011a).

(This table is also available in a machine-readable form in the online journal.)

*sample of massive stars*²⁹ Compared to the results reviewed by Duchêne & Kraus (2013), the SB multiplicity frequency for high-mass stars is on the low side of their value ($70\% \pm 9\%$) but note that our results are not corrected for completeness and that our high value is consistent with theirs. On the other hand, our high value for VBs is significantly larger than theirs ($45\% \pm 5\%$) and that explains why our fraction of total binaries is so high. The difference for the VB multiplicity frequency is likely caused by a better sensitivity to low-mass systems at large separations, a problem that has long plagued this type of studies (Duchêne & Kraus 2013).

Indeed, the fraction of possible binaries is so large that there are only 18 stars for which no sign of binarity is observed. Of those, only four (22.2%) are of luminosity class IV or V, a value that should be compared with the 99 stars (50.8%) that belong to those classes overall. One of those four stars is μ Col, a known runaway, so its singularity needs not be primordial. The remaining three (HD 96 715, HD 99 897, and HD 101 298) are all earlier than O7, i.e., they are more luminous than most O stars of luminosity classes IV and V. What can cause the overabundance of apparently single systems among O giants and supergiants? One explanation is that this is an observational effect. All binary detection methods benefit from a small Δm , so for the earliest dwarfs and for giants and supergiants it is easier for a companion to remain undetected. An alternative explanation for the giants and supergiants is that the difference is real and that those stars are single more frequently. This could be because they have a higher chance of being runaways (because they are older on average than dwarfs) or, perhaps more interestingly, because some of them are the result of mergers (de Mink et al. 2013). If any of those explanations is true and we also consider the fact that we know we are not detecting some binary systems, then it is possible that *all stars above 15–20 M_{\odot} are born in multiple systems*.

Finally, a relatively large fraction (14.9%) are confirmed S+VB systems, i.e., they include at least three objects and two of the orbits have significantly different periods (hierarchical multiple systems). The higher-order multiplicity of O-type stars also shows up when we calculate the average number of components per stellar system. If only certain companions are included, the number is 2.0. If possible companions are added, the value grows to 3.4. Such a large value is not caused by the possible contamination of a few objects with many possible companions, as the median of the distribution is 3, i.e., more than half of the 194 stars are in potentially triple or higher-order multiple systems.

Support for this work was provided by (1) the Spanish Government Ministerio de Ciencia e Innovación through grants AYA2007-64052, AYA2007-64712, AYA 2010-17631, AYA 2010-15081, the Ramón y Cajal Fellowship program, and FEDER funds; (2) the Junta de Andalucía grant P08-TIC-4075; (3) NASA through grants GO-10205, GO-10602, GO-10898, and GO-11981 from the Space Telescope Science Institute, which is operated by the Association of Universities for Research in Astronomy Inc., under NASA contract NAS 5-26555; (4) the Dirección de Investigación de la Universidad

de La Serena (DIULS PR09101); (5) the ESO-Government of Chile Joint Committee Postdoctoral Grant; and (6) the Chilean Government grants FONDECYT Regular 1120668 and FONDECYT Iniciación 11121550. This research has made extensive use of (1) Aladin (Bonnarel et al. 2000), (2) the SIMBAD database, operated at CDS, Strasbourg, France, (3) the Washington Double Star Catalog, maintained at the U.S. Naval Observatory (Mason et al. 2001), and (4) the 2MASS Point Source Catalog (Skrutskie et al. 2006). We would like to thank Miguel Penadés Ordaz for his help in the compilation of data for this paper and the anonymous referee for his/her useful comments.

REFERENCES

- Albacete Colombo, J. F., Morrell, N. I., Niemelä, V. S., & Corcoran, M. F. 2001, *MNRAS*, **326**, 78
- Albacete Colombo, J. F., Morrell, N. I., Rauw, G., et al. 2002, *MNRAS*, **336**, 1099
- Ankay, A., Kaper, L., de Bruijne, J. H. J., et al. 2001, *A&A*, **370**, 170
- Antokhina, E. A., Srinivasa Rao, M., & Parthasarathy, M. 2011, *NewA*, **16**, 177
- Arias, J. I., Barbá, R. H., Gamen, R. C., et al. 2010, *ApJL*, **710**, L30
- Arias, J. I., Barbá, R. H., Maíz Apellániz, J., Morrell, N. I., & Rubio, M. 2006, *MNRAS*, **366**, 739
- Arias, J. I., Morrell, N. I., Barbá, R. H., et al. 2002, *MNRAS*, **333**, 202
- Bagnuolo, W. G., Jr., & Gies, D. R. 1991, *ApJ*, **376**, 266
- Barbá, R. H., Gamen, R. C., Arias, J. I., et al. 2010, *RMxAC*, **38**, 30
- Barbá, R. H., Gamen, R. C., & Morrell, N. I. 2006, *ATel*, **819**, 1
- Barr Domínguez, A., Chini, R., Pozo Núñez, F., et al. 2013, *A&A*, **557**, A13
- Benaglia, P., Cappa, C. E., & Koribalski, B. S. 2001, *A&A*, **372**, 952
- Benaglia, P., Dougherty, S. M., Phillips, C., Koribalski, B., & Tzioumis, T. 2010, *RMxAC*, **38**, 41
- Bohannon, B., & Walborn, N. R. 1989, *PASP*, **101**, 520
- Bonnarel, F., Fernique, P., Bienaymé, O., et al. 2000, *A&AS*, **143**, 33
- Boyajian, T. S., Gies, D. R., Dunn, J. P., et al. 2007, *ApJ*, **664**, 1121
- Burkholder, V., Massey, P., & Morrell, N. I. 1997, *ApJ*, **490**, 328
- Campillay, A., Arias, J. I., Barbá, R. H., et al. 2007, in VI Reunion Anual Sociedad Chilena de Astronomía (SOCHIAS), **63**
- Chini, R., Hoffmeister, V. H., Nasser, A., Stahl, O., & Zinnecker, H. 2012, *MNRAS*, **424**, 1925
- Clark, J. S., Goodwin, S. P., Crowther, P. A., et al. 2002, *A&A*, **392**, 909
- Conti, P. S., Cowley, A. P., & Johnson, G. B. 1975, *PASP*, **87**, 327
- Conti, P. S., & Niemelä, V. S. 1976, *ApJL*, **209**, L37
- Conti, P. S., & Walborn, N. R. 1976, *ApJ*, **207**, 502
- Crowther, P. A. 2007, *ARA&A*, **45**, 177
- Crowther, P. A., & Walborn, N. R. 2011, *MNRAS*, **416**, 1311
- Cvetković, Z., Vince, I., & Ninković, S. 2010, *NewA*, **15**, 302
- De Becker, M., & Rauw, G. 2013, *A&A*, **558**, A28
- De Becker, M., Rauw, G., & Manfroid, J. 2004, *A&A*, **424**, L39
- De Becker, M., Rauw, G., Manfroid, J., & Eenens, P. 2006, *A&A*, **456**, 1121
- de Mink, S. E., Langer, N., Izzard, R. G., Sana, H., & de Koter, A. 2013, *ApJ*, **764**, 166
- Drilling, J. S., Jeffery, C. S., Heber, U., Moehler, S., & Napiwotzki, R. 2013, *A&A*, **551**, A31
- Duchêne, G., & Kraus, A. 2013, *ARA&A*, **51**, 269
- Elías, F., Alfaro, E. J., & Cabrera-Caño, J. 2009, *MNRAS*, **397**, 2
- Evans, C. J., Taylor, W. D., Hénault-Brunet, V., et al. 2011, *A&A*, **530**, A108
- Fernández Lajús, E., & Niemelä, V. S. 2006, in IAU Joint Discussion, **5**, 13
- Ferrero, G., Gamen, R., Benvenuto, O., & Fernández-Lajús, E. 2013, *MNRAS*, **433**, 1300
- Finkbeiner, D. P. 2003, *ApJS*, **146**, 407
- Fitzgerald, M. P., & Mehta, S. 1987, *MNRAS*, **228**, 545
- Forte, J. C., & Orsatti, A. M. 1981, *AJ*, **86**, 209
- Freyhammer, L. M., Clausen, J. V., Arentoft, T., & Sterken, C. 2001, *A&A*, **369**, 561
- Gamen, R. C., Arias, J. I., Barbá, R. H., et al. 2012, *A&A*, **546**, A92
- Gamen, R. C., Gosset, E., Morrell, N. I., et al. 2006, *A&A*, **460**, 777
- Gamen, R. C., Gosset, E., Morrell, N. I., et al. 2008, *RMxAC*, **33**, 91
- García, B., Malaroda, S., Levato, H., Morrell, N. I., & Grosso, M. 1998, *PASP*, **110**, 53
- Garrison, R. F., Hiltner, W. A., & Schild, R. E. 1977, *ApJS*, **35**, 111
- Garrison, R. F., Schild, R. E., & Hiltner, W. A. 1983, *ApJS*, **52**, 1
- Gies, D. R., Mason, B. D., Hartkopf, W. I., et al. 1993, *AJ*, **106**, 2072

²⁹ Note that the $\sim 90\%$ values of the multiplicity fraction provided by some studies such as Kiminki & Kobulnicky (2012) are extrapolated using an expected period distribution, not directly measured as in our data. Other homogeneous studies of multiplicity in O stars give minimum values of 43% (Chini et al. 2012, field), 69%–73% (Chini et al. 2012, non-field), and 44%–67% Sana et al. (2008, 2009, 2011a) for spectroscopic binaries, which are consistent with our results.

- Gies, D. R., Penny, L. R., Mayer, P., Drechsel, H., & Lorenz, R. 2002, *ApJ*, **574**, 957
- Gilmore, G., Randich, S., Asplund, M., et al. 2012, *Msngr*, **147**, 25
- Goto, M., Stecklum, B., Linz, H., et al. 2006, *ApJ*, **649**, 299
- Goy, G. 1973, *A&AS*, **12**, 277
- Grunhut, J. H., Wade, G. A., Sundqvist, J. O., et al. 2012, *MNRAS*, **426**, 2208
- Hammerschlag-Hensberge, G., van Kerkwijk, M. H., & Kaper, L. 2003, *A&A*, **407**, 685
- Hartkopf, W. I., Mason, B. D., Gies, D. R., et al. 1999, *AJ*, **118**, 509
- Havlen, R. J., & Moffat, A. F. J. 1977, *A&A*, **58**, 351
- Hillwig, T. C., Gies, D. R., Bagnuolo, W. G., Jr., et al. 2006, *ApJ*, **639**, 1069
- Hiltner, W. A., Garrison, R. F., & Schild, R. E. 1969, *ApJ*, **157**, 313
- Hoogerwerf, R., de Bruijne, J. H. J., & de Zeeuw, P. T. 2001, *A&A*, **365**, 49
- Hutchings, J. B., Thackeray, A. D., Webster, B. L., & Andrews, P. J. 1973, *MNRAS*, **163**, 13P
- Kiminki, D. C., & Kobulnicky, H. A. 2012, *ApJ*, **751**, 4
- Leep, E. M. 1978, *ApJ*, **225**, 165
- Lesh, J. R. 1968, *ApJS*, **17**, 371
- Leung, K.-C., Moffat, A. F. J., & Seggewiss, W. 1979, *ApJ*, **231**, 742
- Levato, H., & Malaroda, S. 1981, *PASP*, **93**, 714
- Levato, H., & Malaroda, S. 1982, *PASP*, **94**, 807
- Levato, H., Malaroda, S., Garcia, B., Morrell, N. I., & Solivella, G. 1990, *ApJS*, **72**, 323
- Levato, H., Malaroda, S., Garcia, B., et al. 1991, *Ap&SS*, **183**, 147
- Levato, H., Morrell, N. I., Garcia, B., & Malaroda, S. 1988, *ApJS*, **68**, 319
- Linder, N., Rauw, G., Sana, H., De Becker, M., & Gosset, E. 2007, *A&A*, **474**, 193
- Lorenzo, J., Simón-Díaz, S., Negueruela, I., & Vilardell, F. 2010, in ASP Conf. Ser. 435, *Binaries—Key to Comprehension of the Universe*, ed. A. Prša & M. Zejda (San Francisco, CA: ASP), 409
- MacConnell, D. J., & Bidelman, W. P. 1976, *AJ*, **81**, 225
- Mahy, L., Gosset, E., Sana, H., et al. 2012, *A&A*, **540**, A97
- Mahy, L., Rauw, G., De Becker, M., Eenens, P., & Flores, C. A. 2013, *A&A*, **550**, A27
- Mahy, L., Rauw, G., Martins, F., et al. 2010, *ApJ*, **708**, 1537
- Maíz Apellániz, J. 2001, *AJ*, **121**, 2737
- Maíz Apellániz, J. 2008, *ApJ*, **677**, 1278
- Maíz Apellániz, J. 2010, *A&A*, **518**, A1
- Maíz Apellániz, J. 2013, in *Highlights of Spanish Astrophysics, VII, Proc. of the X Scientific Meeting of the Spanish Astronomical Society (SEA)*, ed. J. C. Guirado, et al., 583
- Maíz Apellániz, J., Alfaro, E. J., & Sota, A. 2008a, arXiv:0804.2553
- Maíz Apellániz, J., Pellerin, A., Barbá, R. H., et al. 2012, in ASP Conf. Ser. 465, ed. L. Drissen, C. Robert, N. St-Louis, & A. F. J. Moffat (San Francisco, CA: ASP), 484
- Maíz Apellániz, J., & Sota, A. 2008, *RMxAC*, **33**, 44
- Maíz Apellániz, J., Sota, A., Morrell, N. I., et al. 2013, in *Massive Stars: From α to Ω* , 198
- Maíz Apellániz, J., Sota, A., Walborn, N. R., et al. 2011, in *Highlights of Spanish Astrophysics VI*, ed. M. R. Zapatero Osorio, J. Gorgas, J. Maíz Apellániz, J. R. Pardo, & A. Gil de Paz, 467
- Maíz Apellániz, J., Úbeda, L., Walborn, N. R., & Nelan, E. P. 2005, in *Resolved Stellar Populations*, ed. D. Valls-Gabaud & M. Chávez, arXiv:astro-ph/0506283
- Maíz Apellániz, J., Walborn, N. R., Galué, H. Á., & Wei, L. H. 2004, *ApJS*, **151**, 103
- Maíz Apellániz, J., Walborn, N. R., Morrell, N. I., Niemelä, V. S., & Nelan, E. P. 2007, *ApJ*, **660**, 1480
- Maíz Apellániz, J., Walborn, N. R., Morrell, N. I., et al. 2008b, *RMxAC*, **33**, 55
- Malkov, O. Y., Oblak, E., Snegireva, E. A., & Torra, J. 2006, *A&A*, **446**, 785
- Mannino, G., & Humblet, J. 1955, *AnAp*, **18**, 237
- Mason, B. D., Gies, D. R., Hartkopf, W. I., et al. 1998, *AJ*, **115**, 821
- Mason, B. D., Hartkopf, W. I., Gies, D. R., Henry, T. J., & Helsel, J. W. 2009, *AJ*, **137**, 3358
- Mason, B. D., Wycoff, G. L., Hartkopf, W. I., Douglass, G. G., & Worley, C. E. 2001, *AJ*, **122**, 3466
- Massey, P., DeGioia-Eastwood, K., & Waterhouse, E. 2001, *AJ*, **121**, 1050
- Massey, P., & Johnson, J. 1993, *AJ*, **105**, 980
- Mayer, P., Harmanec, P., & Pavlovski, K. 2013, *A&A*, **550**, A2
- Mayer, P., Lorenz, R., Drechsel, H., & Abseim, A. 2001, *A&A*, **366**, 558
- McSwain, M. V. 2003, *ApJ*, **595**, 1124
- Morgan, W. W., Code, A. D., & Whitford, A. E. 1955, *ApJS*, **2**, 41
- Morgan, W. W., González, G., & González, G. 1953a, *ApJ*, **118**, 323
- Morgan, W. W., Whitford, A. E., & Code, A. D. 1953b, *ApJ*, **118**, 318
- Morrell, N. I., Barbá, R. H., Niemelä, V. S., et al. 2001, *MNRAS*, **326**, 85
- Morrell, N. I., García, B., & Levato, H. 1988, *PASP*, **100**, 1431
- Morris, P. M. 1961, *MNRAS*, **122**, 325
- Morrison, N. D., & Conti, P. S. 1980, *ApJ*, **239**, 212
- Nazé, Y., Antokhin, I. I., Sana, H., Gosset, E., & Rauw, G. 2005, *MNRAS*, **359**, 688
- Nazé, Y., Bagnuolo, S., Petit, V., et al. 2012a, *MNRAS*, **423**, 3413
- Nazé, Y., Mahy, L., Damerdj, Y., et al. 2012b, *A&A*, **546**, A37
- Nazé, Y., Zhekov, S. A., & Walborn, N. R. 2012c, *ApJ*, **746**, 142
- Negueruela, I., Steele, I. A., & Bernabeu, G. 2004, *AN*, **325**, 749
- Nelan, E. P., Walborn, N. R., Wallace, D. J., et al. 2004, *AJ*, **128**, 323
- Nelan, E. P., Walborn, N. R., Wallace, D. J., et al. 2010, *AJ*, **139**, 2714
- Niemelä, V. S., & Gamen, R. C. 2005, *MNRAS*, **356**, 974
- Niemelä, V. S., Morrell, N. I., Fernández Lajús, E., et al. 2006, *MNRAS*, **367**, 1450
- Niemelä, V. S., & Morrison, N. D. 1988, *PASP*, **100**, 1436
- Otero, S. A. 2003, *IBVS*, **5480**, 1
- Otero, S. A. 2006, *OEJV*, **45**, 1
- Otero, S. A. 2007, *OEJV*, **72**, 1
- Otero, S. A., & Claus, F. 2004, *IBVS*, **5495**, 1
- Otero, S. A., & Wils, P. 2005, *IBVS*, **5644**, 1
- Parkin, E. R., Broos, P. S., Townsley, L. K., et al. 2011, *ApJS*, **194**, 8
- Pellerin, A., Maíz Apellániz, J., Simón-Díaz, S., & Barbá, R. H. 2012, in *American Astronomical Society Meeting Abstracts*, Vol. 219, 224.03
- Penny, L. R. 1996, *ApJ*, **463**, 737
- Penny, L. R., Gies, D. R., Wise, J. H., Stickland, D. J., & Lloyd, C. 2002, *ApJ*, **575**, 1050
- Penny, L. R., Seyle, D., Gies, D. R., et al. 2001, *ApJ*, **548**, 889
- Pourbaix, D., Tokovinin, A. A., Batten, A. H., et al. 2004, *A&A*, **424**, 727
- Rauw, G., Nazé, Y., Carrier, F., et al. 2001a, *A&A*, **368**, 212
- Rauw, G., Nazé, Y., Fernández Lajús, E., et al. 2009, *MNRAS*, **398**, 1582
- Rauw, G., Sana, H., Antokhin, I. I., et al. 2001b, *MNRAS*, **326**, 1149
- Rauw, G., Sana, H., Gosset, E., et al. 2000, *A&A*, **360**, 1003
- Rauw, G., Sana, H., Spano, M., et al. 2012, *A&A*, **542**, A95
- Roman-Lopes, A., Barbá, R. H., & Morrell, N. I. 2011, *MNRAS*, **416**, 501
- Sabín-Sanjulián, C., Simón-Díaz, S., Herrero, A., et al. 2014, arXiv:1312.3278
- Sana, H., Gosset, E., & Evans, C. J. 2009, *MNRAS*, **400**, 1479
- Sana, H., Gosset, E., Nazé, Y., Rauw, G., & Linder, N. 2008, *MNRAS*, **386**, 447
- Sana, H., James, G., & Gosset, E. 2011a, *MNRAS*, **416**, 817
- Sana, H., Le Bouquin, J.-B., De Becker, M., et al. 2011b, *ApJL*, **740**, L43
- Sana, H., Le Bouquin, J.-B., Mahy, L., et al. 2013, *A&A*, **553**, A131
- Sánchez-Bermúdez, J., Schödel, R., Alberdi, A., et al. 2013, *A&A*, **554**, L4
- Schild, R. E. 1970, *ApJ*, **161**, 855
- Schild, R. E., Hiltner, W. A., & Sanduleak, N. 1969, *ApJ*, **156**, 609
- Shara, M. M., Moffat, A. F. J., Gerke, J., et al. 2009, *AJ*, **138**, 402
- Simón-Díaz, S., Caballero, J. A., & Lorenzo, J. 2011a, *ApJ*, **742**, 55
- Simón-Díaz, S., Castro, N., García, M., & Herrero, A. 2011b, in *IAU Symp. 272, Active OB Stars: Structure, Evolution, Mass Loss, and Critical Limits*, ed. C. Neiner, G. Wade, G. Meynet, & G. Peters (Cambridge: Cambridge Univ. Press), 310
- Simón-Díaz, S., García, M., Herrero, A., Maíz Apellániz, J., & Negueruela, I. 2011c, in *Stellar Clusters & Associations: A RIA Workshop on Gaia*, ed. E. J. Alfaro Navarro, A. T. Gallego Calvente, & M. R. Zapatero Osorio, 255
- Skrutskie, M. F., Cutri, R. M., Stiening, R., et al. 2006, *AJ*, **131**, 1163
- Smith, N., Barbá, R. H., & Walborn, N. R. 2004, *MNRAS*, **351**, 1457
- Solivella, G. R., & Niemelä, V. S. 1986, *RMxAA*, **12**, 188
- Sota, A., Maíz Apellániz, J., Barbá, R. H., et al. 2013, in *Massive Stars: From α to Ω* , 101
- Sota, A., Maíz Apellániz, J., Walborn, N. R., & Shida, R. Y. 2008, *RMxAC*, **33**, 56
- Sota, A., Maíz Apellániz, J., Walborn, N. R., et al. 2011, *ApJS*, **193**, 24
- Stickland, D. J. 1996, *Obs*, **116**, 294
- Stickland, D. J., & Lloyd, C. 2001, *Obs*, **121**, 1
- Stickland, D. J., Lloyd, C., & Sweet, I. 1998, *Obs*, **118**, 7
- Szczerba, R., Siódmiak, N., Stasińska, G., & Borkowski, J. 2007, *A&A*, **469**, 799
- ten Brummelaar, T. A., O'Brien, D. P., Mason, B. D., et al. 2011, *AJ*, **142**, 21
- Thackeray, A. D., & Andrews, P. J. 1974, *A&AS*, **16**, 323
- Thaller, M. L., Gies, D. R., Fullerton, A. W., Kaper, L., & Wiemker, R. 2001, *ApJ*, **554**, 1070
- Tokovinin, A., Mason, B. D., & Hartkopf, W. I. 2010, *AJ*, **139**, 743
- Turner, N. H., ten Brummelaar, T. A., Roberts, L. C., et al. 2008, *AJ*, **136**, 554
- Urquhart, J. S., Morgan, L. K., & Thompson, M. A. 2009, *A&A*, **497**, 789
- van der Hucht, K. A. 2001, *NewAR*, **45**, 135
- van Leeuwen, F., & van Genderen, A. M. 1997, *A&A*, **327**, 1070
- Vijapurkar, J., & Drilling, J. S. 1993, *ApJS*, **89**, 293
- Wade, G. A., Maíz Apellániz, J., Martins, F., et al. 2012, *MNRAS*, **425**, 1278
- Walborn, N. R. 1971, *ApJL*, **167**, L31
- Walborn, N. R. 1972, *AJ*, **77**, 312

- Walborn, N. R. 1973a, [ApJ](#), **179**, 517
- Walborn, N. R. 1973b, [AJ](#), **78**, 1067
- Walborn, N. R. 1976, [ApJ](#), **205**, 419
- Walborn, N. R. 1982a, [ApJL](#), **254**, L15
- Walborn, N. R. 1982b, [ApJ](#), **256**, 452
- Walborn, N. R. 1982c, [AJ](#), **87**, 1300
- Walborn, N. R. 2001, in ASP Conf. Ser. 242, Eta Carinae and Other Mysterious Stars: The Hidden Opportunities of Emission Spectroscopy, ed. T. R. Gull, S. Johansson, & K. Davidson (San Francisco, CA: ASP), [217](#)
- Walborn, N. R. 2009a, in Stellar Spectral Classification, ed. R. O. Gray & C. J. Corbally (Princeton, NJ: Princeton Univ. Press), 66
- Walborn, N. R. 2009b, in STScI Symposium Series, Massive Stars from Pop. III and GRBs to the Milky Way, ed. M. Livio & E. Villaver, (Vol. 20), 167
- Walborn, N. R., & Fitzpatrick, E. L. 2000, [PASP](#), **112**, 50
- Walborn, N. R., Howarth, I. D., Evans, C. J., et al. 2010a, [AJ](#), **139**, 1283
- Walborn, N. R., Howarth, I. D., Lennon, D. J., et al. 2002, [AJ](#), **123**, 2754
- Walborn, N. R., Maíz Apellániz, J., Sota, A., et al. 2011, [AJ](#), **142**, 150
- Walborn, N. R., & Panek, R. J. 1984, [ApJ](#), **286**, 718
- Walborn, N. R., Sota, A., Maíz Apellániz, J., et al. 2010b, [ApJL](#), **711**, L143
- Walborn, N. R., Stahl, O., Gamen, R. C., et al. 2008, [ApJL](#), **683**, L33
- Werner, K., & Rauch, T. 2001, in ASP Conf. Ser. 242, Eta Carinae and Other Mysterious Stars: The Hidden Opportunities of Emission Spectroscopy, ed. T. R. Gull, S. Johansson, & K. Davidson (San Francisco, CA: ASP), [229](#)
- Wertheimer, J. G., & Laughlin, G. 2006, [AJ](#), **132**, 1995
- Whiteoak, J. B. 1963, *MNRAS*, **125**, 105
- Williams, S. J., Gies, D. R., Hillwig, T. C., McSwain, M. V., & Huang, W. 2013, [AJ](#), **145**, 29
- Wramdemark, S. 1976, *A&AS*, **23**, 231